Investigation On The Spectroscopic And Semiconductive Properties Of Some Organic Compounds

THESIS

SUBMITTED FOR THE DEGREE OF

DOCTOR OF PHILOSOPHY (SCIENCE)

OF THE

UNIVERSITY OF NORTH BENGAL

By

BISWANATH MALLIK, M. Sc.

DEPARTMENT OF OPTICS

INDIAN ASSOCIATION FOR THE CULTIVATION OF SCIENCE

CALCUTTA-700032

1979

PREFACE

The present thesis entitled " Investigation on the spectroscopic and semiconductive properties of some organic compounds " is in fulfilment of the requirements for the degree of Doctor of Philosophy (Science) of the University of North Bengal. It embodies the results of investigation on the spectroscopic and semiconductive properties of some linear conjugated polyenes.

This thesis has two parts and an Appendix. The first part deals with the investigation on the electronic absorption and emission spectroscopy of some polyenes : solvent effect and effect of adsorption of various vapours on their solid films. In the second part results from the studies on the semiconductive properties of these compounds e.g. the effect of adsorption of vapours on the electrical conductivity, on the semiconduction activation energy and on the variation of the pre-exponential factor (in the standard expression for specific conductivity) with the activation energy have been included. There are three chapters in the first part and the second one comprises four chapters. Chapter 1 of both parts contains a general introduction with a brief review of the relevent parts of the existing theories required to interpret the observed results. For collecting the spectroscopic data spectrophotometer and spectrofluorometer have been used. The experimental techniques used for the semiconductive investigation are presented in Chapter 2 of the second part. The chapters 2 and 3 of Part I and chapters 3 and 4 of Part II contain details of the results obtained in the investigation together with the discussion of the results.

Most of the results have been published in the form of papers in different scientific journals. Some are awaiting publication. A list of publications and the available reprints are given in the Appendix.

This work has been carried out in the Department of Physics, North Bengal University, Darjeeling, India and in the Department of Optics, Indian Association for the Cultivation of Science, Calcutta

Department of Optics
Indian Association for the
Cultivation of Science,
Jadavpur,
Calcutta-700 032,
INDIA
The 28th April, 1979.

BISWANATH MALLIK

ACKNOWLEDGEMENTS

To Dr. T.N. Misra, thesis supervisor, to whom I express my deep sense of gratitude for his continuous guidance and untiring supervision throughout the course of the investigation,

to Prof. G.S. Kastha to whom I am extremely grateful for his active interest in the work and for kindly providing with the laboratory facilities,

to Prof. S.N. Sen to whom I am grateful for kindly providing with the laboratory facilities in the Dept. of Physics, North Bengal University, Darjeeling, for some work presented in this thesis,

to Prof. R.K. Mishra who readily made the Aminoco Bowman Spectrofluorometer available for the emission studies,

to Prof. D. Rosenberg for a generous gift of the conducting glass electrodes and the teflon tapes,

to Prof. L.E. Lyons to whom I am thankful for valuable discussions,

to Mr. K.M. Jain, Mrs. A. Ghosh (Banerjee), Dr. K.G. Mandal and many other individuals in the North Bengal University and in Indian Association for the Cultivation of Science, Calcutta-32, to whom I am thankful for their assistance during the progress of the work,

to Mr. S.K. Sarker to whom I am thankful for his competent technical assistance and constant co-operation,

to the authorities of Indian Association for the Cultivation of Science and North Bengal University, and Council of Scientific and Industrial Research, India to whom I am thankful for providing with the research fellowships,

to Mr. D. Ghosal for his expert typing the thesis in a short time.

Department of Optics
Indian Association for the
Cultivation of Science,
Jadavpur, Calcutta-700 032,
INDIA

BISWANATH MALLIK

The 22th April, 1970.

CONTENTS

LIST OF FIGURES

PART I

ABSTRACT

Part I

Electronic absorption and emission spectra of polyenes, all-trans vitamin A alcohol, all-trans vitamin A acetate, β-apo-8'-carotenal, astacene and methyl bixin have been investigated in the solid state. On adsorption of certain vapours on the crystallite surfaces of these polyenes, a new band appears on the low energy side of the well known intense $^1A_g \longrightarrow {}^1B_u$ transition. No significant change in position of this new band is observed with adsorption of different vapours. A good mirror image relationship between the new absorption band and the well known emission band for these molecules indicates that this new absorption band may be due to a transition from the ground state to a low-lying π-electronic state wherefrom the emission initiates. The effect of different solvents on the intense $^1A_g \longrightarrow {}^1B_u$ transition and on the observed emission band of each polyene under investigation is appreciably different. This suggests that different excited states are involved in the absorption and in the emission processes. It has been concluded that in these long-chain polyenes there exists a low-lying forbidden ^1A_g state below the strongly allowed ^1B_u state.

On adsorption of some electron acceptor molecules on the solid films of the polyenes, in addition to the original bands, a new absorption band appears in each case on the longer wavelength side of the spectrum. This new band is energetically much lower than

the emission band of the molecules. The position of this new band is dependent on the electron affinity (E_A) of the acceptor molecules and the intensity depends on the amount of acceptor molecules adsorbed. A linear relationship between the $\bar{\nu}_{max}$ of the new band and E_A has been observed. The ionization potentials of the polyenes have been estimated from this linear relationship. The estimated values agree satisfactorily with the values obtained by other methods. It has been concluded that the polyenes behave as electron donors and in the solid state form charge-transfer complexes with suitable electron acceptors.

Part II

The change in semiconductive properties of some polyenes after adsorption of various vapours on the crystallite surface has been studied at constant sample temperatures. A rapid enhancement in the semiconduction current has been observed. The rise in conductivity has been found to be exponential with increasing vapour pressure of the adsorbed vapour. This adsorption process has been observed to be efficiently reversible. The adsorption and desorption kinetics have been found to follow the modified Roginsky-Zeldovich relation $dm/dt = A \exp(-\beta m/kT)$ where, m is the amount of vapour adsorbed at time 't', A and β are constants at a particular pressure. The activation energies of adsorption and desorption have been estimated from kinetic data analysis. A two-stage adsorption process satisfactorily explains the experimental results.

The change in semiconduction activation energy on adsorption of various vapours has been investigated. The adsorbed vapours change the activation energy by increasing or decreasing it. Such change depends on the chemical nature, amount of the vapour adsorbed and also on the polyene end group. These semiconductors follow the three-constant equation

$$\sigma(T) = \sigma_0' \exp(E/2kT_0) \exp(-E/2kT)$$

where the conventional pre-exponential factor σ_0 has been replaced by $\sigma_0' \exp(E/2kT_0)$ (the so called compensation effect). Here T_0 and σ_0' are constants for a particular substance and T_0 is called the characteristic temperature. T_0 has been found to play a significant role on the dark conduction process. Various methods used for evaluating T_0 and σ_0' have yielded consistent results. Excellent correlation obtained between the relevant parameters in these semiconductors indicates that σ_0 and E are physically related. Various models for conduction mechanism leading to compensation effect have been discussed.

PART I

INVESTIGATION ON THE SPECTROSCOPIC PROPERTIES OF SOME ORGANIC COMPOUNDS

CHAPTER 1

INTRODUCTION

1.1 General

During the last two and a half decades the spectra of organic molecules in different states have been extensively studied to have a more complete understanding of intermolecular as well as intramolecular properties. Particularly, spectroscopic studies of molecules of biological interest have been accelerated in recent years to understand them and their interaction forces which exist within and between molecules of a particular shape in a given situation favourable for a particular biological activity. High speed computers have multiplied the progress greatly. Their use has helped to test theories involving complex calculations of molecular orbitals of large biomolecules. An understanding of the electronic properties of molecules depends on the large accumulation of experimental data. The development of intense UV light sources for absorption and emission studies, UV and visible spectrophotometers has made available more complete sets of experimental data which serve more accurate interpretations of many phenomena associated with the biomolecules concerned.

The present investigation is concerned with the electronic properties of some conjugated molecules (polyenes). The goal of this research is to collect the spectral data experimentally and to interpret the data within the framework of the existing theories. In order to achieve the data the already well established experimental techniques of UV and visible spectroscopy have been adopted.

There are two aspects of the spectroscopic properties of polyenes of current interest. One regarding the existence of a low-lying π-electronic forbidden state[1-6] (^1A_g) below the strongly allowed ^1B_u state in the near UV or visible region of the spectrum and the other is the possibility of formation of charge-transfer complexes[5-10] of these compounds with suitable donor or acceptor molecules.

Adequate interpretation of the spectral data of molecules in different phases rests on modern theories. The free-electron MO theory, LCAO MO theory, resonance force theory, theory of vibrational-electronic interactions and the theory of intermolecular charge-transfer interaction — all aided to interpret the electronic properties of polyene molecules and for explaining some experimental results. The outlines of the relevant parts of these theories are discussed in the following sections of this chapter.

1.2 The Free-Electron MO Theory

The molecular orbital (MO) theory assumes the electrons to be located in the delocalized orbitals. The orbitals of lowest energy for the electrons satisfying the Pauli's exclusion principle are referred to as the ground state of the molecule. An electron when raised from one of these filled orbitals to the other one empty in the ground state corresponds to an excited state.

The free-electron MO theory[11-26] is generally used for determining the allowed energies and state wave functions of the π-electrons in conjugated organic molecules. This theory is based on

the assumption that there is a region in space in which the potential energy of an electron is finite and constant and is infinitely high outside this region. From the molecular point of view the electrons move freely along the length (l) of the conjugated system. Hence the problem of an electron in the conjugated system becomes one-dimensional and the wave equation of an electron in a one-dimensional potential is

$$\frac{d^2\psi}{dx^2} + \frac{2m}{\hbar^2}(E - V)\psi = 0 \qquad (1.1)$$

The electron is assumed to move freely along the length of the molecule and hence $V = 0$. The solutions of the wave equation (1.1) after normalization with the boundary condition $0 \leq x \leq l$ satisfied are

$$\psi_n = \sqrt{\frac{2}{l}} \sin \frac{n\pi x}{l} \qquad (1.2)$$

$$E_n = \frac{n^2\hbar^2}{8ml^2} \qquad (1.3)$$

where n is an interger, m is the electron mass and h is Planck's constant.

The one-dimensional solutions (1.2) and (1.3) will serve as an approximation to the orbitals of a long linear conjugated polyene for example. Thus the MO theory in free-electron approximation gives a simple description of the electronic states of linear conjugated polyenes. A conjugated hydrocarbon of k double

bonds contain 2k π-electrons. Each of k orbitals of the molecule in the ground state is occupied with two electrons. The first electronically excited state of the conjugated molecule is obtained from the corresponding ground state by raising an electron from the highest occupied orbital (n=k) to the lowest empty orbital (n=k+1). Therefore, the energy of excitation, ΔE, is given by

$$\Delta E = E_{k+1} - E_k$$

$$= \frac{(2k+1)h^2}{8ml^2} \qquad (1.4)$$

or $$\lambda = \left(\frac{8mc}{h}\right)\frac{l^2}{2k+1} \qquad (1.5)$$

where the variables are only l and k. It is seen that λ varies as l^2. From the variation of l with the number of double bonds in the system,

$$l \propto (k+1) \qquad (1.6)$$

and from (1.5), $$\lambda \propto \frac{(k+1)^2}{2k+1} \qquad (1.7)$$

At large k, $k+1 \approx k$ and hence

$$\lambda \propto k \qquad (1.8)$$

which indicates that the increase in length of a conjugated system increases the wavelength of absorption. From (1.5) it is understood

that the free-electron method provides a semiquantitative relation between the length of the conjugated system and the wavelength of absorption. The wavelengths of other bands in the higher energy side of the absorption spectrum of the molecule can also be readily predicted by the free-electron MO method.

1.3 The LCAO MO Theory

The LCAO MO theory is based on the expectation that close to one atom of a molecule the influence of that atom will predominate and the molecular wave function will be similar to that of an atomic orbital. Consequently it seems natural to approximate the molecular orbitals as a linear combination of atomic orbitals. Each molecular orbital in the LCAO approximation[26,29-33] is regarded as the sum of various amounts of atomic orbitals. In this approximation the r th molecular orbital is written as

$$\psi_r = \sum_j c_{rj} \phi_j \qquad (1.9)$$

where ϕ_j is the j th atomic orbital and c_{rj} is a coefficient describing the amount of the j th atomic orbital to be found in the r th molecular orbital. These molecular orbitals are assumed to be eigenfunctions of an effective one-electron Hamiltonian for the equilibrium nuclear configuration of the molecule so that

$$H\psi_r = E_r\psi_r \qquad (1.10)$$

The coefficients which correspond to stable molecular orbitals

are to be considered. The orbital energies E_r and the coefficients c_{rj} can be evaluated by using the variation method if the matrix elements H_{ij} of the Hamiltonian and those, S_{ij} of overlap between the atomic orbitals are known. The secular equations are given by

$$\sum_j c_j (H_{ij} - E S_{ij}) = 0 \quad , \text{ for each } i \qquad (1.11)$$

For n atomic orbitals in the expression (1.9) for the molecular orbitals there will be n secular equations of this type. The solutions of these secular equations will be non-trivial only if the n th order secular determinant vanishes :

$$| H_{ij} - E S_{ij} | = 0 \qquad (1.12)$$

If this secular determinantal equation is expanded and solved, this will yield n solutions for the orbital energy E. If each of these solutions for E is substituted back into the secular equations, the coefficients c of the atomic orbital in the molecular orbital can be obtained.

Let us write for convenience

$$\alpha_i = H_{ii} \qquad (1.13)$$

$$\beta_{ij} = H_{ij} = H_{ji} \quad (i \neq j) \qquad (1.14)$$

Here α_i is the Coulomb integral of the atomic orbital ϕ_i . This integral represents the Coulomb energy of an electron in the atomic

orbital ϕ_i. β_{ij} is the resonance integral between the atomic orbitals ϕ_i and ϕ_j and it amounts to the energy of interaction of the two atomic orbitals. Both these integrals α and β correspond to negative energy. If it is assumed that all the atomic orbitals are normalized, the secular equations (1.11) can be written in terms of α and β as

$$\sum_{j \neq i} c_j (\beta_{ij} - E S_{ij}) + c_i(\alpha_i - E) = 0 \quad \text{for each } i \qquad (1.15)$$

It is known that the absorption spectra of hydrocarbons are due to transitions of the π-electrons. The approximations to these secular equations for these π-orbitals, called the Hückel approximations[34-37] are the following :

(1) The Coulomb integrals α_i are taken to be the same for each atomic orbital and this is represented by α.

(2) All the overlap integrals S_{ij} are assumed to be zero for $i \neq j$.

(3) The resonance integrals β_{ij} are considered to be nonzero only between neighbouring atoms. So $\beta_{ij} \neq 0$ if atom i is bonded to j atom ($i \rightarrow j$).

(4) All the resonance integrals for neighbouring carbon atoms are assumed to be equal and are denoted by β.

With the above Hückel approximations the secular equation (1.15) becomes

$$\sum_{j \rightarrow i} c_j \beta + c_i (\alpha - E) = 0 \quad , \qquad \text{for each } i \qquad (1.16)$$

On writing $v = \frac{\alpha - E}{\beta}$, the secular equations (1.16) reduce to

$$\sum_{j \to i} c_j + v c_i = 0 \qquad \text{for each } i \qquad (1.17)$$

Corresponding to the secular equations (1.17), the secular determinant becomes simple : the diagonal elements are v and the off-diagonal elements of row i, column j are 1 if atom i is bonded to atom j, otherwise the off-diagonal elements are zero. Thus the secular determinant for any conjugated π -system wholly of carbon π- centers can be built up. For the linear conjugated π -system, the energies of the Hückel molecular orbitals, v and the coefficients of the carbon $2p\pi$ atomic orbitals in the Hückel molecular orbitals, c, can be expressed in the analytic forms[38] as :

$$v_r = -2 \cos \frac{r\pi}{n+1} \quad , \quad r = 1, 2 \cdots n \qquad (1.18)$$

$$c_{ij} = \left(\frac{2}{n+1}\right)^{\frac{1}{2}} \sin \frac{jr\pi}{n+1} \qquad (1.19)$$

where r signifies the molecular orbitals. The carbon π -centers are numbered as 1,2 .... n from one end of the carbon chain and c_{rj} is the coefficient of j th carbon atom in the r th MO, ψ_r . Substitution of (1.19) in (1.9) gives

$$\psi_r = \left(\frac{2}{n+1}\right)^{\frac{1}{2}} \sum_{j=1}^{n} \sin \frac{jr\pi}{n+1} \phi_j \qquad (1.20)$$

where the linear conjugated system conteins n carbon atoms. The

energy corresponding to ψ_r is

$$E_r = \alpha + 2\beta \cos \frac{r\pi}{n+1} \qquad (1.21)$$

The electronic transition from the highest bonding MO to the lowest antibonding MO gives rise to the first absorption band of the conjugated polyene molecule and the corresponding transition energy is given by

$$\Delta E = 4 \sin \frac{\pi}{2(n+1)} \qquad (1.22)$$

which is in units of $-\beta$. It can be said that for a constant value of $-\beta$ the transition energy decreases as the length of the conjugated polyene chain increases. Since for small angles $\sin\theta \sim \theta$, this simple LCAO MO theory predicts that for a long polyene molecule the wavelength λ_{max} of the first absorption band will be proportional to n, which is evident from (1.22), and will increase to infinity as the length of the conjugated chain increases to infinity. In the preceding section also the MO theory in free-electron approximation predicts for the energy of the transition to the lowest excited electronic state a similar relationship with the length of the conjugated polyene molecules.

1.4 The Resonance Force Theory

One of the basic problems in the application of quantum mechanics to spectroscopic problems is the selection of proper zero-order wave functions - that is, the choice of basic sets that

allow one to obtain directly a reasonable picture of the electronic structure of the molecule in question. For many π-electron systems approaches based on delocalization of electrons such as the LCAO (Hückel) molecular orbital and the free-electron (FE) model have been successful. But these theories show some discrepancies with the experimental results of the polyene. For such molecules the molecular orbital theory both in FE and LCAO approximations discussed earlier predicts that the energy of the lowest excited electronic state approaches that of the ground state as the length of the chain increases. Experimentally this was not found to be so. The energy of the lowest allowed transition of long polyenes appears to have a non-zero limit. However, it has now been shown on theoretical grounds[33-41] that the assumption of equal bond lengths for longer polyenes is incorrect. An alternation of bond lengths, long and short, will always occur if the conjugated system (polyene) is long enough[42]. In the molecular orbital theory electrons are assigned to orbitals delocalized over the whole molecule. According to this theory the low-lying electronic excited states will have an electron raised from one of the bonding molecular orbitals to one of the antibonding set. This simple description of the excited states fails to take account of some important features for long molecules. Although it does predict a nonzero limit for long molecules, it does not necessarily give correct description of the lowest group of excited states. It has been suggested, however, that in situations where one can write only one plausible low energy ground state structure for a molecule, one should consider not delocalization of electrons, but rather delocalization

of excitation, in approaching the low-lying excited states[43], a point of view, which has led to the "resonance force model" for such molecules. The resonance force model[44] of describing the excited states of polyenes treats the molecule as an assembly of ethylene-type units, each with two π-electrons in which exchange forces between the double bonds are omitted, only the electrostatic interaction being considered. The Hamiltonian matrix between the states of the n double bonds is similar to the Hückel matrix for an n-atom chain; the Hückel α is replaced by the ethylene transition energy E_v and β is replaced by Γ , the interaction integral. The eigenvalues of this matrix can be taken from the Hückel problem (1.21)

$$E_r(n) = E_v + 2\Gamma \cos\frac{r\pi}{n+1} \qquad (1.23)$$

The resonance force approach has been applied with success in the interpretation of the spectra of polyenes[44].

1.5 The Theory of Vibrational-Electronic Interactions

The intensity of an optical (electric dipole) transition is proportional to the square of the transition moment between the initial and final states. The transition moment between two states i and j is

$$\vec{M}_{ij} = \int \psi_i(x,X)\, \vec{M}(x,X)\, \psi_j(x,X)\, dx\, dX \qquad (1.24)$$

where $\psi_i(x,X)$ and $\psi_j(x,X)$ are exact solutions of the

Schroedinger equation for the complete Hamiltonian. The collective coordinate symbols x and X form a complete set of internal coordinates and locate respectively all of the electrons and nuclei. $\vec{M}(x,X)$ is the dipole moment operator

$$\vec{M}(x,X) = e\sum_i \vec{r}_i - e\sum_\sigma Z_\sigma \vec{R}_\sigma \qquad (1.25)$$

where $\vec{r}_i$ and $\vec{R}_\sigma$ are the position vectors of the i th electron and σ th nucleus respectively.

In polyatomic molecules exact solutions are not known since the equations of motion of three or more interacting particles cannot be solved. The Born-Oppenheimer approximation[45] is used to obtain a simplification of the mathematical description of the system. This procedure separates the electronic and nuclear motions. The adiabatic wavefunctions are usually further simplified by fixing the nuclear coordinates which appear as parameters in the electronic wavefunctions. Thus the zeroth-order vibronic wavefunction for the μ th vibrational level of the i th electronic state can be written as the product function

$$\Psi_{i\mu}(x,X) = \Psi_i(x,X_0)\chi_{i\mu}(X) \qquad (1.26)$$

where $\Psi_i(x,X)$ is a solution of the electronic Schroedinger equation for the equilibrium nuclear configuration X_0 and $\chi_{i\mu}(X)$ is the vibrational wavefunction.

Since most information concerning the nuclear motions of polyatomic molecules relates to the ground state, it is convenient to express the nuclear coordinates X in terms of a complete set of normal coordinates Q for that state. The normal coordinates completely span the space of infinitesimal nuclear displacements. With appropriate choice of origin, the electronic wavefunctions belonging to the excited electronic states may be expressed in terms of the ground state q . Thus the vibronic wavefunction for μ quanta of any normal mode in the k th excited electronic state is

$$\Psi_{k\mu}(x,Q) = \Psi_k(x,Q_0)\,\chi_{k\mu}(Q,\Delta) \qquad (1.27)$$

where the general displacement vector Δ accounts for the difference in the equilibrium geometry between the ground and excited electronic states.

The number of molecules in a state with energy ΔE greater than the lowest energy state is given by the Boltzmann distribution factor $\exp(-\Delta E/kT)$ so that, at very low temperatures, only the zeroth vibrational level of the ground state will be populated. The probability of the transition from the zeroth vibrational level of the ground state to the μ th vibrational level of the k th excited state is proportional to the squere of the transition moment

$$\vec{M}_{00,k\mu} = \int \Psi_0(x,Q_0)\,\chi_{00}(Q)\left\{e\sum_i \vec{r}_i - e\sum_\sigma Z_\sigma \vec{R}_\sigma\right\}\Psi_k(x,Q_0)\chi_{k\mu}(Q,\Delta)\,dx\,dQ$$

$$= \vec{M}_{0k}(Q_0)\int \chi_{00}(Q)\,\chi_{k\mu}(Q,\Delta)\,dQ$$

where

$$\vec{M}_{0K}(Q_0) = \int \Psi_0(x, Q_0)\, \vec{M}(x)\, \Psi_K(x, Q_0)\, dx \qquad (1.28)$$

and $$\int \chi_{00}(Q)\, \chi_{K\mu}(Q, A)\, dQ$$

is the Franck-Condon overlap factor. The contribution from the operator $e\sum_{\sigma} z_\sigma \vec{R}_\sigma$ vanishes in the integration over the electronic coordinates.

Equation (1.28) accounts for a number of features of a vibronic transition. The vector $\vec{M}_{0K}(Q_0)$ has a definite orientation in relation to the molecular skeleton and therefore predicts the polarization of the transition. Group theoretical[46] considerations classify the transition as symmetry allowed or forbidden. The electronic transition is said to be electric dipole allowed if the decomposition of the direct product of the irreducible representations of $\Psi_0(x, Q_0)$, $\vec{r}_i$, and $\Psi_K(x, Q_0)$ contains the totally symmetric representation of the point group. Otherwise $\vec{M}_{0K}(Q)$ vanishes and the transition is symmetry forbidden.

Experimental evidence shows that the transition moment as defined in equation (1.28) does not give an adequate account of vibronic spectra. The classic example is the weak benzene absorption system at 2600Å which is symmetry forbidden and shows a progression in totally symmetric vibrations built upon single quanta of non-totally symmetric vibrations which act as "false origins"[47]. A theoretical treatment to account for the appearance

of these 'forbidden' components in the transitions of polyatomic molecules by vibronic mixing was formulated by Herzberg and Teller[48]. The theory has been refined and extended by Liehr[49], Murrell and Pople[50], Craig[51], Albrecht[52] and Yeranos[53].

The basis of the Herzberg-Teller theory is to express the dependence of the electronic Schroedinger equation on the motion of the nuclei as a perturbation. The electronic Hamiltonian is expanded as a power series in the normal coordinates Q_q about the equilibrium position of the ground state as

$$H(Q) = H_0 + \sum_q \left(\frac{\partial H}{\partial Q_q} \right)_0 Q_q + \cdots \qquad (1.29)$$

where H_0 is the Hamiltonian for the equilibrium nuclear configuration and the perturbation is $\sum_q \left(\frac{\partial H}{\partial Q_q}\right)_0 Q_q$. The perturbed electronic wavefunction $\psi_{k\mu}(x, Q)$ is then expressed in the basis of the unperturbed wavefunctions $\psi^0_{k,\mu}(x,Q) \equiv \psi^0_{k\mu}$ as the linear combination

$$\psi_{k\mu}(x,Q) = \psi^0_{k\mu} + \sum_{l \neq k} \lambda_{kl} \psi^0_{l0} \qquad (1.30)$$

where $$(E^0_l - E^0_k)\lambda_{kl} = \int \psi^0_{k\mu} \left(\frac{\partial H}{\partial Q_q}\right)_0 Q_q \psi^0_{l0} \, dx \, dQ_q \qquad (1.31)$$

$$= \int \psi^0_k \left(\frac{\partial H}{\partial Q_q}\right)_0 \psi^0_l \, dx \int \chi_{k\mu} Q_q \chi_{l0} \, dQ$$

The ground state is assumed not to mix with excited states since the value of $E^0_k - E^0_0$ is very large (usually greater than 20,000 cm^{-1}).

The transition moment corrected to first order in small displacements is then

$$\vec{M}_{00,K\mu} = \vec{M}_{0K}(Q_0)\int \chi_{00}(Q)\chi_{K\mu}(Q,A)\,dQ + \sum_{\lambda \neq K} \vec{M}_{0\lambda}(Q_0)\int \chi_{00}(Q)\lambda_{K\lambda}\chi_{10}(Q,A)\,dQ$$

where

$$\vec{M}_{0\lambda}(Q_0) = \int \psi_0^\circ M(x)\,\psi_\lambda^\circ\,dx \qquad (1.32)$$

The first term in the equation representing the 'allowed' part of the transition moment integral has already been discussed. The 'forbidden' term is polarized according to the sense of $\vec{M}_{0\lambda}(Q_0)$.

The condition for the non-vanishing of the nuclear dependent or forbidden term in the transition moment expression is that $\vec{M}_{0\lambda}$ and $\lambda_{K\lambda}$ must be nonzero for at least one state λ. For finite $\vec{M}_{0\lambda}$, the direct product of the irreducible representations $\Gamma(\psi_0^\circ)$, $\Gamma(\sum\vec{r}_i)$, $\Gamma(\psi_\lambda^\circ)$ must contain the totally symmetric representation of the point group of the molecule. For finite $\lambda_{K\lambda}$ the direct products of $\Gamma(\psi_K^\circ)$, $\Gamma(\frac{\partial H}{\partial Q_q})_0$, $\Gamma(\psi_\lambda^\circ)$ and $\Gamma(\chi_{K\mu})$, $\Gamma(Q_q)$, $\Gamma(\chi_{10})$ must simultaneously contain the totally symmetric representation. These requirements imply that

$$\Gamma(\psi_K^\circ) \times \Gamma\left(\frac{\partial H}{\partial Q_q}\right)_0 = \Gamma(\psi_\lambda^\circ) = \Gamma\left(\sum\vec{r}_i\right) \qquad (1.33)$$

Further, since the Hamiltonian is invariant to operations of the point group of the molecule, $(\frac{\partial H}{\partial Q_q})_0$ has the same symmetry properties in electron space that Q_μ has in nuclear space. In

equation (1.33), $\Gamma(\psi_k^\circ)$ and $\Gamma(\psi_l^\circ)$ are specified, and $\Gamma(\frac{\partial H}{\partial q_\rho})_0$ can be determined. This is equivalent to specifying the type of vibration that can mix the electronic state ψ_l° with ψ_k°.

A quantitative treatment of the vibrational borrowing via the 606 and 1595 cm^{-1} e_{2g} vibrations between the allowed $^1E_{2u}$ (1800Å) electronic state and the forbidden $^1B_{2u}$ (2050Å) and $^1B_{1u}$ (2000Å) electronic states of benzene has been made[60]. The calculation involves an evaluation of λ_{kl}. The term in H which depends on both the electrons i and the nuclei σ is

$$\sum_i \sum_\sigma \frac{Z_\sigma e^2}{\vec{r}_{i\sigma}} \tag{1.34}$$

and therefore

$$\frac{\partial H}{\partial q_\rho} = \sum_{i=1}^{N} \left\{ \sum_\sigma Z_\sigma e^2 \frac{\partial \vec{r}_\sigma}{\partial q_\rho} \cdot \frac{\vec{r}_{i\sigma}}{r_{i\sigma}^3} \right\}$$

$$= \sum_{i=1}^{N} h_i \tag{1.35}$$

where $\vec{r}_\sigma$ is the position vector of nucleus σ. The nuclear displacements in the normal modes are thus represented by the set of dipoles $ez_\sigma \frac{\partial \vec{r}_\sigma}{\partial q_\rho}$ interacting with electrons i. Since equation (1.35) is the sum of one electron operators h_i the calculation of the integral in (1.31) reduces to the integration of $\sum_{i=1}^{N} h_i$ with the transition density,

$$\rho_{kl} = \int \psi_k^\circ \, \psi_l^\circ \, dx' \tag{1.36}$$

The results of the calculation[31] show that the $^1E_{1u}$ state is mixed most effectively with the $^1B_{2u}$ state by the 606 cm^{-1} vibration and with the $^1B_{1u}$ state by the 1595 cm^{-1} vibration.

1.6 The Franck-Condon Principle

The intensity distribution of an electronic transition among its vibrational members is determined by the Franck-Condon principle, which states that the nuclear positions and velocities do not change during an electronic transition. That is, the starting configuration in the new electronic state represents a displacement from the new equilibrium nuclear configuration without change of symmetry. If the displacement of the equilibrium nuclear configuration is zero ($\Delta = 0$) and if the potential energy surfaces have the same shape in both electronic states, then all the intensity is concentrated in the (0-0) band. If the displacement is non-zero ($\Delta \neq 0$), transitions to higher vibronic states become more probable. The steepness of the potential energy curve in the excited state determines the number of excited state vibrational wavefunctions $\chi_{i\mu}(q, \Delta)$ which will have appreciable overlap with the ground state vibrational wavefunctions $\chi_{00}(q)$ and therefore the length of the progression in an electronic transition.

A number of quantitative applications of the Franck-Condon principle have been made. From a knowledge of the intensity distribution in the benzene band system at 2650Å and the vibrations active in forming the progression (ground state, 992 cm^{-1}, excited state, 923 cm^{-1}), the extension of the C-C bond length of benzene

in the excited state was calculated to be 0.036Å [51]. The lowest benzene triplet state C-C bond length extension relative to the ground state was calculated to be 0.036Å [54] as well. The intensity distribution among the vibrational members of a transition has been calculated from the changes in geometry, the frequencies and the corresponding normal modes of the relevent vibrations in the progressions[55-58].

1.7 Intermolecular Charge-Transfer Complex

A loose reversible association of two or more distinct chemical components is called a complex. Charge-transfer complex (donor-acceptor complex) is formed between an electron donor and an electron acceptor. The acceptor and the donor may in general be molecules, molecule-ions, atoms or atom-ions, with the restriction that they are both in their totally symmetric ground states. The complex is characterized by a new absorption band called the charge-transfer (CT) band. This CT band is absent in the components of the complex. The complex exists in two states, a ground state and an excited state. In the ground state, the donor and the acceptor experience the normal physical forces one would expect from the two components in close proximity i.e., van der Waals forces etc. and in addition a small amount of charge is transferred from the donor to the acceptor which contributes some additional binding energy to the complex. The excited state is promoted when the ground state complex absorbs light of suitable energy. Mulliken[59-64] and other workers[65-67] have explained quantum

mechanically the formation of charge-transfer complexes and their approach is of the valence bond type. Mulliken's valence-bond description provides a very adequate explanation of the characteristic electronic absorption in terms of an intermolecular charge-transfer transition.

According to Mulliken, the ground state of the complex has a wavefunction Ψ_N which is hybrid of two wavefunctions $\Psi_{(A,D)}$ and $\Psi_{(A^-D^+)}$. Here $\Psi_{(A,D)}$ is the no-bond function and is the wavefunction of the donor and the acceptor in close proximity with no charge transfer between them. However it can include contributions from classical electrostatic forces, van der Waals forces and various dispersion forces and dipole interactions. $\Psi_{(A^-D^+)}$ is called the dative function and is the wavefunction of the two components bound together by an electron being totally transferred from the donor D to the acceptor A.

The ground state of the complex is described by

$$\Psi_N = a\,\Psi_{(A,D)} + b\,\Psi_{(A^-D^+)} \quad \text{where } a \gg b \qquad (1.37)$$

The excited state of the complex is described by

$$\Psi_E = b^*\,\Psi_{(A^-D^+)} - a^*\,\Psi_{(A,D)} \quad \text{where } b^* \gg a^* \qquad (1.38)$$

The energy levels of the complex can be found by solving the Schroedinger equation

$$H\,\Psi_N = W\,\Psi_N \qquad (1.39)$$

where H is the Hamiltonian operator and W is the energy. The difference between the two states (i.e., W_g and W_h) of the complex gives the energy (E_{CT}) of the charge-transfer transition and the solution of the equation (1.39) leads to an equation[68,69] for this energy :

$$E_{CT} = h\nu_{CT} = I_D^{v} - E_A^{v} + C_1 + \frac{C_2}{I_D^{v} - E_A^{v} + C_1} \qquad (1.40)$$

where ν_{CT} is the frequency corresponding to the intermolecular charge-transfer transition (lowest energy), I_D^{v} is the vertical ionization potential of the donor, E_A^{v} is the vertical electron affinity of the acceptor and C_1 and C_2 are constants. The last term is often small, so that its variation can be neglected, giving the equation

$$h\nu_{CT} = I_D^{v} - E_A^{v} + C_1 \qquad (1.41)$$

The above discussion from valence bond approach for the understanding of CT complex is useful in case of weak complexes. The formation of CT complex can also be explained in terms of simple molecular orbital (MO) treatment[70-79]. Here the complex is one to be formed by interaction between molecular orbitals of the donor and those of acceptor. This treatment leads to the conclusions similar to those given by the valence bond approach but the MO method seems better in that it gives satisfactory explanation of more then one intermolecular CT band in a complex

often observed[80-87]. There should be bands corresponding to transitions between any of the occupied orbitals of the donor and the empty orbitals of the acceptor. In the MO method, the interaction between the highest occupied orbital of the donor and the lowest empty orbital of the acceptor is in general considered. Due to the interaction the donor orbital is depressed and the empty orbital of the acceptor is raised and the whole system becomes stabilised with a simultaneous transfer of electron from the donor to the acceptor.

References

1. R.S. Hudson and B.E. Kohler, Chem. Phys. Letters, 14, 299 (1972).
2. K. Schulten and M. Karplus, Chem. Phys. Letters, 14, 305 (1972).
3. K. Mandal and T.N. Misra, Chem. Phys. Letters, 27, 57 (1974).
4. R.M. Gavin, Jr., C. Weisman, J.K. McVey and S.A. Rice, J. Chem. Phys., 68, 522 (1978).
5. J.R. Platt, Science, 123, 372 (1956).
6. M.A. Slifkin, Charge-Transfer Interactions of Biomolecules (Academic Press, London and New York, 1971) p 105.
7. B. Pullman and A. Pullman, Quantum Biochemistry (Interscience Publishers, New York, 1963) p 440.
8. F.U. Lichti and J.A. Lucy, Biochem. J., 112, 221 (1969).
9. J.A. Lucy and U.F. Lichti, Biochem. J., 112, 231 (1969).
10. J.A. Lucy, Am. J. Clin. Nut., 22, 1083 (1969).
11. N.S. Bayliss, J. Chem. Phys., 16, 287 (1948).
12. N.S. Bayliss, J. Chem. Phys., 17, 1353 (1949).
13. N.S. Bayliss, Australian J. Sci., 12, 12 (1949).
14. N.S. Bayliss, Quart. Rev. Chem. Soc., 6, 319 (1952).
15. H. Kuhn, Helv. Chim. Acta., 31, 1441 (1948).
16. H. Kuhn, Helv. Chim. Acta., 32, 2247 (1949).
17. H. Kuhn, J. Chem. Phys., 16, 840 (1948).
18. H. Kuhn, J. Chem. Phys., 17, 1198 (1949).
19. H. Kuhn, Chimica, 4, 203 (1950).
20. J.R. Platt, J. Chem. Phys., 17, 484 (1949).
21. J.R. Platt, J. Chem. Phys., 21, 1597 (1953).
22. W.T. Simpson, J. Chem. Phys., 16, 1124 (1948).
23. W.T. Simpson, J. Chem. Phys., 17, 1218 (1949).

24. K. Rudenberg and C.W. Scherr, J. Chem. Phys., 21, 1565 (1953).

25. C.W. Scherr, J. Chem. Phys., 21, 1582 (1953).

26. J.N. Murrell, The Theory of the Electronic Spectra of Organic Molecules (Chapman and Hall Ltd., London, 1971).

27. H.H. Jaffe and M. Orchin, Theory and Applications of Ultraviolet Spectroscopy (John Wiley and Sons, Inc., New York and London, 1962).

28. J.R. Platt, Radiation Biology, edited by A. Hollaender (McGraw-Hill, New York, 1956) p 71.

29. R.S. Mulliken, J. Chem. Phys., 7, 14 (1939).

30. R.S. Mulliken, J. Chem. Phys., 7, 364 (1939).

31. C.C.J. Roothaan, Revs. Mod. Phys., 23, 69 (1951).

32. H. Suzuki, Electronic Absorption Spectra and Geometry of Organic Molecules (Academic Press, New York and London, 1967).

33. A. Streitwieser, Jr., Molecular Orbital Theory for Organic Chemists (John Wiley and Sons, Inc., New York and London, 1961).

34. E. Hückel, Z. Physik, 70, 204 (1931).

35. E. Hückel, Z. Physik, 72, 310 (1931).

36. E. Hückel, Z. Physik, 76, 628 (1932).

37. E. Hückel, Z. Physik, 83, 632 (1933).

38. C.A. Coulson, Proc. Roy. Soc. (London), A 169, 413 (1939).

39. H. Labhart, J. Chem. Phys., 27, 957 (1957).

40. Y. Ooshika, J. Phys. Soc. Japan, 12, 1238 (1957).

41. Y. Ooshika, J. Phys. Soc. Japan, 12, 1246 (1957).

42. H.C. Longuet-Higgins and L. Salem, Proc. Roy. Soc., A251, 172(1959).

43. W.T. Simpson, J. Am. Chem. Soc., 78, 3585 (1956).

44. W.T. Simpson, J. Am. Chem. Soc., 73, 5363 (1951).

45. M. Born and K. Huang, Dynamical Theory of Crystal Lattices (Oxford University Press, London and New York, 1954).

46. M. Tinkham, Group Theory and Quantum Mechanics (McGraw-Hill, New York, 1964).

47. F.M. Garforth, C.K. Ingold and H.G. Poole, J. Chem. Soc., 406(1948).

48. G. Herzberg and E. Teller, Z. Physik Chim., B21, 410 (1933).

49. A.D. Liehr, Z. Naturforsch, 13a, 311 (1958).

50. J.N. Murrell and J.A. Pople, Proc. Phys. Soc. (London), A69, 245 (1956).

51. D.P. Craig, J. Chem. Soc., 59 (1950).

52. A.C. Albrecht, J. Chem. Phys., 33, 156 (1960).

53. W.A. Yeranos, Z. Naturforsch, 22a, 183 (1967).

54. A. Grabowska, J. Mol. Spectrosc., 20, 96 (1966).

55. E.F. McCoy and I.G. Ross, Aust. J. Chem., 15, 573 (1962).

56. J.B. Coon, R.E. de Wames and C.M. Lloyd, J. Mol. Spectrosc., 8, 285 (1962).

57. K. Miller and J.N. Murrell, Theoret. Chim. Acta (Berl.), 2, 281(1965).

58. K. Miller and J.N. Murrell, Theoret. Chim. Acta (Berl.), 7, 69 (1967).

59. R.S. Mulliken, J. Am. Chem. Soc., 72, 600 (1950).

60. R.S. Mulliken, J. Am. Chem. Soc., 74, 811 (1952).

61. R.S. Mulliken, J. Phys. Chem., 56, 801 (1952).

62. R.S. Mulliken, J. Chem. Phys., 51, 341 (1964).

63. R.S. Mulliken, J. Chem. Phys., 23, 397 (1955).

64. R.S. Mulliken, J. Chem. Phys., 21, 20 (1964).

65. S.P. McGlynn, Chem. Rev., 58, 1113 (1958).

66. G. Briegleb, Elektronen-Donator-Acceptor-Komplexe (Springer-Verlag, Berlin, 1961).

67. W.B. Person and R.S. Mulliken, A. Rev. Phys. Chem., 13, 107 (1962).

68. M.A. Slifkin, Charge-Transfer Interactions of Biomolecules (Academic Press, London and New York, 1971) p 4.

69. E.C.M. Chen and W.E. Wentworth, J.Chem.Phys., 63, 3183 (1975).

70. M.J.S. Dewar and A.R. Lepley, J. Am. Chem. Soc., 83, 4560 (1961).

71. M.J.S. Dewar and H. Rogers, J. Am. Chem. Soc., 84, 395 (1962).

72. A.R. Lepley, J.Am. Chem. Soc., 84, 3577 (1962).

73. A.R. Lepley, J. Am. Chem. Soc., 86, 2545 (1964).

74. A.R. Lepley, Tetrahedron Letters, 2823 (1964).

75. A.R. Lepley and C.C. Thomson, Jr., J.Am.Chem. Soc., 89, 5623(1967).

76. J.N. Murrell, J. Am. Chem. Soc., 81, 5037 (1959).

77. F. Fukui, A. Imamura, T. Yonezawa and C. Nagata, Bull. Chem. Soc. Japan, 34, 1076 (1961).

78. F. Fukui, A. Imamura, T. Yonezawa and C. Nagata, Bull. Chem. Soc. Japan, 35, 33 (1962).

79. R.L. Flurry, Jr., J. Phys. Chem., 69, 1927 (1965).

80. S. Iwata, J. Tanaka and S. Nagakura, J. Am. Chem. Soc., 89, 2813 (1967).

81. H. Kuroda, I. Ikemoto and H. Akamatu, Bull. Chem. Soc. Japan, 39, 1842 (1966).

82. H. Kuroda, M. Kobayashi, M. Kinoshita and S. Takemoto, J. Chem. Phys., 36, 457 (1962).

83. L.E. Orgel, J. Chem. Phys., 23, 1852 (1955).

84. A. Mier, Rec. Trav. Chim. Pay-Bas, 75, 866 (1956).

86. R.E. Merrifield and W.D. Phillips, J. Am. Chem. Soc., 80, 2778 (1958).

86. A. Kuboyama, J. Chem. Soc. Japan, Pure Chem. Sect. (Nippon Kagaku Zasshi), 81, 658 (1960).

87. G. Briegleb, J. Czekalla and G. Reuss, Z. Physik. Chim. N.F., 30, 316 (1961).

CHAPTER 2

ON THE EVIDENCE OF A LOW-LYING FORBIDDEN STATE IN SOME POLYENES

2.1 Introduction

In recent years, spectroscopic investigation of the linear conjugated polyenes[1-7] has been a subject of much interest. Many earlier calculations[8-11] based on approximate theories of molecular electronic structure were carried out to know the electronic behaviour of the polyenes. The basic result obtained from spectroscopic experiments is that there is a strongly allowed electronic transition for all polyenes in the near UV or visible region whose intensity increases and energy decreases as the conjugated chain length increases.[12] The experimental results[13-16] show that the energy of this transition appears to approach an asymptotic value. This apparent convergence is not predicted by the simplest versions of free electron or Hückel (LCAO) molecular orbital theory unless the observed alternation of bond length[8,17] is included into the theory. Then the proper limiting behaviour is observed at the expense of an increased number of parameters. All - trans polyenes possess a center of inversion. In simple Hückel and free electron molecular orbital approaches the energy ordered one-electron molecular orbitals have alternately odd and even symmetry with respect to this inversion. Each of the theories predicts the lowest energy electronic transition to be strongly electric dipole allowed; this is the feature maintained by semi-empirical and a priori methods which include single excitation configuration interaction for the excited states. According to semi-empirical and a-priori calculations[18], the excited electronic states of linear conjugated polyenes are ^1A_g, ^1B_u, ^1A_g, ^1A_g, ^1B_u in order of increasing energy. The lowest energy electronic transition

is $^1A_g \rightarrow {}^1B_u$, which is said to be the strongly allowed $\pi \rightarrow \pi^*$ transition.

Investigations[3] on the electronic spectra of linear conjugated polyenes have shown that the maxima of absorption and emission bands in the visible region have little or no overlap. This has led to the speculation that the absorption and emission bands in these molecules are severely Franck-Condon forbidden. For the 0 - 0 band of a very strong absorption having a high extinction coefficient, as is the case with the intense absorption band of polyenes, such forbiddenness is not easy to rationalise. The energy difference between the lowest energy peak of the absorption spectrum and the highest λ^{energy} peak of the emission spectrum is not consistent with the theoretical value obtained by semi-empirical and a priori methods.

Recently Hudson and Kohler[5,19] have presented some experimental evidence that there exists a low-lying forbidden state below the well-defined lowest π -electronic state in α,ω-diphenyloctatetraene (DPO). This experimental evidence has also been supported by theoretical treatment of Schulten and Karplus[4]. They have included double-excitation configurations in semi-empirical and a priori calculations of polyenes to improve the π -electron energy level calculations. The inclusion of double-excitation configurations in addition to the singly excited configurations brings about the change in order of excited electronic states. One of the two excited ^1A_g states of all-trans polyenes is significantly lowered in energy and this ^1A_g state is calculated to be at lower energy than the ^1B_u state responsible for the strongly allowed transition in the polyenes.

Thus they have demonstrated that the inclusion of double-excitation configuration for excited states of polyenes leads to the existence of a low-lying weak π -electronic state which has ^1A_g symmetry in the all-trans form. The transition from the ground state ^1A_g to this low-lying π -electronic excited ^1A_g state is forbidden. The low-lying state is present in other isomers[4] as well. Recently, Mandal and Misra[6] have reported that adsorption of certain gas molecules on the solid films of some polyenes makes this transition allowed. The present investigation was undertaken to extend such experiment to some more polyenes. In addition to this the solvent behaviour on the absorption and emission spectra of these polyenes has also been studied for collecting information about the absorbing and the emitting states.

2.2 Experimental and Results

The polyenes employed in the present investigation are all-trans vitamin A alcohol, all-trans vitamin A acetate, β - apo-8'-carotenal, astacene and methyl bixin. The structure of these chemicals is shown in Fig. 2.1. These compounds of high purity were obtained from Hoffman-La Roche Co., Switzerland. We have used these chemicals without further purification. Organic solvents used in this experiment were either of spectrograde quality of B.D.H. (England) and E. Merck (Germany) or purified by usual procedures. The absorption spectra were recorded by a Perkin-Elmer recording Spectrophotometer-202 and Spectronom-202. The emission spectra were recorded by Aminoco Bowman Spectrofluorometer.

FIG. 2.1 : Structure of some linear conjugated polyenes.

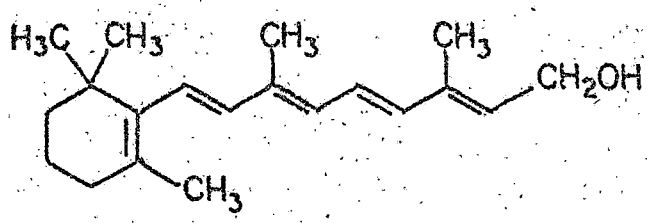

1. Vitamin A alcohol.

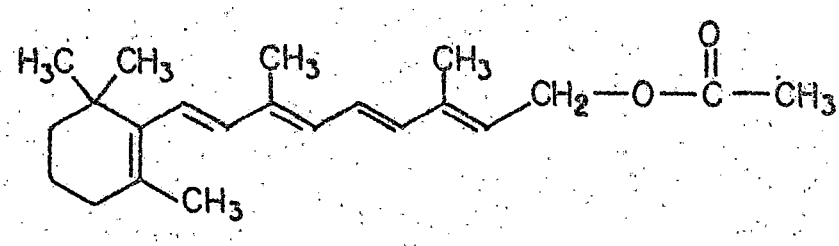

2. Vitamin A acetate.

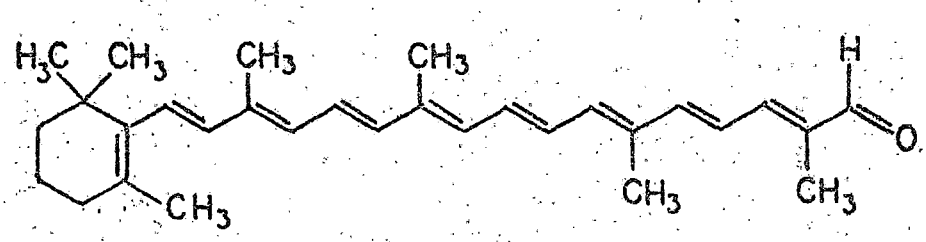

3. β—apo—8′—carotenal.

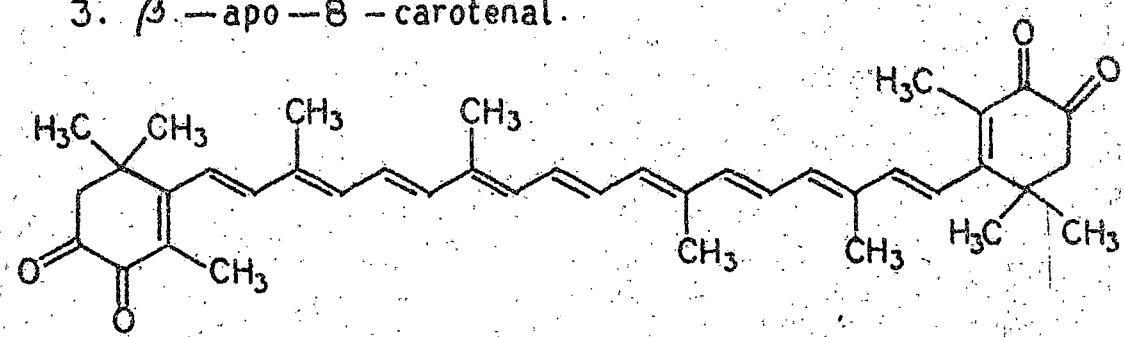

4. Astacene

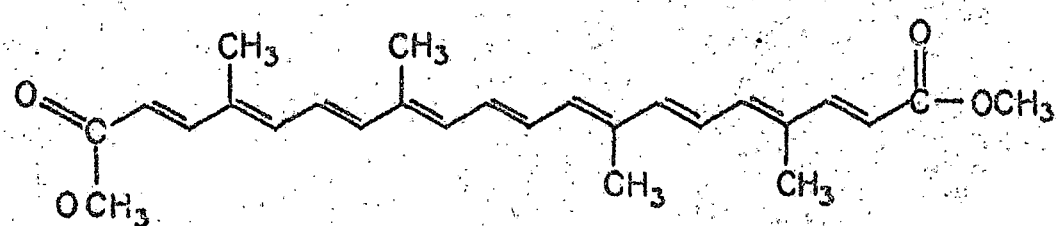

5. Methyl bixin

FIG. 21

Thin films of polycrystals of the polyenes were made on the quartz surface by gently rubbing the material. Solid films thus made were exposed to vapours of some organic solvents like aniline, acetone, benzene, carbontetrachloride, dimethyl aniline, ethanol, methanol, pyridine etc. The exposure was made by holding the films for about 5 minutes over a beaker containing the chemicals at room temperature (28°C) and the absorption spectra were then recorded immediately after the exposure.

The room temperature absorption spectra of the polyenes under investigation are shown in Figs. 2.2 - 2.6. On adsorption of vapours, a new band appears on the longer wavelength side of the spectrum in each case. With all the vapours studied the effect is almost similar except that with certain of these, the effect is more pronounced than with others. Pyridine vapour adsorption on β -apo-8'-carotenal affects absorption spectra intensely whereas aniline vapour shows a strong effect on astacene spectrum. However, no appreciable change in position of the new band is observed with different vapours adsorption. Effect of adsorption of various vapours on the intensity of the weak low energy band system is summarized in tables 2.1 - 2.5 for vitamin A alcohol, acetate, β -apo-8'-carotenal, astacene and methyl bixin respectively.

The absorption spectra of <u>all-trans</u> vitamin A alcohol are shown in Fig. 2.2. When exposed to different vapours, a new week band appears at about 24000 cm^{-1} along with the bands observed before vapour adsorption. The other bands do not show appreciable shift after vapour adsorption. The absorption spectrum of vitamin A alcohol

Table 2.1

Effect of adsorption of various vapours on the intensity of the weak low energy band system of all-trans vitamin A alcohol

Vapour adsorbed	Relative Intensity
Aniline	1
Acetone	1
Benzene	2
Carbontetrachloride	2
Dimethyl aniline	2
Ethanol	1
Methanol	1
Pyridine	1

Table 2.2

Effect of adsorption of various vapours on the intensity of the weak low energy band system of all-trans vitamin A acetate

Vapour adsorbed	Relative Intensity
Aniline	1
Acetone	2
Benzene	2
Carbontetrachloride	1
Dimethyl aniline	1
Ethenol	1
Methanol	1
Pyridine	1

Table 2.3

Effect of adsorption of various vapours on the intensity of the weak low energy band system of β -apo-8'-carotenal.

Vapour adsorbed	Relative Intensity
Aniline	2
Acetone	1
Benzene	1
Carbontetrachloride	2
Dimethyl aniline	1
Ethanol	2
Methanol	2
Pyridine	3

Table 2.4

Effect of adsorption of various vapours on the intensity of the weak low energy band system of octacene.

Vapour adsorbed	Relative Intensity
Aniline	3
Acetone	2
Benzene	1
Carbontetrachloride	2
Dimethyl aniline	1
Ethanol	2
Methanol	2
Pyridine	2

Table 2.5

Effect of adsorption of various vapours on the intensity of the weak low energy band system of methyl bixin

Vapour adsorbed	Relative Intensity
Aniline	1
Acetone	1
Benzene	2
Carbontetrachloride	2
Dimethyl aniline	1
Ethanol	1
Methanol	2
Pyridine	1

FIG. 2.2 : Electronic absorption spectra of <u>all-trans</u> vitamin A alcohol at room temperature (26°C).
1, spectrum in methanol; 2, spectrum for the solid film; 3, spectrum after CCl_4 vapour adsorption.
Qualitative resolution of the total absorption spectrum for the solid film after CCl_4 vapour adsorption : 4, band of the solid film; and 5, new band.

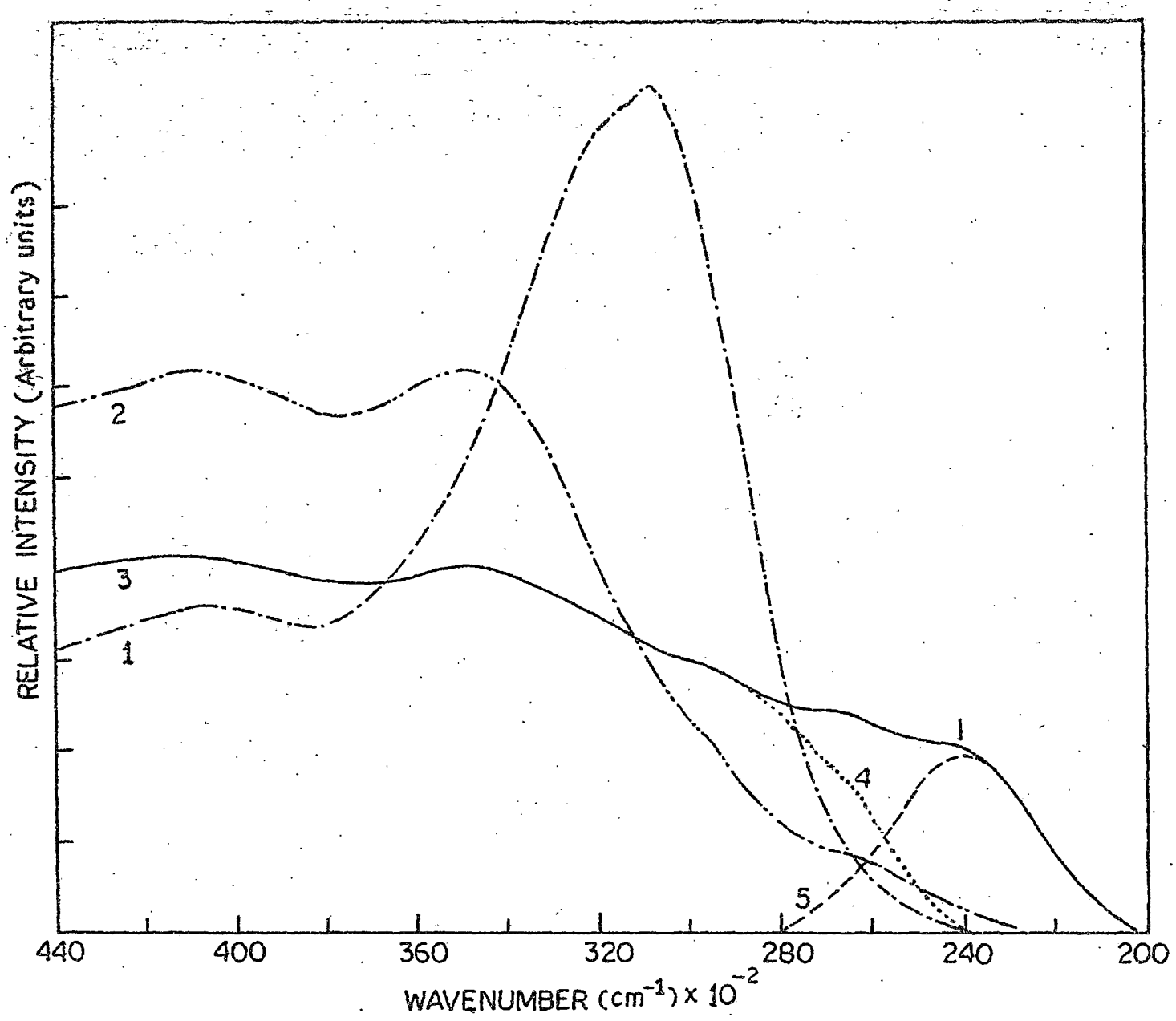
RELATIVE INTENSITY (Arbitrary units)
2
3
1
1
4
5
440
400
360
320
280
240
200
WAVENUMBER (cm^{-1}) x 10^{-2}

FIG. 2·2

in methanol has two strong bands, one at 40600 cm^{-1} and the other at 30864 cm^{-1}. There is a weak hump at about 31900 cm^{-1}. The crystal spectrum shows four main absorption bands at about 41 000, 34900, 29500 and 26666 cm^{-1}. The positions of the absorption bands are given in table 2.6.

In Fig. 2.3, the absorption spectra of <u>all-trans</u> vitamin A acetate in the solid state and in solution are shown. Both in solution and in the solid state, the spectrum of vitamin A acetate is broad. The position of the $\bar{\nu}_{max}$ of the band in solution and in solid state is at about 30534 and 29400 cm^{-1} respectively. After adsorption of acetone vapour, a new band appears at about 26000 cm^{-1} and the original band of vitamin A acetate shifts slightly towards the blue. The position of the bands are summarized in table 2.7.

The absorption spectrum of β-apo-8'-carotenal in n-hexane as shown in Fig. 2.4 appears with bands at 22790, 21790 and 20790 cm^{-1} seperated by about 1000 cm^{-1}. The spectrum in the solid state (Fig. 2.4) loses its vibrational structure. The band is broad and shifts little towards longer wavelength. On being exposed to different vapours a new band appears at 18200 cm^{-1}. The band in the solid state on vapour adsorption is little redshifted. The results are summarized in table 2.8

The absorption spectra of astacene in different states are shown in Fig. 2.5. The spectrum in CCl_4 is broad and structureless with $\bar{\nu}_{max}$ at 20242 cm^{-1}. In the solid state the band is further broadened with $\bar{\nu}_{max}$ at about 19650 cm^{-1}. After exposure to

Table - 2.6

Absorption bands of all-trans vitamin A alcohol

Solution spectrum in methanol at 25°C		Solid state film at 25°C before vapour adsorption		Solid state film at 25°C after adsorption of CCl_4 vapour	
Wavenumber (cm^{-1})	Assignment	Wavenumber (cm^{-1})	Assignment	Wavenumber (cm^{-1})	Assignment
				24000 (w)	Newband system ($^1A_g \longrightarrow {}^1A_g$)
30864 (vs)	0(A)	26666(v)	Factor group split component of A	26666(v)	Factor group split component of A
31000(w)	0+1036	29500(vw)	Factor group split component of A	29500(vw)	Factor group split component of A
		34900(vs)	Factor group split component of A	34800(ms)	Factor group split component of A
40600(ms)	0(B)	41000(ms)	Band maxima	41000(ms)	Band maxima

v — very ; s — strong; m — medium; w — weak.

FIG. 2.3 : Electronic absorption spectra of all-trans vitamin A acetate at room temperature (25°C).
1, spectrum in ethyl acetate; 2, spectrum for the solid film; 3, spectrum after acetone vapour adsorption. Qualitative resolution of the total absorption spectrum for the solid film after acetone vapour adsorption : 4, band of the solid film; and 5, new band.

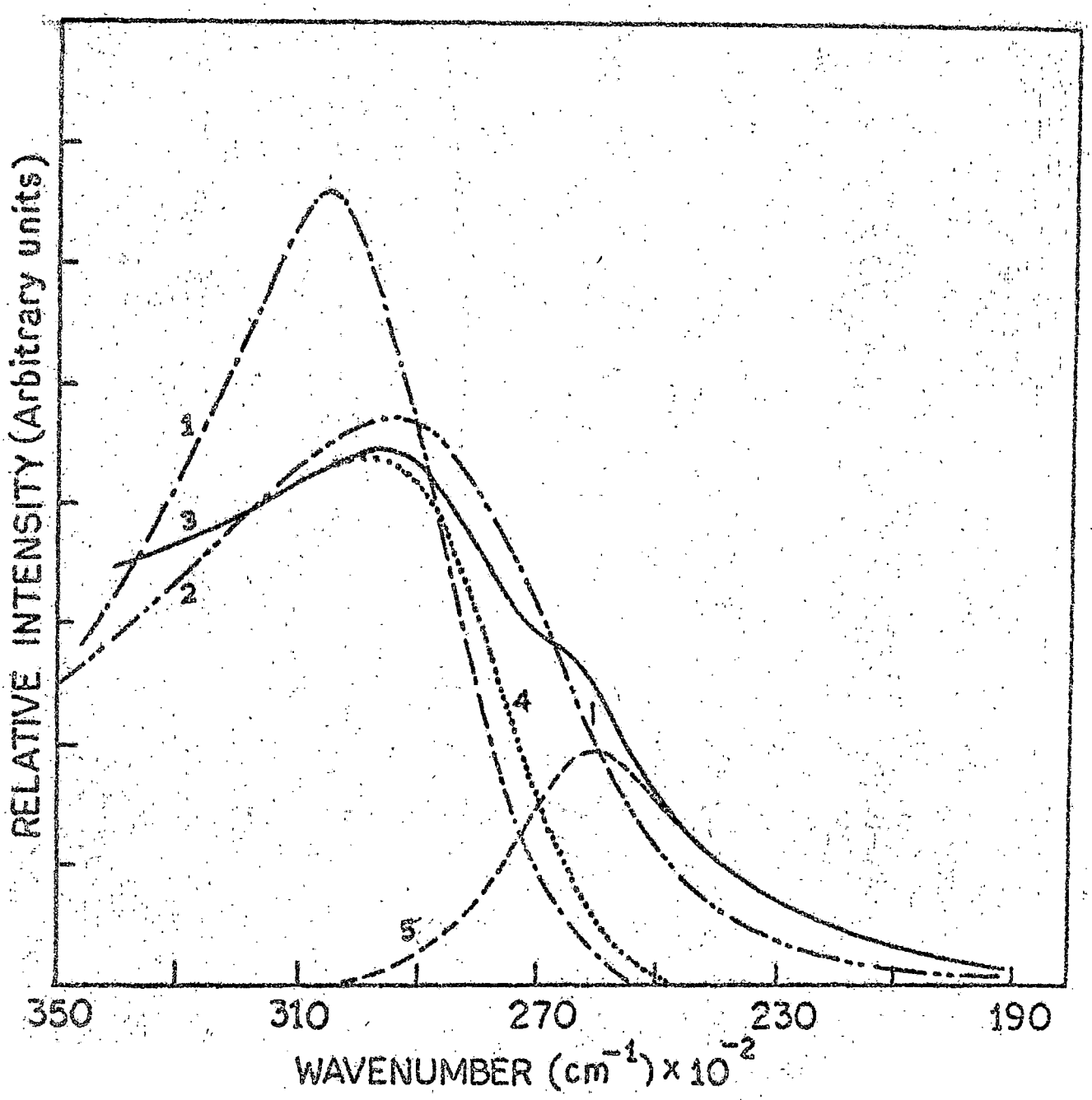
RELATIVE INTENSITY (Arbitrary units)
1
2
3
4
5
350
310
270
230
190
WAVENUMBER (cm^{-1}) x 10^{-2}

FIG. 2-3

Table - 2.7

Absorption bands of all-trans vitamin A acetate

Solution spectrum in ethyl acetate solution at 25°C		Solid state film at 25°C before vapour adsorption		Solid state film at 25°C after adsorption of acetone vapour	
Wavenumber (cm^{-1})	Assignment	Wavenumber (cm^{-1})	Assignment	Wavenumber (cm^{-1})	Assignment
				26000(v)	New band system ($1_{A_g} \longrightarrow 1_{A_g}$)
Broad structure-less band with $\tilde{\nu}_{max}$ at 30534(vs)	Band maxima	Broad structure-less band with $\tilde{\nu}_{max}$ at 29400(vs)	Band maxima	Broad structure-less band with $\tilde{\nu}_{max}$ at 29500(vs)	Band maxima

v - very
s - strong
w - weak

FIG. 2.4 : Electronic absorption spectra of β-apo-8'-carotenal at room temperature (25°C).
1, spectrum in n-hexane; 2, spectrum for the solid film; 3, spectrum after pyridine vapour adsorption. Qualitative resolution of the total absorption spectrum for the solid film after pyridine vapour adsorption : 4, band of the solid film; and 5, new band.

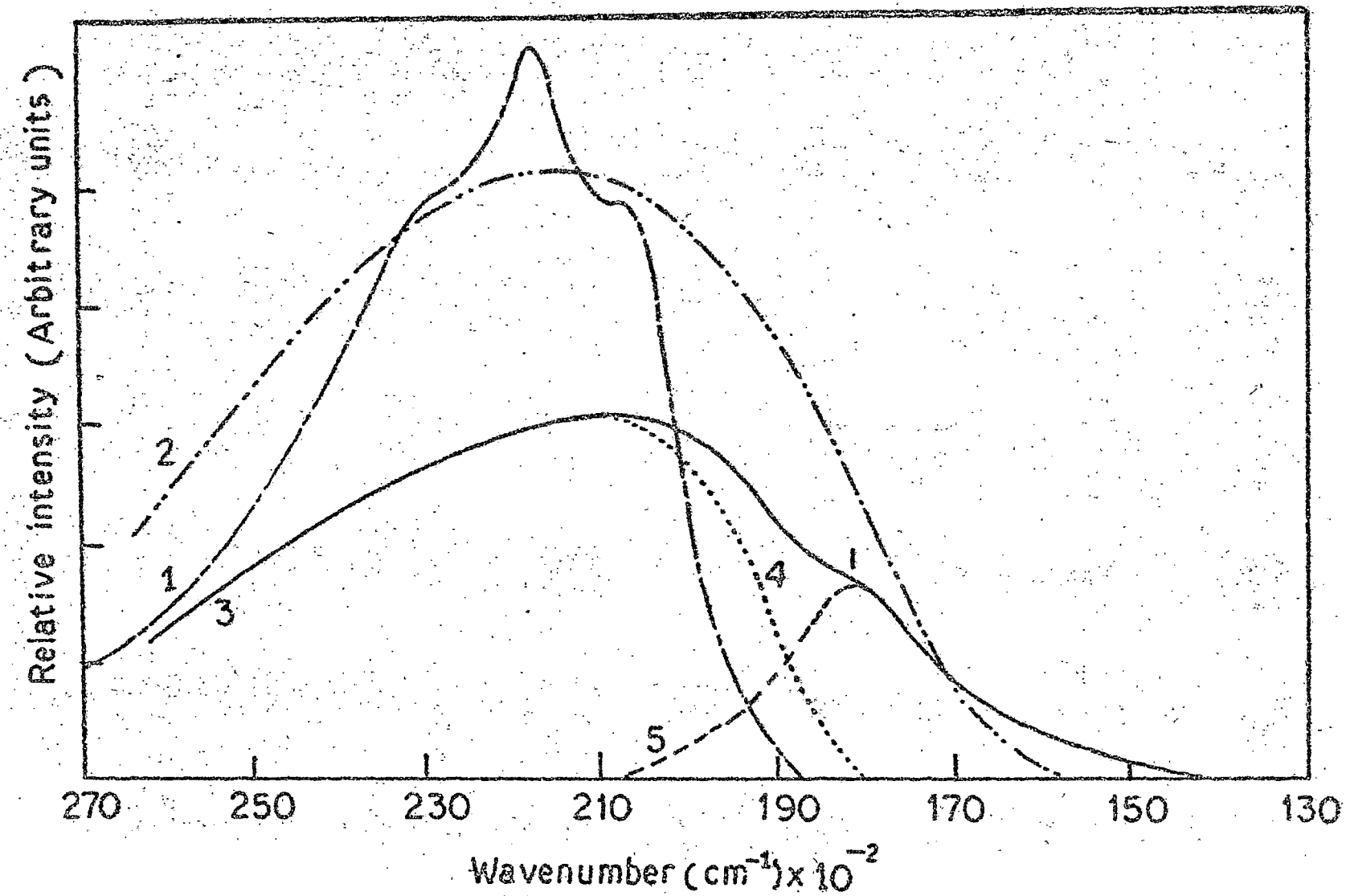
Relative intensity (Arbitrary units)
1
2
3
4
5
270
250
230
210
190
170
150
130
Wavenumber (cm^{-1}) x 10^{-2}

FIG. 2.4

Table-2.8

Absorption bands of β -apo-2'-carotenal visible band system

Solution spectrum in n-Hexane at 25°C		Solid state film at 25°C before vapour adsorption		Solid state film at 25°C after adsorption of pyridine vapour	
Wavenumber (cm^{-1})	Assignment	Wavenumber (cm^{-1})	Assignment	Wavenumber (cm^{-1})	Assignment
				18200(ms)	New band system ($1A_g \rightarrow 1A_g$)
20790(s)	0	Broad structureless band with $\bar{\nu}_{max}$ at 21650(sb)	Band maxima	Broad structureless band with $\bar{\nu}_{max}$ at 21050(sb)	Band maxima
21790(vs)	0+1000				
22790(ms)	0+2x1000				

s - strong
v - very
m - medium
b - broad

FIG. 2.6 : Electronic absorption spectra of asteeene at room temperature (25°C).
1, spectrum in CCl_4; 2, spectrum for the solid film; 3, spectrum for the solid film after aniline vapour adsorption. Qualitative resolution of the total absorption spectrum after aniline vapour adsorption : 4, band of the solid film; and 5, new band.

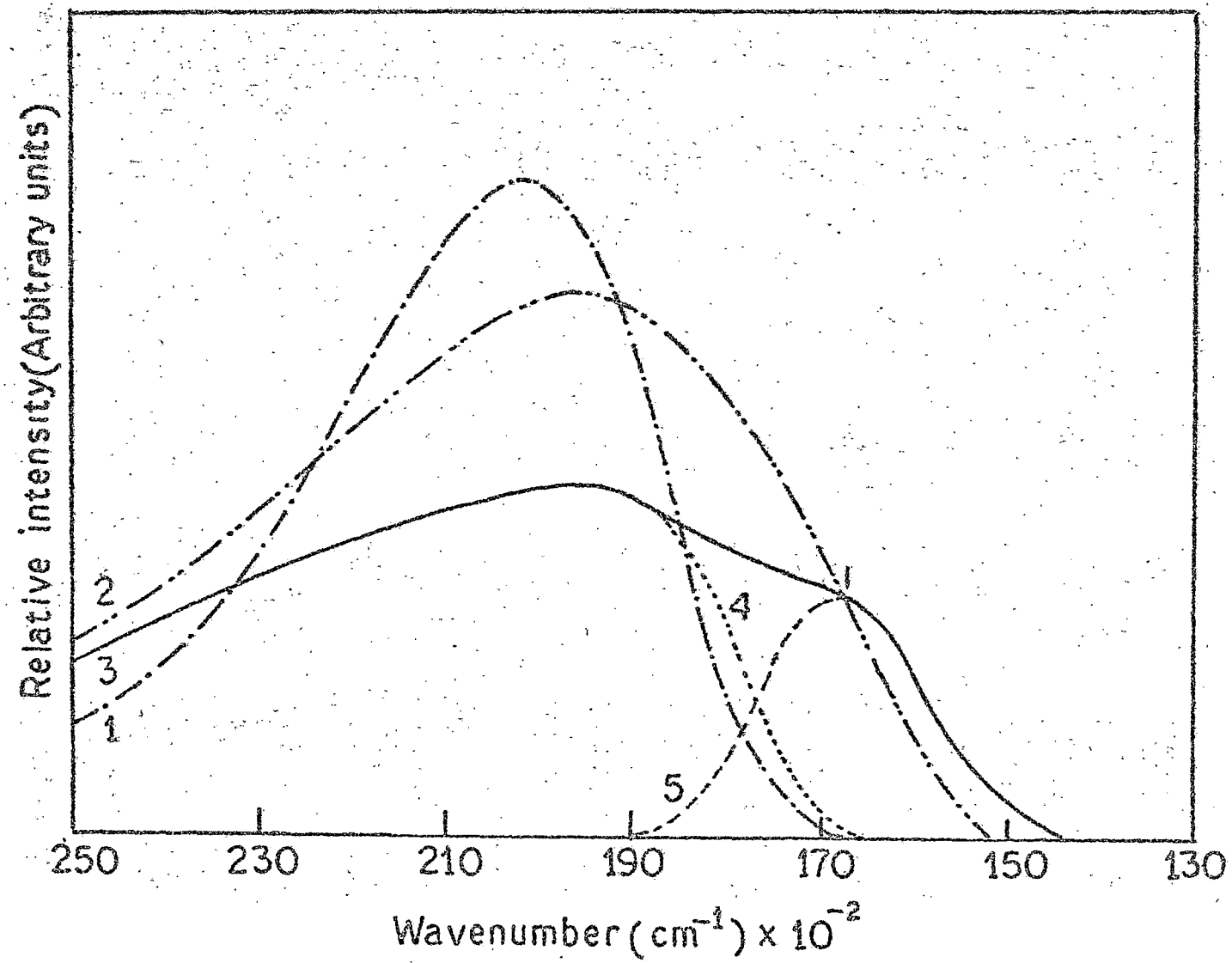
Relative intensity(Arbitrary units)
2
3
1
4
5
250
230
210
190
170
150
130
Wavenumber (cm^{-1}) x 10^{-2}

FIG. 2·5

various vapours the solid state spectrum appears with a new band at about 16660 cm^{-1} with a small change in position of the band in the crystalline state as shown in table 2.9.

The absorption spectrum of methyl bixin in acetone consists of three bands at 20660, 21660 and 23160 cm^{-1} (Fig. 2.6). In the solid state film as shown in Fig. 2.6, the spectrum is broad and redshifted. When various vapours are adsorbed on the surfaces of the crystallites in the films, a marked change in the solid film spectrum is observed. On being exposed in methanol vapour as shown in Fig. 2.6 a new band appears at about 17500 cm^{-1} in addition to the original bands of methyl bixin in the solid state. The results are summarized in table 2.10.

Table-2.9

Absorption bands of extreme visible band system

Solution spectrum in CCl_4 at 25°C		Solid state film at 25°C before vapour adsorption		Solid state film at 25°C after adsorption of aniline vapour	
Wavenumber (cm^{-1})	Assignment	Wavenumber (cm^{-1})	Assignment	Wavenumber (cm^{-1})	Assignment
				16660(ms)	New band system ($^1A_g \rightarrow {}^1A_g$)
Broad structure-less band with $\bar{\nu}_{max}$ at 20242(s)	Band maxima	Broad structure-less band with $\bar{\nu}_{max}$ at 19660(s)	Band maxima	Broad structure-less band with $\bar{\nu}_{max}$ at 19450(sb)	Band maxima

s - strong
m - medium
b - broad

FIG. 2.6 : Electronic absorption spectra of methyl bixin at room temperature (25°C).
1, spectrum in acetone; 2, spectrum for the solid film; 3, spectrum for the solid film after methanol vapour adsorption. Qualitative resolution of the total absorption spectrum after methanol vapour adsorption : 4, band of the solid film; and 5, new band.

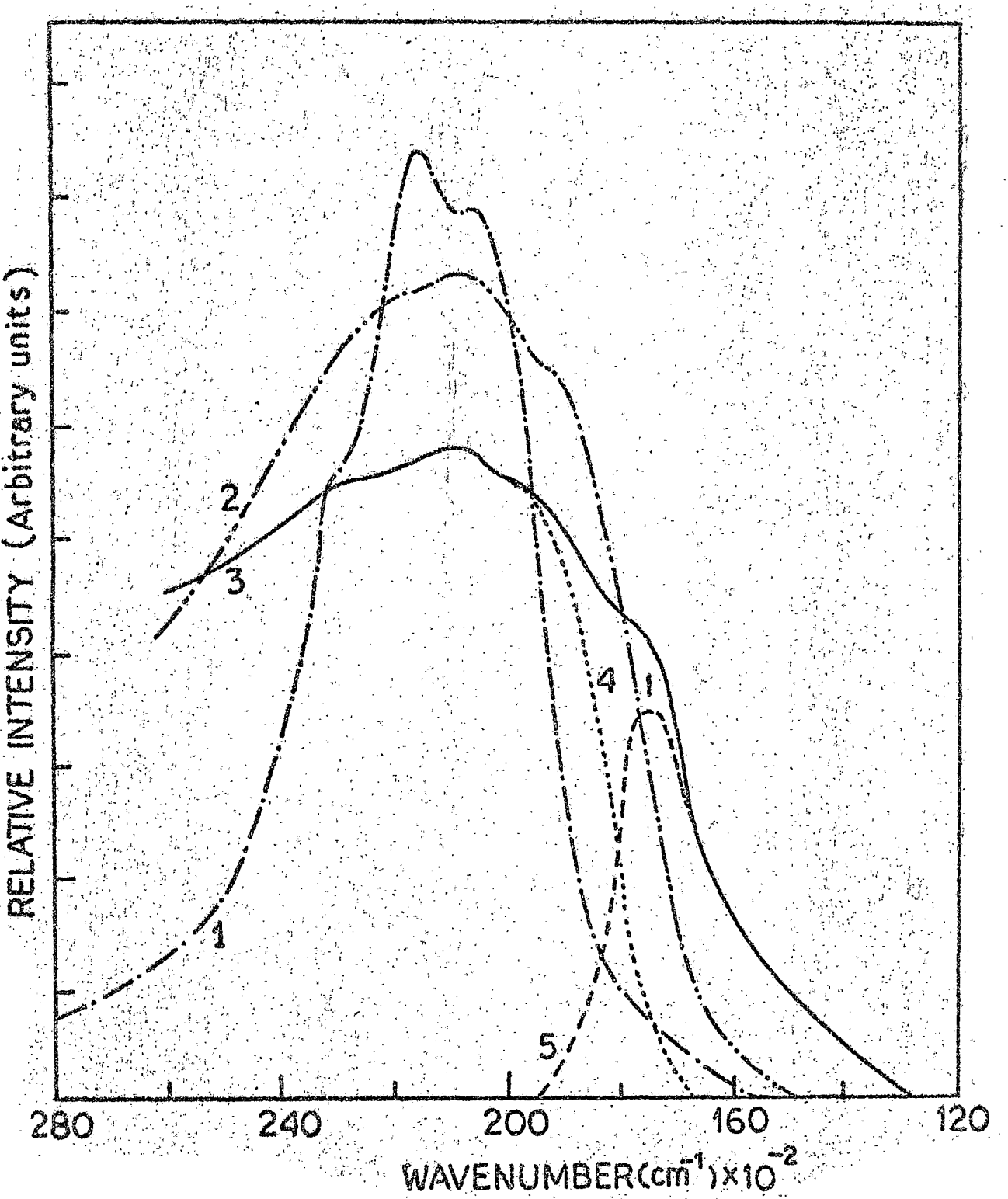
RELATIVE INTENSITY (Arbitrary units)
280
240
200
160
120
WAVENUMBER(cm⁻¹)×10⁻²
1
2
3
4
5

FIG. 2.6

Table - 2.10

Absorption bands of methyl bixin visible band system

Solution spectrum in acetone at 25°C		Solid state film at 25°C before vapour adsorption		Solid state film at 25°C after adsorption of methanol vapour	
Wavenumber (cm^{-1})	Assignment	Wavenumber (cm^{-1})	Assignment	Wavenumber (cm^{-1})	Assignment
				17500(w)	New band system ($^1A_g \rightarrow {}^1A_g$)
20550(ms)	0	19500(wb)	0	19700(wb)	0
21550(vs)	0 + 1000	20800(sb)	0 + 1300	21000(ms)	0 + 1300
23150(w)	0 + 2 x 1000	22100(vw)	0 + 2x1300	23000(w)	0 + 2x1300

m - medium
s - strong
v - very
w - weak
b - broad

2.3 Discussion

2.3.1 Low-lying Forbidden Electronic Transition

Our experimental results show that in all the polyenes studied a new band appears when certain vapours are adsorbed on the surface of the polyene crystals. The intensity of this new band depends on the polyenes used and also on the vapour adsorbed. But the position of this new band in a particular polyene remains almost unchanged with different vapours adsorption. This excludes this band to be a charge-transfer absorption band. There is a large overlap between the well-studied long wavelength band system and the new band. So it is difficult to locate exactly the position of this new band. In order to get the longer wavelength band contour out of the total spectrum we have resolved qualitatively the whole spectrum into two parts. One part corresponds to the spectral shape of the new band and the other part corresponds to the solid film spectrum before vapour adsorption. Reasonably good resolved spectra are achieved in most of the polyenes. In vitamin A alcohol, to resolve the total absorption spectrum in two components becomes complicated as the intensity of the factor group split components are affected by vapour adsorption.

Of the polyenes studied, vitamin A is known to fluoresce strongly. In ethylacetate solution, the absorption and the emission spectra of vitamin A (alcohol and acetate) are shown in Fig. 2.7. Here, practically no overlap between the absorption and the emission spectra is observed which indicates that possibly the absorbing and the emitting states are different.

FIG. 2.7 : Electronic absorption and emission spectra of vitamin A in ethyl acetate at room temperature (25°C).
Vitamin A alcohol : 1, absorption; 2, emission.
Vitamin A acetate : 3, absorption; 4, emission.

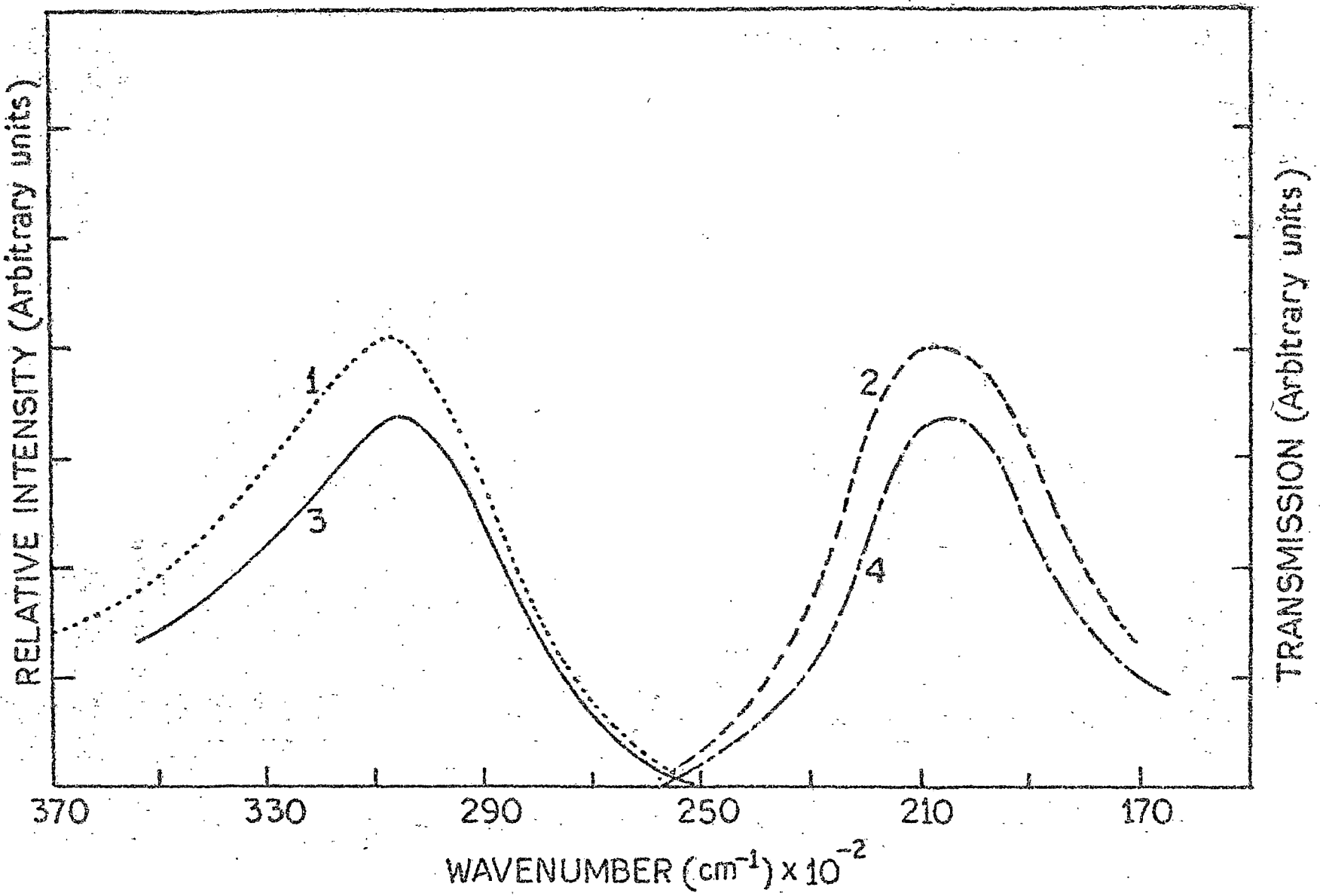
RELATIVE INTENSITY (Arbitrary units)
TRANSMISSION (Arbitrary units)
1
2
3
4
370
330
290
250
210
170
WAVENUMBER (cm^{-1}) x 10^{-2}

FIG. 2·7

The crystal emission spectra of the polyenes studied except vitamin A acetate[3] are not available. However, we have recorded the crystal emission spectra of vitamin A alcohol and have compared the emission band of vitamin A (alcohol and acetate) with the new band in the solid film (Figs. 2.8 and 2.9). The heights of the absorption and emission maxima are normalized. It is evident from the Figs. 2.8 and 2.9 that there is a good overlap between the emission and the new absorption band in vitamin A alcohol and acetate. The mirror image relationship is also satisfied. We have plotted transmission against the wavenumber (cm^{-1}) instead of ϵ_ν/ν against ν for the emission spectra as suggested by Birks and Dyson[20]. Unfortunately, the emission from the crystalline films of β-apo-8'-carotenal, astacene and methyl bixin could not be recorded. In these polyenes, the emission in solution is slightly on the high energy side of the new band in the crystal films. In view of the fact that free molecular electronic energy states are generally lowered in the state of aggregation, the emission of these polyene crystal films is expected to be on the lower energy side of that in solution. One can then reasonably expect to get good overlap between the new absorption band and the emission band of these polyenes in the crystalline state. Thus, our experimental results[21] suggest that the excited electronic state involved in the new absorption band and the reported emission band of the polyenes studied is the same and may be the low-lying weak π-electronic state suggested by Schulten and Karplus[4]. The transition from the ground state to this low-lying π-electronic state is forbidden since this state in <u>all-trans</u> polyenes has ^1A_g symmetry[4]. Our vapour adsorption method thus opens a new avenue in

FIG. 2.8 : Electronic absorption and emission spectra of all-trans vitamin A alcohol.
1, total spectrum after CCl_4 vapour adsorption;
2, resolved part for solid film; 3, new band; and
4, emission spectrum in the solid state.

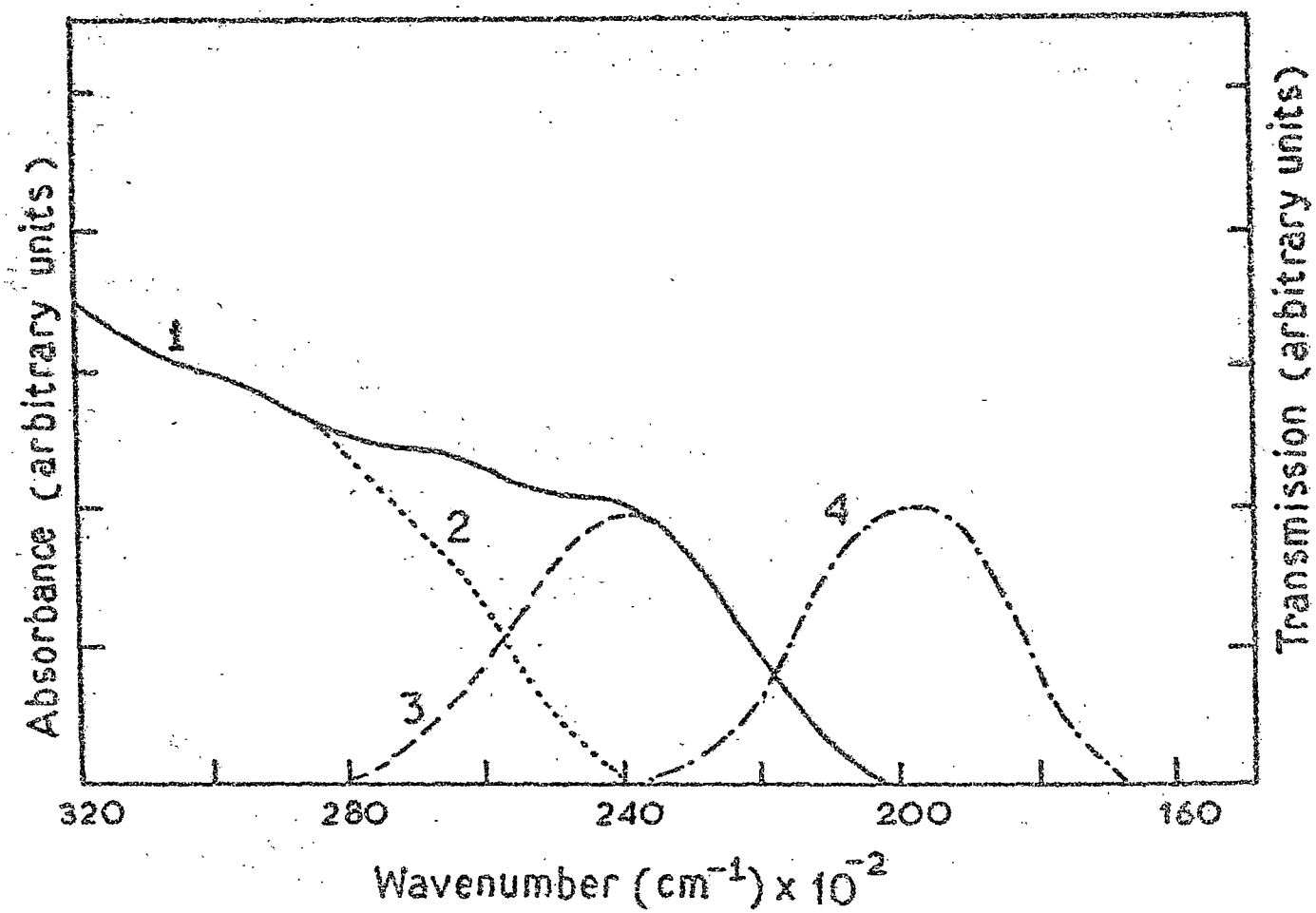
Absorbance (arbitrary units)
Transmission (arbitrary units)
1
2
3
4
320
280
240
200
160
Wavenumber (cm^{-1}) x 10^{-2}

FIG. 2·8

FIG. 2.9 : Electronic absorption and emission spectra of all-trans vitamin A acetate.
1, total spectrum after acetone vapour adsorption; 2, resolved part for the solid film; 3, new band; and 4, emission spectrum in the solid state.

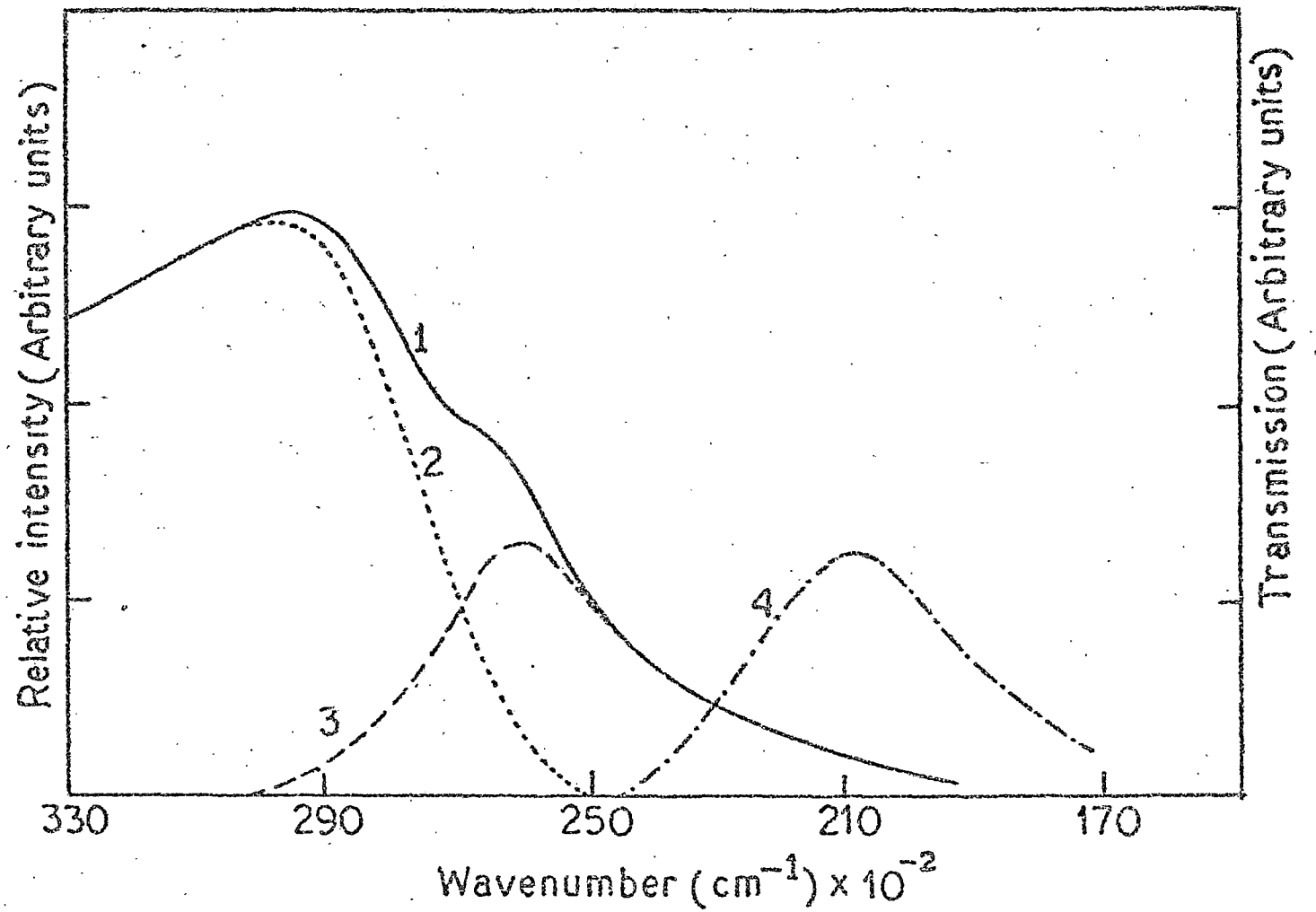
Relative intensity (Arbitrary units)
Transmission (Arbitrary units)
1
2
3
4
330
290
250
210
170
Wavenumber (cm^{-1}) x 10^{-2}

FIG. 2.9

making this low-lying forbidden transition allowed at room temperature.

The adsorbed vapour molecules introduce the perturbation required for the enhancement of a low-lying forbidden transition. The exact nature of the perturbation is not yet resolved.

2.3.2 Solvent Behaviour

The study of the solvent shift of the absorption and the emission bands helps in understanding the nature of the corresponding states. The major contribution to the solvent shift of the strong transition has the form[22]

$$hc(\bar{\nu}-\bar{\nu}_{gas}) = -\frac{2}{a^3}\cdot\frac{n^2-1}{n^2+2}\cdot\frac{E}{E'+E}\left[|P_{eg}|^2 - E(\alpha_g-\alpha_e)\right] \qquad (2.1)$$

where $hc\bar{\nu}$ is the transition energy, a is a characteristic molecular size parameter, n is the solvent refractive index, E is an average excitation energy of the solvent, E' is an average excitation energy for the solute, P_{eg} is the transition dipole for the transition from the state g to e and α's are the ground and excited state polarisabilities. Equation (2.1) can be written as

$$\Delta\bar{\nu} = K\cdot f\cdot\frac{n^2-1}{n^2+2} \qquad (2.2)$$

where K is a parameter which is constant for a given molecule, f is the oscillator strength for a particular transition. Solvents

of different refractive indices were chosen to study the solvent effect on the absorption and emission bands of the polyenes. The effect of different solvents on the absorption and emission bands of the polyenes under investigation are presented in tables 2.11 - 2.15. From the tables it is seen that the absorption bands of the polyenes show a large red-shift with the increase of the refractive index of the solvents. But in case of emission, this shift is very small compared to that for absorption. Our experimental results[21,23] show that in all the polyenes studied, the plot of $\bar{\nu}_{max}$ for both absorption and emission against $(n^2-1)/(n^2+2)$ is a straight line. The plots of $\bar{\nu}_{max}$ (the frequency of the first intense absorption band usually observed in solution and the highest energy emission band) vs. $(n^2-1)/(n^2+2)$ are shown in Figs. 2.10 - 2.14 for vitamin A alcohol, vitamin A acetate, β -apo-8'-carotenal, astacene and methyl bixin respectively. The slope for the first absorption band of all the polyenes is about six to eight times greater than that for the emission band. This estimate of the relative strengths of the absorption and emission oscillator strengths indicates that the absorption and the emission under discussion involve two different excited states of the molecules. The fluorescence originates from a state other than that involved in the intense absorption band observed in solution. Thus it seems that there is a weakly absorbing singlet state with an energy lower than the strongly allowed excited state ^1B_u reached by absorption. The forbidden electronic state which has been allowed by our vapour adsorption method is the low-lying singlet excited state.

Table - 2.11

Solvent effect on the absorption and emission bands of vitamin A alcohol at room temperature ($25^{0}C$)

Solvent	$\frac{n^2-1}{n^2+2}$	$\bar{\nu}_{max}(cm^{-1})$ for emission	$\bar{\nu}_{max}(cm^{-1})$ for absorption
Methanol	0.203	21008	30864
Ethanol	0.221	20964	30769
Ethyl acetate	0.227	20942	30722
1,4-Dioxane	0.254	20942	30534
Carbon tetrachloride	0.275	20964	30303
Benzene	0.294	20920	30303

FIG. 2.10 : Plots of $\bar{\nu}_{max}$ against $(n^2-1)/(n^2+2)$ for the lowest energy absorption band and the highest energy emission band of <u>all-trans</u> vitamin A alcohol.

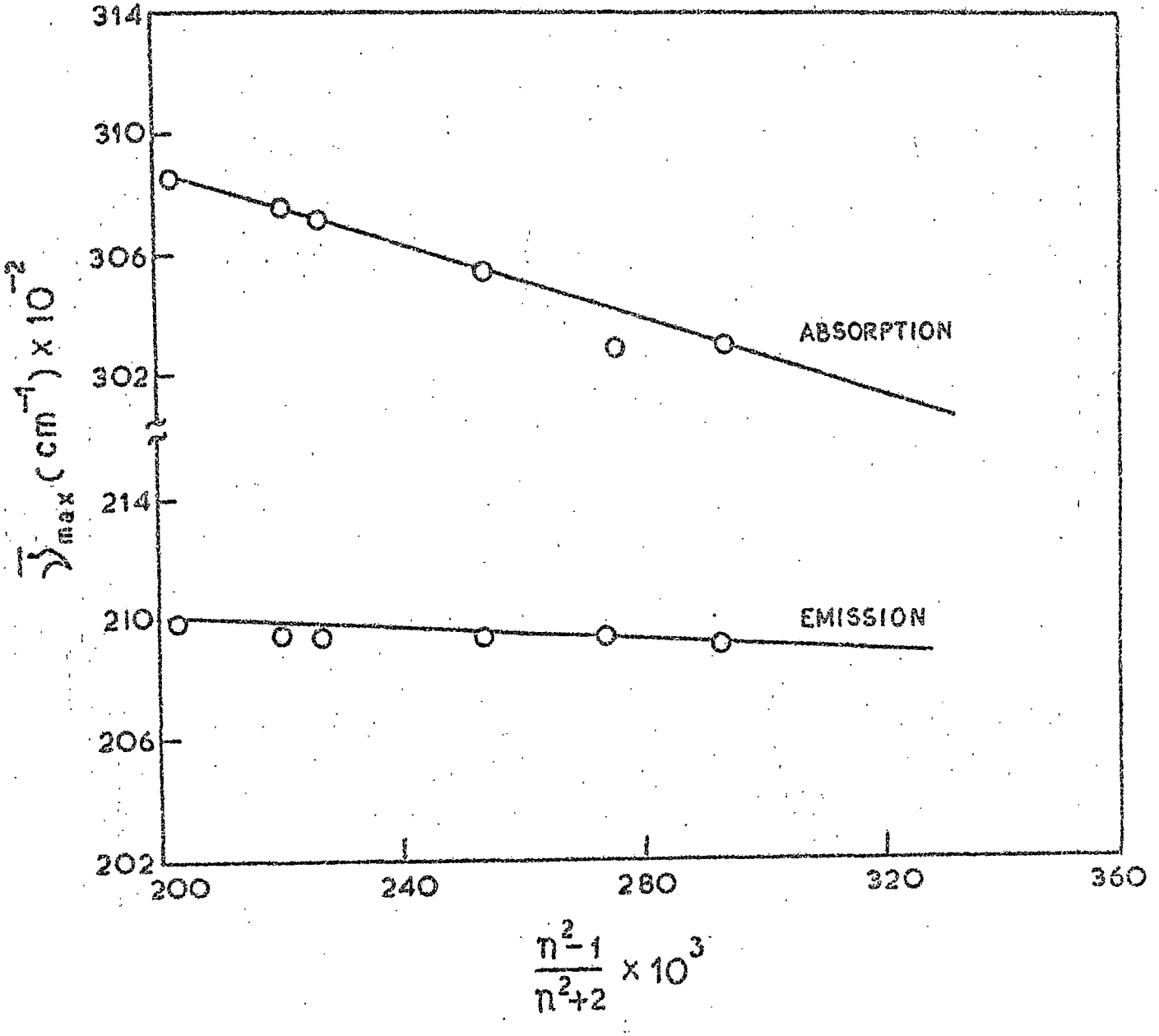
314
310
306
302
214
210
206
202
200
240
280
320
360
ABSORPTION
EMISSION
$\tilde{\nu}_{max}$ (cm^{-1}) x 10^{-2}
$\frac{n^2-1}{n^2+2} \times 10^3$

FIG. 2·10

Table - 2.12

Solvent effect on the absorption and emission bands of vitamin A acetate at room temperature (25°C)

Solvent	$\frac{n^2-1}{n^2+2}$	$\bar{\nu}_{max}(cm^{-1})$ for emission	$\bar{\nu}_{max}(cm^{-1})$ for absorption
Methanol	0.203	20833	30614
Ethanol	0.221	20833	30581
Ethyl acetate	0.227	20730	30534
1,4-Dioxane	0.254	20790	30487
Carbon tetrachloride	0.275	20876	30030
Benzene	0.294	20790	30030

FIG. 2.11 : Plots of $\bar{\nu}_{max}$ against $(n^2-1)/(n^2+2)$ for the lowest energy absorption band and the highest energy emission band of <u>all-trans</u> vitamin A acetate.

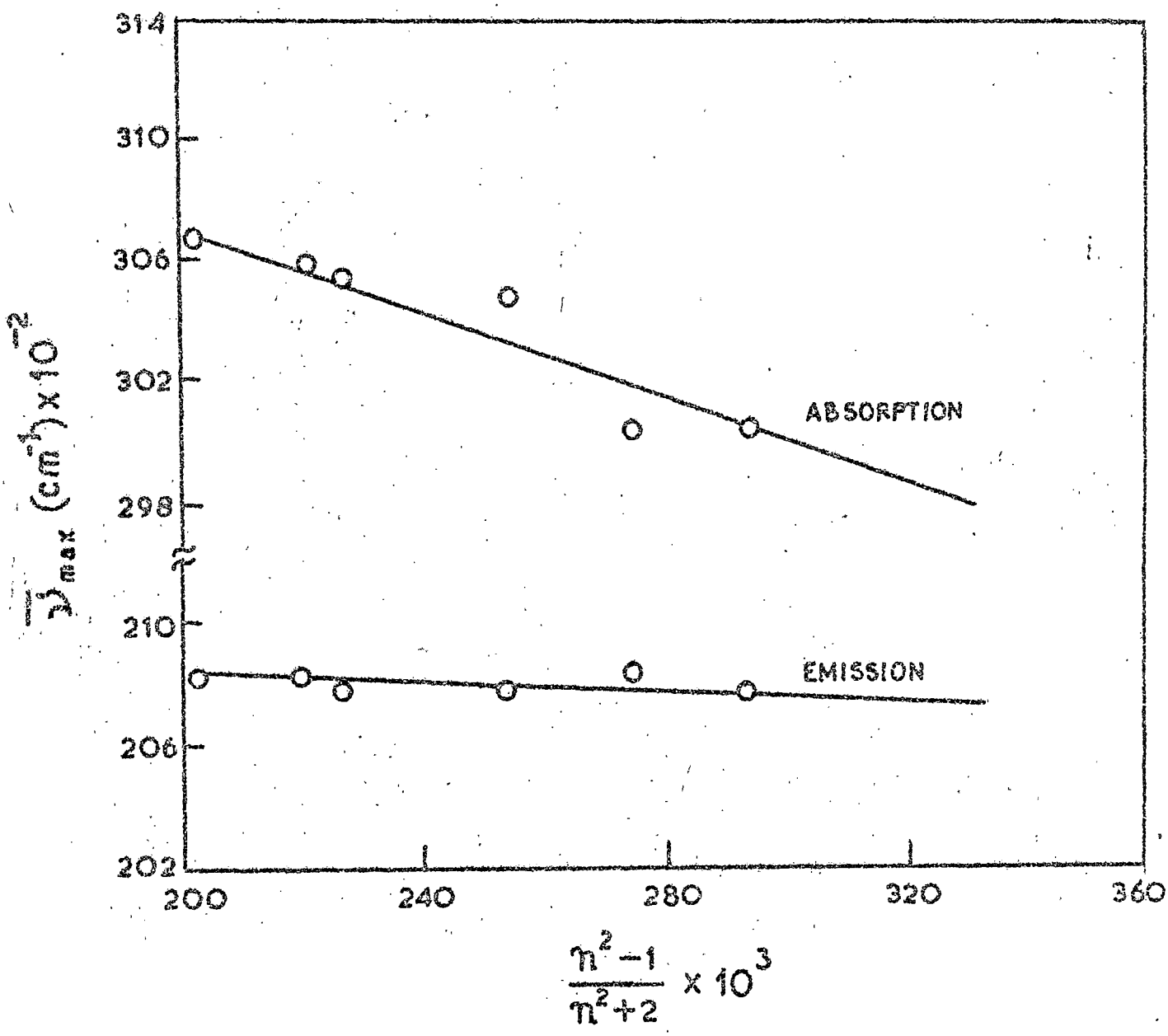
314
310
306
302
298
210
206
202
200
240
280
320
360
ABSORPTION
EMISSION
$\bar{\nu}_{max}$ (cm^{-1}) x 10^{-2}
$\frac{n^2-1}{n^2+2} \times 10^3$

FIG. 2·11

Table - 2.13

Solvent effect on the absorption and emission bands of β -apo-8'-carotenal at room temperature (25°C)

Solvent	$\frac{n^2-1}{n^2+2}$	$\bar{\nu}_{max}(cm^{-1})$ for emission	$\bar{\nu}_{max}(cm^{-1})$ for absorption
Acetone	0.219	19157	21880
Ethyl acetate	0.227	19157	21739
n-Hexane	0.228	19011	21790
1,4-Dioxane	0.254	19083	21459
Cyclohexane	0.257	19120	21600
Carbon tetrachloride	0.275	19047	21270
Benzene	0.294	19083	21229

FIG. 2.12 : Plots of $\overline{\nu}_{max}$ against $(n^2-1)/(n^2+2)$ for the lowest energy absorption band and the highest energy emission band of β-apo-8'-carotenal.

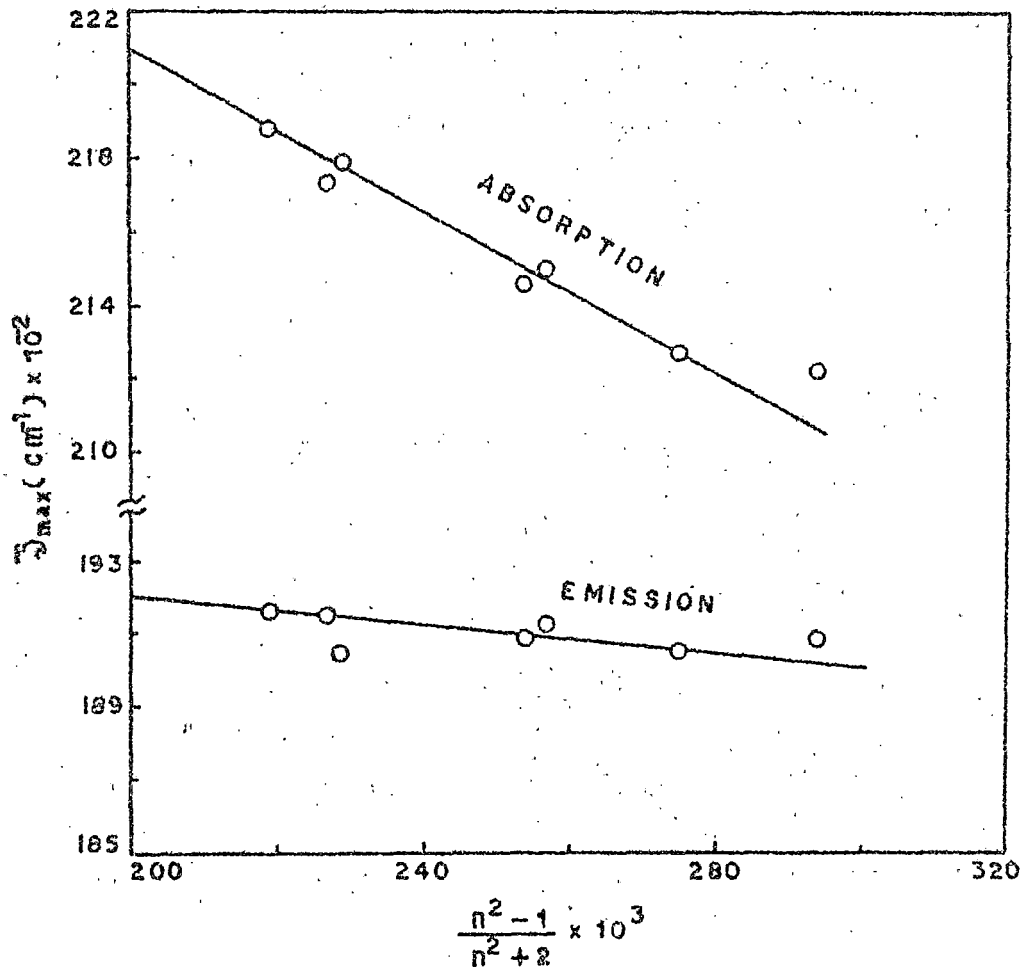
222
218
214
210
193
189
185
200
240
280
320
ABSORPTION
EMISSION
$\bar{\nu}_{max}(cm^{-1}) \times 10^{-2}$
$\frac{n^2-1}{n^2+2} \times 10^3$

FIG. 2.12

Table - 2.14

Solvent effect on the absorption and emission bands of astacene at room temperature ($25^{0}C$)

Solvent	$\frac{n^2-1}{n^2+2}$	$\bar{\nu}_{max}(cm^{-1})$ for emission	$\bar{\nu}_{max}(cm^{-1})$ for absorption
Acetone	0.219	18018	20746
Ethyl acetate	0.227	17857	20661
1,4-Dioxane	0.254	17921	20408
Carbon tetrachloride	0.275	17889	20242
Benzene	0.284	17889	20202

FIG. 2.13 : Plots of $\bar{\nu}_{max}$ against $(n^2-1)/(n^2+2)$ for the lowest energy absorption band and the highest energy emission band of estacene.

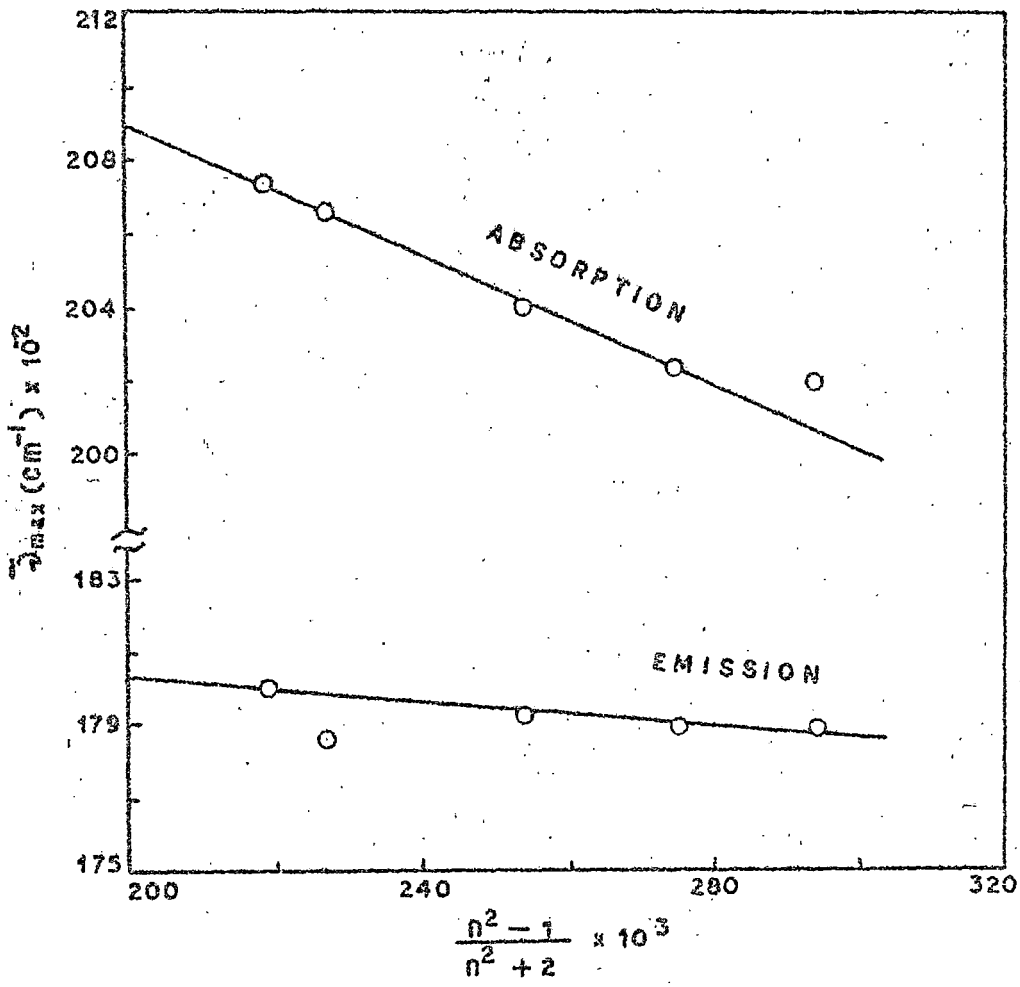
212
208
204
200
183
179
175
200
240
280
320
ABSORPTION
EMISSION
$\bar{\nu}_{max}$ (cm^{-1}) x 10^{-2}
$\frac{n^2-1}{n^2+2}$ x 10^3

FIG. 2.13

Table - 2.15

Solvent effect on the absorption and emission bands of methyl bixin at room temperature (26°C)

Solvent	$\frac{n^2-1}{n^2+2}$	$\bar{\nu}_{max}(cm^{-1})$ for emission	$\bar{\nu}_{max}(cm^{-1})$ for absorption
Acetone	0.219	18796	21645
Ethanol	0.221	18761	21598
Ethyl acetate	0.227	18726	21505
1,4-Dioxane	0.254	18691	21220
Cyclohexane	0.257	18796	21186
Carbon tetrachloride	0.275	18726	20920
Benzene	0.294	18691	20920

FIG. 2.14 : Plots of $\bar{\nu}_{max}$ against $(n^2-1)/(n^2+2)$ for the lowest energy absorption band and the highest energy emission band of methyl bixin.

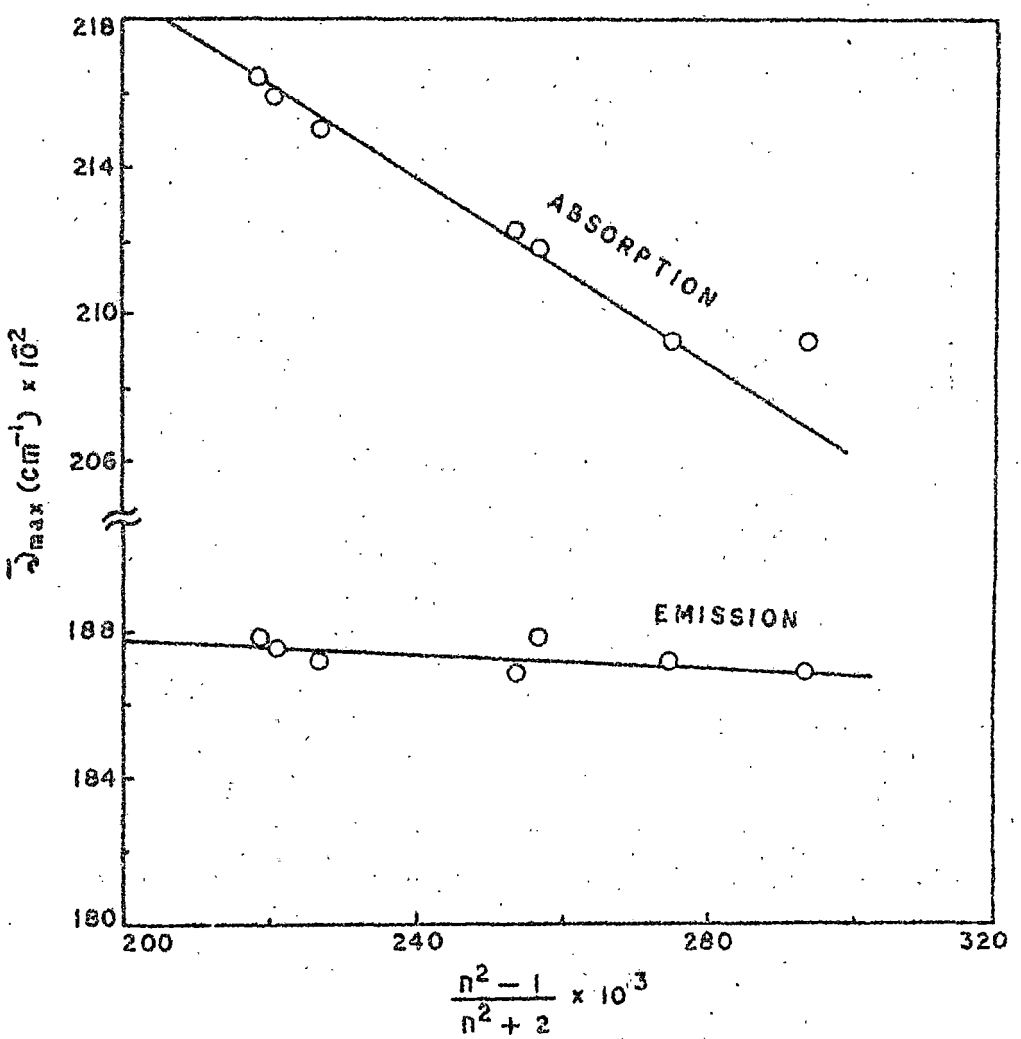
218
214
210
206
188
184
180
200
240
280
320
ABSORPTION
EMISSION
$\tilde{\nu}_{max}$ (cm^{-1}) x 10^2
$\frac{n^2-1}{n^2+2}$ x 10^3

FIG. 2·14

This lowest excited electronic state in polyenes is ^1A_g state which is symmetry forbidden. The life-time of this state is long because of its forbidden nature. Therefore, this lowest state seems to be involved in the photochemical processes.

2.3.3 Factor Group Splitting

The wavefunctions of the translationally non-equivalent interacting molecules in the crystal produce splitting of the molecular energy levels[24,25]. It is of interest to note this factor group splitting in vitamin A alcohol solid film. The weak absorption band of vitamin A alcohol in solution at about 40600 cm^{-1} evidently corresponds to the band at 41000 cm^{-1} in the solid state (Fig. 2.2). The two bands in solution at about 31900 and 30864 cm^{-1} have a separation of 1036 cm^{-1}. In the solid film none of the bands at 34900, 33500 and 28666 cm^{-1} seems to correspond to the weak solution band at 31900 cm^{-1}. It is likely that these three bands in the solid state are the factor group split components of the band at 30864 cm^{-1} in solution. The weak band at 31900 cm^{-1} in the solution spectrum is possibly masked by the strong absorption at 34900 cm^{-1} in the crystalline state.

Unfortunately the crystal structure of vitamin A alcohol and molecular orientations in the lattice are not known. It is, therefore, not possible to estimate the factor group splitting in the crystal.

In the solid film spectra of other polyenes, no factor group splitting could be detected.

2.4 Conclusion

The new absorption band appearing on the long wavelength side of the $^1A_g \longrightarrow {}^1B_u$ transition due to adsorption of various vapours on the solid films of polyenes studied shows a good overlap and mirror image relationship with the emission band of these polyene solid films. The solvent effect on the $^1A_g \longrightarrow {}^1B_u$ absorption band and on the observed emission band suggests that two different electronic states are involved in the absorption and in the emission. It is suggested that the low energy band appearing on vapour adsorption is due to the transition from the ground ^1A_g state to the next excited ^1A_g state wherefrom the emission in these polyenes also originates. Thus, we conclude that a low energy ^1A_g state lies below the ^1B_u state in these polyenes.

References

1. T.N. Misra and B. Rosenberg, J. Chem. Phys., 48, 5734 (1968).
2. K. Mandal and T.N. Misra, Indian J. pure appl. Phys., 10, 86 (1972).
3. A. J. Thomson, J. Chem. Phys., 51, 4106 (1969).
4. K. Schulten and M. Karplus, Chem. Phys. Letters, 14, 305 (1972).
5. B.S. Hudson and B.E. Kohler, Chem. Phys. Letters, 14, 299(1972).
6. K. Mandal and T.N. Misra, Chem. Phys. Letters, 27, 67 (1974).
7. R.M. Gavin, Jr., C. Weisman, J.K. McVey and S.A. Rice, J. Chem. Phys., 68, 522 (1978).
8. N.S. Bayliss, J. Chem. Phys., 16, 287 (1948).
9. J.R. Platt, Radiation Biology (Daniel Davy, Hartford, 1956) Vol. 3
10. W.G. Penny, Proc. Roy. Soc. (London), A 158, 306 (1937).
11. J.E. Lennard Jones, Proc. Roy. Soc. (London), A 158, 280 (1937).
12. K.W. Hausser, R. Kuhn, A. Smakula and K.H. Kreuchen, Z. Phys. Chem., B 29, 363 (1935).
13. K.W. Hausser, Z. Tech. Phys., 15, 10 (1934).
14. P. Baylor and M.C. Whiting, J. Chem. Soc. (London), 3037 (1955).
15. F. Bohlmann and H.J. Hennhardt, Chem. Ber., 89, 1307 (1956).
16. F. Sondheimer, D.A. Ben-Efraim and R. Wolovsky, J. Am. Chem. Soc., 83, 1675 (1961).
17. H. Kuhn, J. Chem. Phys., 17, 1198 (1949).
18. H. Suzuki, Electronic Absorption Spectra and Geometry of Organic Molecules (Academic Press, New York, 1967).
19. B.S. Hudson and B.E. Kohler, J. Chem. Phys., 59, 4984 (1973).

20. J.D. Birks and D.J. Dyson, Proc. Roy. Soc. (London), A275, 135 (1963).

21. B. Mallik, K.M. Jain, K. Mandal and T.N. Misra, Indian J. Pure Appl. Phys., 13, 699 (1975).

22. S. Basu, Advances in Quantum Chemistry edited by P.O. Lowdin (Academic Press, Inc., New York, 1964) Vol. 1, p 145.

23. B. Mallik, K.M. Jain, K. Mandal and T.N. Misra, Indian J. Pure Appl. Phys., 15, 289 (1977).

24. A.S. Davydov, Zh. Eksperim. i Teor. Fiz., 18, 210 (1948).

25. T.N. Misra, Rev. Pure. Appl. Chem., 15, 40 (1965).

CHAPTER 3

CHARGE-TRANSFER COMPLEXES OF SOME POLYENES

3.1 Introduction

Mulliken[1] suggested that charge-transfer (CT) complexes may play an important role in biological systems. Some possible implications have been discussed in a book by Szent-Györgyi[2]. Many workers have produced evidence which, it is claimed, supports this proposition. The idea is that the charge-transfer complexes possess certain properties which could be important in biological systems. The first most obvious property is the transfer of charge from one molecule to another. Electron and charge transfer or transport systems are vitally important in biology.

The balance of electron donors and acceptors of varied biopotential is one of the basic parameters of life and is used in the regulation of activity and the physical state of the cell[3]. Medium range charge-transfer is possibly the most frequent and fundamental in biological reactions. The forces developed due to charge-transfer may bring about the association of two and more entities. It may further influence equilibrium and reactivity. The preferred conformation resulting from CT in turn may confer a biological activity. It has been suggested[2,4] that CT complex formation plays a role in respiratory chain of oxidative phosphorylation, chemical carcinogenesis, drug action and photosynthesis.

The presence of carotenoids (polyenes) in living systems and in plants is well recognised. Some carotenoid pigments are present in cone layers of eyes[5], in olfactory areas[6-8], in skin and in membranes[9,10] of animals. Presence of carotenoids in chloroplasts

strongly suggests its involvement in photosynthesis. It was Platt[11] who suggested that donor-carotene-acceptor trimolecular complex could be involved in primary photosynthesis process. Such a complex would shift the carotene absorption band to much longer wavelength below the absorption bands of chlorophylls and the complex would be the energy sink of the whole system. Simple binolecular CT complex may also work in the same way. Charge-transfer mechanism involving other polyenes may well be responsible for many other biological activities.

Usually CT bands are studied in solutions. Of the polyenes of our interest only vitamin A is well studied[12-16] Lupinski[17] observed a new absorption band at 10000Å in a mixture of β-carotene and iodine in $ClCH_2Cl$ solution and attributed this to a CT band of β-carotene ....I^+ complex. Ebrey[18], on the other hand, agrued that the band observed by Lupinski, instead of being a charge-transfer band of donor-acceptor type, was a band of β-carotene shifted to longer wavelength due to charge-transfer effect, thus suggesting that β-carotene. I^+ complex has several resonance structures for the β-carotene ground state that would equalise bond length and cause its shifting to longer wavelength. Thus it appears that the usual method of observing the CT bands in solution with suitable acceptors has not been successful with the polyenes except with vitamin A.

The important property of the charge-transfer complex forces is that they are relatively long-range as compared to chemical

forces and the typical distances between the molecules in these complexes are 3.2 to 3.4 Å whereas chemical bond lengths are less than about 1.5 Å. Before a charge-transfer interaction can take place, the donor and the acceptor molecule or parts of the molecules must be in sufficient proximity to each other so that the difference in electro-potential can be recognized. In many cases the physical forces (e.g., dipole-dipole force, viscous force etc.) operating between the molecules can prevent such close approach and the formation of the charge-transfer complex is not favoured. In solution, the molecules are not isolated and the interaction between the molecules cannot be divorced from the effects of the immediate surroundings. Generally the polarity and the viscosity of a medium are observed to have a strong effect on the charge-transfer interaction. In the media of low viscosity, Brownian motion which causes the molecules to move about reduces the possibility of their close approach. In a rigid matrix, the molecules do not experience any Brownian motion and are held in such close proximity that charge-transfer are generally facilitated. Thus, the molecules which seem not to interact in solution may do so in the solid state. It was, therefore, thought worthwhile to study the charge-transfer complexes of all-trans-β-carotene, β-apo-8'-carotenal, astacene and methyl bixin in the solid state. For this purpose, we have allowed the vapours of some acceptors to be adsorbed on the transparent solid films of the polyenes in quartz cells and have collected the spectroscopic data to see if CT complexes are really formed in the solid state. In this chapter the results of such studies are presented.

3.2 Experimental and Results

The sample of all-trans- β -carotene like other polyenes was obtained from Hoffman-La-Roche Co. Ltd., Switzerland. This was used without further purification. The structure of this polyene is shown in Fig. 3.1.

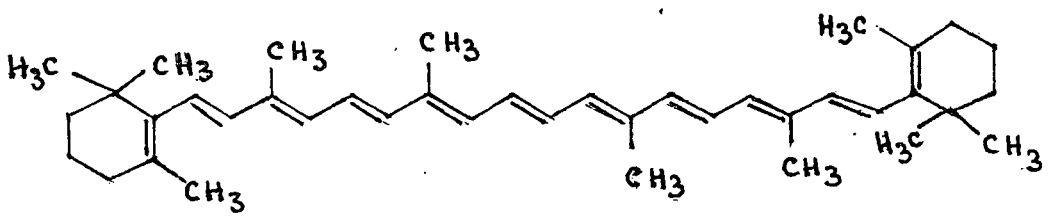

Fig. 3.1 Structure of all-trans- β -carotene

Thin films of polycrystals of the polyenes were made on the quartz surface in the same procedure as mentioned in the previous chapter. The solid films thus made were exposed to vapours of nitric acid, iodine, bromine and iodine monochloride. These chemicals were of high quality. The absorption spectra at room temperature (28°C) were recorded immediately after exposing the solid films to vapours by a spectromom - 202 spectrophotometer of Hungarian Optical Works.

The room-temperature (28°C) absorption spectra of all-trans- β -carotene, β -apo-8'-carotenal, astacene and methyl bixin in the solid state and the spectra after adsorption of different acceptor vapours are shown in Figs. 3.2 - 3.6. It is seen that on adsorption

FIG. 3.2 : Electronic absorption spectra of all-trans-β-carotene solid film at 28°C after adsorption of different electron acceptor vapours : (1), solid film spectrum without vapour adsorption; (2), nitric acid vapour adsorption; (3), iodine vapour adsorption; (4), bromine vapour adsorption; (5), iodine monochloride vapour adsorption. (The positions, $\bar{\nu}_{max}$, of the new bands are indicated by vertical marks. Spectra on adsorption of different vapours are not normalized).

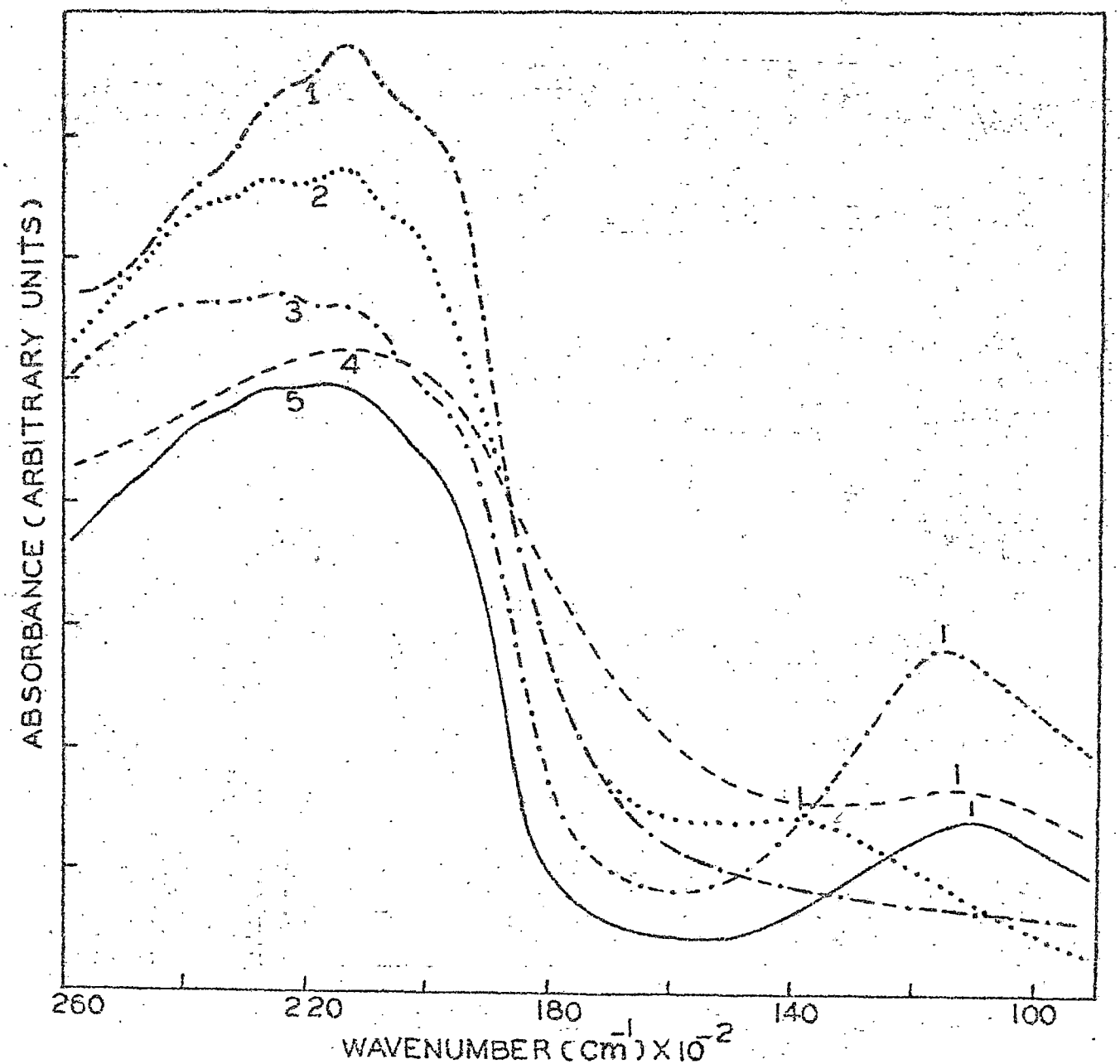
ABSORBANCE (ARBITRARY UNITS)
1
2
3
4
5
260
220
180
140
100
WAVENUMBER (cm⁻¹) X 10⁻²

FIG: 3·2

FIG. 3.3 : Electronic absorption spectra of β -apo-8'-carotenal solid film at 28°C after adsorption of different electron acceptor vapours : (1), solid film spectrum without vapour adsorption; (2), iodine vapour adsorption; (3), bromine vapour adsorption; (4), iodine monochloride vapour adsorption. (The positions, $\tilde{\nu}_{max}$, of the new bands are indicated by vertical marks. The spectra on adsorption of various vapours are not normalized).

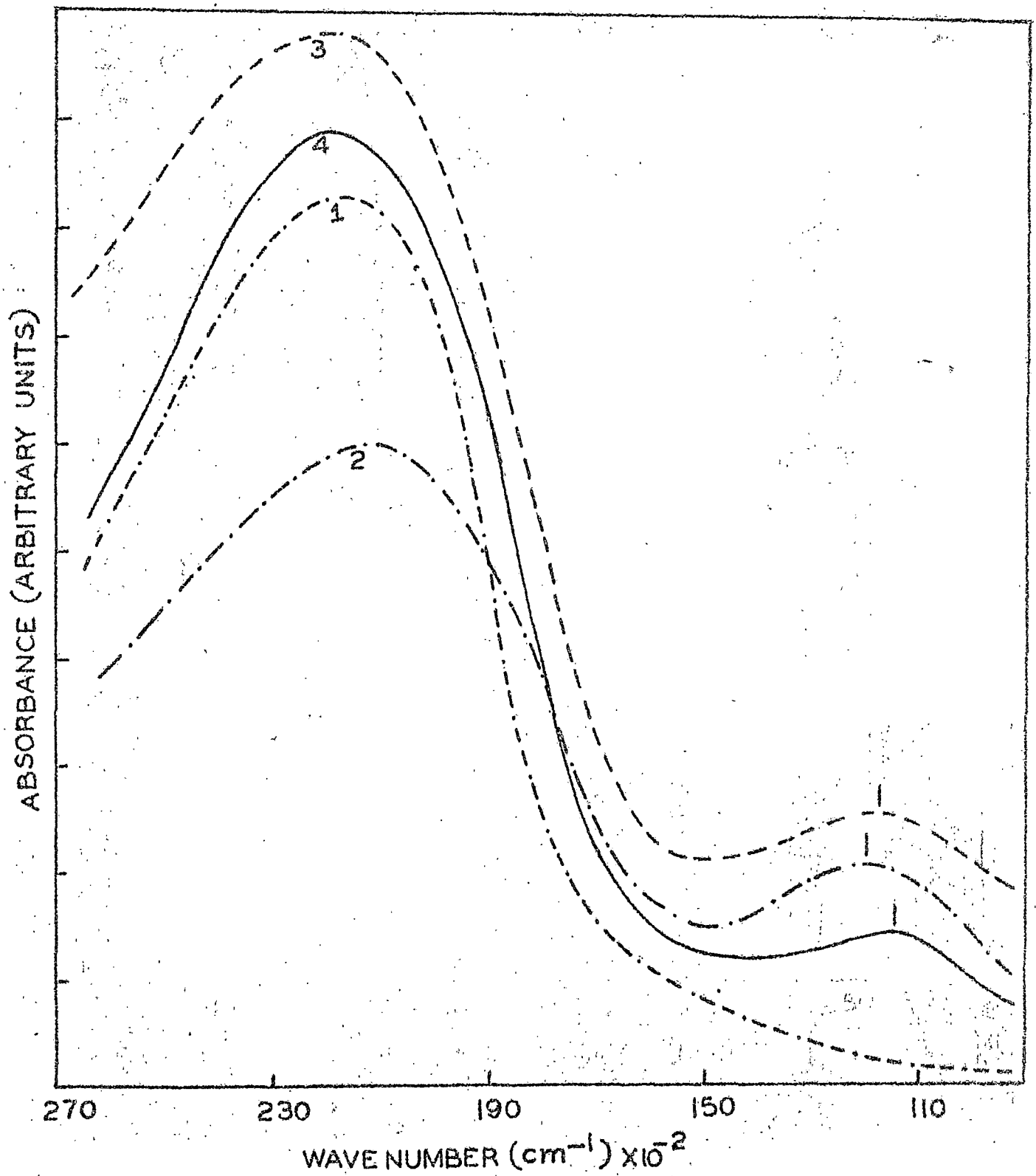
3
4
1
2
ABSORBANCE (ARBITRARY UNITS)
270
230
190
150
110
WAVE NUMBER (cm⁻¹) X10⁻²

FIG. 3·3

FIG. 3.4 : Electronic absorption spectra of astacene solid film at 28°C after adsorption of different electron acceptor vapours : (1), solid film spectrum without vapour adsorption; (2), iodine vapour adsorption; (3), bromine vapour adsorption; (4), iodine monochloride vapour adsorption (The positions, $\bar{\nu}_{max}$, of the new bands are indicated by vertical marks. The spectra on adsorption of various vapours are not normalised).

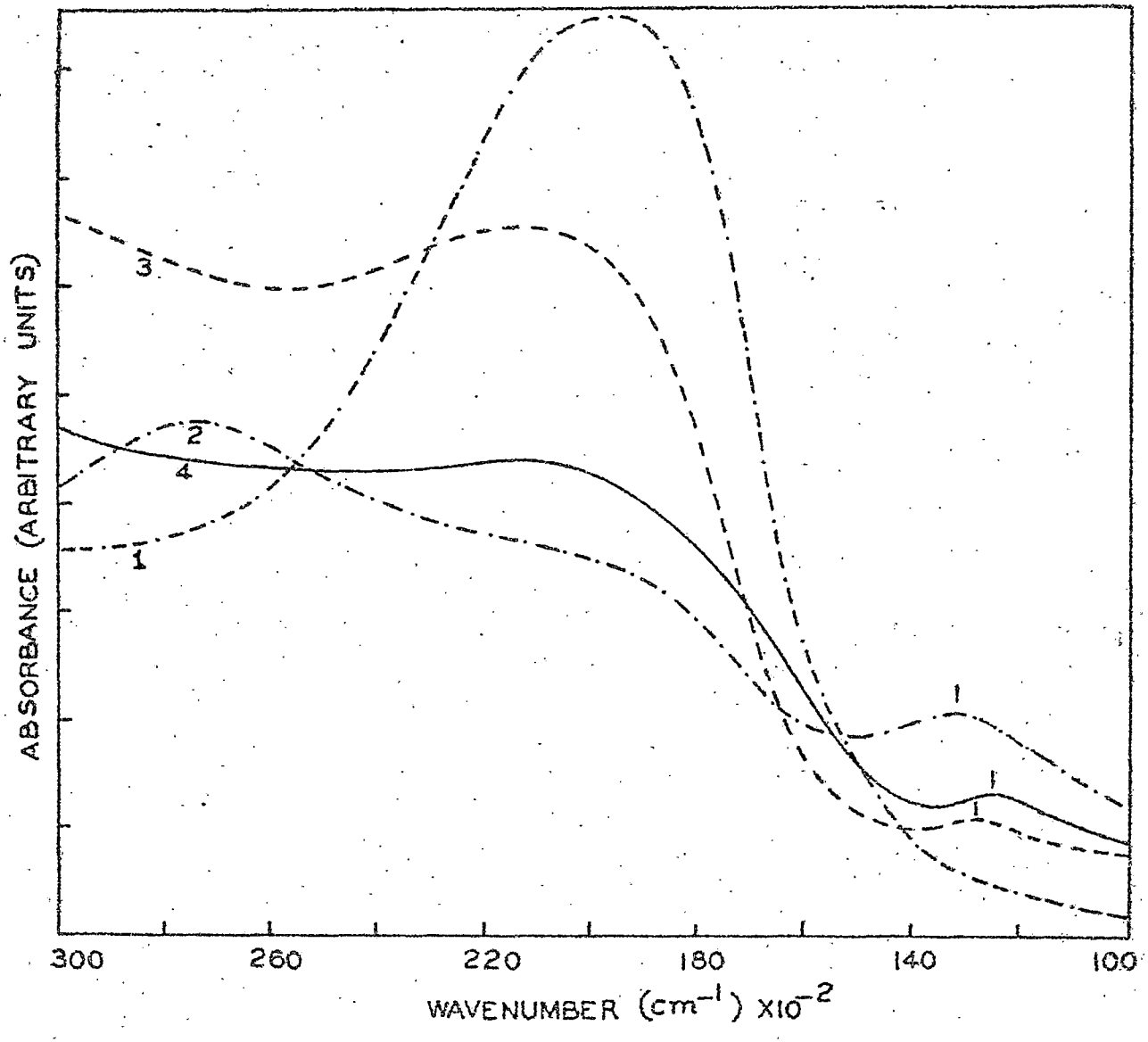
ABSORBANCE (ARBITRARY UNITS)
3
2
4
1
1
1
1
300
260
220
180
140
100
WAVENUMBER (cm⁻¹) X10⁻²

FIG-3·4

FIG. 3.5 : Electronic absorption spectra of methyl bixin solid film at 28°C after adsorption of different electron acceptor vapours : (1), solid film spectrum without vapour adsorption; (2), iodine vapour adsorption; (3), bromine vapour adsorption; (4), iodine monochloride vapour adsorption. (The positions, $\bar{\nu}_{max}$, of the new bands are indicated by vertical marks. The spectra on adsorption of various vapours are not normalized).

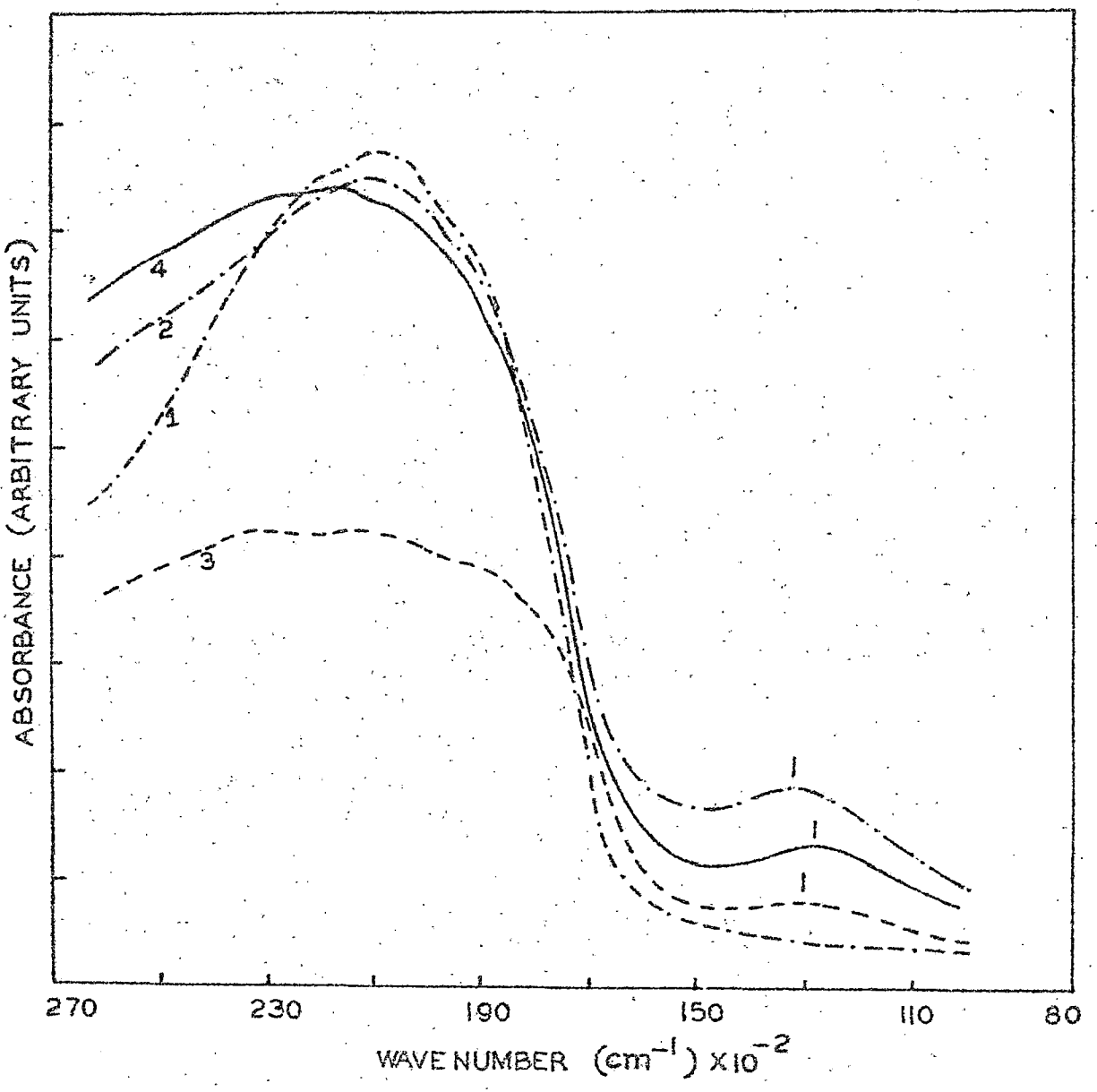
ABSORBANCE (ARBITRARY UNITS)
4
2
1
3
270
230
190
150
110
80
WAVE NUMBER (cm^{-1}) X10^{-2}

FIG. 3·5

of acceptor vapours, in each polyene a new band appears on the long wavelength side of the spectra in addition to the original bands of the polyene solid films. With the increasing amount of acceptor molecules adsorbed on the film surface, the intensity of this new band increases as is usually observed in case of a charge-transfer band. This observation is shown in Figs. 3.6-3.9 for all-trans- β -carotene, β -apo-8'-carotenal, astacene and methyl bixin, respectively. The position of the new band in each polyene is found to be dependent on the acceptor vapours used and shows appreciable red-shift with the increasing electron affinity of the acceptor molecules. Only acceptors fairly volatile at ordinary temperatures are suitable for such experiment. As the number of such acceptors are very limited, only a few acceptors could be used. The position of the new bands in different polyenes appearing on adsorption of various acceptor vapours are summarized in table 3.1.

3.3 Discussion

In each polyene the new band appears on the lower energy side of the observed emission band of the polyene and its separation is about 5000 - 7000 cm^{-1} from the $\bar{\nu}_{max}$ of the emission band. This excludes the possibility of this band to be the low-lying forbidden band as discussed in the previous chapter. The results presented in the previous section suggest this band to be a charge-transfer band.

FIG. 3.6 : Enhancement of the intensity of the new band with the amount of adsorbed acceptor molecules on the solid film of all-trans β -carotene at 28°C. The solid line is for the neat solid film spectrum. The broken lines represent the spectra after iodine vapour adsorption; (1-4), in order of increasing amount of iodine molecules.

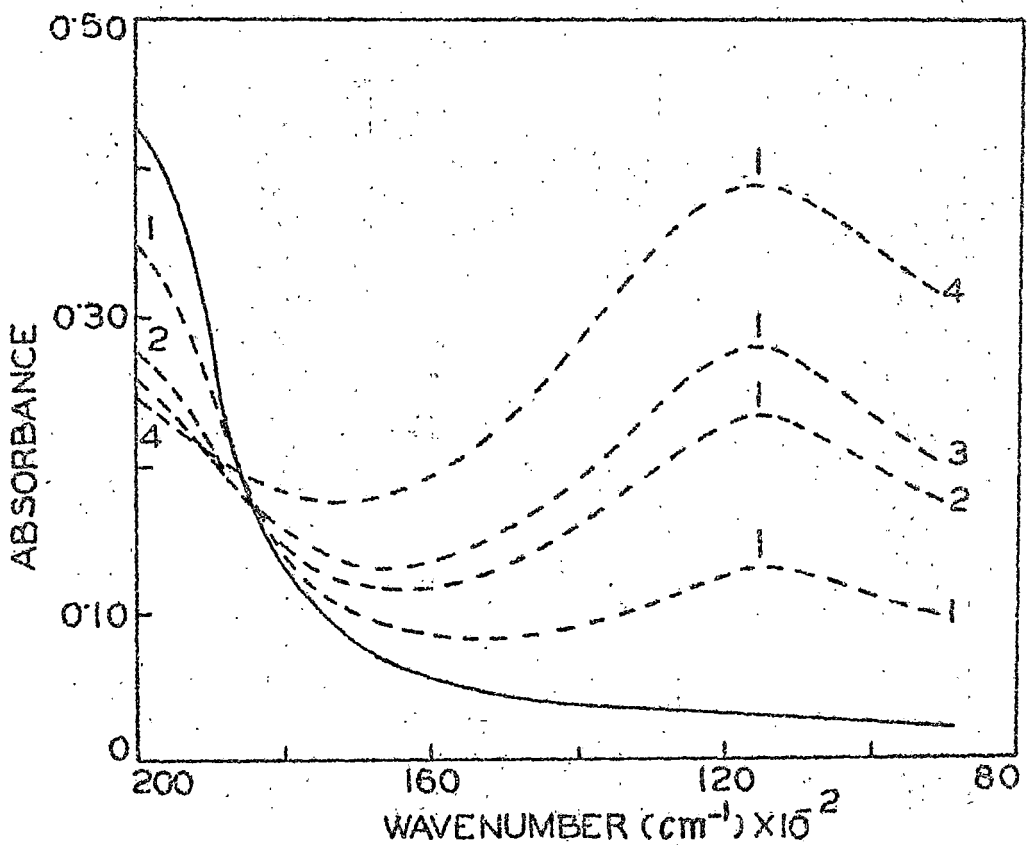
0·50
0·30
0·10
0
ABSORBANCE
200
160
120
80
WAVENUMBER (cm⁻¹) X10⁻²
1
2
4
1
4
1
3
1
2
1
1

FIG. 3·6

FIG. 3.7 : Enhancement of the intensity of the new band with the amount of adsorbed acceptor molecules on the solid film of β -apo-8'-carotenal at 28°C. The solid line is for the neat solid film spectrum. The broken lines represent the spectra after iodine vapour adsorption; (1-4), in order of increasing amount of iodine molecules.

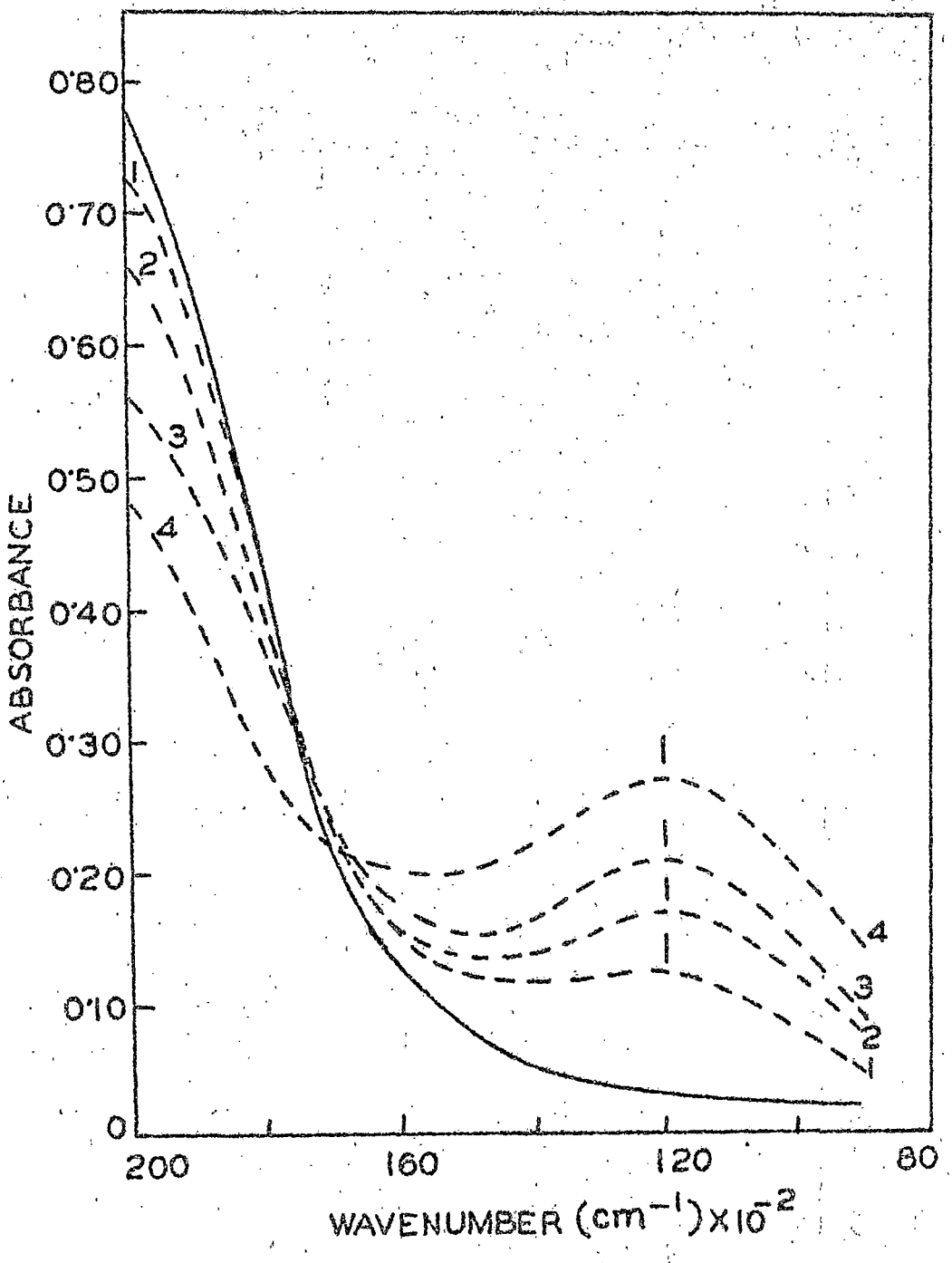
0·80
0·70
0·60
0·50
0·40
0·30
0·20
0·10
0
ABSORBANCE
1
2
3
4
200
160
120
80
WAVENUMBER (cm⁻¹) X 10⁻²

FIG. 3·7

FIG. 3.8 : Enhancement of the intensity of the new band with the amount of adsorbed acceptor molecules on the solid film of astacene at 28°C. The solid line for the neat solid film spectrum. The broken lines represent the spectra after iodine vapour adsorption; (1-4), in order of increasing amount of iodine molecules.

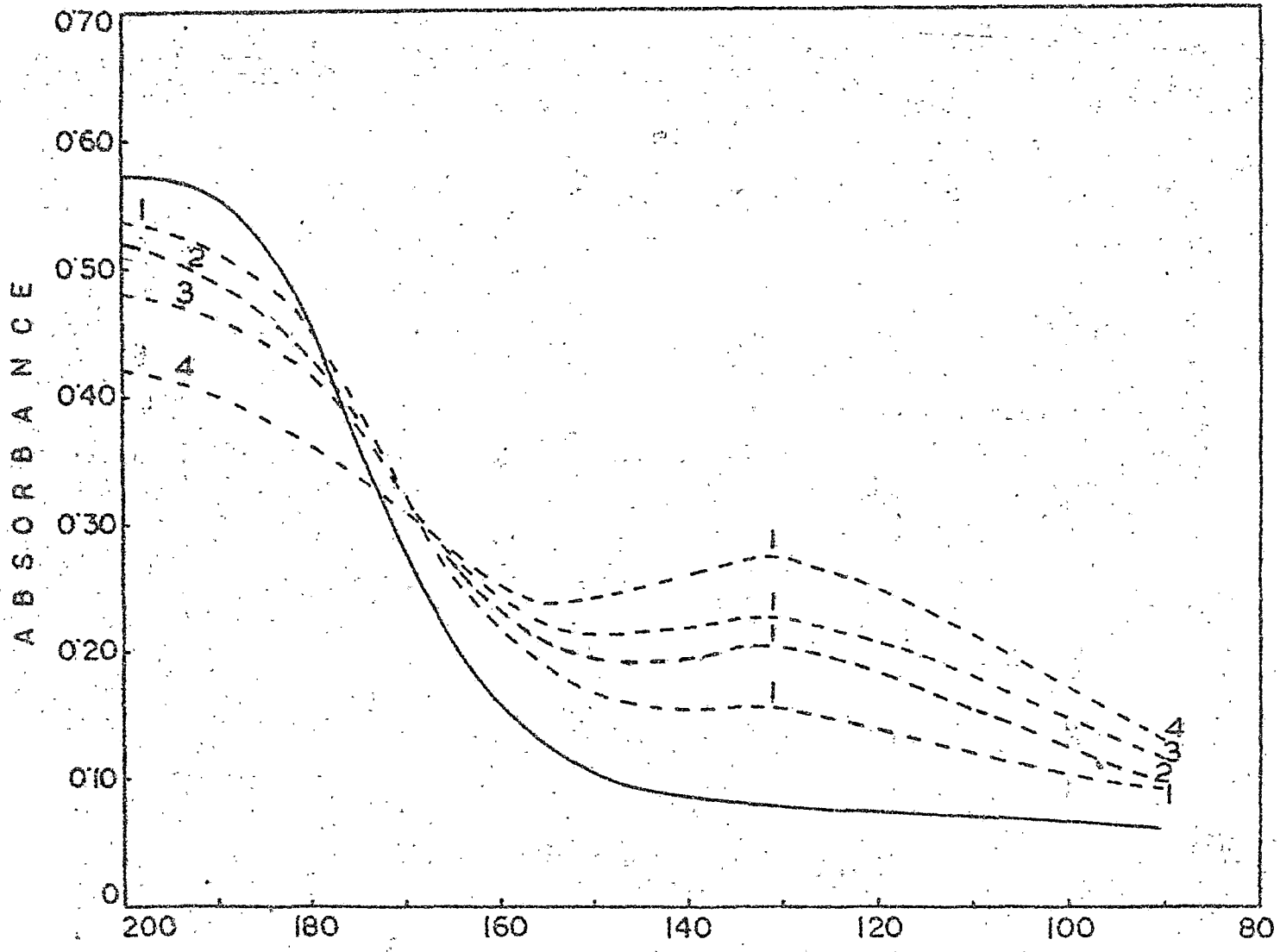
0·70
0·60
0·50
0·40
0·30
0·20
0·10
0
ABSORBANCE
1
2
3
4
200
180
160
140
120
100
80
WAVENUMBER (cm⁻¹) × 10⁻²

FIG.3·8

FIG. 3.9 : Enhancement of the intensity of the new band with the amount of adsorbed acceptor molecules on the solid film of methyl bixin at 28°C. The solid line is for the neat solid film spectrum. The broken lines represent the spectra after iodine vapour adsorption; (1-4), in order of increasing amount of iodine molecules.

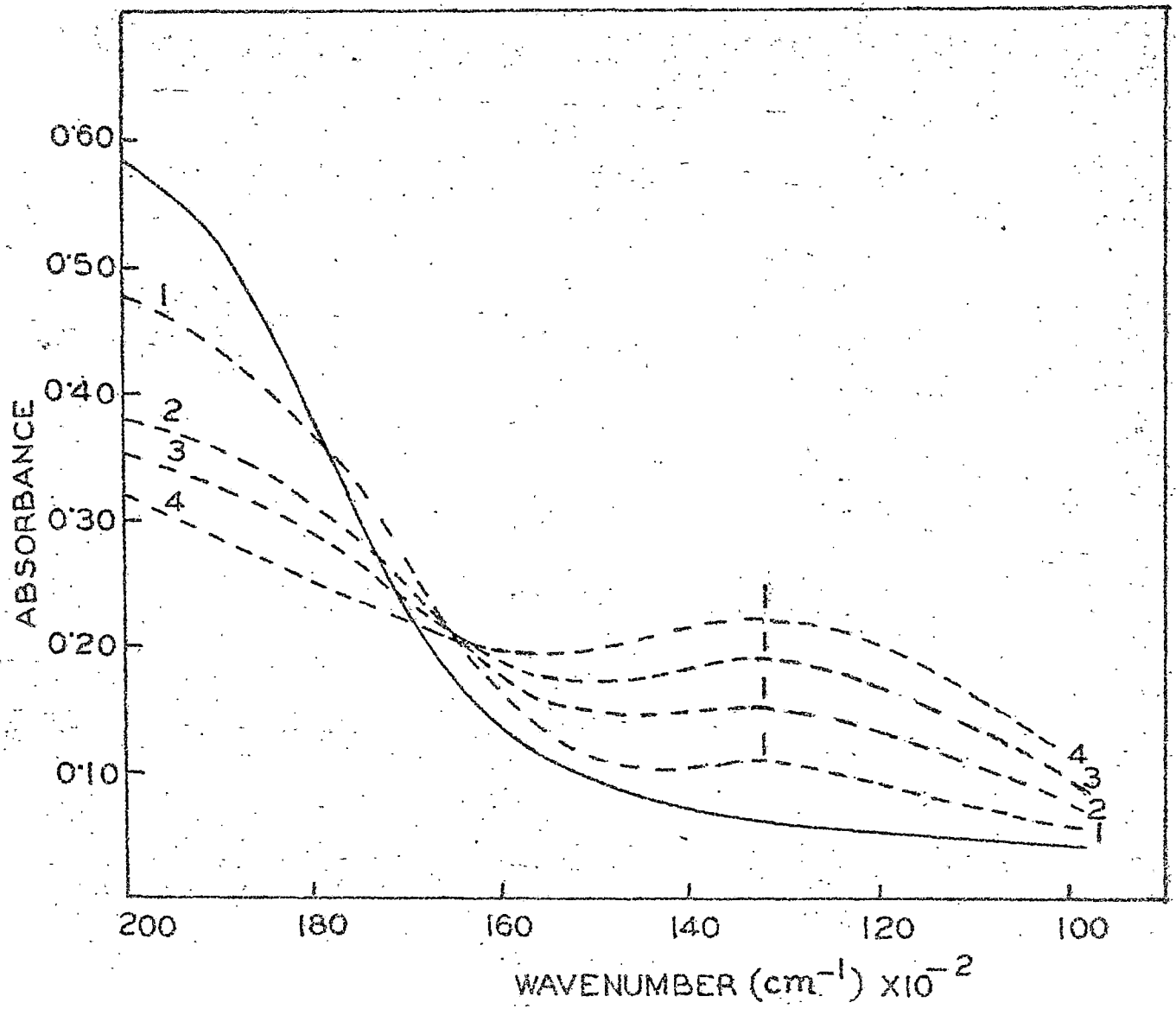
0·60
0·50
0·40
0·30
0·20
0·10
ABSORBANCE
1
2
3
4
200
180
160
140
120
100
WAVENUMBER (cm⁻¹) X10⁻²

FIG. 3·9

Table - 3.1

Position ($\bar{\nu}_{max}$) of the new band appearing on adsorption of different acceptor vapours on the solid films of some polyenes

Acceptor used	E_A(eV)	$\bar{\nu}_{max}$ (Cm^{-1}) for			
		all-trans-β-Carotene	β-apo-8'-Carotenal	Astacene	Methyl bixin
Nitric acid	1.83	13900	-	-	-
Iodine	2.40	11550	12000	13150	13200
Bromine	2.60	11300	11800	12800	13000
Iodine monochloride	2.70	11100	11500	12500	12700

It has already been discussed in chapter 1 that Mulliken's theory for charge-transfer complex formation leads to the equation (from eqn. (1.41))

$$h\nu_{CT} = I_D^V - E_A^V + C_1 \qquad (3.1)$$

Thus for a particular donor, a plot of ν_{CT} against E_A^V should be linear. Unfortunately, reliable values of vertical electron affinities are very scarce. Apart from the necessary distinction between the vertical and adiabatic values, different experimental methods yield different results and also sometimes the substance of interest has not been studied at all. The value of E_A^V for nitric acid is not available in the literature. Recently, Chen and Wentworth[19] have emphasized that the correlation of $h\nu_{CT}$ with the absolute electron affinities (E_A) of acceptors is consistent with the usual linear equations and their associated assumptions. The adiabatic electron affinities of I_2, Br_2 and ICl estimated theoretically by Person[20] were 2.4 ± 0.3, 2.6 ± 0.3 and 2.7 ± 0.3 eV respectively agreeing satisfactorily with the experimental absolute values measured by Hughes et al.[21] We have, therefore, used these adiabatic electron affinity values as the absolute values. The value of E_A for nitric acid has been taken from Chen and Wentworth's table[19].

A plot of $\bar{\nu}_{max}$ (cm^{-1}) of the new band of all-trans- β - carotene against E_A is shown in Fig. 3.10. A satisfactory straight line is obtained. The ionization potential of β-carotene can be

FIG. 3.10 : Plot of $\bar{\nu}_{max}$ (cm^{-1}) against E_A for <u>all-trans-</u> β -carotene.

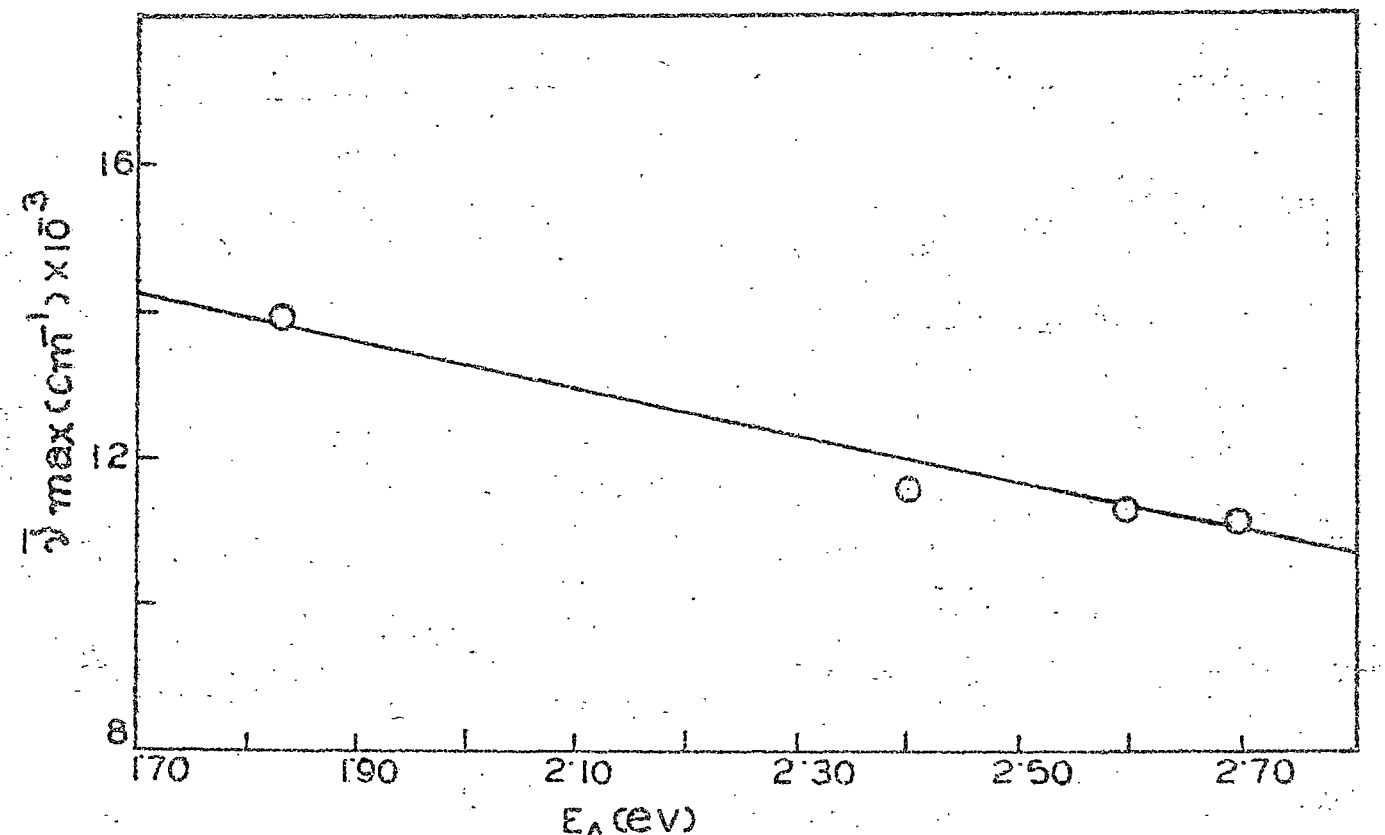

FIG.3·10

estimated from this $\bar{\nu}_{max}$ vs. E_A plot. The intercept of this curve gives $I_D + C_1 = 2.44$ eV. In typical donor-acceptor CT complexes, $-C_1$ is usually around 3 eV[19,22]. This gives a value of the ionization potential of β-carotene as 5.44 eV. The experimental value[23,24] of ionization potential (measured from photoemission thresholds) of β-carotene is 5.5 eV. This agreement leads credence to the above linear plot and also to the CT concept[88] for this complex. From equation (3.1), one expects a slope of unity for $\bar{\nu}_{CT}$ vs. E_A^V plot. Fig. 3.10 gives a slope of 0.44. This low value of slope could be due to that the electron affinity values used for the plot being absolute rather than vertical. Further, equation (3.1) is only approximate and there is no reason to expect that the last term in equation (1.40) is negligible for all the pairs of donors and acceptors. Indeed, such deviation of slope from unity is a general observation in these types of experiments[26,27].

The relationship between the ionization potentials of two donors and the values of $\bar{\nu}_{max}$ corresponding to their CT complexes with a common acceptor can be written (assuming that the C_1 values do not differ much in the two complexes) as

$$I_D\ (\text{donor-2}) = I_D\ (\text{donor-1}) + h\bar{\nu}_{CT}(2) - h\bar{\nu}_{CT}(1) \qquad (3.2)$$

From this equation (3.2), one can estimate the value of ionization potential of donor-2 if the ionization potential of the donor-1 and the associated values of the $\bar{\nu}_{CT}$ are known. We have estimated the value of ionization potential of β-apo-8'-carotenal, astacene and methyl bixin from this equation (3.2) considering I_D (donor - 1)

as 6.50 eV for β -carotene and taking $\bar{\nu}_{max}$ of the new band for iodine vapour adsorption in all these polyenes. The estimated values are 5.56, 5.69 and 5.70 eV for β -apo-8'-carotenal, astacene and methyl bixin respectively. For charge-transfer bands, the estimated values of ionization potential should show a good agreement with the values obtained by other methods. As the values of ionization potential of these polyenes are not reported, we have alternatively evaluated these values from the I_p vs. $\bar{\nu}_{CT}$ plot for a large number of other donors[22] with iodine acceptor as shown in Fig. 3.11. These values are shown in table 3.2 for comparison with our estimated values. The excellent agreement between these two sets of values confirms that the new bands are charge-transfer bands of the polyenes.

The weak low-lying $^1A_g \rightarrow {}^1A_g$ band is not observed on adsorption of these acceptor vapours possibly due to the broadening of the intense $^1A_g \rightarrow {}^1B_u$ band.

The room-temperature absorption spectra of all-trans- β -carotene, β -apo-8'-carotenal, astacene and methyl bixin after adsorption of I_2 vapour are shown in Figs. 3.12 - 3.15. From these spectra, it is observed that in addition to the new band in the longer wavelength side another new absorption band is also observed at about 27800 cm^{-1} in each case. This is the well-known absorption band of I_3^- ion[29]. The other absorption band of this molecular ion expected at about 33900 cm^{-1} has possibly been merged with the

FIG.3.11 : Plot of $\bar{\nu}_{CT}$ against I_D for CT complexes of a number of donors with iodine acceptor. The donors are : (1), benzene; (2), toluene; (3), m-xylene; (4), mesitylene; (6), naphthalene; (6), durene; (7), pentamethylbenzene; (8), triphenylene; (9), hexamethylbenzene; (10), chrysene; (11), anthracene; (12), pyrene. (Values of $\bar{\nu}_{CT}$ and I_D have been taken from Refs. 23 and 10 respectively).

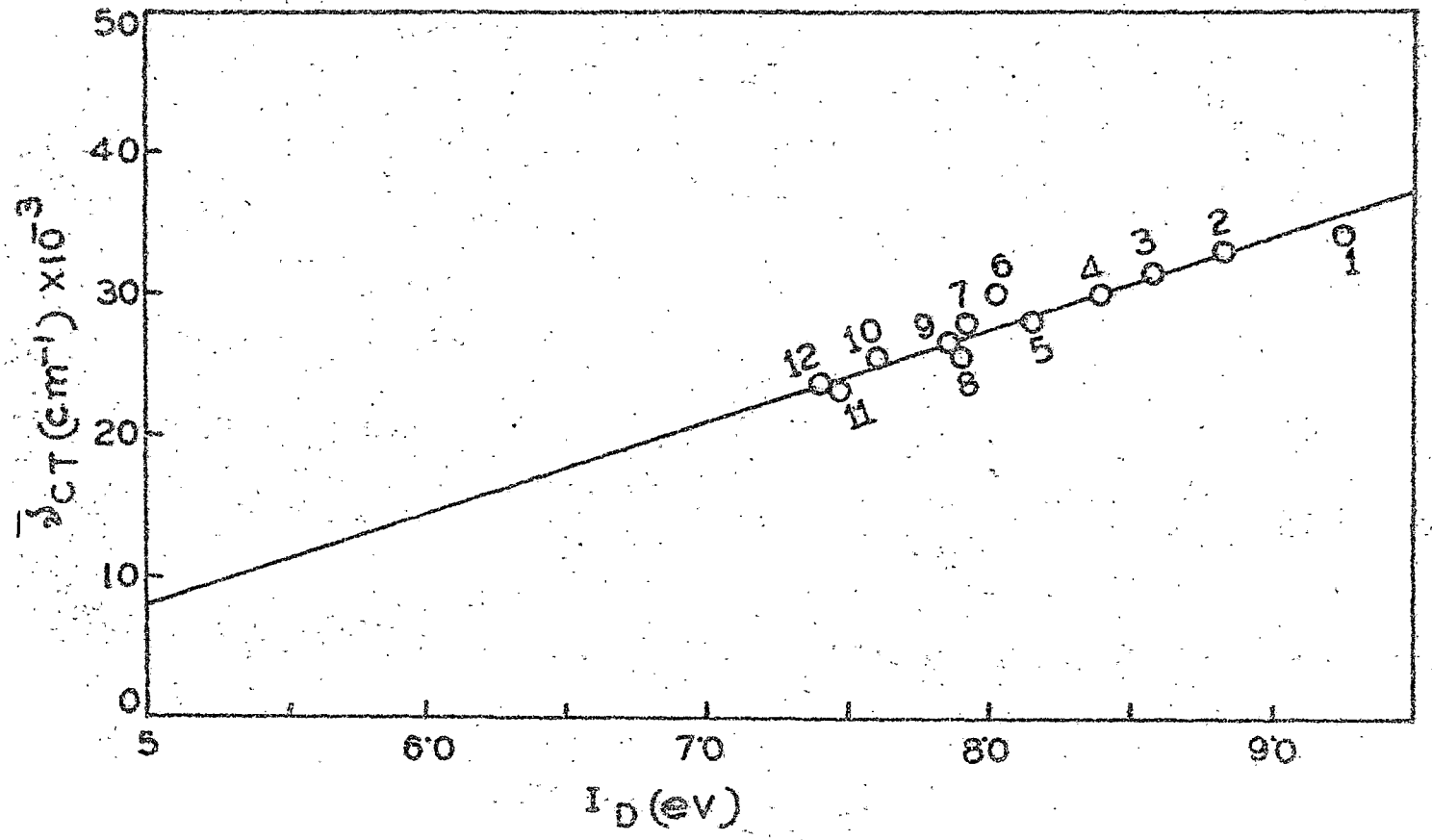
50
40
30
20
10
0
5
6·0
7·0
8·0
9·0
λ_{CT}^{-1} (cm^{-1}) x10^{-3}
I_D (eV)
0
1
2
3
4
5
6
7
8
9
10
11
12

FIG. 3.11

Table - 3.2

Comparison of the values of ionization potential of some polyenes estimated from this experiment and obtained from Fig. 3.11

Polyenes	Estimated I_p(eV)	Value of I_p(eV) obtained from Fig.3.11
all-trans- β -Carotene	5.44	5.56
β-apo-8'-Carotenal	5.56	5.62
Astecene	5.69	5.67
Methyl bixin	5.70	5.70

FIG. 3.12 : Electronic absorption spectra of <u>all-trans-</u> β -carotene solid film (28°C) : (1), spectrum without adsorption of vapour; (2), spectrum after adsorption of iodine vapour. (The positions of the new bands are indicated by vertical marks).

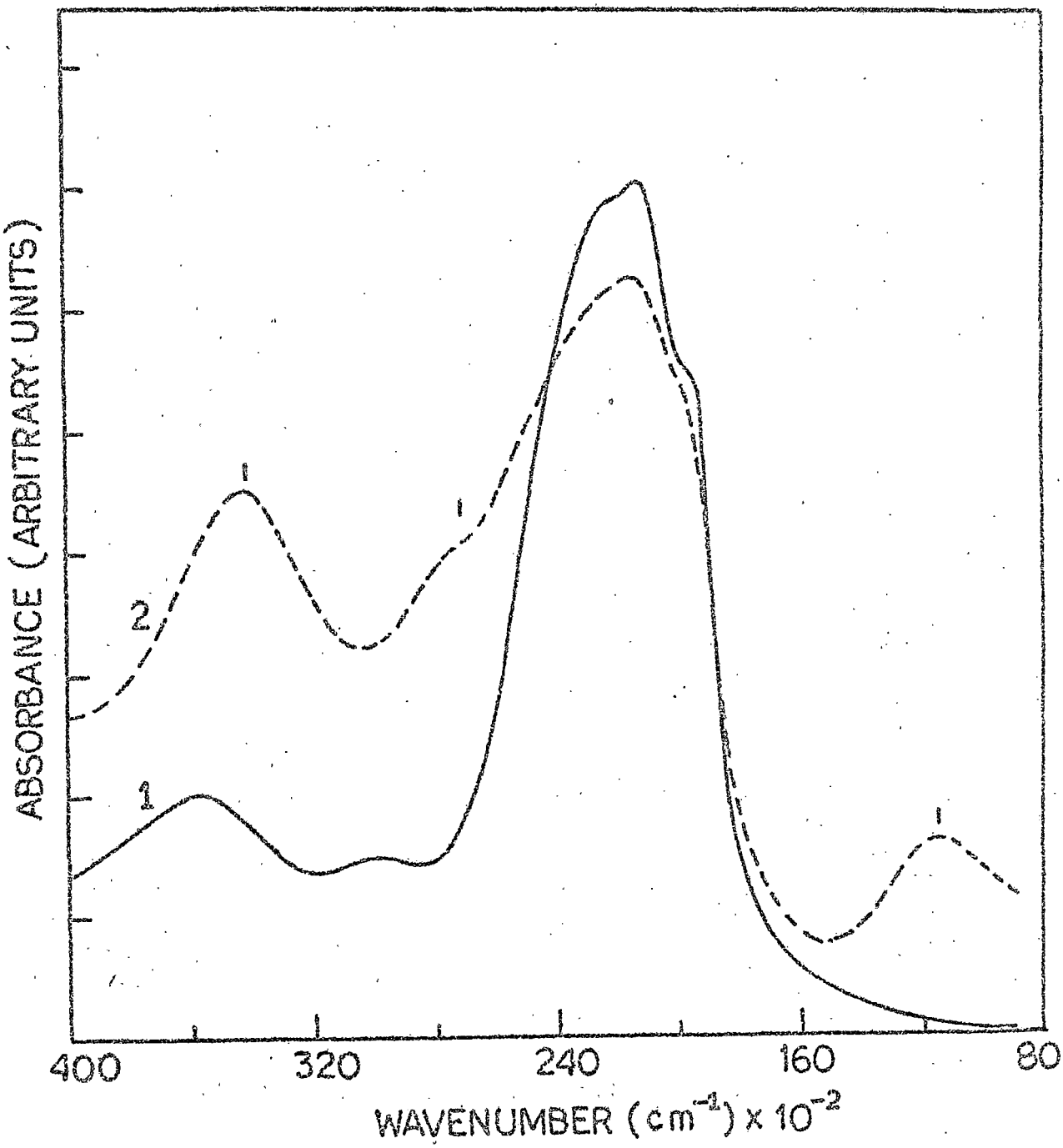
ABSORBANCE (ARBITRARY UNITS)
2
1
400
320
240
160
80
WAVENUMBER (cm^{-1}) x 10^{-2}

FIG. 3·12

FIG. 3.13 : Electronic absorption spectra of β-apo-8'-carotenal solid film (28°C) : (1), spectrum without adsorption of vapour; (2), spectrum after adsorption of iodine vapour. (The positions of the new bands are indicated by vertical marks).

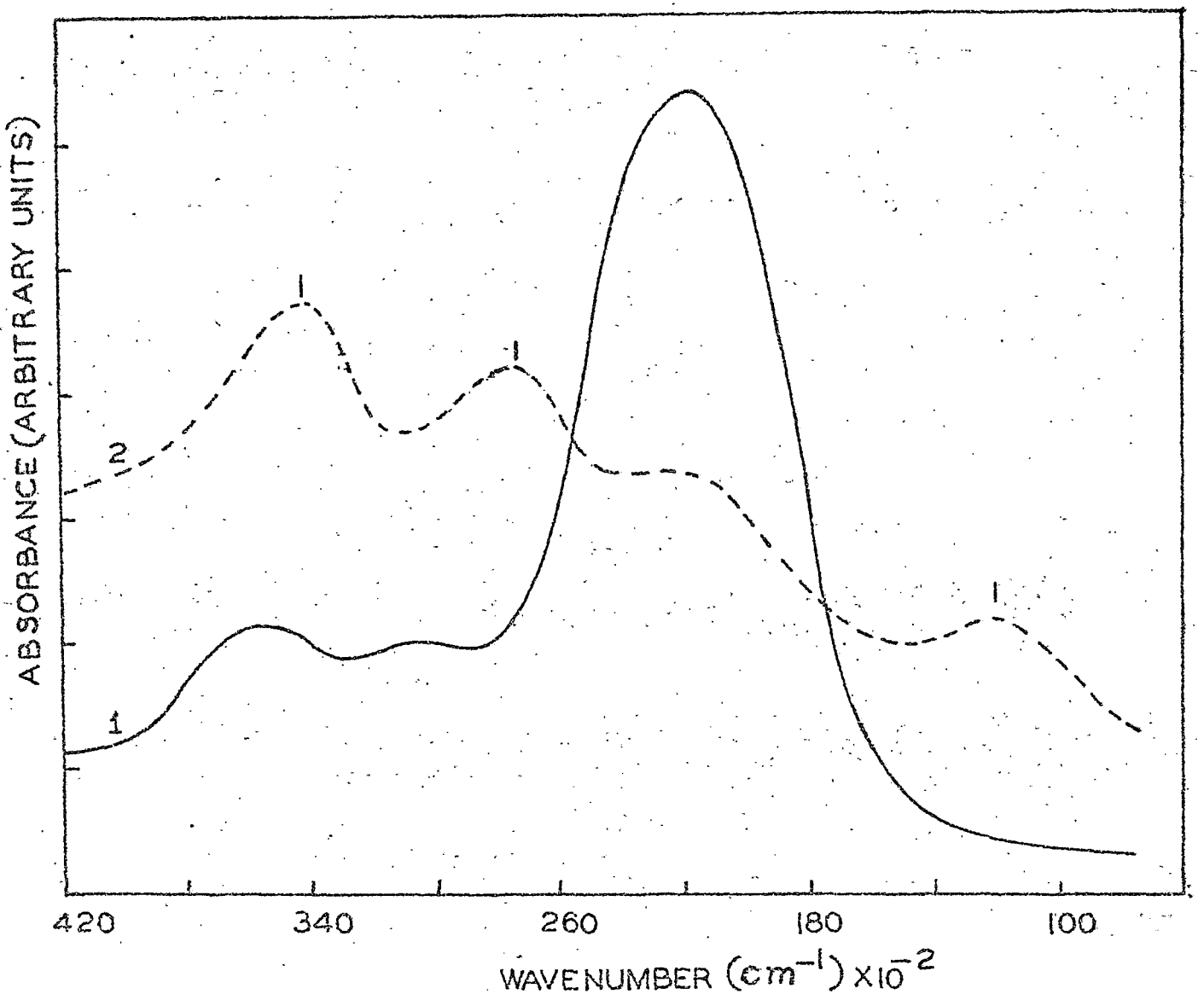
ABSORBANCE (ARBITRARY UNITS)
1
2
420
340
260
180
100
WAVENUMBER (cm⁻¹) X10⁻²

FIG.3·13

FIG. 3.14 : Electronic absorption spectra of astacene solid film (28°C) : (1), spectrum without adsorption of vapour; (2), spectrum after iodine vapour adsorption. (The positions of the new bands are indicated by vertical marks.)

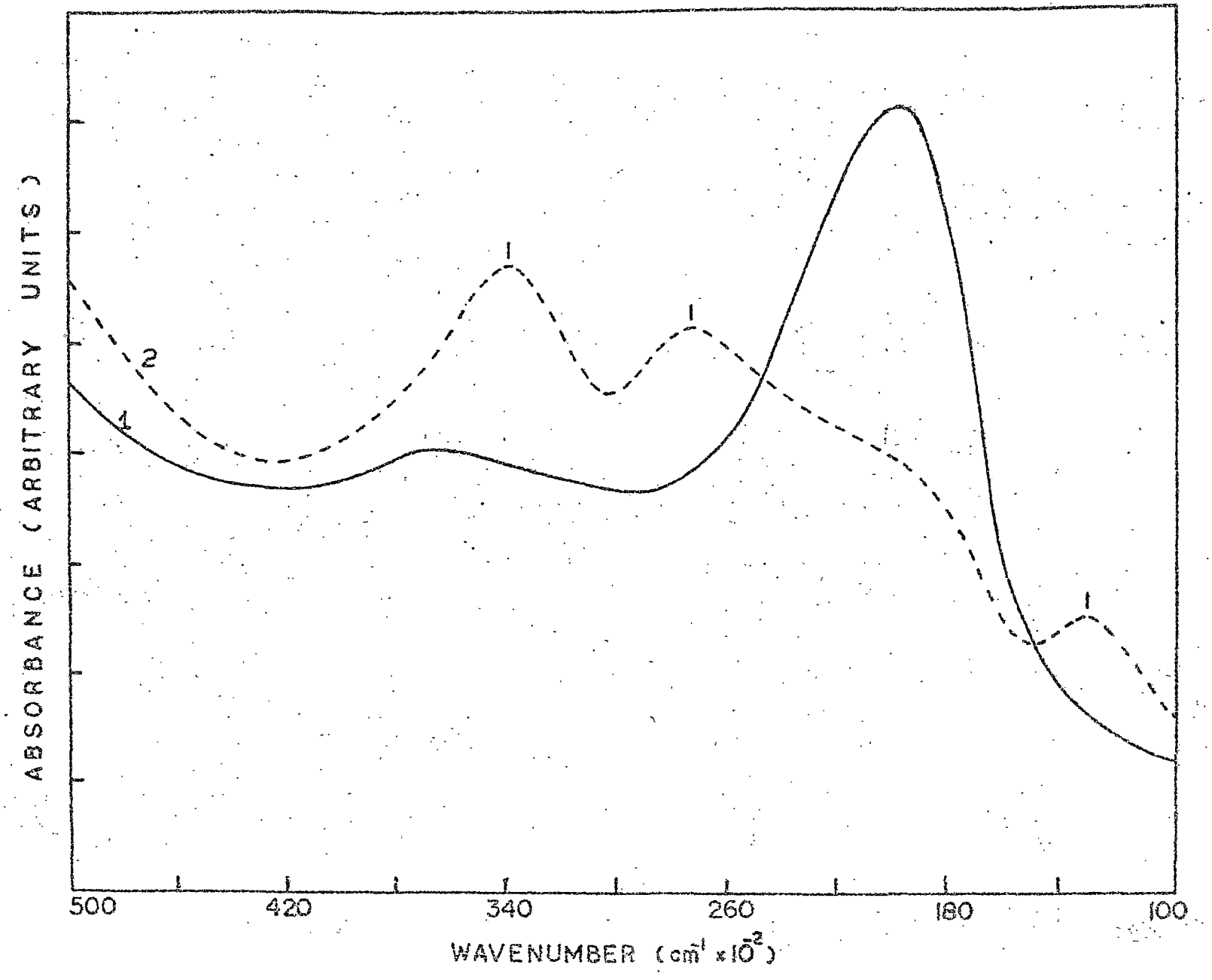
ABSORBANCE (ARBITRARY UNITS)
2
1
1
1
500
420
340
260
180
100
WAVENUMBER (cm⁻¹ x 10⁻²)

FIG.3·14

FIG. 3.15 : Electronic absorption spectra of methyl bixin solid film (22°C) : (1), spectrum without adsorption of vapour; (2), spectrum after iodine vapour adsorption. (The positions of the new bands are indicated by vertical marks).

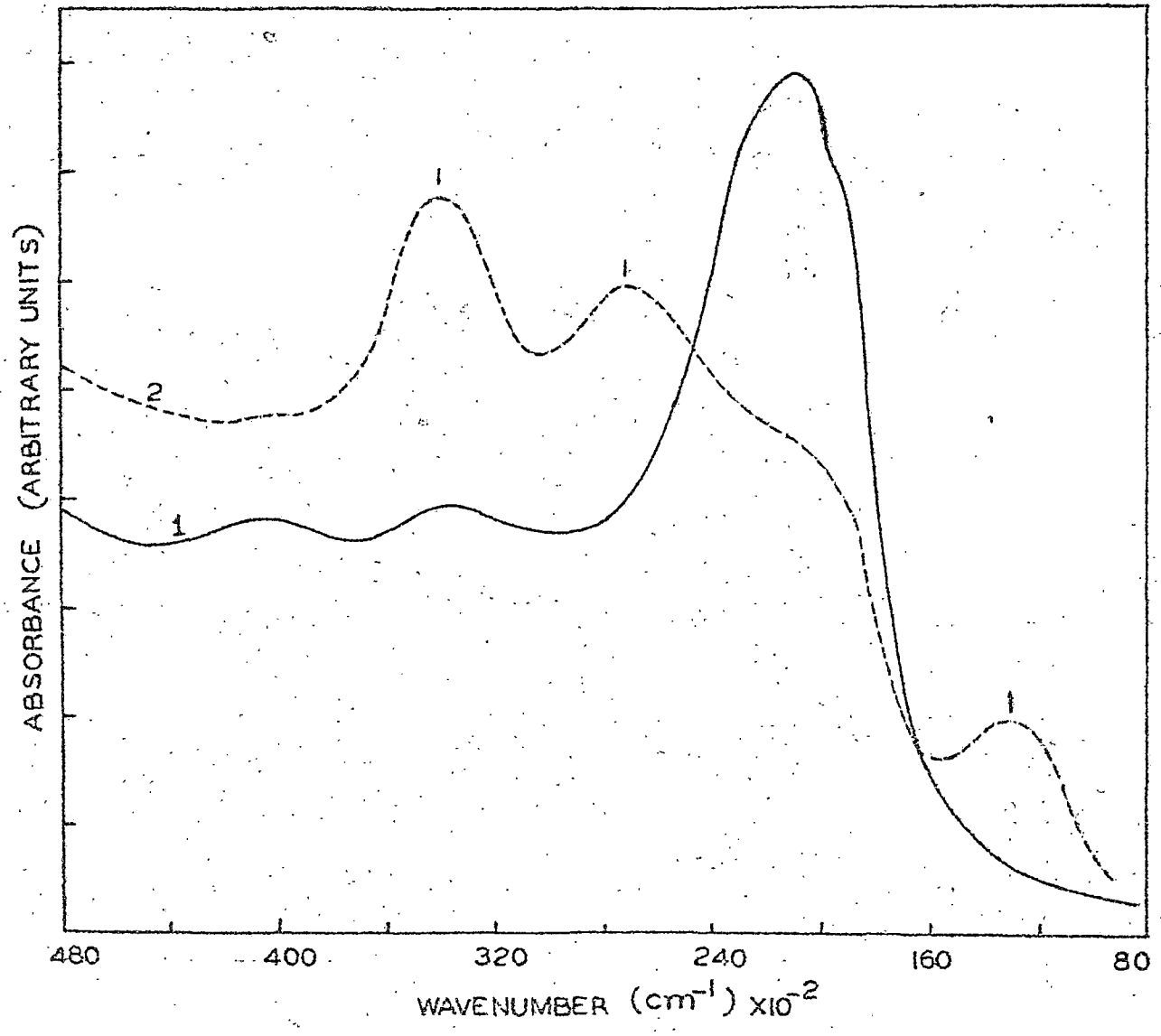
ABSORBANCE (ARBITRARY UNITS)
480
400
320
240
160
80
WAVENUMBER (cm⁻¹) X10⁻²
1
2
1
1

FIG. 3·15

original bands of these polyenes in this region. In case of iodine, possibly through the reaction

$$\text{Polyene} + 2I_2 \rightleftharpoons (\text{Polyene} \ldots\ldots I)^+ + I_3^-$$

the polyenes form CT complexes with iodine. The new band arises due to transition from the ground state (Polyene $\ldots\ldots I^+$) to the excited state ($\text{Polyene}^+ \ldots\ldots I$) of the complex.

Contrary to that suggested by Ebrey[18] our results for the polyenes studied indicate that at least in the solid state single resonance structure

$$C = C - (C = C)_n - C = C \ldots\ldots \overset{+}{I}$$

is quite stable and usual donor acceptor complexes are formed.

3.4 Conclusion

The polyenes under investigation can form charge-transfer complexes with suitable acceptors in the solid state.

References

1. R.S. Mulliken, J. Am. Chem. Soc., 74, 811 (1952).
2. A. Szent - Györgyi, Introduction to a Submolecular Biology (Academic Press, London and New York, 1960).
3. A.G. Györgyi, Bioelectronics (Academic Press, Inc., New York, 1968) p.79.
4. R. Foster, Organic Charge - Transfer Complexes (Academic Press, London and New York, 1969) p.336.
5. H. Popper and R. Greenberg, Archs Path., 32, 11 (1941).
6. E. Miles, W.H. Postman and R.R. Meggio, J. Am. Chem. Soc., 61, 1929 (1939).
7. M.H. Briggs and R.D. Duncan, Nature, 191, 1310 (1961).
8. D.G. Moulton, Nature, 174, 693 (1962).
9. E.A. Edwards, N.A. Finklestein and E.Q. Duntley, J. Invest. Derm., 16, 311 (1951).
10. P. Flesch, A. Setanove and S.E. Crawford, J. Invest. Derm., 25, 269 (1955).
11. J.R. Platt, Science, 122, 372 (1969).
12. F.U. Lichti and J.A. Lucy, Biochem. J., 112, 221 (1969).
13. J.A. Lucy and F.U. Lichti, Biochem. J., 112, 231 (1969).
14. F.U. Lichti and J.A. Lucy, Biochem. J., 103, 34 (1967).
15. J.A. Lucy, Am. J. Clin. Nut., 22, 1033 (1969).
16. J.A. Lucy, Proc. Biochem. Soc., 96, 12 (1965).
17. J.H. Lupinski, J. Phys. Chem., 67, 2725 (1963).
18. T.G. Ebrey, J. Phys. Chem., 71, 1963 (1967).

19. E.C.M. Chen and W.E. Wentworth, J. Chem. Phys., 63, 3183(1975).

20. W.B. Person, J. Chem. Phys., 38, 109(1963).

21. B.M. Hughes, C. Lifshitz and T.O. Tiernan, J. Chem. Phys., 59, 3162(1973).

22. A.L. Ferragher and F.M. Page, Trans. Faraday. Soc.,63, 2369(1967).

23. F.I. Vilesov, Dokl. Akad. Nauk. SSSR.Ser. Fiz., 132, 632(1960).

24. F.I. Vilesov and A.N. Terenin, Dokl. Akad. Nauk. SSSR. Ser. Fiz., 133, 1059 (1960).

25. D. Mallik, K.M. Jain and T.N. Misra, Ind. J. Biochem. Biophys., 16, 233 (1979).

26. H. McConnel, J.S. Ham and J.R. Platt, J. Chem. Phys., 21,66(1953).

27. R. Foster, Tetrahedron,19, 96 (1960).

28. R. Foster, Organic Charge Transfer Complexes (Academic Press, London and New York, 1969) p.40.

29. M.A. Slifkin, Charge Transfer Interactions of Biomolecules (Academic Press, London and New York, 1971) p.66.

PART - II

INVESTIGATION ON THE SEMICONDUCTIVE PROPERTIES OF SOME ORGANIC COMPOUNDS

CHAPTER 1

INTRODUCTION

1.1 General

Interest in the electrical conduction processes in organic compounds has steadily increased in the past two decades. The major lines of investigation have fairly clear origins. For example, studies of the temperature dependence of the conductivity of aromatic and polymeric solids have been stimulated in part by the suggestion of Szent-Györgyi[1,2] that perhaps the motion of electrons in living systems may be associated with semiconduction process. Since that time, a great many papers have dealt[3,4] with the application of solid state concepts to biological and biochemical phenomena. However, Szent-Györgyi later suggested[5] that, as a general proposition, this idea cannot be accepted because the energy gap commonly encountered in proteins is far too wide; there is simply not enough energy available, generally, in biological systems to raise an electron across a gap of the order of 2.3 eV. However, these concepts have been applied successfully to processes like photosynthesis[6-22] and vision[23-30] for which relatively energetic quanta are indeed available. Moreover, quite a few biochemically important semiconductors have been found[31] which do have substantially lower values of energy gap, notably the carotenes, chlorophylls and at least some amino acids. In fact, most significant contribution which the study of organic semiconductors may bring to the progress of science in general may well be in the broad field of " bioenergetics ".

The biological importance of vitamin A and other long chain polyenes is well known. These compounds are thought[32-35] to be involved in some biological processes like photosynthesis, vision, bacterial respiration and olfactory transduction etc. A significant

feature of these compounds is their conjugated chain structure of alternating single and double bonds. Possibly this may allow them to function as electron mediators in the biological processes. Such conjugation may also manifest itself in semiconduction and superconduction effects. The present investigation is concerned with the semiconductive properties of some linear conjugated polyenes. There has been considerable interest in the electrical conductivity of biologically important semiconductors in recent years[14,15,36-41]. Our interest is centered particularly on two rather remarkable properties, (1) effect of adsorption of gases or vapours on the electrical conductivity and (2) the "compensation behaviour"[39-46] namely a linear relationship between the logarithm of the pre-exponential factor (σ_0) [in the standard[39,40] expression $\sigma(T) = \sigma_0 \exp(-E/2RT)$ for specific conductivity] and the semiconduction activation energy (E).

Adequate interpretation of the semiconduction data of the polyene compounds rests on modern theories of solid state physics. The band theory of solids, the theory of semiconductors, tunneling and hopping model of charge transport and the theory of polaron conduction in solids - all aided to understand the electrical conduction in the conjugated polyene compounds. In the following sections of this chapter, outlines of the relevant parts of these theories are discussed.

1.2 Band Theory of Molecular Crystals

The band theory originally developed for metals, ionic and valence crystals has been applied with some success to molecular crystals[46-49] as well.

In one electron approximation, the wave function for a single electron can be written[50,51] as

$$\Psi_K = \phi_K(\vec{r}) \exp i\vec{K}.\vec{r} \qquad (1.1)$$

where $\vec{K}$ is the wave number vector of the electron; $|\vec{K}| = \frac{2\pi}{\lambda}$, where λ is the associated wavelength; and $\vec{r}$ is the position vector of the electron in the crystal; ϕ_K is a function which has the translational periodicity of the crystal lattice.

If $\phi_K(\vec{r})$ is constant throughout the crystal, then Ψ_K becomes a function which describes a free electron[51]. So this is precisely the type of function which is applicable in metals. The field in which the electrons move is the sum of three components and can be expressed in terms of the operators of the Hartree-Fock type[52-54] operating on ϕ, as

$$V = V' + V'' + V''' \qquad (1.2)$$

where

$$V'' \equiv \int \left\{ \left[\sum_j \phi_j^*(\vec{r_2})\, \phi_j(\vec{r_2}) \right] / r_{12} \right\} dV_2$$

and

$$V''' \equiv -\left\{ \int \left[\sum_j \phi_j^*(\vec{r_2})\, \phi_j(\vec{r_1}) \right] \phi_i(\vec{r_2}) / r_{12}\, dV_2 \right\} / \phi_i(\vec{r_1})$$

Here, V' is the field acting on electron 1 that arises from all the nuclei; V'' is the coulomb potential of the electronic charge distribution and V''' gives rise to a term known as the "exchange" term. In these equations, atomic units of charge are used; volume elements include the spin; ϕ_j is a one-electron function including the spin; $\vec{r}_1$ is the position vector of electron 1; r_{12} is the distance between electrons 1 and 2. V is almost same for all electrons. If V is nearly constant as in most metals, the energy $\varepsilon(\vec{k})$ of an electron with a given value of $\vec{k}$ is given by[51]

$$\varepsilon(\vec{k}) = \left(\frac{\hbar^2}{2m}\right)\vec{k}^2 \qquad (1.3)$$

Due to the fact that the values of $\vec{k}$ are very closely spaced, $\varepsilon(\vec{k})$ is almost a continuous function of $\vec{k}$ and separated bands of permissible $\varepsilon(\vec{k})$ values are not observed. If $\phi_K(\vec{r})$ varies greatly within a unit cell and falls to zero between adjacent cells, then the motion obtained is the opposite extreme of free-electron motion, known as the "tight-binding" condition.[51,52,55] This "tight-binding" is a characteristic of molecular crystals. Under this approximation the one-electron crystal wave functions ψ_K are constructed[56,57] from linear combinations of one-electron molecular wave functions χ_n:

$$\psi_K(\vec{r}) = N^{-\frac{1}{2}} \sum_{n=1}^{N} \exp\left(i\vec{k}.\vec{r}_n\right) \chi_n\left(\vec{r}-\vec{r}_n\right) \qquad (1.4)$$

Here $\vec{r}_n$ locates the geometrical centre of molecule n, and the sum extends over the N molecules in the crystal. The molecular wave function χ_n is oriented in the crystal in the same way as molecule

n i.e., χ_n is the same function for all n. It is assumed that the integrals $\int \chi_m^* \chi_n \, d\tau = 0$ if $m \neq n$.

Applying the periodic boundary conditions[68] an elementary cell in $\vec{K}$ space can be defined whose volume is given by the conditions

$$-\pi < \vec{K}.\vec{\alpha}\,,\ \vec{K}.\vec{\beta}\,,\ \vec{K}.\vec{c} \leq +\pi \qquad (1.5)$$

where $\vec{a}$, $\vec{b}$, and $\vec{c}$ are unit cell vectors in a monoclinic lattice with two molecules in unit cell situated at (0,0,0) and at (a/2, b/2, 0) $\vec{\alpha}$ and $\vec{\beta}$ are defined by $\vec{\alpha} = \frac{1}{2}(\vec{a}+\vec{b})$ and $\vec{\beta} = \frac{1}{2}(-\vec{a}+\vec{b})$; $\vec{\alpha}$, $\vec{\beta}$ and $\vec{c}$ connect the centers of nearest neighbour molecules. The conditions represented by equation (1.5) define a zone in $\vec{K}$ space which is not identical with the conventional Brillouin zone.[51,52,55]. There is a one-to-one correspondence between the points in the Brillouin zone and the points in the elementary cell defined by equation (1.5). Since the Brillouin zone is extremely complex in shape, the equation (1.5) is generally used to set the limits on $\vec{K}$.

The crystalline field is approximated by

$$V(\vec{r}) = \sum_n V_n \left(\vec{r} - \vec{r}_n\right) \qquad (1.6)$$

where V_n is the Hartree potential of an isolated neutral molecule. The eigenvalue of ψ_n is written[68] as

$$\mathcal{E}'(\vec{K}) = \mathcal{E}_0 + \mathcal{E}_1 + 2 \sum_s{}' \mathcal{E}_s \cos \vec{K}.\vec{r}_s \qquad (1.7)$$

where, $$\varepsilon_o = \int \chi_n \left[-(h^2\Delta/2m) - eV_n \right] \chi_n \, d\tau \qquad (1.8)$$

$$\varepsilon_1 = \sum_s{}' \int |\chi_n|^2 V_{n+s} \, d\tau \,, \quad s \neq 0 \qquad (1.9)$$

$$\varepsilon_s = \int \chi_{n+s} V_{n+s} \chi_n \, d\tau \qquad (1.10)$$

and the lattice vectors $\vec{r_s}$ and $-\vec{r_s}$ are counted as one in the sum (eqn. 1.7). The prime sign on $\sum$ indicates that the term with $\vec{r_s} = 0$ is omitted from the summation. The eigenfunctions obtained from equation (1.4) are for a fictional triclinic lattice. These are single valued functions of $\vec{k}$ in a Brillouin zone defined by the conditions in equation (1.6) and can be transformed to the proper notation for the monoclinic space group by choosing a Brillouin zone half as big :

$$-\pi < \vec{k}.\vec{a}, \ \vec{k}.\vec{b}, \ \vec{k}.\vec{c} \leq +\pi \qquad (1.11)$$

and taking two eigen functions per $\vec{k}$,

$$\psi_k^{\pm} = \left(\tfrac{1}{N}\right)^{\frac{1}{2}} \sum_n \left[\left(\exp 2\vec{k}.\vec{n_1} \right) \chi_{n_1} \pm \left(\exp 2\vec{k}.\vec{n_2} \right) \chi_{n_2} \right] \qquad (1.12)$$

where n_1 and n_2 are the two molecules in unit cell n. The eigen values in this notation are

$$\varepsilon^{\pm}(\vec{k}) = \varepsilon_o + \varepsilon_1 + 2\sum_s{}' \varepsilon_s \cos \vec{k}.\vec{r_s} \pm 2\sum_s \varepsilon_{s+\alpha} \cos\left[\vec{k}.(\vec{r_s}+\vec{\alpha})\right] \qquad (1.13)$$

The intermolecular resonance integrals ε_s determine the structure of the band. The resonance integrals fall off rapidly with intermolecular distance and only a few nearest neighbour interactions are found to be important. Functional forms for V_n and the appropriate χ_n are required to evaluate[56,57] ε_s. The band structure depends on the structure of the crystal lattice. In case of anthracene, the integral between molecules connected by $\vec{\alpha}$ is the same as that between molecules connected by $\vec{\beta}$ and we call them both ε_α. The other significant terms are $\varepsilon_b\,(\vec{r}_s = \vec{b})$ and $\varepsilon(\vec{r}_s = \vec{c}+\vec{\alpha}$ and $\vec{r}_s = \vec{c}-\vec{\beta})$. The integral between molecules connected by $\vec{c}$ is negligible, as is that between molecules connected by $\vec{a}$. The one-electron energy for each band, then, neglecting the constant energy terms ε_o and ε_1, is given by

$$\varepsilon(\vec{K}) = 2\varepsilon_\alpha\left[\cos\vec{K}\cdot\vec{\alpha} + \cos\vec{K}\cdot\vec{\beta}\right] + 2\varepsilon_b\cos\vec{K}\cdot(\vec{\alpha}+\vec{\beta}) + 2\varepsilon_\gamma\cos\vec{K}\cdot(\vec{c}+\vec{\alpha}) + \cos\vec{K}\cdot(\vec{c}-\vec{\beta}) \qquad (1.14)$$

1.3 The Conduction Equation

If n_i is the concentration of the ith species of charge carriers having mobility μ_i and total charge z_i times the electronic charge (e), the net conductivity of the medium for i different species of carriers is given by

$$\sigma = \sum_i \left[z_i e n_i \mu_i \right] \qquad (1.15)$$

It is assumed that there is negligible interaction between different carrier species.

In case of semiconductors where the charge carriers are electrons and holes, the equation (1.15) can be written as

$$\sigma = n_c e \mu_e + n_h e \mu_h \qquad (1.16)$$

Here n_c is the concentration of electrons in the conduction band, n_h is the concentration of holes in the valence band, μ_e is the mobility of electrons and μ_h is the mobility of holes.

The concentration of electrons in the conduction band, n_c, can be expressed by[51,55]

$$n_c = \int_{E_c}^{top} \rho(E)\, F(E)\, dE \qquad (1.17)$$

where E_c represents the bottom of the conduction band, $\rho(E)$ is the density of states and $F(E)$ is the Fermi-Distribution function. Integration of expression (1.17) with assumption[56] $(E_c - E_F) \geq 4kT$, gives

$$n_c = 2(2\pi m_e^* kT/h^2)^{3/2} \exp(E_F - E_c)/kT \qquad (1.18)$$

where m_e^* is the effective mass of the electron near E_c and E_F is the Fermi-Energy.

The concentration of holes, n_h, in the valence band may be written as[51,56]

$$n_h = \int_{bottom}^{E_v} \rho(E)\left[1 - F(E)\right] dE \qquad (1.19)$$

where the integration extends over the valence band; E_v is the energy

corresponding to the top of the valence band. If it is assumed[66] that the Fermi-level lies more than about $4kT$ above E_v, then $1 - F(E) \approx \exp(E - E_F)/kT$ and integration of (1.19) gives

$$n_h = 2(2\pi m_h^* 2k/h^2)^{3/2} \exp(E_v - E_F)/kT \qquad (1.20)$$

where m_h^* represents the effective mass of a hole near the top of the valence band. Employing the fact that $n_c = n_h$ one can get from (1.18) and (1.20)

$$E_F = (E_c + E_v)/2 + \frac{3}{4} kT \log(m_h^*/m_e^*) \qquad (1.21)$$

Substitution of this value of E_F in (1.18), yields

$$n_c = n_h = 2(2\pi kT/h^2)^{3/2} (m_e^* m_h^*)^{3/4} \exp(-E/2kT) \qquad (1.22)$$

where E represents the energy gap between the valence and the conduction bands. This is applicable only to an intrinsic semiconductor in thermal equilibrium. Thus, from equation (1.16) the conductivity of an intrinsic semiconductor is given by

$$\sigma = \sigma_0 \exp(-E/2kT) \qquad (1.23)$$

where,
$$\sigma_0 = 2e(2\pi kT/h^2)^{3/2} (m_e^* m_h^*)^{3/4} (\mu_e + \mu_h) \qquad (1.24)$$

The effective mass m^* of an electron or a hole is a concept which is much used in band theory. It is defined[51,55] by the equation

$$m^* = h^2 / \frac{d^2\epsilon}{dk^2} \qquad (1.25)$$

where ϵ is the energy of an electron with wavenumber $\vec{k}$ ($k = 2\pi/\lambda$, where λ is the de Broglie wavelength). A large value of the

effective mass corresponds to a low mobility; both are determined by the width of the band. The mobility μ in general is a tensor μ_{ij} and is thus anisotropic[66]. The velocity $\vec{v}(\vec{k})$ associated with an electron in a level characterized by the wavenumber vector $\vec{k}$, which has the energy $\varepsilon(\vec{k})$ is given[51,69] by

$$\vec{v}(\vec{k}) = \left(\frac{\partial \pi}{h}\right)\left(\frac{\partial \varepsilon(\vec{k})}{\partial \vec{k}}\right) \qquad (1.20)$$

The mobility can be expressed in terms of the components of the velocity and of a function which depends on the scattering of the electrons as they move through the lattice.

1.4. Tunneling Model of Dark Conduction

Tunneling is a quantum mechanical phenomenon in which a particle such as an electron passes through a potential energy barrier without acquiring enough energy to pass over the top of the barrier.

The tunneling mechanism generally considered was proposed by Eley and Willis[60] is illustrated in Fig. 1.1. Here three adjacent similar molecules are shown : (a) in the absence of an applied voltage gradient V (volts cm^{-1}); and (b) after application of V and after the excitation of an electron in the central molecule. The diagram is schematic and the energy levels in a molecule are shown as equally spaced which is not observed in real molecules. After excitation of the electron from the $(\frac{N}{2})$ th level to the $(\frac{N}{2}+1)$ th level both the electron and the hole can tunnel as shown in Fig. 1.1(b)

FIG. 1.1 : Tunnel model[60] of an organic semiconductor

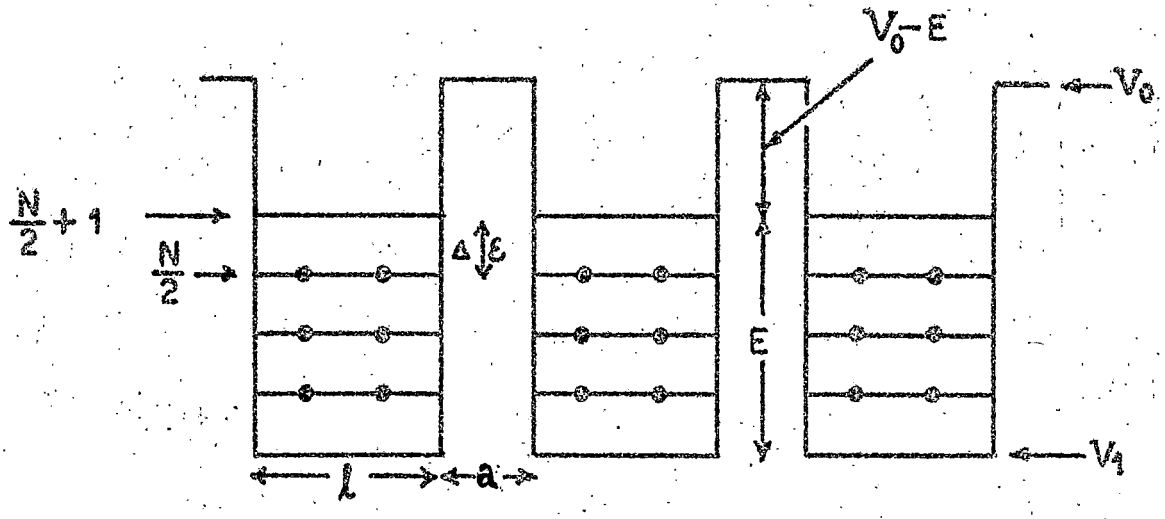
$V_0 - E$
V_0
$\frac{N}{2}+1$
$\frac{N}{2}$
$\Delta\varepsilon$
E
V_1
l
a

(a)

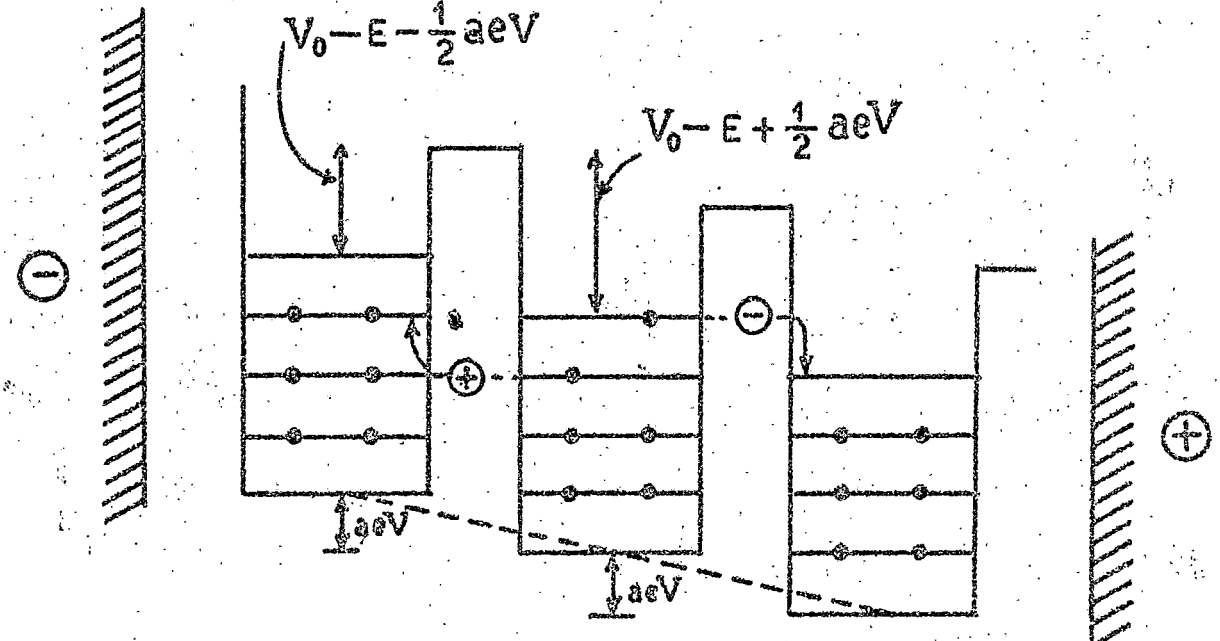
$V_0 - E - \frac{1}{2}aeV$
$V_0 - E + \frac{1}{2}aeV$
$\frac{1}{2}aeV$
aeV

(b)

FIG. 1·1

The total energy change for transferring the electron is

$$\Delta E = I_G - A_G - a e V - \left(\frac{e^2}{\epsilon r}\right) \qquad (1.27)$$

where I_G , A_G are the ionization energy and electron affinity of the organic molecule; 'a' the barrier width; aeV, the energy change caused by the applied field V indicated in Fig. 1.1 (b) by a vertical displacement of a potential well relative to its neighbour. The term $e^2/\epsilon r$ expresses the coulombic interaction of the opposite charges separated by a distance r. The effective permittivity ϵ for the region between the charges is generally high because of the polarisability of surrounding π-electrons. Since the ion pair will polarize the surrounding medium, a correction term should be applied to the formula (1.27).

The number of times an electron penetrates an intermolecular barrier gives a measure of its drift velocity. It is proportional to the product of the number of times it strikes the barrier and the probability of penetration. The electron in the $\left(\frac{N}{2}+1\right)$ th level is regarded as moving between the potential walls with a velocity v_e given by

$$v_e = \left(\frac{N}{2}+1\right)\frac{h}{2lm_e^*} \qquad (1.28)$$

where l is the distance across the well and m_e^* , the effective mass of the electron. If P_f and P_r represent the probability of penetrating the barrier of width 'a' in the direction of the field and in the reverse direction respectively, the drift velocity v_{de} of the electron in the field is

$$v_{de} = \left(\frac{v_e}{2l}\right)(a+l)\left(P_f - P_r\right)$$

$$= \left[\left(\frac{N}{2}\right)+1\right]\left(h/4l^2 m_e^*\right)(a+l)\left(P_f - P_r\right) \qquad (1.29)$$

and the current density is given by

$$i = n e v_{de} \qquad (1.30)$$

In the equation (1.29) it is assumed that the net displacement of the electron upon going through the barrier is $(a+l)$.

Thus considering the value of n as n_c obtained from equation (1.22), the equation for 'i' can be given by

$$i = \left[2\left(2\pi m_e^* kT\right)^{3/2}/h^3\right]\left[\exp\left(-E/2kT\right)\right]\left(\frac{N}{2}+1\right),$$

$$e h (a+l)\left(P_f - P_r\right)/4l^2 m_e^* \qquad (1.31)$$

which is an equation of the form

$$i = \sigma_o V \exp\left(-E/2kT\right) \qquad (1.32)$$

An evaluation of P_f and P_r now enables σ_o to be calculated. Here P_f and P_r depend on the shape of the barrier.

1.5 The Hopping Model for Dark Conduction

If two molecules are separated by a potential barrier, a carrier on one can move to the other by moving over the barrier via an activated state — the process is called hopping.

A simple hopping model has been applied by Pohl[61] and by Pohl and Opp[62] to the motion of carriers in an organic solid. The carriers are considered to move by hopping to neighbouring molecules in a manner which is random except for the anisotropy caused by the applied field (F). If the carriers are electrons, then

$$i = ne\mu F \tag{1.33}$$

where n is the concentration of electrons.
It can be shown that

$$\mu = \left[f a^2 e N_s (kT)^2 / (h^3 \nu^2) \right] \exp\left(-E_s / kT\right) \tag{1.34}$$

where f is the average angle of hopping with regard to the direction of F; a, the intermolecular distance; N_s, the number of neighbouring sites; ν, the frequency of vibration in the two directions normal to the direction of carrier motion across the barrier; E_s, the height of the barrier. The interaction of the carrier with vibration in the lattice[63] may also give hopping of charge carriers without having these to cross a potential barrier. Considering such electron-lattice interaction using the localized representation[64] the value of μ becomes

$$\mu = (ea^2/\hbar)\left[2\pi \beta_u^2 / (kT + \hbar\omega_0) \right] \exp\left[-\gamma_u (2S+1)\right] \cdot I_0\left\{ 2\gamma_u \left[S(S+1) \right]^{\frac{1}{2}} \right\} \tag{1.35}$$

where β_u denotes the matrixelement connecting molecular functions on sites seperated by a distance u ; ω_0 is Debye frequency for acoustic waves; γ is a dimensionless parameter and accounts for

the electron-lattice interaction; S is given by

$$S = 1 / [\exp(\hbar\omega_0 / kT) - 1] \qquad (1.36)$$

and I_0 denotes a Bessel function. For the hopping model to be valid not only $\hbar\omega_0$ is to be much greater than β , but the carrier must also remain on a lattice site much longer than the period of a vibration; that is, the relaxation time (τ_u) in which the electron hops from a site j to a site $j+u$ must be much greater than $2\pi/\omega_0$. Then the equation representing the mobility in case of hopping model i.e.,

$$\mu = (ea^2) / kT\,(1/\tau_u) \qquad (1.37)$$

suggests that $\mu << (ea^2/\hbar)(\hbar\omega_0/kT) \approx 1\ cm^2\ volt^{-1}\ sec^{-1}$.

Thus one criterion which arises for the validity of the hopping model is that the mobility should be less than about 1 cm^2 $volt^{-1}$ sec^{-1}. The other criterion which has sometimes been quoted is that a positive temperature dependence of mobility indicates that a hopping model applies. However, Glerum[64] has shown that, although the mobility increases with temperature when the interaction between the carrier and the lattice is large, when $\gamma < 10$ the mobility either does not change or it decreases with increasing temperature.

1.6 Polerons in Molecular Crystals

In some circumstances the interaction of electrons and phonons can lead to the electrons being trapped in self-induced potential

wells. The entity which then moves through the crystal is not an electron by itself, but an electron accompanied by a localized vibration, a combination which is called a polaron[63].

Fiebrand[65,66] has considered a molecular crystal with one excess electron. The half-width of the one-electron band in the tight binding approximation is given by

$$J_k = \sum_u \langle \chi^0_{j+u} | V_j | \chi^0_j \rangle \qquad (1.38)$$

where $|\chi^0_j\rangle$ is a molecular ionic function centered at the lattice point j and unperturbed by nuclear motions. Intermolecular vibrations of the lattice which interact only weakly with carriers and which have a low velocity are neglected, but molecular vibrations, taken to be harmonic, are regarded as contributing to the formation of polarons. Considering these assumptions and writing the electron phonon interaction as linear in the vibrational co-ordinates one finds that the binding energy of the polaron is of the order

$$E_b \approx \tfrac{1}{2} \sum_q M_q^2 \omega_q (\Delta x_q)^2 \qquad (1.39)$$

where M_q is the reduced mass of the qth oscillator; ω_q, the frequency; Δx_q, the difference between the equilibrium distances of molecule and ion.

The formation of Bloch-type bands from the polarons, by treating the electronic overlap as a perturbation, now becomes possible. Such bands are narrower than the corresponding electron band by a vibrational overlap factor. Their width, when the phonon velocity is

small compared with that of the polaron, is given by

$$J_\sigma(v^\circ+v) = J_K \langle v_j | v_j^\circ \rangle^2 \qquad (1.40)$$

where v° and v are vibrational quantum numbers of the neutral molecule and the ion; $|v_j\rangle$ and $|v_j^\circ\rangle$ are the corresponding ion and molecular vibrational wave functions at center j. Approximately then,

$$J_\sigma(v^\circ+v) \approx J_K (E_b/\hbar\omega)^{v^\circ+v} [\exp(-E_b/\hbar\omega)] \qquad (1.41)$$

Thus there exists, below the electron band, a series of polaron bands with widths J_σ.

When the polarons are strongly bound, i.e., $E_b \gg J_K$ and $E_b \gg \hbar\omega \gg 2\pi J_\sigma$, a number of important conclusions can be drawn. At very low temperatures, the carriers will occupy the lowest-lying polaron band. They will have low mobilities which are limited by lattice phonon scattering, in which case $\mu \propto T^{-3/2}$ to T^{-1}. At higher temperatures, the higher energy bands will be populated, and the effective band width will increase exponentially with temperature. It follows that $d\mu/dT$ will gradually change sign. As T approaches E_b/k, the mobility is governed by the distribution between polaron bands and the electron band, so that transport becomes an activated hopping process. As T exceeds E_b/k, the distribution over the bands is approximately independent of T and again $\mu \propto T^{-3/2}$ to T^{-1}.

Another interesting conclusion regarding the effects of temperature arises from the condition that

$$\hbar\omega >> 2\pi J_\sigma \tag{1.42}$$

which is itself a consequence of the uncertainty principle. It means that for polaron formation the time an electron remains on a lattice site should be long compared with the period of a vibration, $2\pi/\omega$. This is the reason why lattice phonons in molecular crystals generally are not expected to participate in the formation of polarons. Now let us consider the temperature T_t equal to E_b/k. Here the polaron will dissociate thermally, and the electron will move without an accompanying molecular vibration. When the width of a polaron band is such that $\hbar\omega \approx 2\pi J_\sigma$, the polaron can be said to dissociate kinetically, the electron not remaining on the lattice site longer than the period of a vibration. Siebrand applies this notion to the case in which the carrier moves by activated hopping from a polaron band to the electron band and has an effective band width J' at $T=T'$. For an activated hoping process,

$$\mu = ea^2/\tau kT' \tag{1.43}$$

$$\text{since} \qquad \omega/2\pi = 1/\tau \gg J'/\hbar \tag{1.44}$$

also, it follows that $\mu < 1 cm^2 volt^{-1} sec^{-1}$, if $a = 5\text{Å}$ and $\hbar\omega = kT'$. This conclusion agrees with that of Glarum[64].

The polaron band structure, equation (1.41), having been determined, transport is discussed by assuming that the polarons interact weakly with lattice vibrations. The polarons thus are scattered in a way which gives rise to a relaxation time $\tau(\vec{k})$.

Then the band structure and carrier mobility are connected by well-known formulas

$$\vec{v}(\vec{K}) = \hbar^{-1} \vec{\nabla}_K \varepsilon(\vec{K})$$
$$D_{ij} = \langle v_i(\vec{K})\, v_j(\vec{K})\, \tau(\vec{K}) \rangle \qquad (1.45)$$
$$\mu_{ij} = e D_{ij} / kT$$

where $\vec{v}(\vec{K})$ is the velocity of a carrier in state $|\vec{K}\rangle$; $\varepsilon(\vec{K})$ is the energy of $|\vec{K}\rangle$; D_{ij}, μ_{ij} are components of the diffusivity and mobility tensors.

When the carriers interact strongly with molecular vibrations, this interaction should be included in the zeroth order carrier wave function. This implies that the complete wave function for the crystal no longer separates into electronic and vibrational parts. The electron-vibration interaction results in a narrower band widths.

The coupling criteria has been discussed by McRae and Siebrand[67]. These criteria can be generalized to three dimensions, as is done by Siebrand[68]. He uses the dimensionless parameters

$$\gamma \equiv - E_b / \hbar\omega \qquad (1.46)$$

and $$\beta \equiv |\vec{J}| / \hbar\omega \qquad (1.47)$$

for a one-dimensional array of one dimensional oscillators. When γ is large, the carriers are effectively localized. This theory assumes a simple form when the intermolecular coupling is either strong or weak, but is more complicated when coupling is intermediate.

1.6.1 The Tunneling and Hopping of Polarons

When an electron is surrounded by a cloud of phonons, a transition from site j to site j' results in the destruction of the cloud at j and the creation of a new cloud at j'. There is thus a large number of phonon emissions and absorptions accompanying the transition, and the electron is scattered many times during a single jump to a neighbouring site. The electron on a site is trapped in a potential well and has to pass a barrier of a height equal to the binding energy of the polaron in order to move to the neighbouring site. This passage[68] is a tunneling in molecular solids. Tunneling, which is analogous to a wave-like motion, applies when the vibrational states involve only a few quanta and are well separated; hopping applies when a large number of highly excited vibrational levels are crowded together and consists of randomly performed jumps. The translational symmetry of the lattice necessarily implies[69] wave-like motion. However, translational symmetry may be destroyed by thermal motion. If the phonon band width exceeds that of the polaron band, the disperaion of the lattice frequencies introduces enough randomness to annihilate the polaron band structure. The crystal may then, behave like a liquid with respect to carrier transport (hopping being the mechanism) and the mobility should not change much upon melting contrary to that generally observed.[70,71] Polaron tunneling is therefore thought to be the mechanism of carrier transport in molecular solids.

The probability P_{hj} that the electron jumps from a site h to a site $j = h \pm 1$ is calculated by time-dependent perturbation theory as[68]

$$P_{hj} = 4|\langle h|H'_e|j\rangle|^2 \sin^2(xt/2)\, t^2 x^2 \qquad (1.48)$$

where $\hbar x = E_j - E_h$ and H'_e refers to that part of the Hamiltonian of which the eigenfunctions describe the motion of the electron between the molecules. In the matrix element $\langle h|H'_e|j\rangle$, h and j refer to molecular wave functions. Here P_{hj} can be expressed more explicitly as

$$P_{hj} = (2\pi/\hbar)\rho(0)\, t\, J^2 S_{oo}^4 \exp\left[-4E_b \sum_{\sigma} v_{\sigma}(1-\cos\sigma)/N\hbar\omega(\sigma)\right] \qquad (1.49)$$

where N is the number of lattice sites; ω, the vibrational angular frequency; t, the time; σ, 2π times the phonon wave number; $\rho(0)$, a density of states at $x=0$; J, the intermolecular electronic coupling between nearest neighbours; S_{oo}, the vibrational overlap integral for zero values of the vibrational quantum numbers v.

A detailed treatment of equation (1.49) is given by Holstein[72]. The diffusivity D is given by

$$D = a^2 \bar{P}_{hj} / t \qquad (1.50)$$

where a is the lattice spacing and $\bar{P}_{hj}$ is the thermal average of P_{hj} obtained by substituting in equation (1.49), the thermal averages of v_{σ} denoted by $\bar{v}_{\sigma}$, where

$$\bar{v}_{\sigma} = N/\left\{\exp\left[\hbar\omega(\sigma)/kT\right]-1\right\} \qquad (1.51)$$

For temperatures $T \gg \hbar\omega/k$, mobility is expected to increase exponentially as T increases. If $T \gg \hbar\omega/k$, Holstein has shown that

$$D \sim \exp\left(-E_a/kT\right) \qquad (1.52)$$

where E_a, the activation energy, is of the order of but smaller than $-E_b$.

References

1. A. Szent-Györgyi, Science, 23, 609 (1941).
2. A. Szent-Györgyi, Nature, 148, 157 (1941).
3. A. Szent-Györgyi, Bioenergetics edited by L.G. Augenstine (Academic Press, New York, 1957).
4. C. Reid, Excited States in Chemistry and Biology (Academic, New York, 1957).
5. A. Szent-Györgyi, Discussions Faraday Soc., No. 27, 111, 239 (1959).
6. M. Calvin and P.D. Sogo, Science, 125, 499 (1957).
7. G. Tollin, P.D. Sogo and M. Calvin, Ann. N.Y. Acad. Sci., 74, 310 (1958).
8. M. Calvin, Rev. Mod. Phys., 31, 157 (1959).
9. M. Calvin and G.M. Androes, Microalgae and Photosynthetic Bacteria, 319 (1963).
10. D.P. Ilten and M. Calvin, J. Chem. Phys., 42, 3760 (1966).
11. P.A. Loach, G.M. Androes, A.F. Maksim and M. Calvin, Photochem. Photobiol., 2, 443 (1963).
12. E. Katz, Photosynthesis in Plants edited by M.E. Loomis and J. Franck (Iowa State Coll. Press, Ames, Iowa, 1949) p 291.
13. S.S. Brody, Z. Elektrochem., 64, 187 (1960).
14. B. Rosenberg and J.F. Camiscoli, J. Chem. Phys., 35, 982(1961).
15. B. Rosenberg, J. Chem. Phys., 34, 812 (1961).
16. H.T. Witt, R. Morew, A. Müller, B. Rumberg and G. Zieger, Z. Elektrochem., 64, 181 (1960).

17. M. Calvin, "Light and Life Conference" (The Johns Hopkins University, Baltimore, Md., 1960).

18. D.F. Bradley and M. Calvin, Proc. Nat. Acad. Sci. U.S.A., 41, 563 (1955).

19. M. Kotani, Rev. Mod. Phys., 35, 717 (1963).

20. D.R. Keans and M. Calvin, J. Am. Chem. Soc., 83, 2110 (1961).

21. M. Calvin, Rev. Mod. Phys., 31, 147 (1959).

22. E. Rabinowitch, Discussions Faraday Soc., No. 27, 161 (1959).

23. B. Rosenberg, R.A. Orlendo and J.M. Orlando, Arch. Biochem. Biophys., 93, 395 (1961).

24. E.W. Abrahamson, J. Marquisee, P. Gavuzzi and J. Roubie, Z. Elektrochem., 64, 177 (1960).

25. B. Rosenberg, J. Chem. Phys., 31, 233 (1959).

26. W.A. Hagins and W.H. Jennings, Discussions Faraday Soc., No. 27, 180 (1959).

27. G. Wald, Exptt. Cell Res. Suppl., 5, 338 (1958).

28. H. Fernandez - Moran, Rev. Mod. Phys., 31, 319 (1959).

29. F.S. Sjostrand, Rev. Mod. Phys., 31 301 (1959).

30. B. Rosenberg, Symposium on Electrical Conductivity in Organic Solids, edited by H. Kallmann and M. Silver (Interscience, New York, 1961) p 291.

31. F. Gutmann and L.E. Lyons, Organic Semiconductors (John Wiley and Sons, Inc., New York, London and Sydney, 1967) p 758-765.

32. J.R. Platt, Science, 123, 372 (1959).

33. B. Rosenberg, Advances in Radiation Biology edited by L.G. Augenstein, R. Mason and M.R. Zelle(Academic Press, New York, 1966) Vol.-2, p 193.

34. D.G. Moulton, Handbook of Sensory Physiology edited by L.M. Beidler (Springer-Verlag Berlin, Heidelberg, New York, 1971) Vol.-4, p 59.

35. B. Rosenberg, T.P. Misra and R. Switzer, Nature, 217, 423(1968).

36. T.P. Misra, B. Rosenberg and R. Switzer, J. Chem. Phys., 48, 2036 (1968).

37. D.D. Eley and R.S. Snart, Biochem. Biophys. Acta, 102, 379(1965).

38. B. Rosenberg, J. Chem. Phys., 36, 816 (1962).

39. B. Rosenberg, B. Bhowmik, H.C. Harder and E. Postow, J. Chem. Phys., 49, 4108 (1968).

40. G. Kemeny and B. Rosenberg, J. Chem. Phys., 53, 3549 (1970).

41. G. Kemeny and I.M. Ceklany, J. Theor. Biol., 40, 107 (1973).

42. G. Kemeny and B. Rosenberg, J. Chem. Phys., 52, 4151 (1970).

43. T.A. Kaplan and S.D. Mahanti, J. Chem.Phys., 62, 100 (1975).

44. G. Kemeny and S.D. Mahanti, Proc. Nat.Acad.Sci.,U.S.A., 72, 909 (1975).

45. H. Masui, H. Nagasaka and K. Yahagi, Japan J. Appl. Phys., 16, 177 (1977).

46. J.L. Katz, S.A. Rice, S.I. Choi and J. Jortner, J. Chem. Phys., 39, 1683 (1963).

47. R. Silbey, J. Jortner, S.A. Rice and M.T. Vala, Jr., J. Chem. Phys., 42, 733 (1965).

48. R. Silbey, J. Jortner, S.A. Rice and M.T. Vala, Jr., J. Chem. Phys., 43, 2925 (1965).

49. R.G. Kepler, Organic Semiconductors edited by J.J. Brophy and J.W. Buttrey (Macmillan, New York, 1962) p 1.

50. F. Bloch, Z. Physik, 52, 555 (1928).

51. C. Kittel, Introduction to Solid State Physics (Wiley Eastern Private Ltd., New Delhi, 1971) 3rd. Edition.

52. W.A. Harrison, Solid State Theory (Tata McGraw-Hill Publishing Co. Ltd., Bombay and New Delhi, 1970) TMH Edition.

53. F. Gutmann and L.E. Lyons, Organic Semiconductors (John Wiley and Sons. Inc., New York, London and Sydney, 1967) p 826.

54. L. Pauling and E.B. Wilson, Introduction to Quantum Mechanics (McGraw-Hill Logakusha Ltd., Japan, 1935).

55. A.J. Dekker, Solid State Physics (Macmillan and Co. Ltd., London, 1967).

56. O.H. Le Blanc, Jr., J. Chem. Phys., 35, 1275 (1961).

57. O.H. Le Blanc, Jr., J. Chem. Phys., 36, 1032 (1962).

58. F. Seitz, The Modern Theory of Solids (McGraw-Hill, New York and London, 1940).

59. W. Shockley, Electrons and Holes in Semiconductors, Van Nostrand and Co. Inc., Princeton, N.J.,1950) p 308.

60. D.D. Eley and M.R. Willis, Symposium on Electrical Conductivity in Organic Solids edited by H. Kallmann and M. Silver (Interscience Publishers, New York, 1961)p 257

61. H.A. Pohl, Modern Aspects of the Vitreous State edited by J.D. Mackenzie (Butterworth, London, 1962) p 105.

62. H.A. Pohl and D.A. Opp, J. Phys. Chem., 66, 2121 (1962).

63. H. Fröhlich and G.L. Sewell, Proc. Phys. Soc.(London), 74, 643 (1959).

64. S.H. Glarum, Phys. Chem. Solids, 24, 1577 (1963).

65. W. Siebrand, Abstr. Organic Crystal Symposium (N.R.C., Ottawa, 1962) p 56.

66. W. Siebrand, Doctorate Thesis (University of Amsterdam, 1963).

67. E.G. McRae and W. Siebrand, J. Chem. Phys., 41, 905 (1964).

68. W. Siebrand, J. Chem. Phys., 41, 3574 (1964).

69. B.L. Nageev, Soviet Phys. Solid State, 3, 1267 (1962).

70. O.H. Le Blanc, Jr., Abstr. of Organic Crystal Symposium (N.R.C., Ottawa, 1962) p 82.

71. O.H. Le Blanc, Jr., J. Chem. Phys., 37, 916 (1962).

72. T. Holstein, Ann. Phys. (N.Y.), 8, 325, 343 (1959).

CHAPTER 2

EXPERIMENTAL : MATERIALS, METHODS AND APPARATUS

2.1 Experimental

The general descriptions of the experimental techniques used in this research are given below. Details of a particular experimental method will be described in conjunction with the discussion of the results thereby obtained.

2.2 Chemicals

The polyene semiconductors used in this work are vitamin A alcohol (all-trans), vitamin A acetate (all-trans), β -apo-8'-carotenal, astacene and methyl bixin. Chemical structures of these polyenes have already been shown in chapter 2, part I. The organic liquids used in this investigation are toluene, benzene, ethyl acetate, n-heptane, ethanol and methanol. These liquids were of spectrograde or equivalent quality of B.D.H (England) and E. Merck (Germany). The teflon spacers and sheets, and the conducting glass electrodes required for this work were obtained from Dielectrix Corporation (U.S.A.) and Fisher Scientific Co. (U.S.A.) respectively.

2.3 Preparation of the " Sandwich " Conductivity Cell

Applying the usual procedure[1-4] the conductivity cells were made in air by placing about 5 mgs of the semiconductive materials on a clean stainless steel electrode (plate) in safe light illumination. Two teflon spacers, 2 mils (0.005 cm) thick, were positioned near the edges of the electrode, and the powdered crystals were

flattened by gently rotating a piece of conducting glass electrode on the top with the conducting side making contact with the specimen. The teflon spacer maintained the separation between the electrodes. To maintain the sandwich cell, two spring clips were fixed at a moderate pressure to the ends of the electrodes.

2.4 Experimental Arrangements :

A schematic diagram of the experimental set-up for the studies of semiconductivity presented in Fig. 2.1 is similar to that of Rosenberg et al[2,5]. The sandwich cells were placed in a conductivity chamber made of brass and fashioned entirely with teflon - all the electrical surface leakage parts were of teflon. The stainless steel electrode was placed on a thermal copper bar platform in good thermal contact through thermal paste and thus the temperature of the sandwich cell could be controlled from outside. A d.c. voltage of 22.5 volts from dry batteries was applied across the cells. There was a gas inlet and an outlet in the chamber for gas adsorption study and an arrangement for connecting the outlet with a suction pump. The chamber atmosphere could circulate freely through the opposite open sides of the sandwich cell. Temperature measurements were made by using a copper-constantan thermocouple attached at the top of the metal electrode and a millivolt potentiometer of Toshniwal Brothers Pvt. Ltd., India. The semiconduction current measurements were made with an electrometer amplifier, EA 815, of the Electronic Corporation of India Ltd. In order to eliminate the effect of oxygen, water vapour or any other vapours or gases adsorbed by the sample before

FIG. 2.1 : A schematic diagram of the apparatus used to test the effects of the adsorbed vapours (or gases) on the conductivity of the polyene semiconductors.

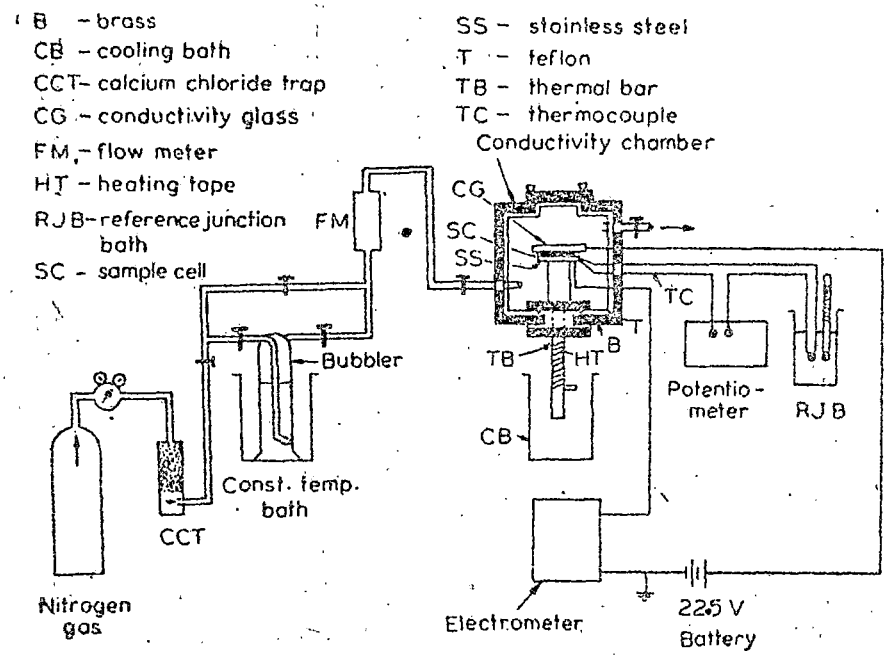
B – brass
CB – cooling bath
CCT – calcium chloride trap
CG – conductivity glass
FM – flow meter
HT – heating tape
RJB – reference junction bath
SC – sample cell
SS – stainless steel
T – teflon
TB – thermal bar
TC – thermocouple
Conductivity chamber
CG
SC
SS
FM
TC
T
B
TB
HT
CB
Bubbler
Const. temp. bath
CCT
Nitrogen gas
Potentio-meter
RJB
Electrometer
22.5 V Battery

FIG. 2·1

experiment, the chamber was thoroughly flushed with dry nitrogen gas and the sample was then given repeated heating and cooling treatments in nitrogen atmosphere over the temperature range to be used. To pass various vapours inside the chamber, dry nitrogen gas was used as a carrier which was passed through the bubbler containing the organic liquid kept at a required temperature to maintain a fixed partial vapour pressure less than the saturation vapour pressure at sample cell temperatures. For desorption studies, dry nitrogen gas was allowed to pass directly through the chamber. The measurements of dark currents at a constant or different cell temperatures were carried out maintaining the conductivity cells at nitrogen, vacuum or different ambient atmospheres according to our experimental requirement.

References

1. T.N. Misra, B. Rosenberg and R. Switzer, J. Chem. Phys., 48, 2096 (1968).

2. B. Rosenberg and E.C. Harder, Photochemistry and Photobiology, 6, 629 (1967).

3. B. Rosenberg, J. Chem. Phys., 34, 63 (1961).

4. B. Rosenberg, J. Chem. Phys., 31, 232 (1959).

5. B. Rosenberg, T.N. Misra and R. Switzer, Nature, 217, 423 (1968).

CHAPTER 3

EFFECT OF ADSORPTION OF VAPOURS ON THE ELECTRICAL CONDUCTIVITY OF SOME POLYENE SEMICONDUCTORS : ADSORPTION AND DESORPTION KINETICS

3.1 Introduction

Adsorption of gases changes the semiconductive properties of both organic[1-6] and inorganic[7-10] solids. Adsorption of oxygen produces a pronounced increase of semiconduction current in phthalocyanine[1], anthracene[2,11,12] and chlorophylls[13]. Number of other gases also affect the current. Adsorption of various gases and vapours enhances the specific conductivity of β-carotene[4,6]. It has been observed that the conductivity change is generally reversible[5,6,14] — one can return to the initial value of conductivity simply by desorbing the gases or vapours.

Gray and Darby[10] have studied in detail the semi-conductivity changes during the adsorption and desorption of oxygen gas on oxides of copper, nickel, manganese and zinc of extremely high purity. They have considered the first order, second-order and exponential relationships $(dm/dt) = Km$, $(dm/dt) = Km^2$ and $(dm/dt) = K \exp(-\epsilon m)$ respectively where m is the number of adsorbed atoms at time t; K and ϵ are constants. These relationships have been derived by many authors making direct measurements of the amount of gases adsorbed Gray et al[10] have shown that the exponential plot is a better over-all approximation for the complex order process than for one obeying the first order kinetics, or a combination of the second and first order processes at the initial and final period of adsorption respectively. In working out the kinetics, Gray and Darby have assumed that the measured conductivity is either proportional to $\sqrt{m}$ or to m.

In case of hydration of proteins[15] and adsorption of gases on β -carotene[6], it has been observed that the adsorption-time curves follow the Roginsky-Zeldovichs'[16,17] exponential equation in a slightly modified form. The derivation of this equation assumes that the rate of adsorption (dm/dt) possesses an activation energy which increases linearly with the amount (m) of the adsorbed gas or vapour,

$$\frac{dm}{dt} = A \exp(-\beta m / kT) \qquad (3.1)$$

where for a particular pressure A and β are constants. These workers, unlike that of Gray et al.[10] have shown with a good degree of certainty that at a constant temperature and for lower percentage of gas or vapour adsorption, the relationship between the conductivity (σ) and the amount of gas or vapour adsorbed is given by[5,6,18]

$$\sigma_A(m) = \sigma_V \exp(\alpha m) \qquad (3.2)$$

where σ_V and σ_A are the specific conductivities before and after adsorption of m percent of gas or vapour; α is a constant.

However, experiments clearly show that there is a direct correlation between the rate of adsorption of gases or vapours and the change in semiconduction current. It is therefore, necessary to examine this correlation in detail to determine the most reasonable and accurate correlation. As the rate of adsorption of gases or vapours depends on its pressure, the consideration of formal adsorption kinetics is incomplete without an examination of the pressure

dependence of the adsorption process and hence of the conductivity change.

In this chapter, we first discuss how the conductivity of polyene semiconductors depends on the pressure of the adsorbed vapours and then examine the validity of the Hopinsky - Zeldovich relation.

3.2 Experimental and Results

3.2.1 Semiconduction of some polyenes and the effect of adsorption of vapours on the semiconduction current.

The effects of adsorption of some vapours were studied in the usual manner as described in the previous chapter. The sandwich cell was temperature cycled and in addition to that dry nitrogen gas was allowed to pass through the chamber to desorb any vapour or gas adsorbed by the sample prior to the experiment. The cell was then kept at room temperature (28°C) and the carrier gas, dry nitrogen, was passed through the reagent liquid which was kept at a constant temperature to maintain a required vapour pressure. After a few moments as the powder sample started to adsorb the vapour from the chamber-atmosphere, the current began to increase and attained a saturation value after half an hour approximately. The current enhancement was by several orders of magnitude in some cases. The result of such a measurement for ethyl acetate vapour adsorption in vitamin A alcohol is shown in Fig. 3.1. The curve (b) of Fig. 3.1

FIG. 3.1 : The change in dark current in a vitamin A alcohol powder cell kept at 25°C with (a) adsorption and (b) desorption of ethyl acetate vapour at 43.5 mm pressure.

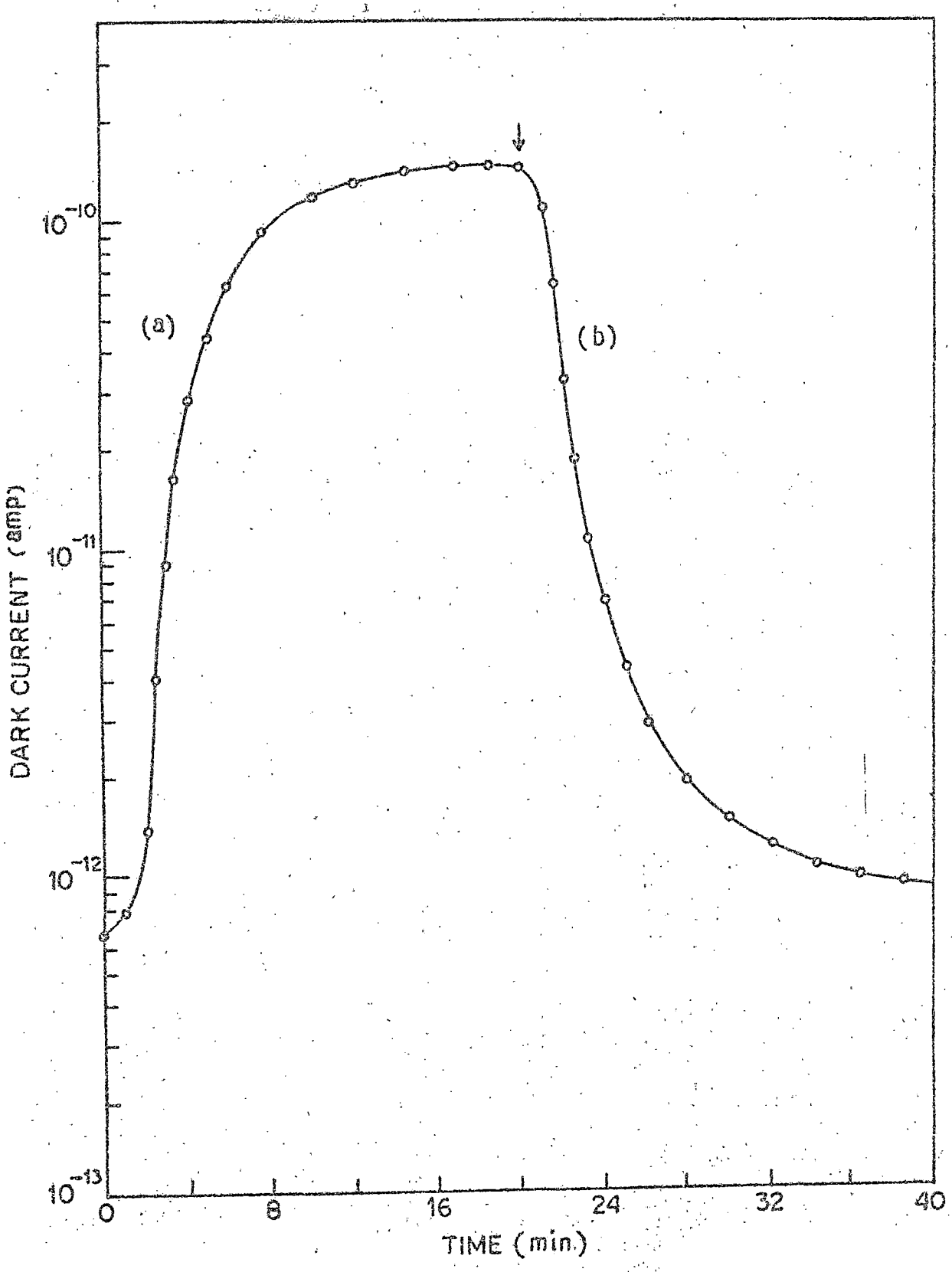

FIG: 3.1

shows the decrease in conductivity back to its initial value when the chamber is flushed with dry nitrogen gas and the vapour is desorbed from the crystallite surfaces. The arrow indicates the time when desorption starts. Such adsorption and desorption kinetic curves for vitamin A acetate, β -apo-8'-carotenal, astacene and methyl bixin for ethyl acetate vapour adsorption are shown in Figs. 3.2 - 3.5, respectively. All these curves show excellent reversibility of current on desorption of vapours. Similar curves are obtained for toluene, benzene, n-heptane, ethanol and methanol vapour adsorption also. The maximal value of current reached under particular experimental conditions, depends on the vapour pressure of the reagent liquid at its temperature and also on the temperature of the sample cell; time to reach this value depends also on the flow rate. To test the sensitivity of a particular polyene semiconductor for different vapours, saturation current values were noted after adsorption of various vapours at a fixed partial vapour pressure with a constant flow rate and a constant sample cell-temperature. The sensitivity as measured by σ_A/σ_V values of the different polyene semiconductors in sandwich cells for adsorption of various vapours are summarized in tables 3.1 and 3.2. Apparently, the sensitivity depends on the chemical nature of the adsorbed molecules.

3.3.2 Semiconduction as a function of vapour pressure

We have studied the magnitude of the current increase at a constant sample cell temperature as a function of the partial pressure of the vapours in the chamber. The temperature of the reagent liquid through which dry nitrogen gas was passed and fed

FIG. 8.2 : The change in dark current in a vitamin A acetate powder cell kept at 25°C with (a) adsorption and (b) desorption of ethyl acetate vapour at 42.0 mm pressure.

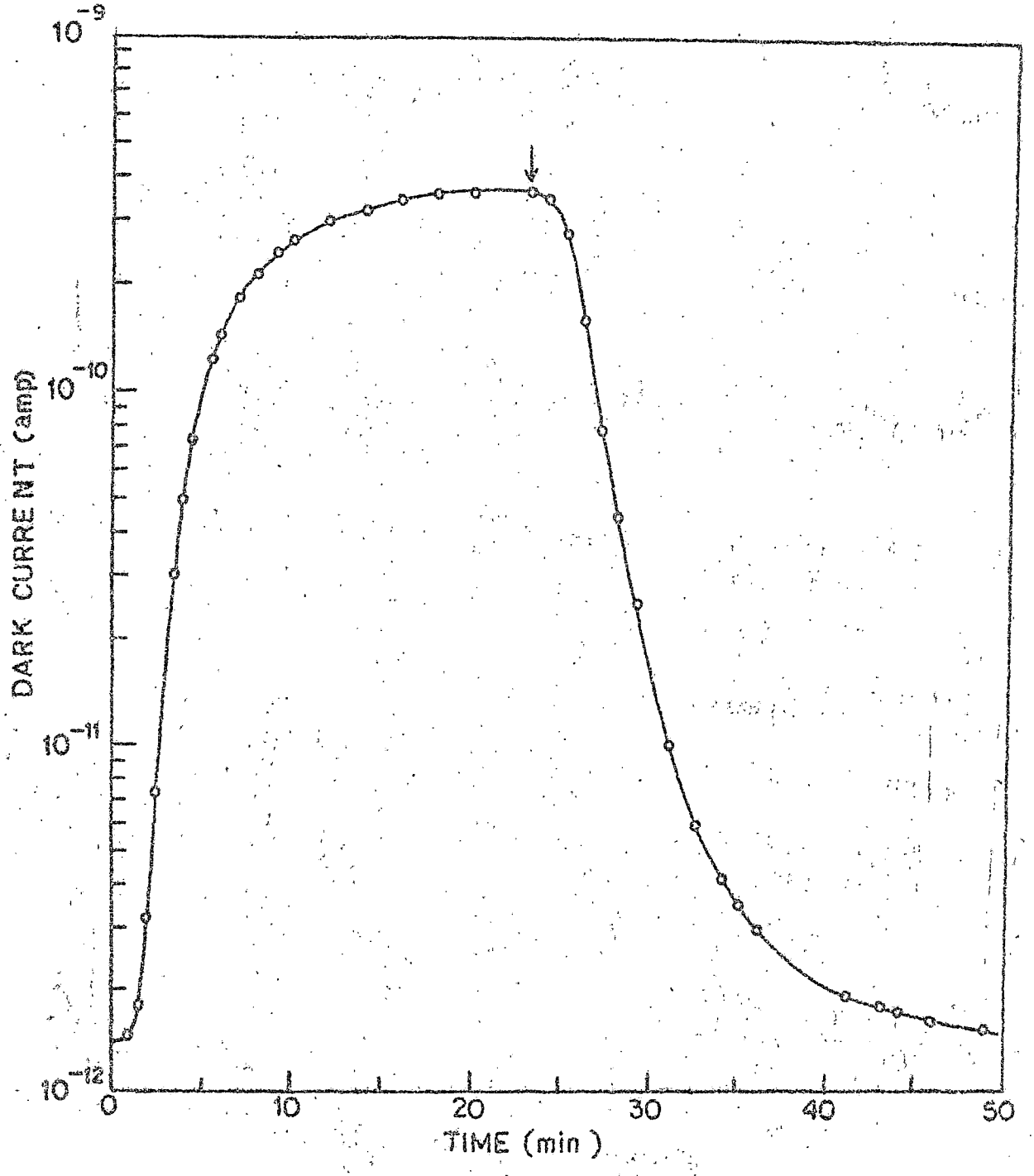

FIG. 3·2

FIG. 3.3 : The change in dark current in a β -apo-8'-carotenal powder cell kept at 25°C with (a) adsorption and (b) desorption of ethyl acetate vapour at 53.8 mm pressure.

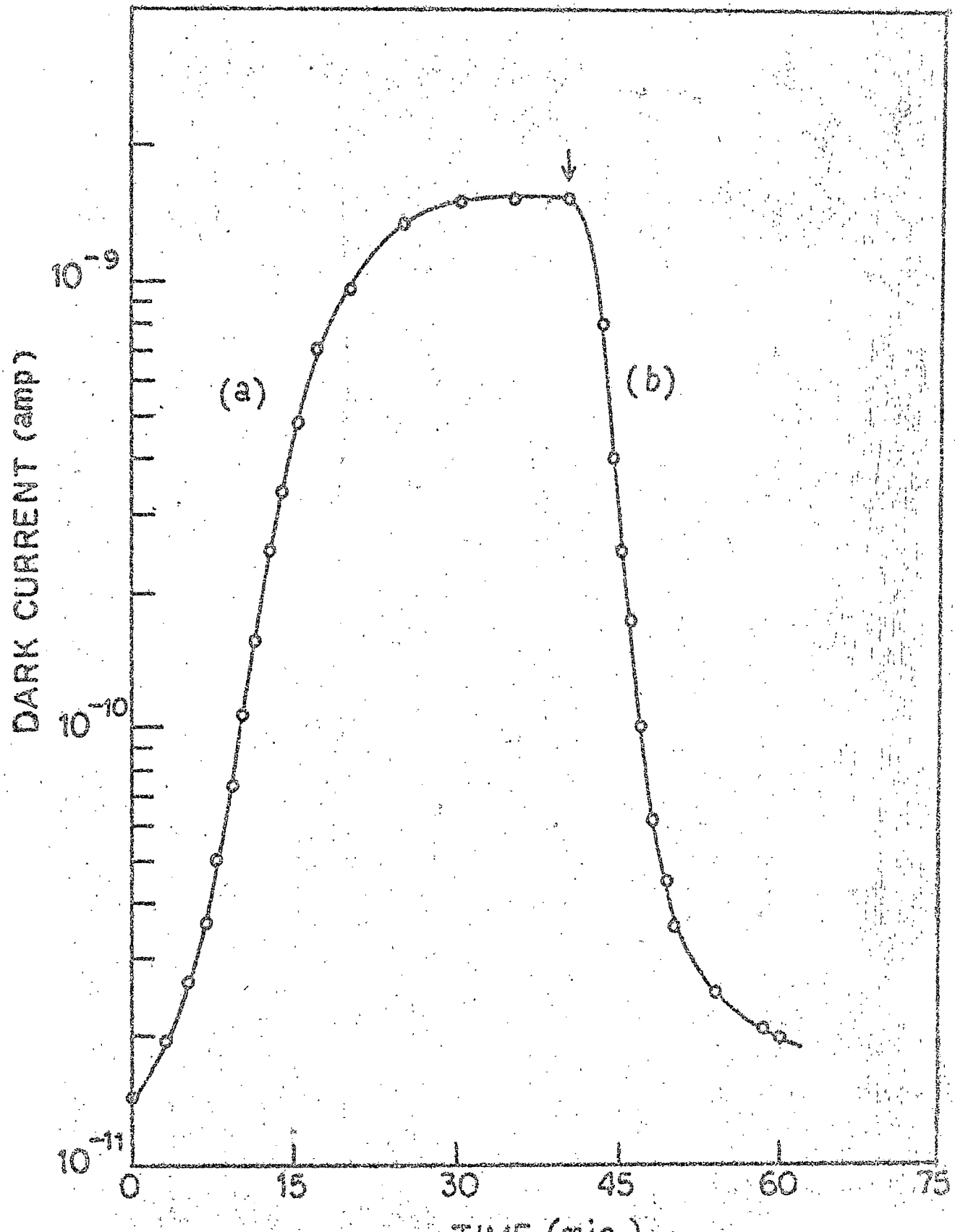

FIG. 3.3

FIG. 3.4 : The change in dark current in an anthracene powder cell kept at 25°C with (a) adsorption and (b) desorption of ethyl acetate vapour at 70.0 cm pressure.

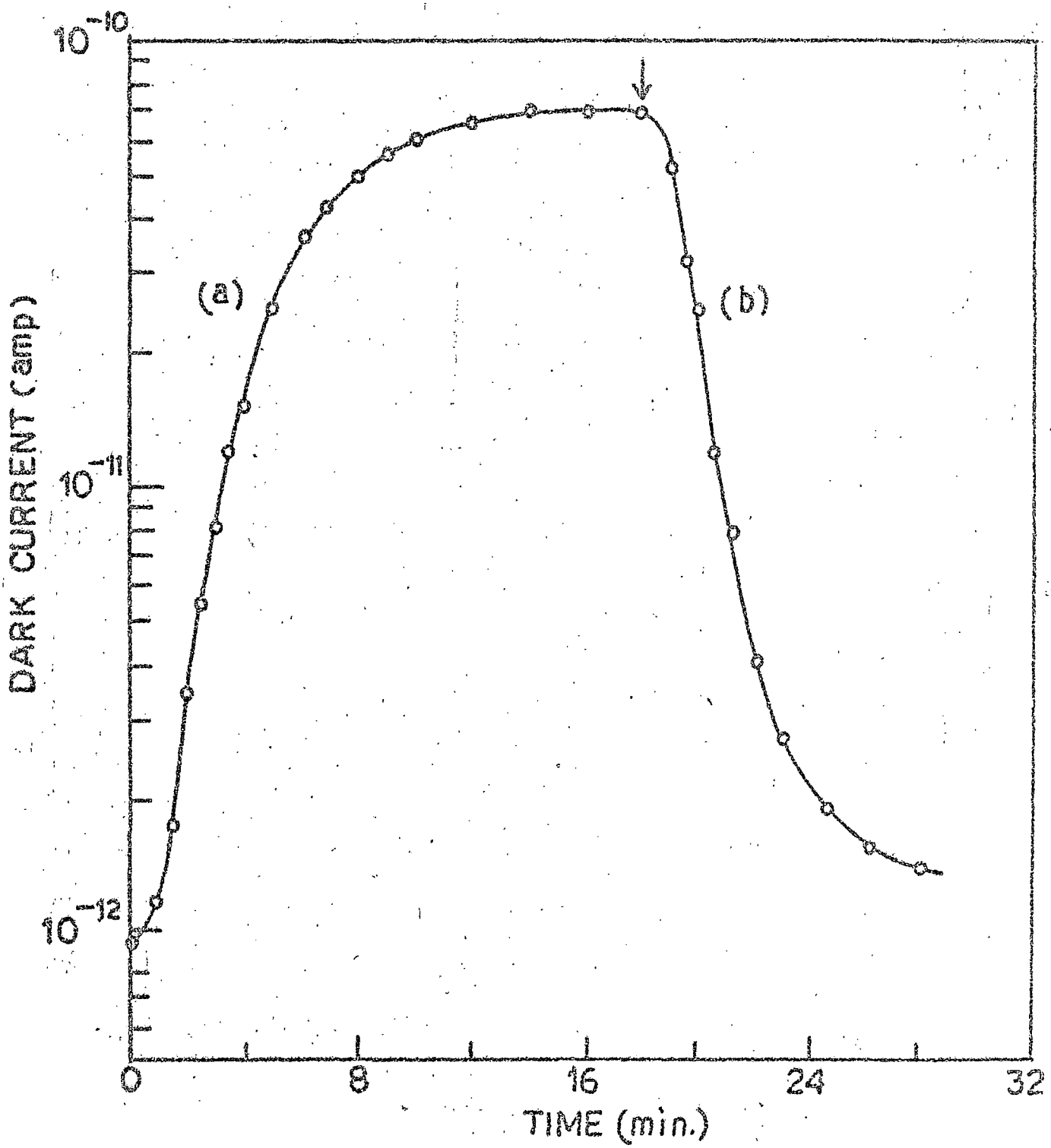

FIG. 3·4

FIG. 3.5 : The change in dark current in a methyl bixin powder cell kept at 25°C with (a) adsorption and (b) desorption of ethyl acetate vapour at 80.0 mm pressure.

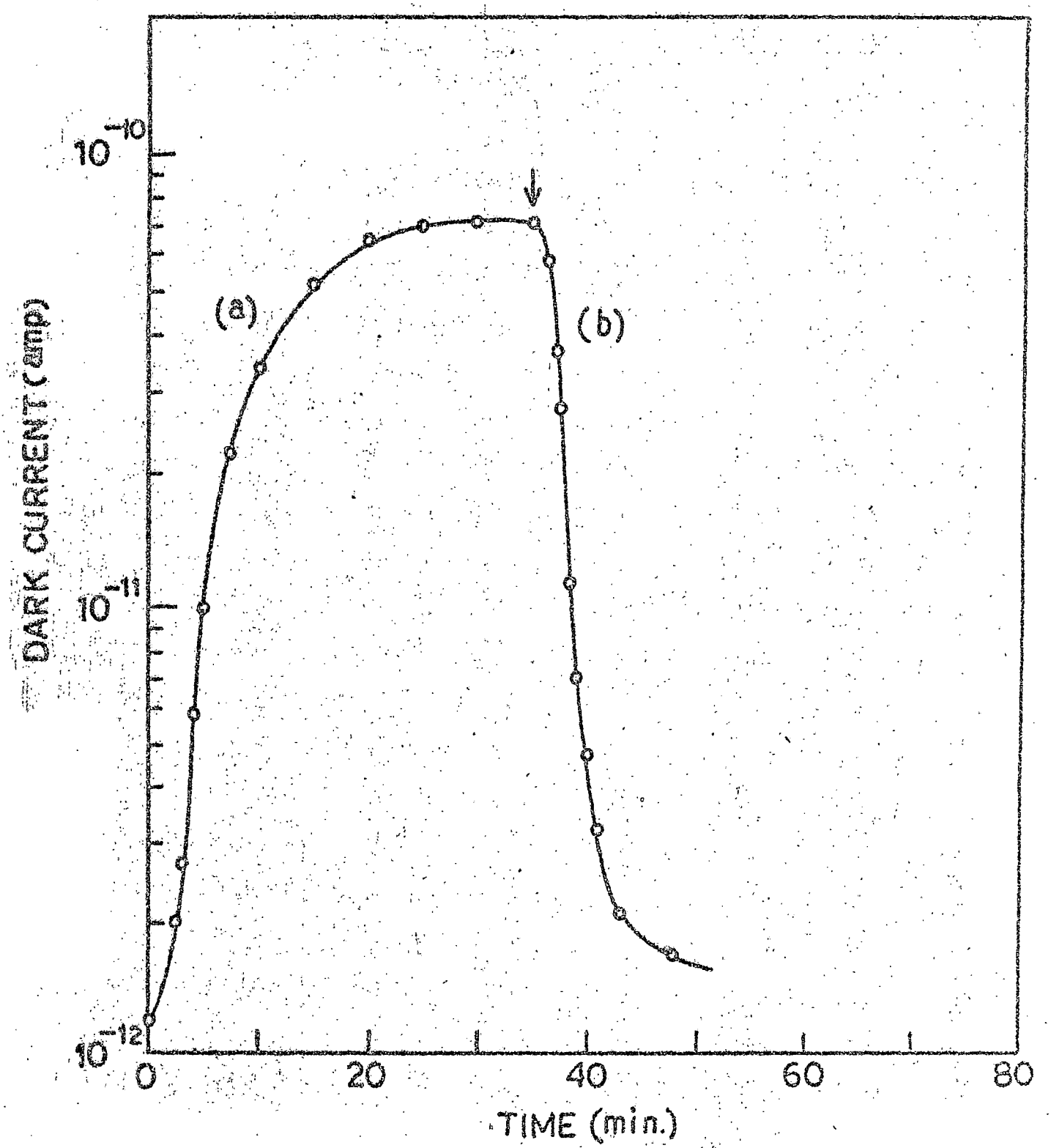

FIG. 3·5

Table - 3.1

Rise in the dark current in vitamin A (alcohol and acetate) powder cells at 12.5°C due to adsorption of various vapours at the same pressure of 40 mm.

Vapour adsorbed	Dielectric constant[1] at 25°C	Ionisation potential[2] (eV)	σ_A / σ_V	
			vitamin A alcohol	vitamin A acetate
Toluene	2.38	8.81	2.3×10^4	5.0×10^4
Benzene	2.28 (20°C)	9.24	6.7×10^3	1.7×10^4
Ethyl acetate	6.00	10.11	6.5×10^3	1.3×10^4
n-Heptane	1.93 (20°C)	10.35	4.0×10^3	3.8×10^3
Ethanol	24.30	10.50	3.0×10^2	2.0×10^3
Methanol	32.60	10.85	4.5×10	3.2×10^2

1. Ref. 19
2. Ref. 20 and 21

Table - 3.2

Rise in the dark current in the powder cells of some polyenes at 18.5°C due to adsorption of various vapours at the same pressure (p) for a particular polyene

Vapour adsorbed	Dielectric constant	Ionisation potential (eV)	σ_A / σ_V		
			β-apo-8'-carotenal p = 42 mm	Octacene p = 60 mm	Methyl bixin p = 60 mm
Toluene	2.38	8.81	7.3	1.8	1.6
Benzene	2.28 (20°C)	9.24	4.2	2.5	3.3
Ethyl acetate	6.00	10.11	5.0×10^2	1.5×10^2	1.0×10^1
n-Heptane	1.93 (20°C)	10.35	4.4	-	-
Ethanol	24.30	10.50	5.0×10^3	4.0×10^3	1.0×10^2
Methanol	32.60	10.85	6.5×10^2	5.0×10^2	3.3×10^1

into the conductivity chamber was varied. At a constant flow rate, the partial pressure of the reagent liquid vapour in the chamber atmosphere was proportional to the vapour pressure of the liquid at the temperature it was kept. The steady state current (i.e., saturation current) was noted for different vapour pressures. The kinetics for the dark current enhancement for different partial pressures of ethyl acetate ambient vapour for vitamin A alcohol, vitamin A acetate, β -apo-8'-carotenal, astacene and methyl bixin semiconductors are shown in Figs. 3.6 - 3.10 respectively.

3.3 Discussion

3.3.1 Sensitivity of the semiconductors for various vapours

It is seen from the tables 3.1 and 3.2 that there may be a rough correlation of the sensitivity of a semiconductor with the ionization potential of the adsorbed molecules but none with their static dielectric constant. As regards the correlation of conductivity enhancement with the ionization potential, the polyenes can be divided into two groups. In one, namely vitamin A alcohol and acetate the sensitivity is more, the lower is the ionization potential (table 3.1) while in the other, namely β -apo-8'-carotenal, astacene and methyl bixin, the sensitivity is more the higher is the ionization potential (table 3.2). Indeed, charge-transfer type of interaction has often been thought[22-24] to be responsible for the conductivity enhancement on gas or vapour adsorption.

FIG. 8.6 : The change in dark current in a vitamin A alcohol powder cell kept at 26°C after adsorption of ethyl acetate vapour at different pressures.

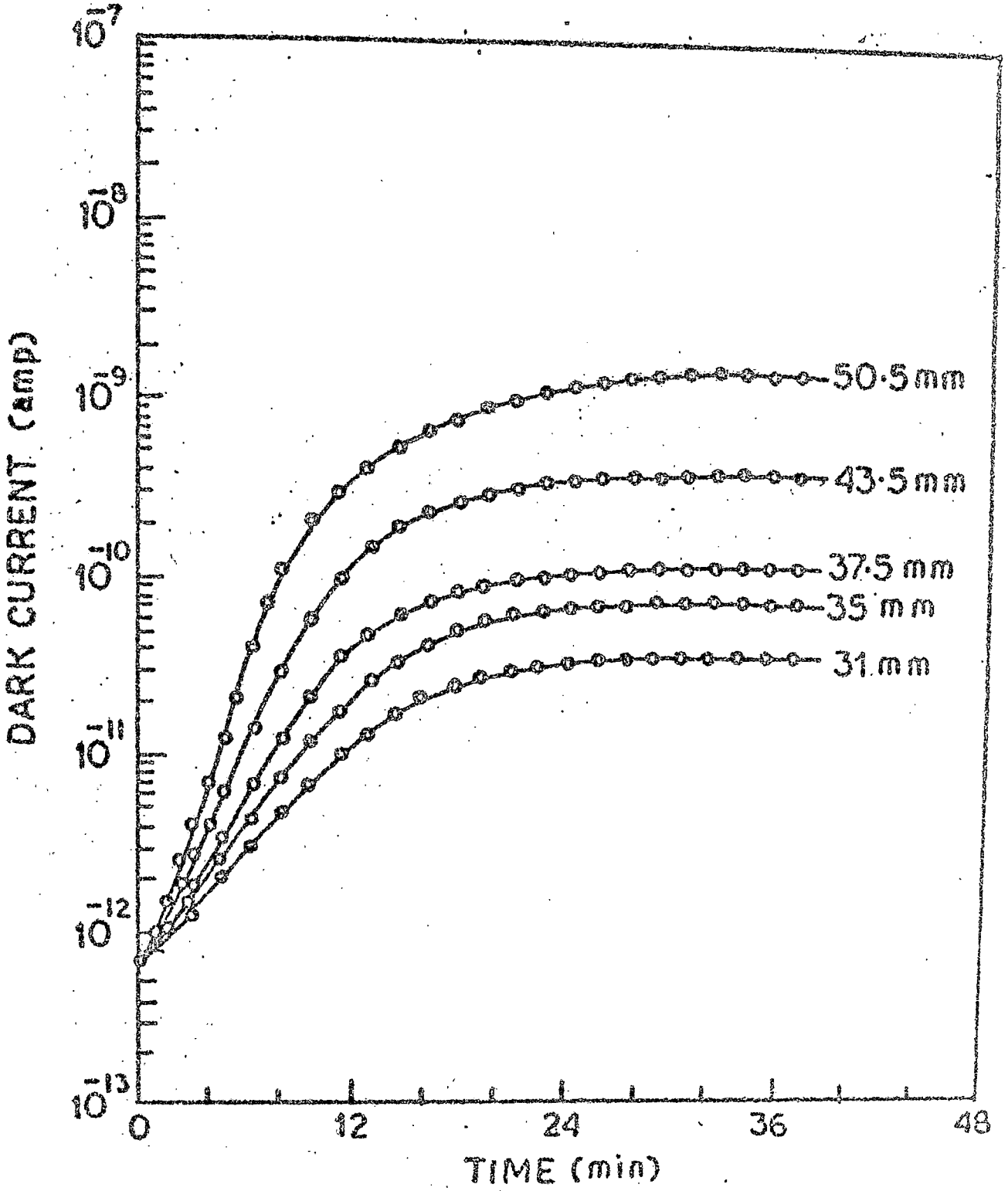
DARK CURRENT (amp)
10^{-7}
10^{-8}
10^{-9}
10^{-10}
10^{-11}
10^{-12}
10^{-13}
50·5 mm
43·5 mm
37·5 mm
35 mm
31 mm
0
12
24
36
48
TIME (min)

FIG. 3·6

FIG. 3.7 : The change in dark current in a vitamin A acetate powder cell kept at 25°C after adsorption of ethyl acetate vapour at different pressures.

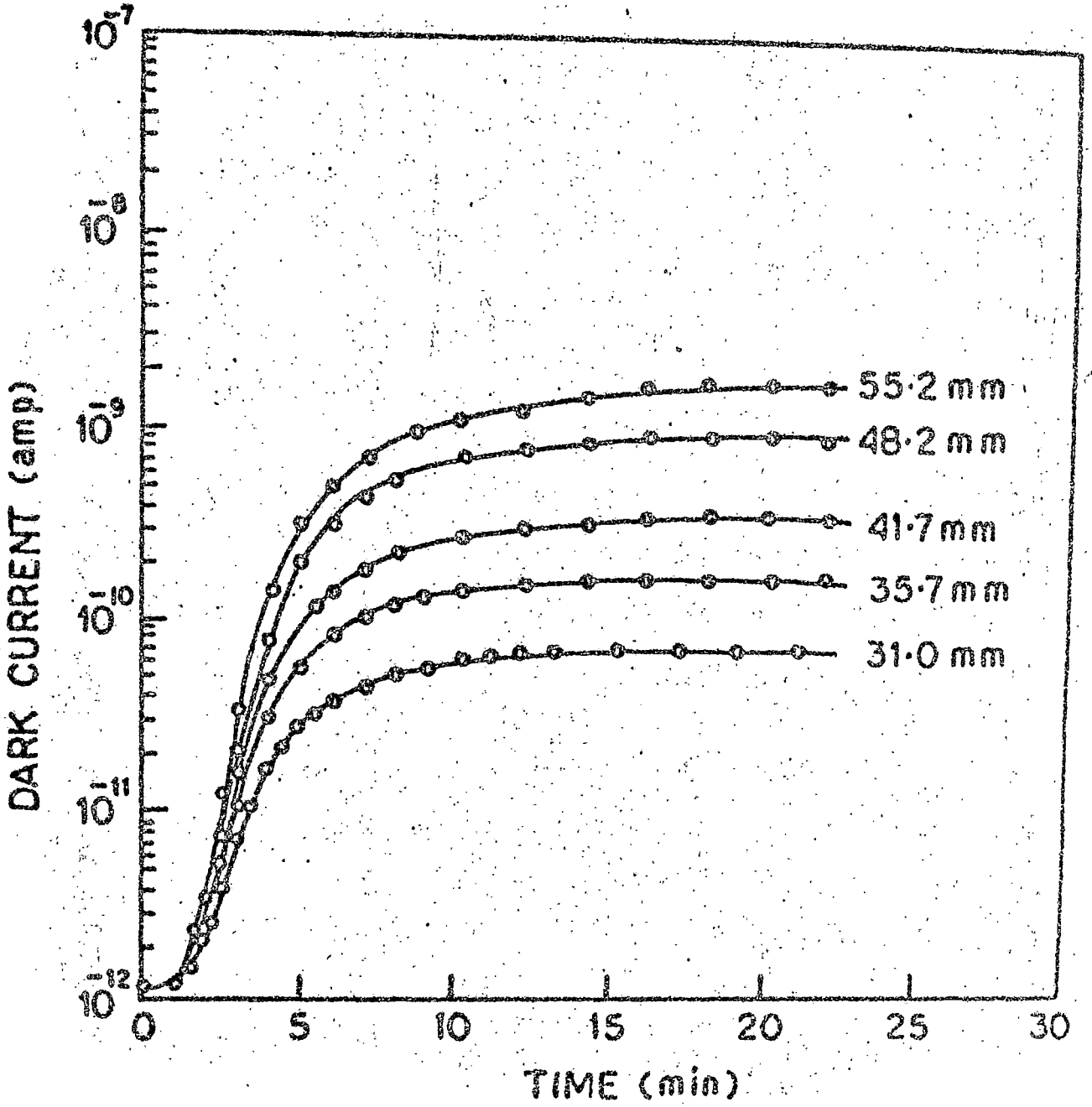
DARK CURRENT (amp)
10^{-7}
10^{-8}
10^{-9}
10^{-10}
10^{-11}
10^{-12}
55·2 mm
48·2 mm
41·7 mm
35·7 mm
31·0 mm
0
5
10
15
20
25
30
TIME (min)

FIG. 3·7

FIG. 3.8 : The change in dark current in a β -apo-8'-carotenal powder cell kept at 26°C after adsorption of ethyl acetate vapour at different pressures.

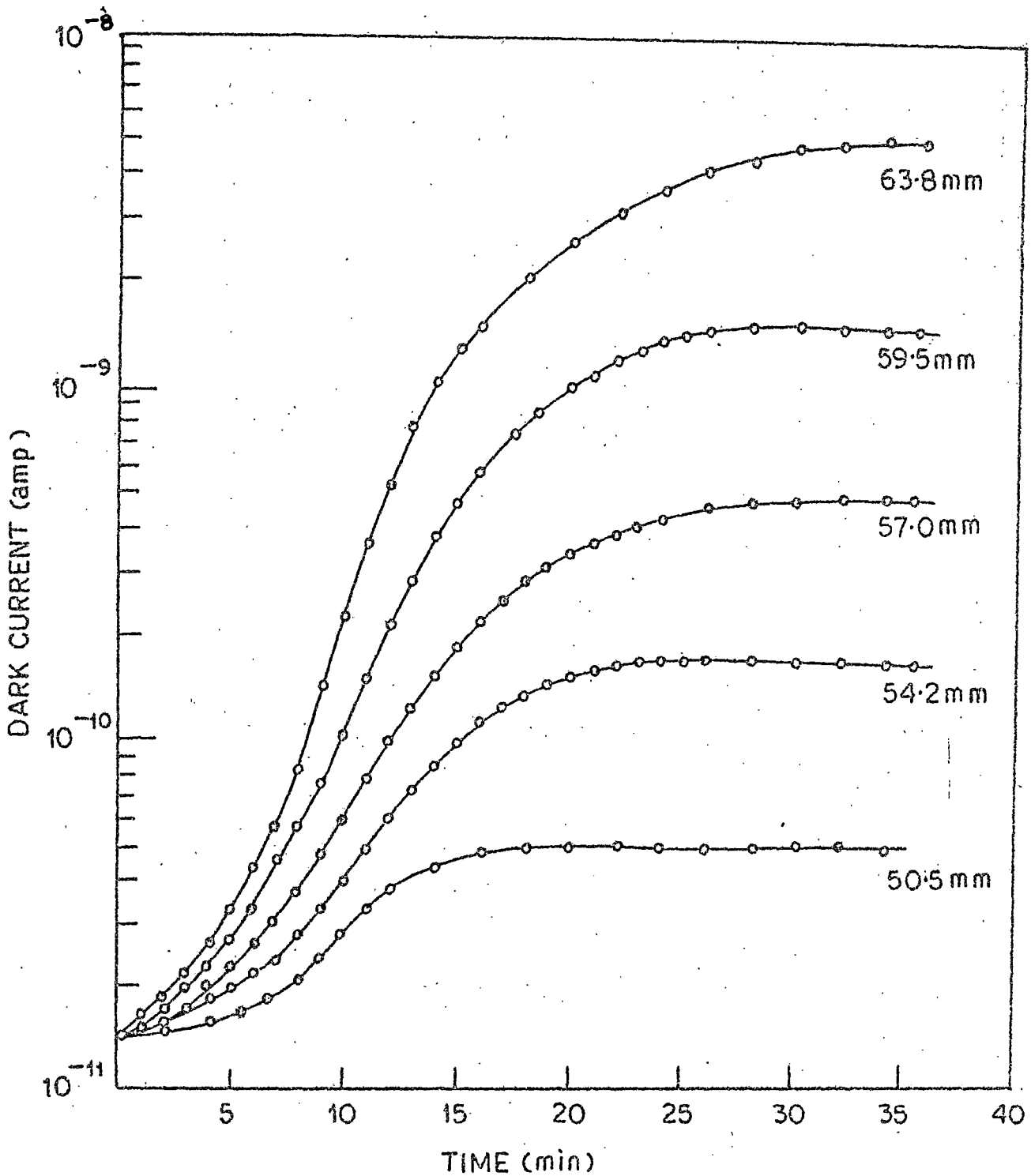
10^{-8}
10^{-9}
10^{-10}
10^{-11}
DARK CURRENT (amp)
63·8mm
59·5mm
57·0mm
54·2mm
50·5mm
5
10
15
20
25
30
35
40
TIME (min)

FIG. 3·8

FIG. 3.9 : The change in dark current in an antacene powder cell kept at 25°C after adsorption of ethyl acetate vapour at different pressures.

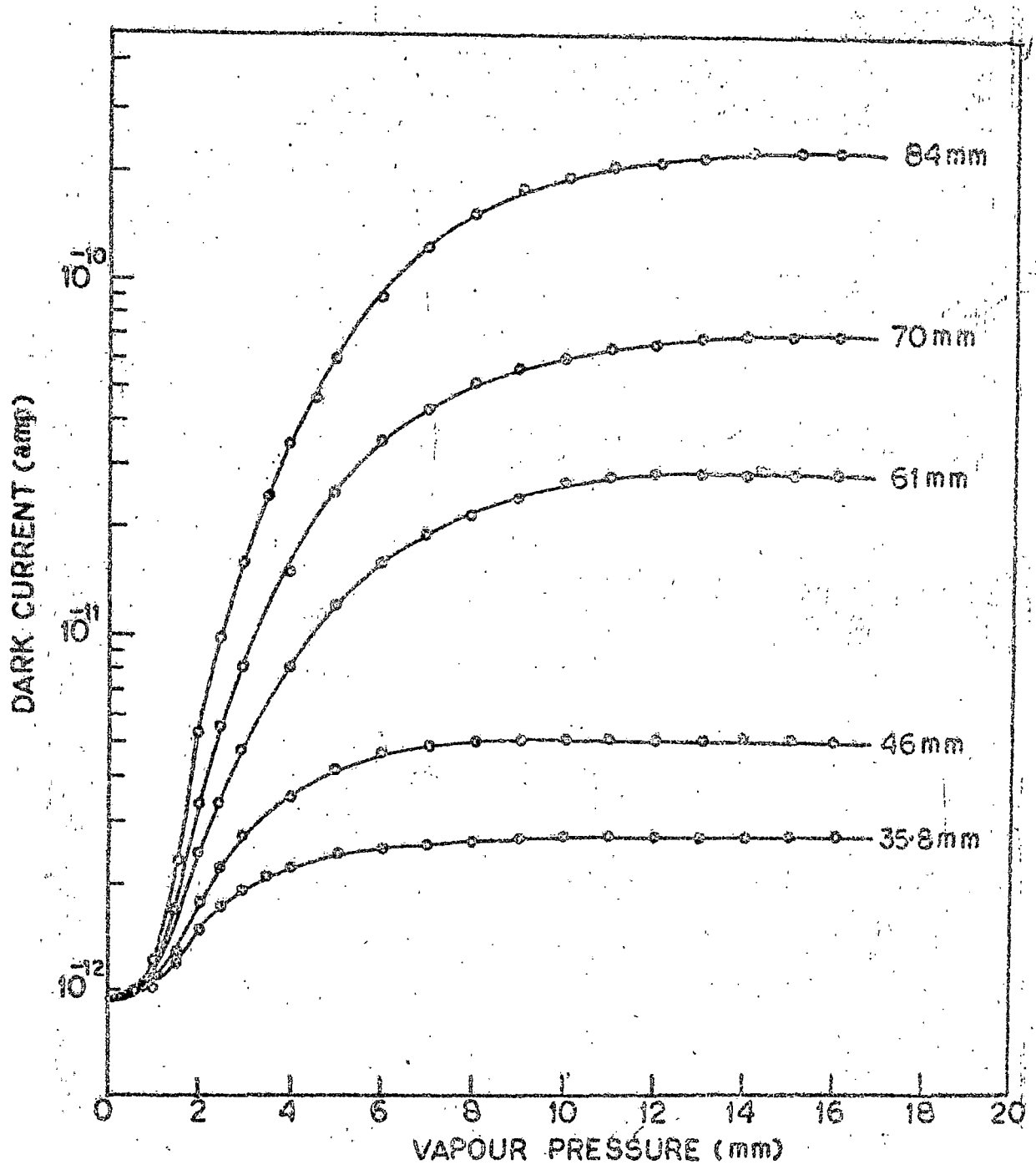
84 mm
70 mm
61 mm
46 mm
35·8 mm
10^{-10}
10^{-11}
10^{-12}
DARK CURRENT (amp)
0
2
4
6
8
10
12
14
16
18
20
VAPOUR PRESSURE (mm)

FIG. 3·9

FIG. 3.10 : The change in dark current in a methyl bixin powder cell kept at 25°C after adsorption of ethyl acetate vapour at different pressures.

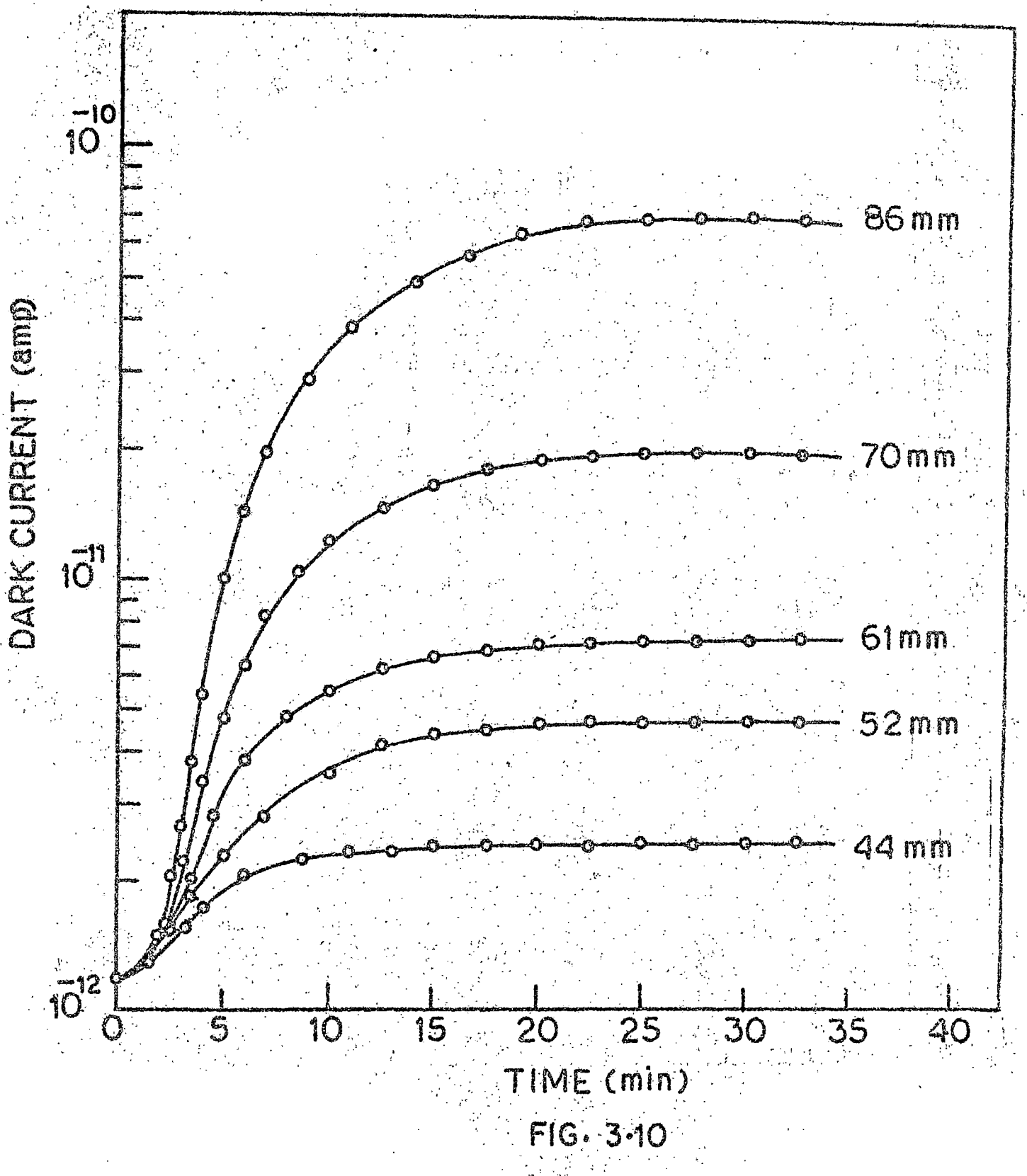
DARK CURRENT (amp)
10^{-10}
10^{-11}
10^{-12}
86 mm
70 mm
61 mm
52 mm
44 mm
0
5
10
15
20
25
30
35
40
TIME (min)

FIG. 3·10

3.3.2 Dependence of the conductivity on vapour pressure

The rise in conductivity of the polyene semiconductors was studied at a constant sample temperature (25°C) as a function of partial pressure of ethyl acetate vapour.

It is assumed that 'm' depends on the partial pressure (p) of the reagent liquid and in the initial period, also on the time of exposure. After some time, however, an equilibrium is established. Thus we assume[25] that in the initial region

$$m(t) = Q(t) \cdot p \qquad (3.3)$$

where Q(t) is a function of time.

At equilibrium,

$$m_0 = Q_0 \cdot p \qquad (3.4)$$

where Q_0 now becomes independent of time. This is expected from Langmuir's[26] adsorption isotherm, when a small fraction of the surface is covered by the gas or vapour molecules. Combining (3.2) and (3.3), we get

$$\sigma_A \{m(t)\} = \sigma_V \exp\{\alpha \cdot Q(t) \cdot p\} \qquad (3.5)$$

and at equilibrium for (3.4),

$$\sigma_A(m_0) = \sigma_V \exp(\alpha \cdot Q_0 \cdot p) \qquad (3.6)$$

A plot of log $\sigma_A(m_0)$ or logarithm of saturation current vs. the

vapour pressure (ϕ) at equilibrium is expected from (3.6) to be linear.

In Figs. 3.11 and 3.12 we show such plots of logarithm of the saturation current versus vapour pressure (ϕ) at equilibrium for ethyl acetate adsorption on the various polyene semiconductors. Fairly good straight lines are obtained (Figs. 3.11 and 3.12). The slope of these curves (αQ_o) is a measure of the strength of interaction between the vapour molecules and the semiconductors. These linear plots prove the applicability of the Langmuir adsorption isotherm for small fraction of surface coverage in these cases of vapour adsorption on polyene crystallites.

3.3.3 Adsorption kinetics

We have examined if the adsorption kinetics follow the Roginsky-Zeldovich equation.

Integrating equation (3.1), we get,

$$m(t) = \frac{kT}{\beta} \log(t+t_o) + \text{Constant} \qquad (3.7)$$

From equations (3.2) and (3.7),

$$\log \sigma_A = \frac{\alpha kT}{\beta} \log(t+t_o) + \text{Constant} \qquad (3.8)$$

Thus, from any empirically chosen t_o, a linear plot of either log σ_A vs. log ($t+t_o$) or logarithm of current vs. logarithm of time is suggested from equation (3.8). Results in Figs. 3.13 - 3.17 for vitamin A alcohol, vitamin A acetate, β -apo-8'-carotenal, ostacene

FIG. 3.11 : Change in the dark current of vitamin A (alcohol and acetate) powder cells at 25°C as a function of the vapour pressure of ethyl acetate.
The lines (1) and (2) correspond to vitamin A alcohol (left scale) and vitamin A acetate (right scale) respectively.

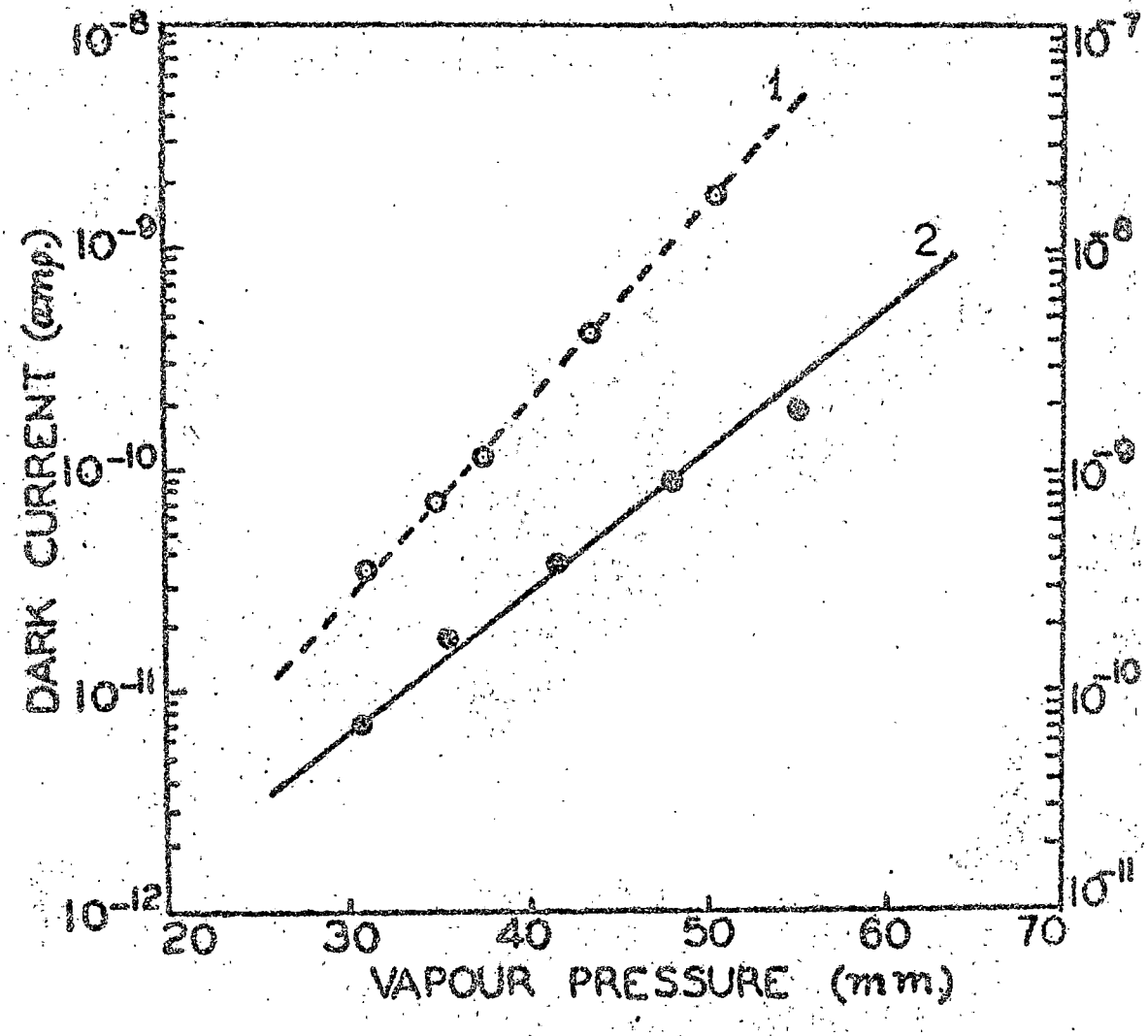
DARK CURRENT (amp.)
10⁻⁸
10⁻⁹
10⁻¹⁰
10⁻¹¹
10⁻¹²
10⁻⁷
10⁻⁸
10⁻⁹
10⁻¹⁰
10⁻¹¹
1
2
20
30
40
50
60
70
VAPOUR PRESSURE (mm.)

FIG. 3·11

FIG.3.12 : Change in the dark current of β -apo-8'-carotenal, astacene and methyl bixin powder cells kept at 25°C as a function of the vapour pressure of ethyl acetate. The lines 1, 2 and 3 correspond to β -apo-8'-carotenal, astacene and methyl bixin respectively.

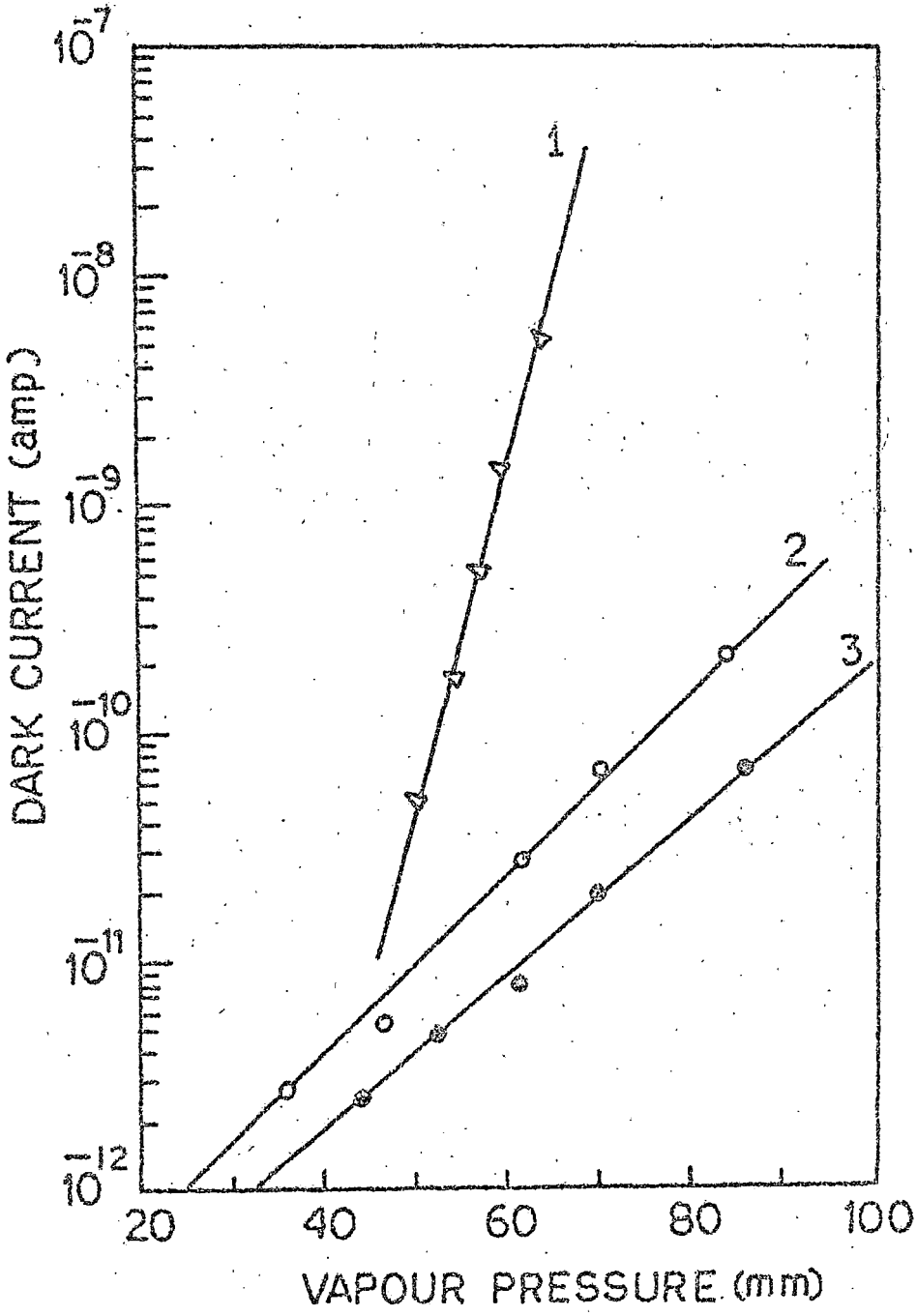
DARK CURRENT (amp.)
10^{-7}
10^{-8}
10^{-9}
10^{-10}
10^{-11}
10^{-12}
1
2
3
20
40
60
80
100
VAPOUR PRESSURE (mm)

FIG. 3·12

FIG.3.13 : Adsorption kinetics data plotted according to Roginsky-Zeldovich equation for vitamin A alcohol.

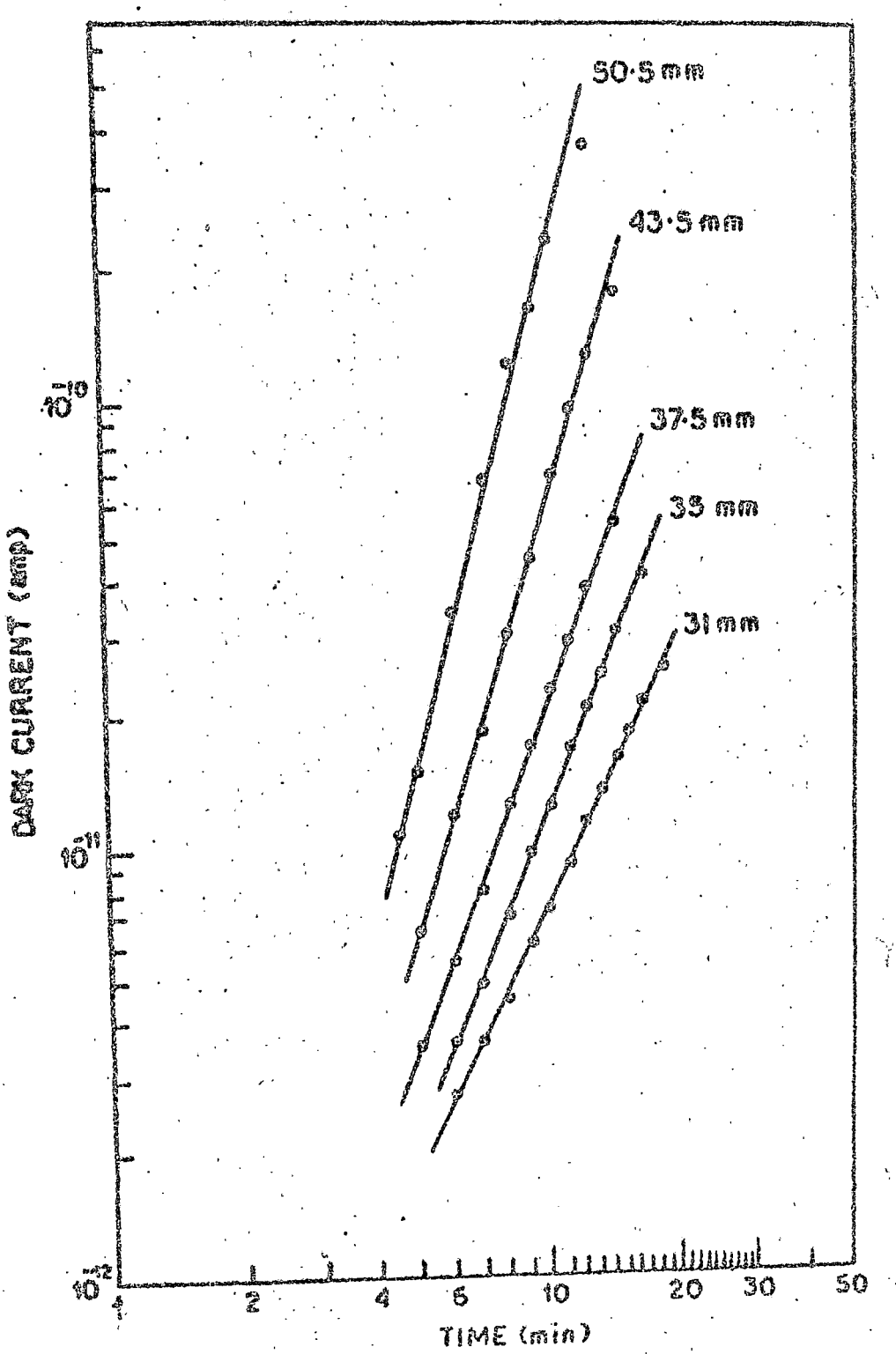
50·5 mm
43·5 mm
37·5 mm
33 mm
31 mm
DARK CURRENT (amp)
10^{-10}
10^{-11}
10^{-12}
1
2
4
6
10
20
30
50
TIME (min)

FIG. 3·13

FIG.3.14 : Adsorption kinetics data plotted according to Roginsky-Zeldovich equation for vitamin A acetate.

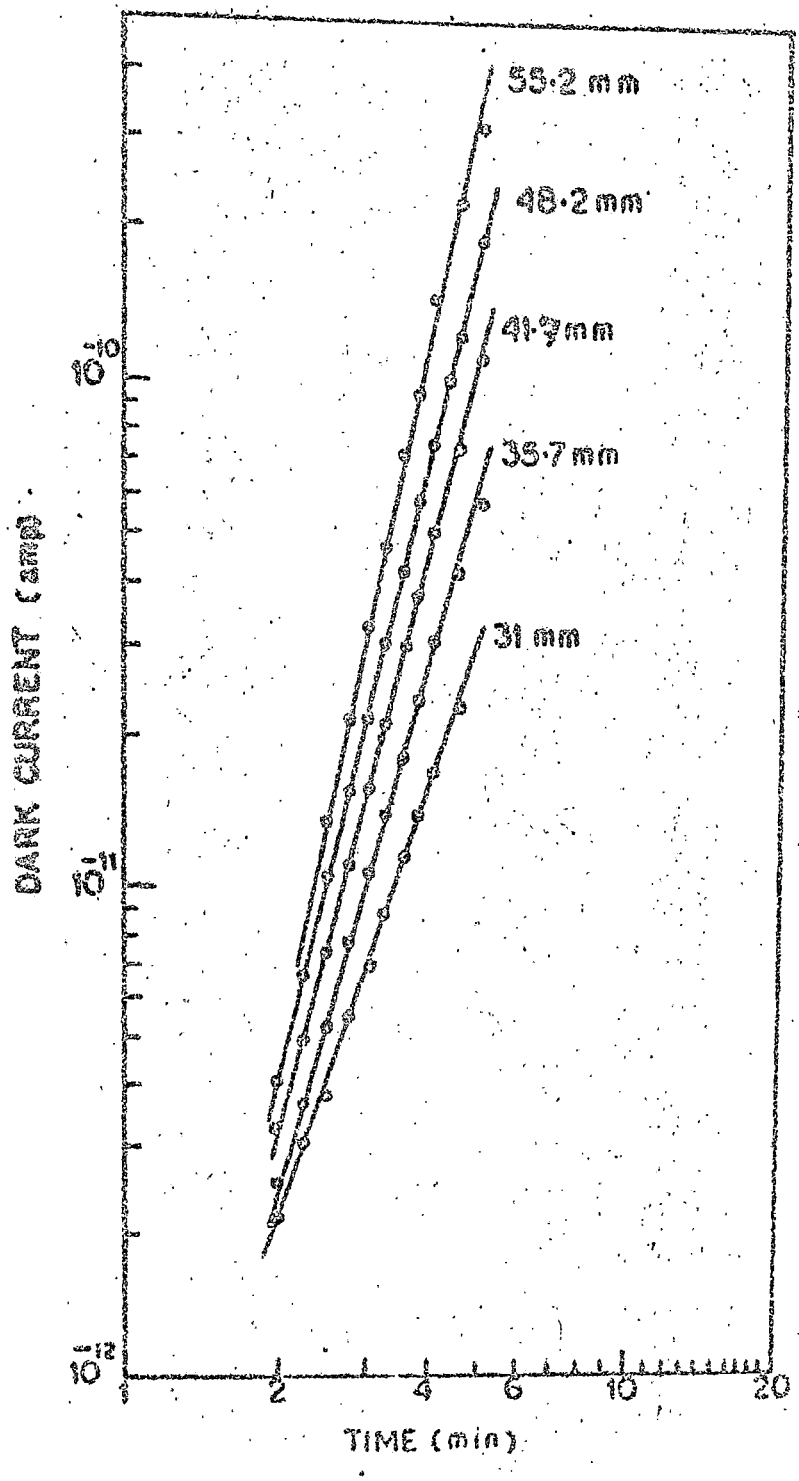
55·2 mm
48·2 mm
41·7 mm
35·7 mm
31 mm
DARK CURRENT (amp)
10^{-10}
10^{-11}
10^{-12}
2
4
6
10
20
TIME (min)

FIG. 3·14

FIG.3.15 : Adsorption kinetics data plotted according to Roginsky-Zeldovich equation for β -apo-8'-carotenal .

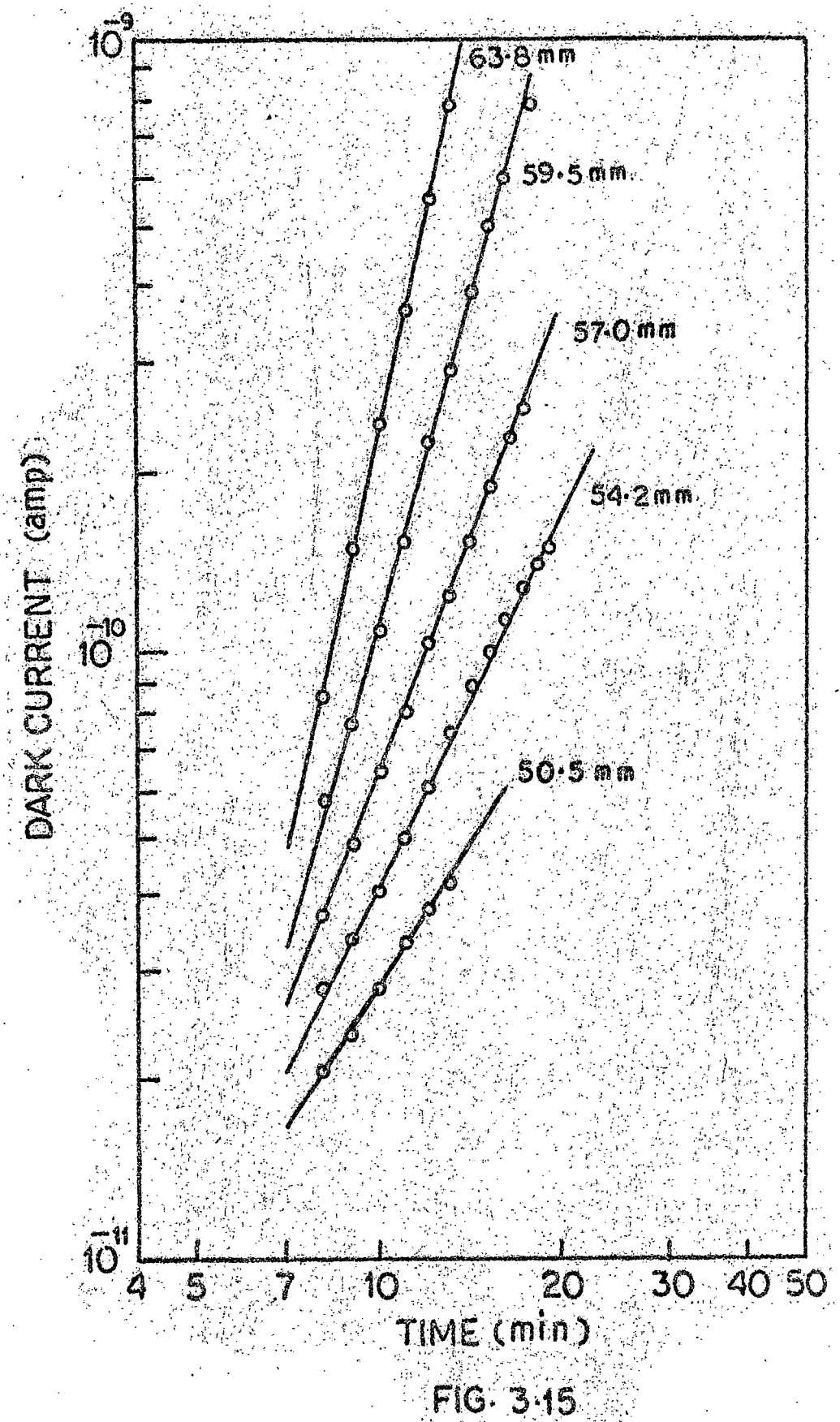
63·8 mm
59·5 mm
57·0 mm
54·2 mm
50·5 mm
DARK CURRENT (amp)
10^{-9}
10^{-10}
10^{-11}
4
5
7
10
20
30
40
50
TIME (min)

FIG. 3·15

FIG.3.16 : Adsorption kinetics data plotted according to Roginsky-Zeldovich equation for antacene.

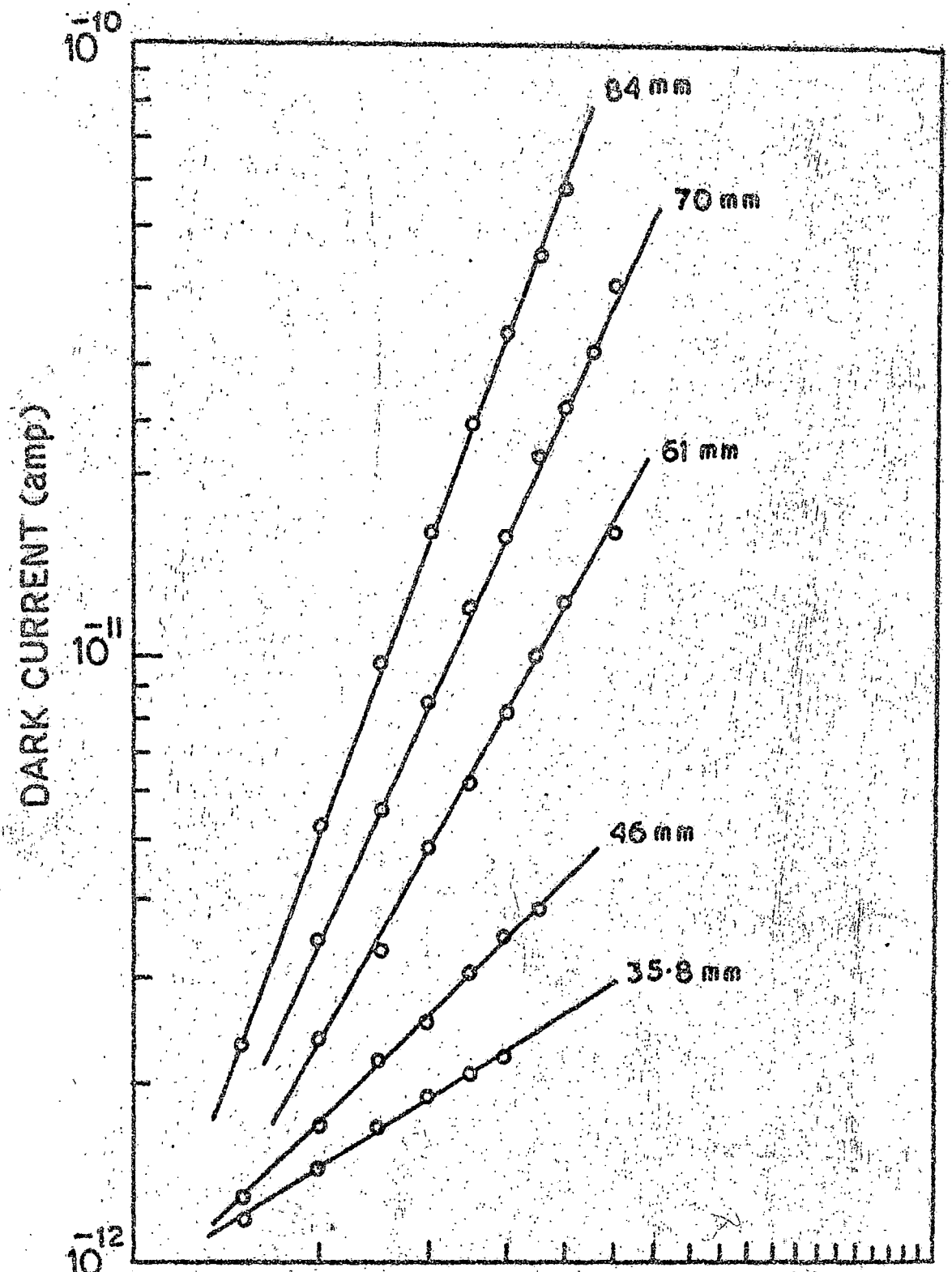
10^{-10}
10^{-11}
10^{-12}
DARK CURRENT (amp)
84 mm
70 mm
61 mm
46 mm
35·8 mm
1
2
4
6
10
20
TIME (min)

FIG. 3.16

FIG.3.17 : Adsorption kinetics data plotted according to Roginsky-Zeldovich equation for methyl bixin.

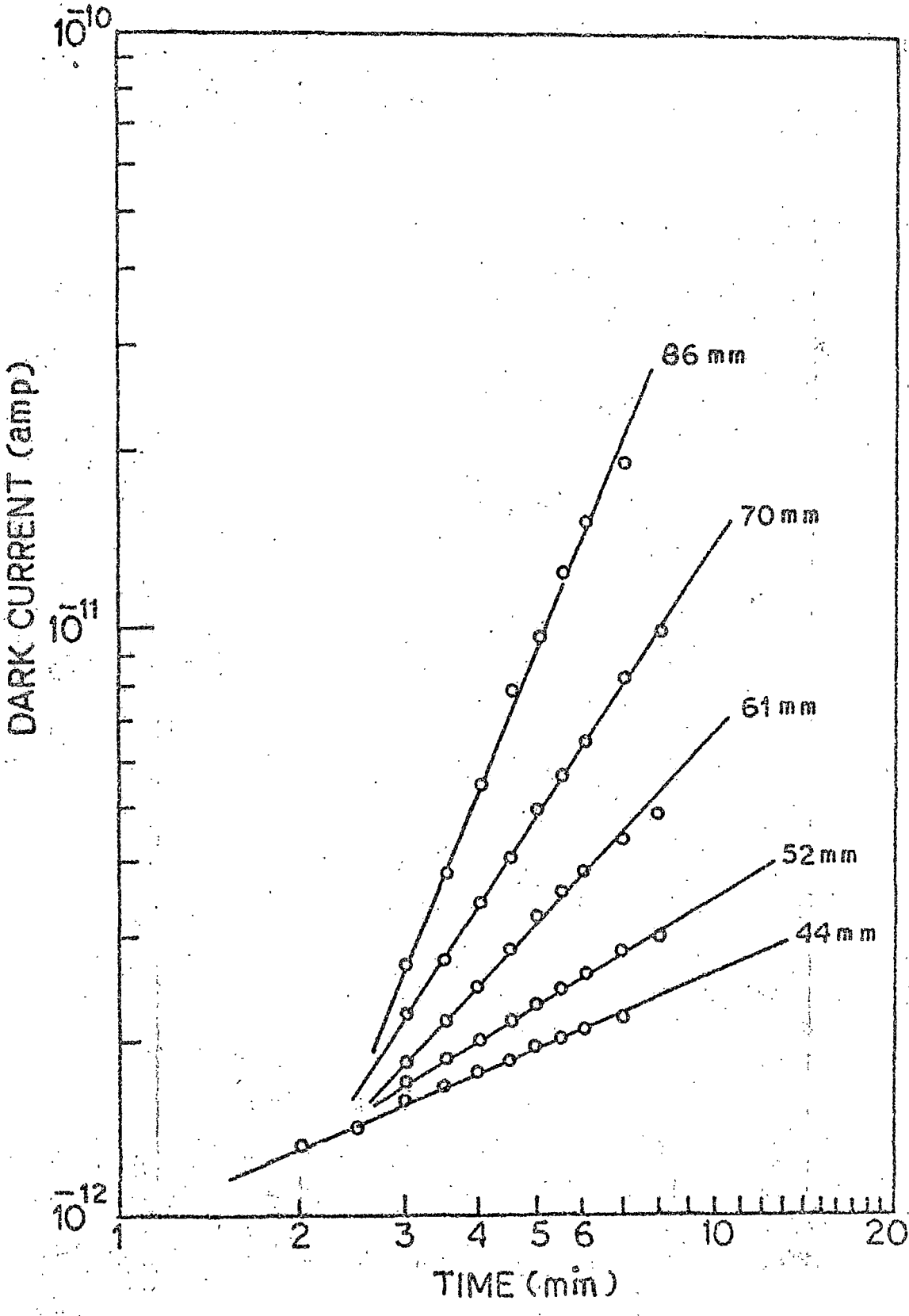
10^{-10}
10^{-11}
10^{-12}
DARK CURRENT (amp)
86 mm
70 mm
61 mm
52 mm
44 mm
1
2
3
4
5
6
10
20
TIME (min)

FIG. 3.17

and methyl bixin respectively are in good agreement with this. In the initial region, different slopes observed at different vapour pressures show the vapour pressure-dependence of β (since α is pressure independent). The higher the partial vapour pressure, the larger is the slope. This justifies the assumption made in expression (3.3) and shows an inverse relationship between p and β. As we are unable to estimate a numerical value of α from this experiment, we can not evaluate the numerical value of β from the measured slopes. However, we have estimated the values of β/α $(=\beta')$ from the slopes to see its pressure dependence. In table 3.3 variation of β' with vapour pressure is shown.

3.3.4 Desorption Kinetics

Equation (3.1) is valid for the rate of adsorption. Since desorption is a reverse process of adsorption, expression for the rate of desorption can be written in a similar form with a positive sign in the exponent i.e., by

$$-\frac{dm}{dt} = A^* \exp\left(\frac{\beta^* m}{RT}\right) \qquad (3.9)$$

Here $\beta^* m$ is the activation energy for desorption. In the measurement of desorption, the experimental condition is so arranged that there is no re-adsorption. The plots of logarithm of current vs. logarithm of time for desorption of ethyl acetate vapour from vitamin A alcohol, vitamin A acetate, β -apo-8'-carotenal, octacene and methyl bixin crystallites are shown in Figs. 3.18 - 3.22 respectively.

Table - 3.3

Vapour pressure dependence of the factor β' for ethyl acetate vapour adsorption kinetics.

Polyenes	Vapour pressure (mm)	β' (eV)
Vitamin A alcohol	31.0	1.202×10^{-2}
	35.0	1.005×10^{-2}
	37.5	0.930×10^{-2}
	43.5	0.759×10^{-2}
	50.5	0.648×10^{-2}
Vitamin A acetate	31.0	0.819×10^{-2}
	35.7	0.758×10^{-2}
	41.7	0.660×10^{-2}
	48.2	0.601×10^{-2}
	55.2	0.518×10^{-2}

contd.

Table - 3.3 (contd.)

Polyenes	Vapour pressure (mm)	β' (eV)
	50.5	1.629×10^{-2}
β -apo-8'-	54.2	1.245×10^{-2}
Carotenal	57.0	0.994×10^{-2}
	59.5	0.718×10^{-2}
	63.8	0.555×10^{-2}
	35.8	3.973×10^{-2}
Astacene	46.0	2.568×10^{-2}
	61.0	1.422×10^{-2}
	70.0	1.168×10^{-2}
	84.0	0.931×10^{-2}
	44.0	5.714×10^{-2}
Methyl	52.0	4.131×10^{-2}
bixin	61.0	2.526×10^{-2}
	70.0	1.638×10^{-2}
	86.0	1.039×10^{-2}

FIG. 3.18 : Desorption kinetics data plotted according to Roginsky - Zeldovich equation for vitamin A alcohol.

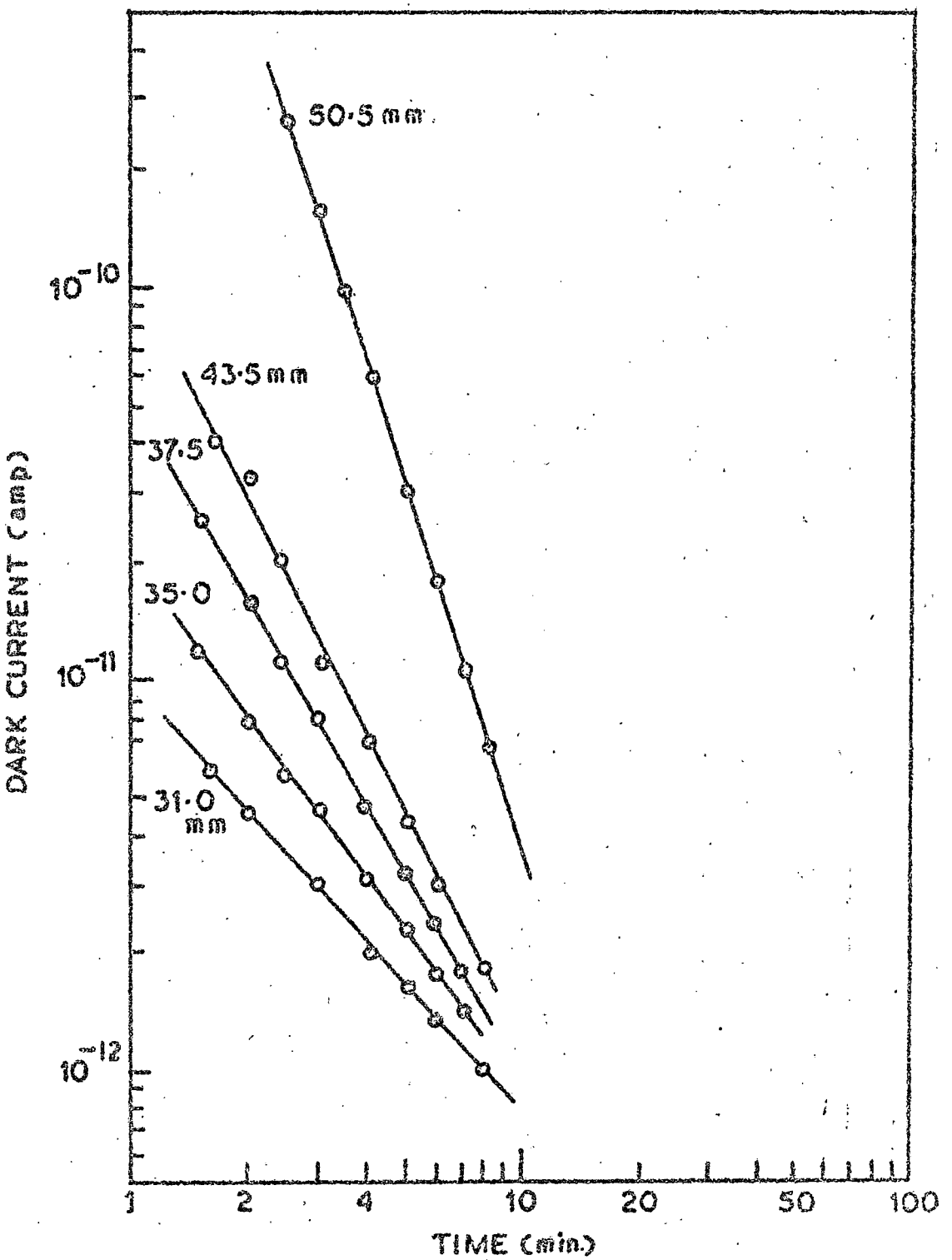
50·5 mm
43·5 mm
37·5
35·0
31·0 mm
10^{-10}
10^{-11}
10^{-12}
DARK CURRENT (amp.)
1
2
4
10
20
50
100
TIME (min.)

FIG. 3·18

Fig.2.13 : Desorption kinetics data plotted according to Roginsky-Zeldovich equation for vitamin A acetate.

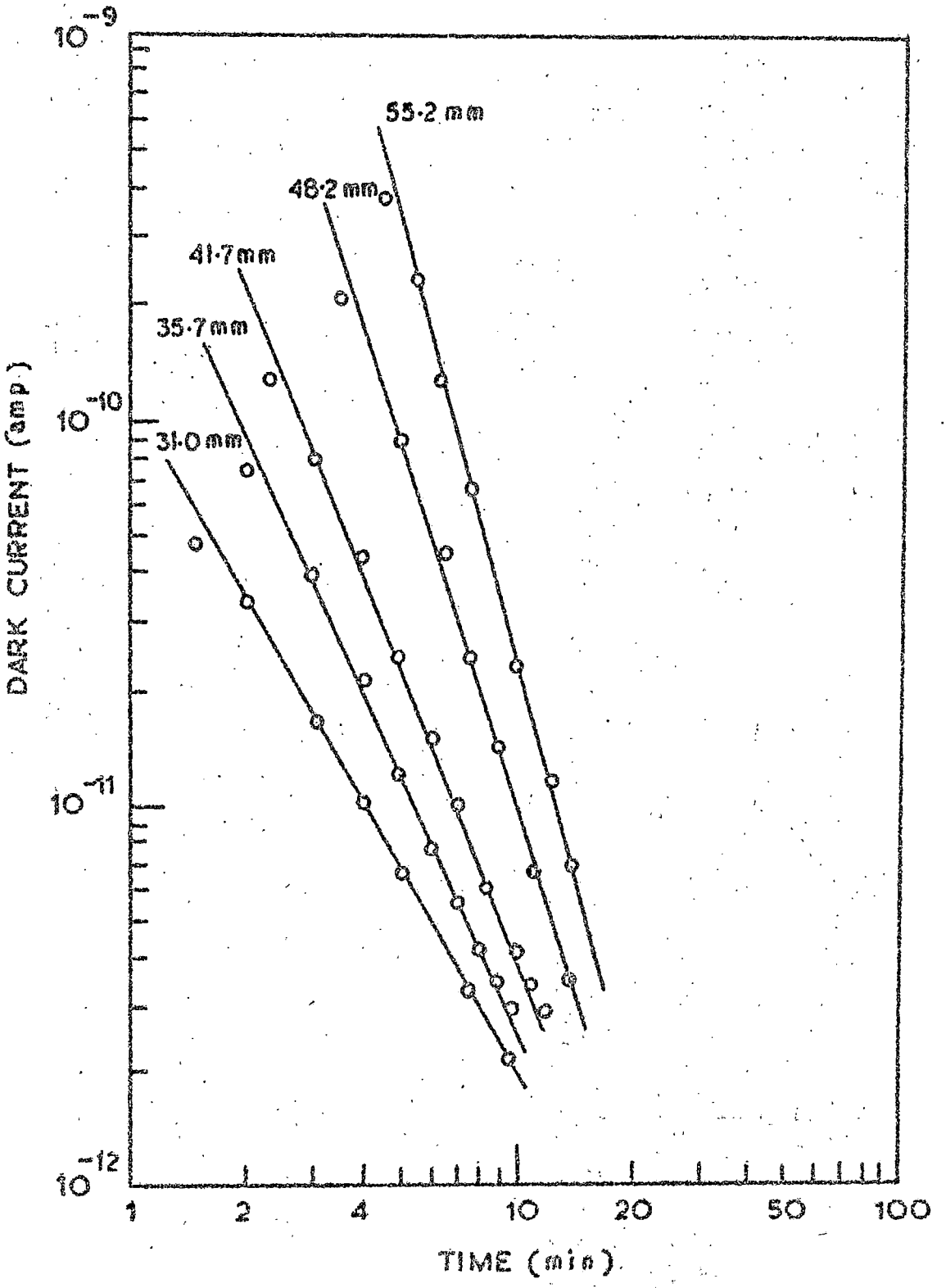
DARK CURRENT (amp)
10^{-9}
10^{-10}
10^{-11}
10^{-12}
55·2 mm
48·2 mm
41·7 mm
35·7 mm
31·0 mm
1
2
4
10
20
50
100
TIME (min)

FIG. 3·19

FIG. 3.20 : Desorption kinetics data plotted according to Roginsky-Zeldovich equation for β -apo-8'-carotenal.

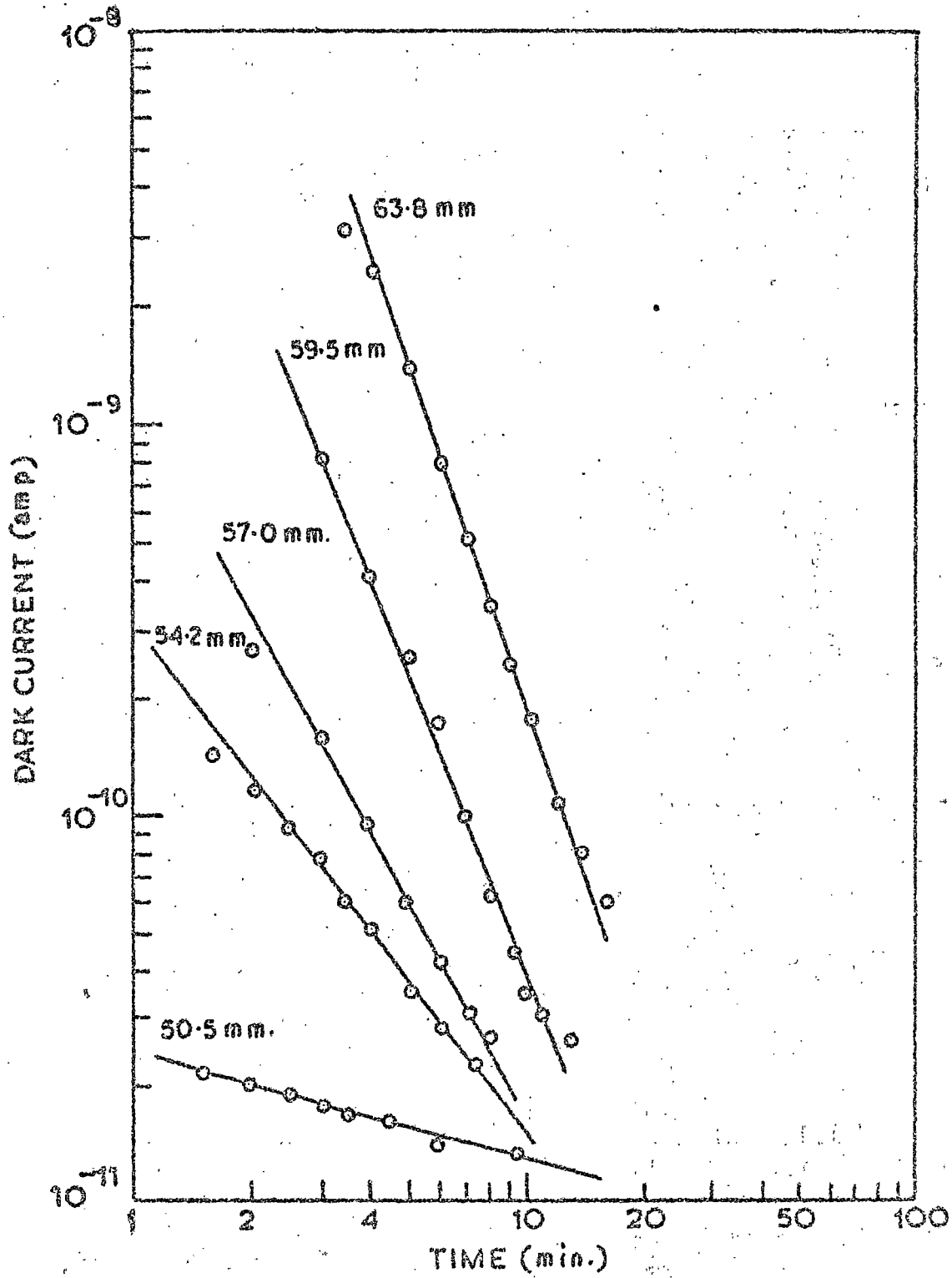
DARK CURRENT (amp)
10^{-8}
10^{-9}
10^{-10}
10^{-11}
63·8 mm
59·5 mm
57·0 mm.
54·2 mm
50·5 mm.
1
2
4
10
20
50
100
TIME (min.)

FIG. 3·20

FIG.3.21 : Desorption kinetics data plotted according to Roginsky - Zeldovich equation for ostacene.

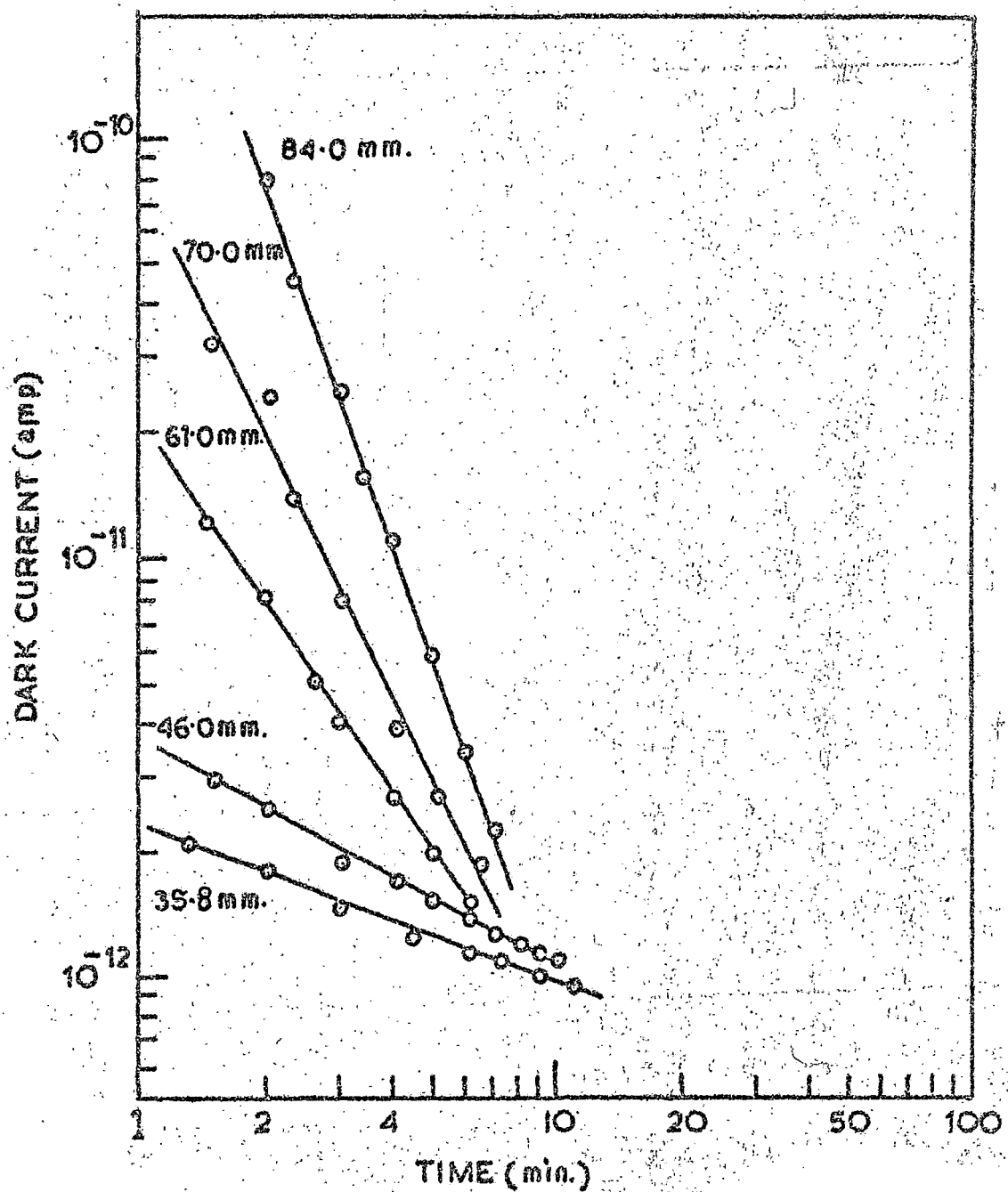
84·0 mm.
70·0 mm.
61·0 mm.
46·0 mm.
35·8 mm.
10^{-10}
10^{-11}
10^{-12}
DARK CURRENT (amp)
1
2
4
10
20
50
100
TIME (min.)

FIG. 3·21

FIG.3.22 : Desorption kinetics data plotted according to Roginsky-Zeldovich equation for methyl bixin.

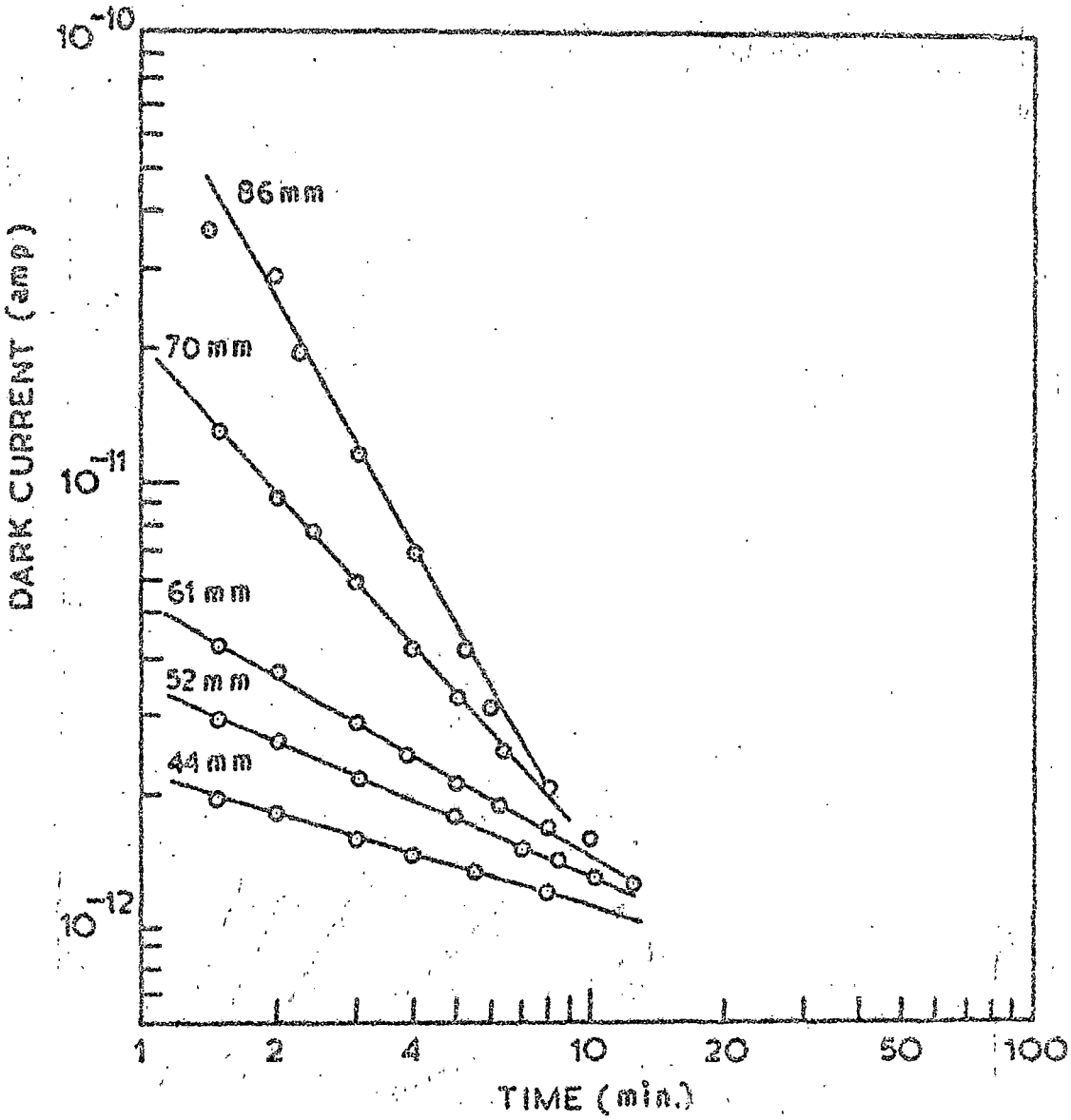
DARK CURRENT (amp)
10^{-10}
10^{-11}
10^{-12}
86 mm
70 mm
61 mm
52 mm
44 mm
1
2
4
10
20
50
100
TIME (min.)

FIG. 3·22

In table 3.4, we present the experimental values of $\beta^{*\prime}$ $(= \beta^*/\alpha)$ obtained from these plots for ethyl acetate vapour desorption from different polyene crystallites. As like that β, β^* also decreases with increasing vapour pressure. For any particular pressure of ambient vapour, β^* is larger than β.

There are number of different treatments[27] for the Roginsky-Zeldovich equation. A simple two stage-process after Riley and Leslie[16] as shown in Fig. 3.23 seems quite satisfactory to account for the experimental observations. In the first stage, a mobile van der Waals adsorption on the crystal surface gives a Lennard-Jones potential energy curve which is assumed to depend on the fraction of surface coverage. This stage is followed by a rate-determining transition over a potential energy barrier to the final stage of adsorption forming weakly bound complexes between the vapour molecules and the polyene crystallites. The barrier is formed by the intersection of the two potential curves. As more vapour molecules get physically adsorbed (van der Waals), a repulsive interaction between the dipoles will raise the potential energy curve for the first stage thereby lowering the barrier height giving decreasing activation energy of adsorption with increasing vapour pressure. As the surface coverage of the second stage rises, this potential curve also rises resulting in lowering of desorption activation energy with increasing pressure. The rise of the second stage curve is such that the minimum of this curve is always at lower energy than the minimum of the first stage, the energy difference between these two minima decreasing with increasing vapour pressure.

Table - 3.4

Vapour pressure dependence of the factor $\beta^{*\prime}$ for ethyl acetate vapour desorption kinetics.

Polyenes	Vapour pressure(mm)	$\beta^{*\prime}$ (eV)
Vitamin A alcohol	31.0	2.304×10^{-2}
	35.0	1.847×10^{-2}
	37.5	1.492×10^{-2}
	43.5	1.201×10^{-2}
	50.5	0.798×10^{-2}
Vitamin A acetate	31.0	1.431×10^{-2}
	35.7	1.151×10^{-2}
	41.7	1.023×10^{-2}
	48.2	0.802×10^{-2}
	55.2	0.648×10^{-2}

contd.

Table - 3.4 (contd.)

Polyenes	Vapour pressure (mm)	$\beta^{x'}$ (eV)
β -apo-8'-carotenal	60.5	8.621×10^{-2}
	64.2	1.919×10^{-2}
	57.0	1.322×10^{-2}
	50.5	1.015×10^{-2}
	63.8	0.808×10^{-2}
Astacene	35.8	6.733×10^{-2}
	46.0	4.591×10^{-2}
	61.0	1.720×10^{-2}
	70.0	1.250×10^{-2}
	84.0	0.969×10^{-2}
Methyl bixin	44.0	8.312×10^{-2}
	52.0	5.971×10^{-2}
	61.0	4.322×10^{-2}
	70.0	2.215×10^{-2}
	86.0	1.421×10^{-2}

FIG. 3.23 : Potential energy curves for vapour adsorption in two stages in polyenes, explaining modified Roginsky-Zeldovich plots. E_d^1, E_d^2 and E_d^3 are activation energies of desorption in order of increasing pressure. Similarly E_a's are activation energies for adsorption.

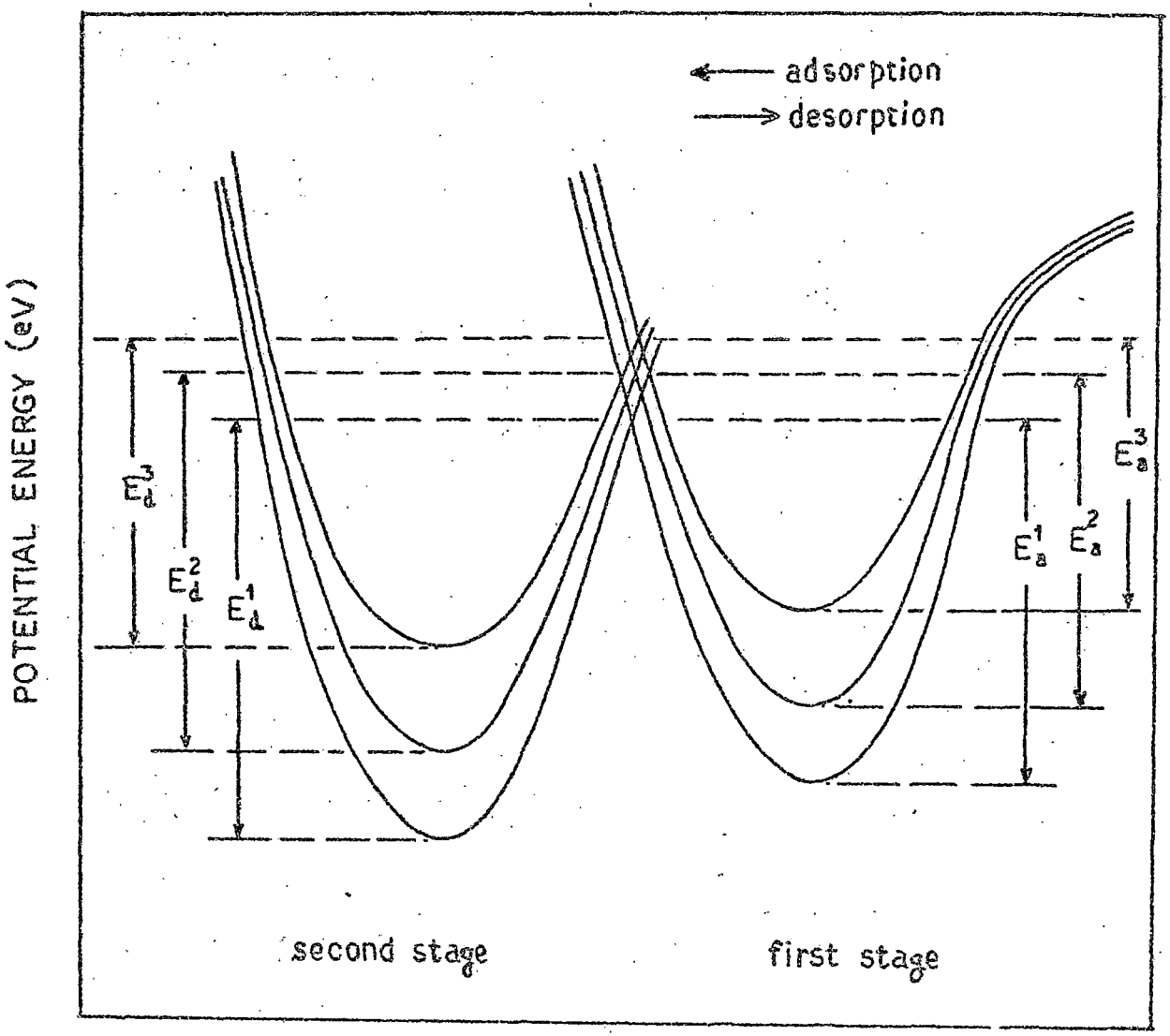
adsorption
desorption
POTENTIAL ENERGY (eV)
E_d^3
E_d^2
E_d^1
E_a^1
E_a^2
E_a^3
second stage
first stage
REACTION PATH

FIG. 3·23

Here β^*_m, the activation energy for desorption should, apart from a small entropy factor, be equal to the vapour-surface molecular complex. In table 3.4, we have shown the experimental values of $\beta^{*\prime}$. Unfortunately neither our experiments give any numerical value of α, nor we have been able to measure n, the amount of vapour adsorbed. Any reliable estimate of the binding energy of various vapours with different polyenes has therefore, not been possible. In case of hydration of proteins, Rosenberg[18] estimated $\alpha \approx 2.6$. A similar value of α for these cases of vapour desorption from polyene crystallites, the value of binding energy are $\approx 10^{-2}$ eV per unit of 'm' desorbed. This low value of the binding energy accounts for easy and efficient desorption of these vapours from the polyene crystals.

3.4 Conclusion

The adsorption of vapours enhances the semiconductivity of the polyenes appreciably. This enhancement depends on the chemical nature and also on the pressure of the adsorbed vapour. The adsorption and desorption kinetics follow the modified Roginsky-Zeldovich relation. A two stage adsorption process, the first stage of which gives a Lennard - Jones potential energy curve and is followed by a rate-determining transition over a potential energy barrier to the second state of adsorption forming weakly bound complexes between the vapour molecules and the polyene crystallites, can explain satisfactorily the experimentally observed kinetics data.

References

1) A.T. Vartanyan, Zhur. Fiz. Khim., 22, 769 (1948).

2) A.T. Vartanyan, Doklady Akad. Nauk. S.S.S.R., 71, 641 (1950).

3) A.G. Chynoweth, J. Chem. Phys., 22, 1029 (1954).

4) B. Rosenberg, J. Chem. Phys., 34, 812 (1961).

5) K.M. Jain, A. Ghosh, B. Mallik and T.N. Misra, Indian J. Phys., 52A, 643 (1978).

6) T.N. Misra, B. Rosenberg and R. Switzer, J. Chem. Phys., 48, 2096 (1968).

7) O. Fritsch, Ann. Physik, 22, 375 (1935).

8) W. Hartmann, Z. Physik, 102, 709 (1936).

9) W. Mayer and H. Neldel, Physik, Z.38, 1014 (1937).

10) T.J. Gray and P.W. Darby, J. Chem. Phys., 60, 201 (1956).

11) A. Bree and L.E. Lyons, J. Chem. Soc., 5 179 (1960).

12) A. Bree and L.E. Lyons, 25, 384 (1956).

13) B. Rosenberg and J.F. Camiscoli, J. Chem. Phys., 35, 932 (1961).

14) W.G. Schneider and T.C. Waddington, J. Chem. Phys., 25, 358 (1956).

15) D. D. Eley and R.B. Leslie, Advances in Chemical Physics (New York: Interscience Publishers) 7, 238 (1964).

16) Ya. Zeldovich, Acta Physicochim URSS, 1, 449 (1934).

17) S. Roginsky and Ya. Zeldovich, Acta Physicochim URSS, 1, 554, 595 (1934).

18) B. Rosenberg, Physical Processes in Radiation Biology edited by L. Augenstein, R. Mason and B. Rosenberg (Academic Press, New York and London, 1964) p 111.

19) S. Treiber and M. Koren, Natt. Bur. Stand. Circ., 514 (1951).

20) F. Gutmann and L.E. Lyons, Organic Semiconductors (John Wiley and Sons, New York, London and Sydney, 1967) p 669.

21) J.C. Lorquet, Mol. Phys., 9, 101 (1965).

22) M.M. Labes and O.N. Rudyj, J. Am. Chem. Soc., 85, 1955(1963).

23) P.J. Neucroft, O.N. Rudyj and M.M. Labes, J. Am. Chem. Soc., 85, 2059 (1963).

24) P.J. Neucroft, O.N. Rudyj, R.F. Salomon and M.M. Labes, J. Phys. Chem., 66, 779 (1962).

25) B. Mallik, A. Ghosh and T.N. Misra, Proc. Indian Acad. Sci., 93A, 25 (1979).

26) S. Glasstone, Text Book of Physical Chemistry (Macmillan and Co. Ltd., London, 1951) p 1200.

27) F.S. Stone, Chemistry of the solid state edited by W.E. Garner (Butterworths, London, 1955) p 367.

CHAPTER 4

COMPENSATION EFFECT IN SOME POLYBIC SEMICONDUCTORS

4.1 Introduction

The electrical conductivity of conjugated π-electronic organic compounds follows the operational definition of a semiconductor

$$\sigma(T) = \sigma_0 \exp(-E/2kT) \tag{4.1}$$

where $\sigma(T)$ is the specific conductivity at any absolute temperature T, σ_0 is a pre-exponential factor, E the semiconduction activation energy and k is Boltzmann constant (E/2 is often written as E', however, we shall use the former throughout this chapter). Experimentally, E is obtained from the slope of the linear plot of $\log \sigma(T)$ [or $\log i(T)$] versus $\frac{1}{T}$ and the extrapolated intercept of the line on the ordinate at $T^{-1} = 0$ yields the value of σ_0. Recently, the so called pre-exponential factor σ_0 has been the subject of much discussion[1-6] as experimental evidence accumulated shows that σ_0 contains exponential functions. Gutmann and Lyons[7] showed that a linear relationship of the form

$$\log \sigma_0 = \alpha E + \beta \tag{4.2}$$

holds good for one entire class of organic compounds. Here α and β are constants. Rosenberg et al[2] showed evidence that if E is varied by hydration or by complex formation relation (4.2) is valid for a single organic substance as well and they suggested an expression for the specific conductivity of the form

$$\sigma(T) = \sigma_0' \exp(E/2kT_0) \exp(-E/2kT) \tag{4.3}$$

where $$\sigma_0 = \sigma_0' \exp(E/2kT_0) \tag{4.4}$$

Here the additional constant T_0 is called the characteristic temperature of the material. σ_0' and T_0 for the same compound remain invariant. The linear relationship between the logarithm of the pre-exponential factor and the activation energy is called the compensation effect. σ and E change in such a manner that their effect on σ_0 are mutually compensated. Johnston and Lyons[4] believe that the linear relationship between log σ_0 and E may originate solely from the calculation of these parameters and the compensation effect requires no physical interpretation. However, they have suggested that if σ_0 and E are physically related, one should get a linear relationship between log σ and E yielding the semiconductive parameters in agreement with the values obtained from other sources. Exner[8] also has pointed out that, in certain limited conditions, a compensation law may occur accidently, and he has provided a set of similar criteria for judging the validity of the rule.

From equation (4.3), for any particular temperature T_1, the specific conductivity is given by

$$\log \sigma(T_1) = \log \sigma_0' + \left[\frac{1}{T_0} - \frac{1}{T_1}\right] \frac{E}{2k} \qquad (4.5)$$

Thus, the plot of log $\sigma(T_1)$ vs. E is expected to be linear with a slope $\left[\frac{1}{T_0} - \frac{1}{T_1}\right] \frac{1}{2k}$ and an intercept of log σ_0'. The value of σ_0' obtained from this plot should also show a good agreement with the values obtained from the log σ_0 vs. E and log σ vs. $\frac{1}{T}$ plots. In the experiment of Johnston and Lyons[4] in one component crystal of anthracene it has been observed by changing its purity and doping with tetracene that log σ_0 vs. E plots are linear. A very poor

correlation between log σ and E was, however, observed[4]. Some recent theoretical work[9-11] suggest that in biological semiconductors the compensation effect arises due to the dark conduction process. In view of the scanty experimental work available on this effect, it was thought worthwhile to investigate the conduction process in more biological semiconductors. To test the validity of this compensation effect, E is generally varied by various ways[5,6,12] and log σ_0 is plotted against E.

In the previous chapter we have seen that the adsorption of various vapours changes the specific conductivity of the polyenes. Such change is generally associated with a change of the semiconduction activation energy. As for example, adsorption of moisture on dry protein[13] and various vapours on β - carotene[14] increases the semiconduction current and decreases the activation energy. Epstein and Wildi[15] have reported that the removal of oxygen from polymeric copper phthalocyanine causes a sharp drop in the resistivity with a concomitent drop of the activation energy. In this chapter we present the results of our investigations on the effect of adsorption of various vapours on the semiconduction activation energy values of some polyenes. Using these changed activation energy values we further show the validity of the compensation rule in these cases. The results are in conformity with the idea that σ_0 and E are indeed physically related.

4.2 Experimental and Results :

4.2.1 Effect of vapour adsorption on activation energy :

The semiconduction activation energy of crystalline powders of vitamin A alcohol, vitamin A acetate, β - apo - 8'- carotenal, astecene and methyl bixin was measured several times in dry nitrogen atmosphere and also in vacuum. All measurements gave consistent values. Almost same values were obtained in dry nitrogen and in vacuum. The observed values are 2.06, 3.50, 1.36, 1.30 and 1.32 eV (approx.) for the alcohol, acetate, β -apo-8'-carotenal, astecene and methyl bixin respectively. The adsorption of vapours changes the activation energy appreciably.

To determine the effect of adsorbed vapour on the semiconduction activation energy, the sample was allowed to adsorb the vapour at a fixed pressure and come to a steady state at a constant sample cell temperature in the chamber atmosphere containing the vapour in nitrogen. The pressure of the total gas mixture in the chamber was atmospheric and the partial pressure of the vapour was the saturation vapour pressure of the reagent liquid at the temperature at which it was kept. Both inlet and the outlet of the chamber was then sealed and the value of the saturation current was noted with time. The saturation current was found to be almost constant even after four hours indicating that the conduction in the system was mainly electronic[16,17]. The cell was then rapidly cooled to about - 40°C. The chamber was then flushed gently with dry nitrogen gas. The outlet of the chamber was kept open and the atmospheric pressure

was maintained inside the chamber. The temperature was then slowly increased and the semiconduction current was measured with the increasing temperature of the sample cell. The result of one such typical experiment for ethyl acetate vapour adsorption on vitamin A acetate are shown in Fig. 4.1. For the region upto the point A, the current increases uniformly with temperature and the curve has a straight line portion. As the temperature increases further, there is gradual slowing down of the rate of current rise with temperature. At the point B, the current drops off, first slowly, then very fast until the point C is reached when the current gradually rises again. At the point D, the current rise becomes uniform and the curve is again a straight line. Evidently, the straight line portion in the low temperature region shows the semiconductive properties of vitamin A acetate powder with adsorbed ethyl acetate vapour and the slope of this line gives the activation energy (0.62 eV) of the system. At considerable higher temperatures, the adsorbed vapour starts desorbing and the rate of desorption increases with increasing temperature and the current begins to diminish. At the point C, the desorption is nearly complete and the current returns to the initial value before vapour adsorption. The straight line portion of the curve at the higher temperature region above the point C, gives the activation energy of vitamin A acetate powder in dry nitrogen atmosphere. The observed value (3.43 eV) is slightly lower possibly due to incomplete desorption of adsorbed vapours. Similar curves were also obtained with other vapours. Vitamin A alcohol shows similar behaviour on vapour adsorption. The effect of adsorption of ethyl acetate vapour on the activation energy of

FIG. 4.1 : Semiconductivity in an ethyl acetate adsorbed vitamin A acetate powder cell as a function of temperature.

Ambient vapour pressure 50 mm adsorbed at sample cell temperature 12.5°C.

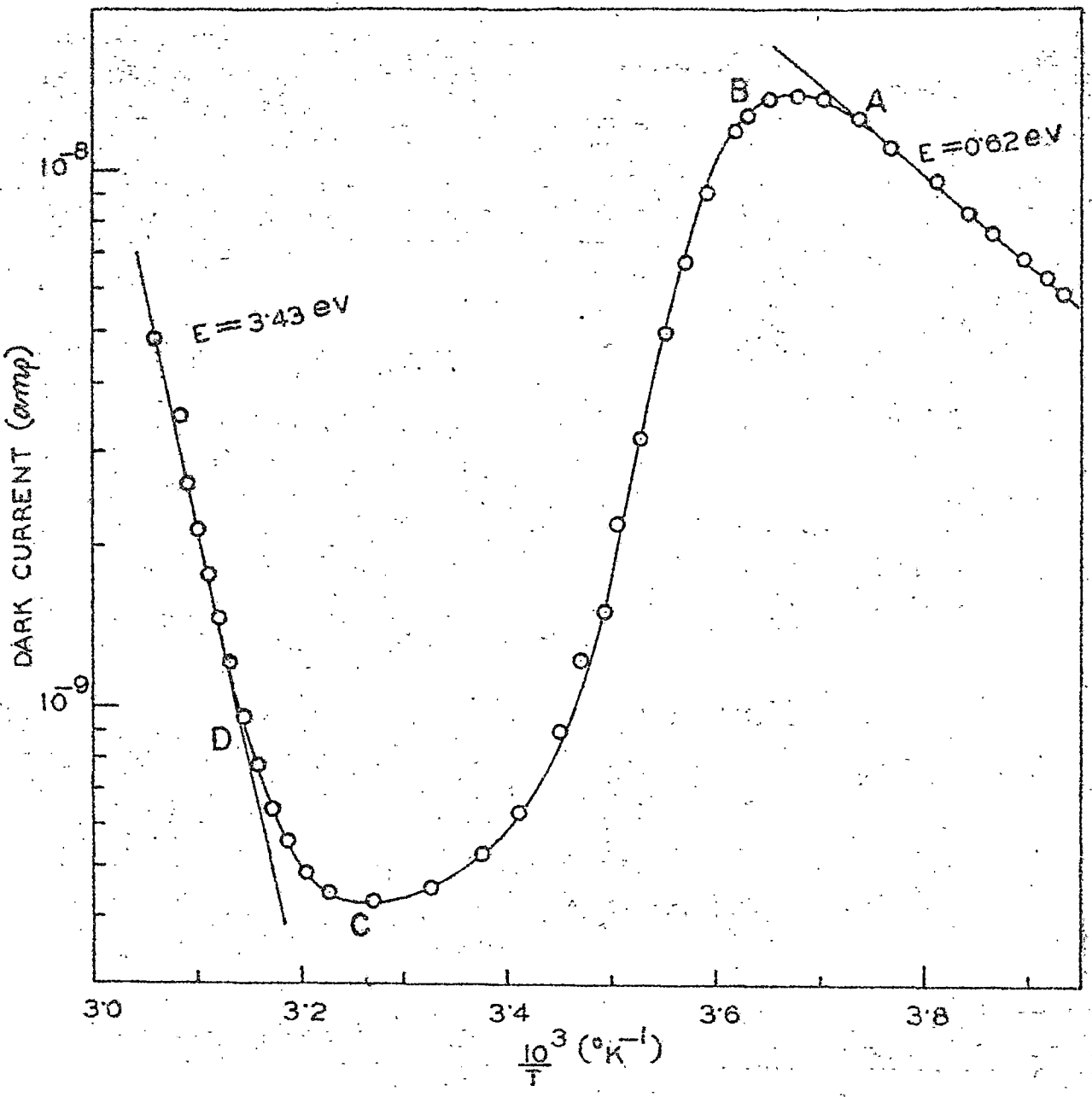
DARK CURRENT (amp)
10^{-8}
10^{-9}
E = 3·43 eV
E = 0·62 eV
A
B
C
D
3·0
3·2
3·4
3·6
3·8
$\frac{10^3}{T}$ (°K^{-1})

FIG. 4·1

a vitamin A alcohol cell is shown in Fig. 4.2. In this case the straight line in the low temperature region gives the activation energy of 0.58 eV which is also less than the value observed in dry nitrogen. The activation energy (1.7 eV) obtained from the straight line at higher temperature region is slightly lower than the value at nitrogen atmosphere (2.06 eV). This is what we have seen in case of Vitamin A acetate also. Similar curves were obtained with toluene, benzene, n-heptane, ethanol and methanol vapours.

The effect of adsorption of ethyl acetate vapour on the activation energy of other polyene semiconductors is shown in Figs. 4.3 - 4.5 for β -apo-8'-carotenal, astacene and methyl bixin powders respectively. From the figures it is seen that in these cases also these plots give two portions of good straight lines — one in the low temperature and the other in the higher temperature region. The activation energy after adsorption of vapours in these polyenes are, however, appreciably higher than that in dry nitrogen atmosphere. The value of the activation energy obtained from the straight line at higher temperature region in all these plots agree satisfactorily to the value in nitrogen atmosphere though in case of methyl bixin (Fig. 4.5) this value is slightly higher possibly due to incomplete desorption.

In the previous chapter we have shown that the enhancement of conductivity depends on the chemical nature of the adsorbed vapours. We have studied the effect of different vapours on the activation energy of these polyene semiconductors and have measured the activation energy of each semiconductor after adsorbing different

FIG. 4.2 : Semiconductivity in an ethyl acetate adsorbed vitamin A alcohol powder cell as a function of temperature.
Ambient vapour pressure 60 mm adsorbed at sample cell temperature 12.5°C.

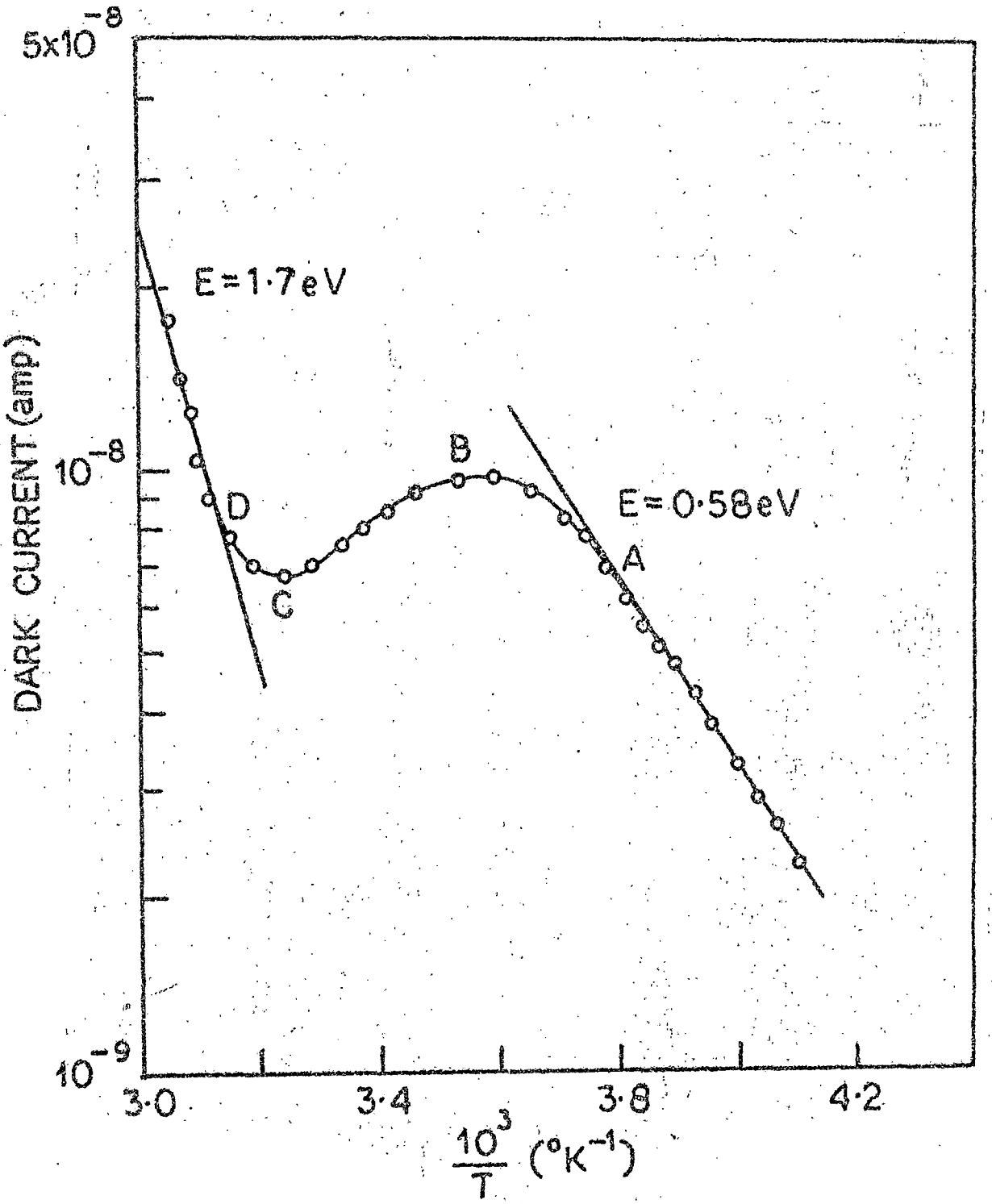
5x10⁻⁸
10⁻⁸
10⁻⁹
DARK CURRENT (amp)
E=1·7eV
E=0·58eV
A
B
C
D
3·0
3·4
3·8
4·2
10³/T (°K⁻¹)

FIG. 4·2

FIG. 4.3 : Semiconductivity in an ethyl acetate adsorbed β-apo-8'-carotenal powder cell as a function of temperature.
Ambient vapour pressure 40 mm adsorbed at sample cell temperature 18.5°C.

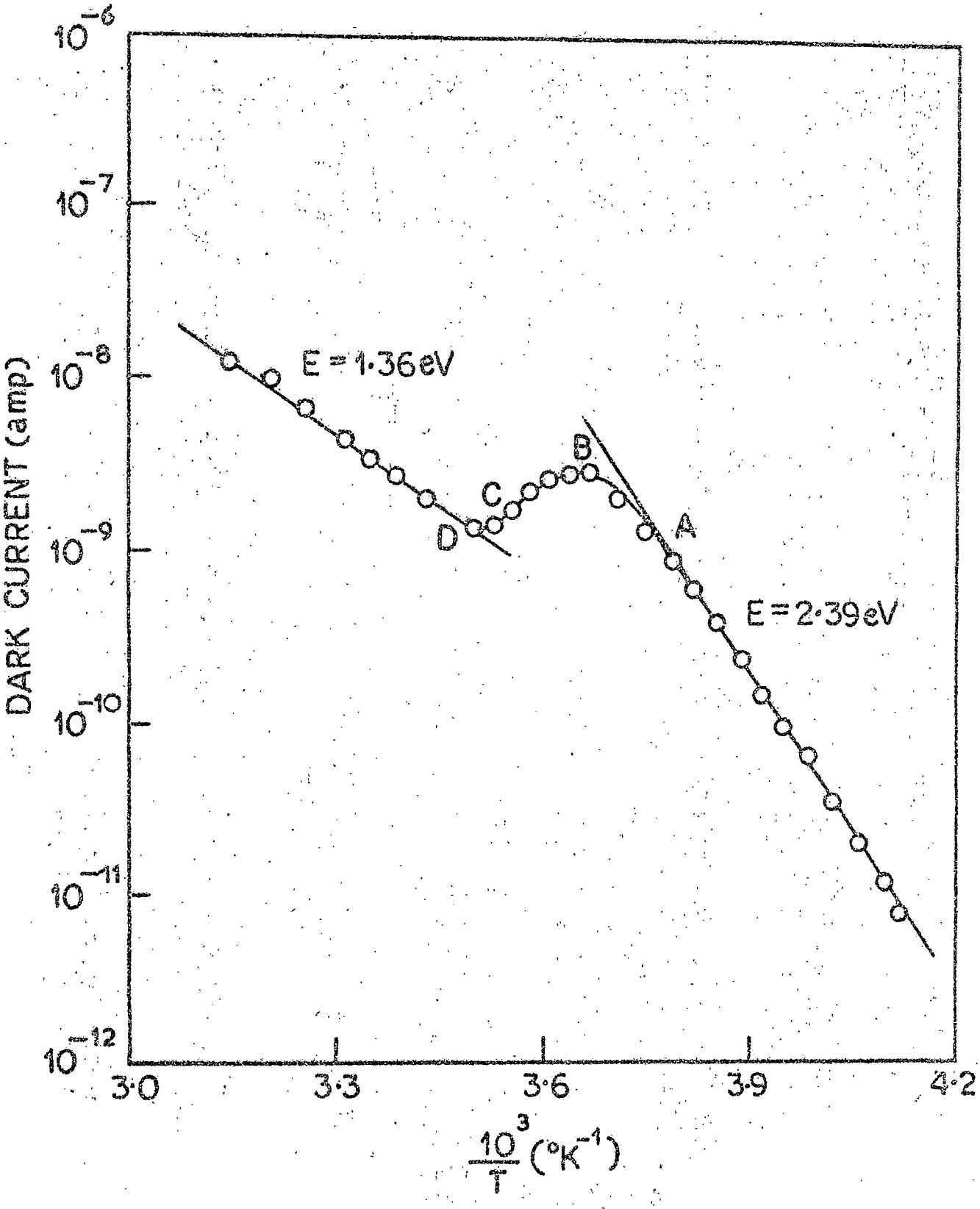
DARK CURRENT (amp)
10^{-6}
10^{-7}
10^{-8}
10^{-9}
10^{-10}
10^{-11}
10^{-12}
E = 1·36eV
E = 2·39eV
A
B
C
D
3·0
3·3
3·6
3·9
4·2
$\frac{10^3}{T}$ (°K^{-1})

FIG. 4·3

FIG. 4.4 : Semiconductivity in an ethyl acetate adsorbed octacene powder cell as a function of temperature. Ambient vapour pressure 45 mm adsorbed at sample cell temperature 18.6°C.

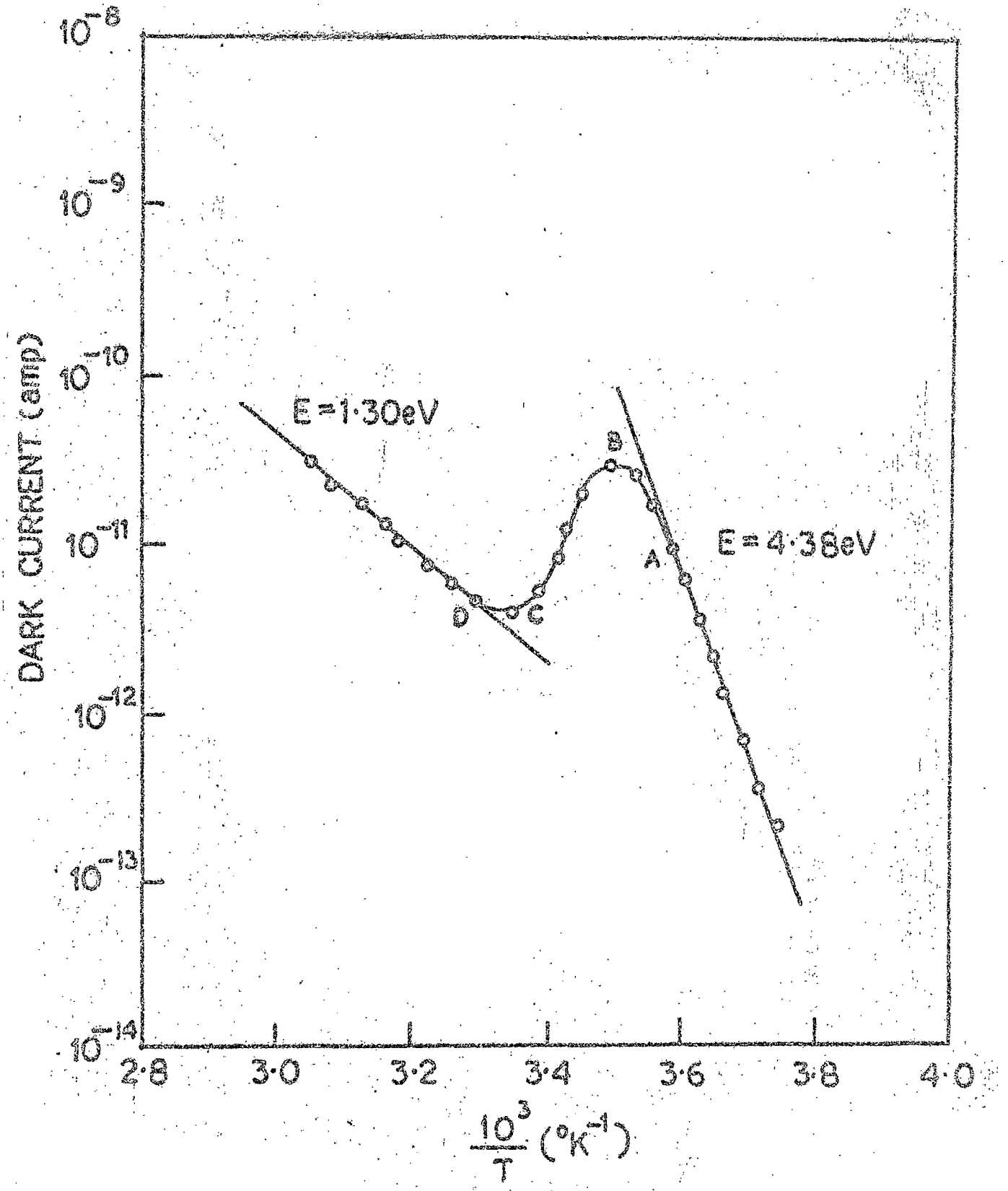
DARK CURRENT (amp)
10^{-8}
10^{-9}
10^{-10}
10^{-11}
10^{-12}
10^{-13}
10^{-14}
E = 1·30eV
E = 4·38eV
A
B
C
D
2·8
3·0
3·2
3·4
3·6
3·8
4·0
$\frac{10^3}{T}$ (°K^{-1})

FIG.4.4

FIG. 4.6 : Semiconductivity in an ethyl acetate adsorbed methyl bixin powder cell as a function of temperature. Ambient vapour pressure 65 mm adsorbed at sample cell temperature 18.6°C.

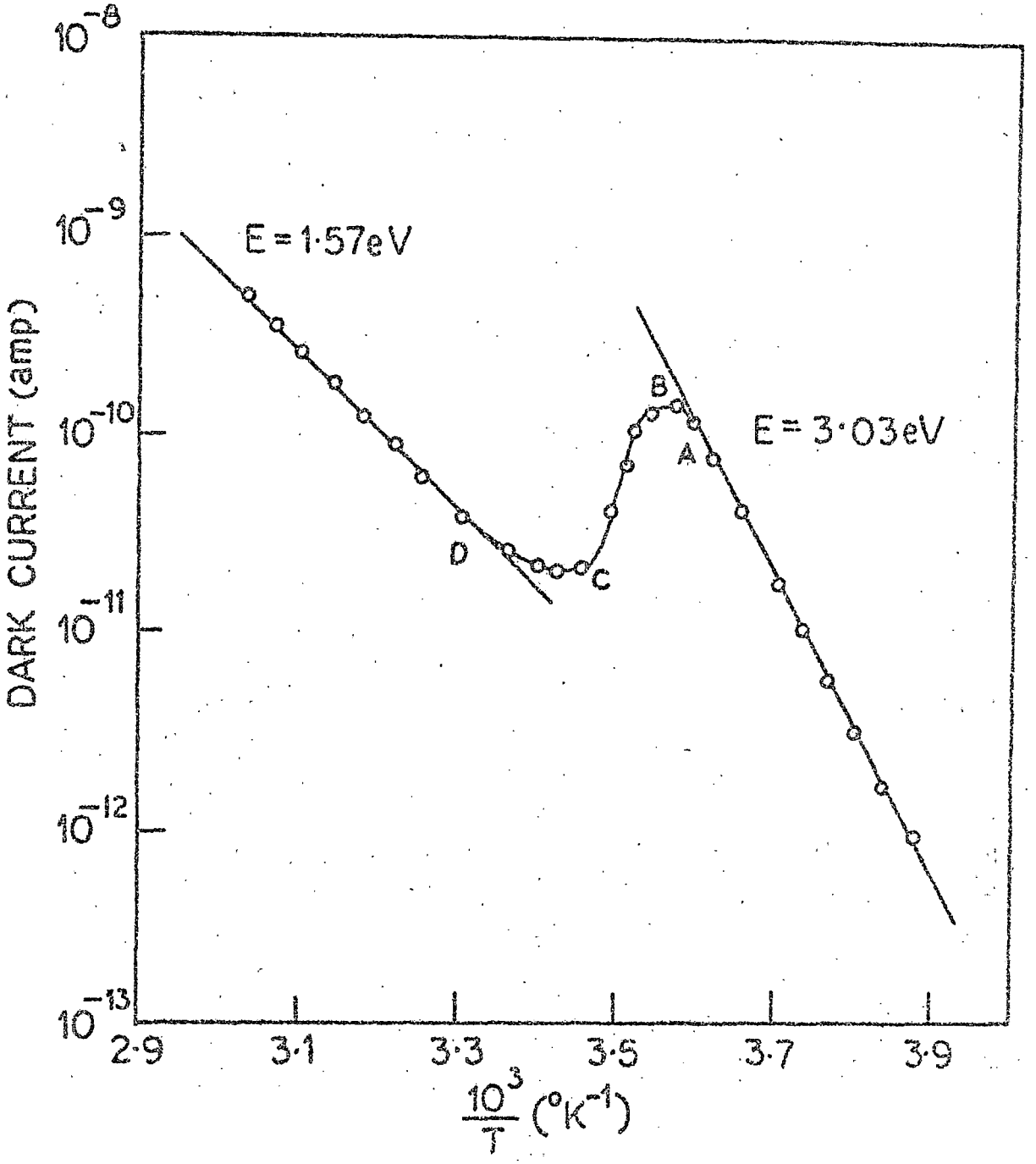
DARK CURRENT (amp)
10^-8
10^-9
10^-10
10^-11
10^-12
10^-13
E = 1·57eV
E = 3·03eV
A
B
C
D
2·9
3·1
3·3
3·5
3·7
3·9
10^3/T (°K^-1)

FIG. 4·5

vapours at a fixed partial pressure and maintaining the sample cell at a constant temperature. In Fig. 4.6, we show the straight line portion in the low temperature region for toluene, ethyl acetate, n-heptane, ethanol and methanol vapours adsorption in vitamin A alcohol. It is observed that with the adsorption of different vapours at the same pressure, the activation energy values are different for different vapurs. In Figs. 4.7 - 4.10 we show similar $\log \sigma$ vs. $\frac{1}{T}$ plots for Vitamin A acetate, β - apo - 8' - carotenal, astacene and methylbixin respectively. We see that the decrease [for Vitamin A alcohol and acetate in Figs. 4.6 and 4.7] and increase [for β - apo-8'-carotenal, astacene and methyl bixin in Figs. 4.8-4.10] in activation energy depends on the nature of the vapours.

4.2.2 <u>Semiconduction activation energy as a function of the amount of vapour adsorbed</u> :

To study the dependence of the activation energy change on the amount of a particular vapour adsorbed in a sample cell, measurements were done by repeated heating, partially desorbing and cooling cycles. A set of straight lines in the low temperature region for $\log \sigma$ vs. $\frac{1}{T}$ plots is shown in Figs. 4.11 and 4.12 for adsorption of different amounts of ethyl acetate vapour in Vitamin A alcohol and Vitamin A acetate respectively. The slopes of these lines depend on the amount of ethyl acetate adsorbed. It is seen that the value of activation energy increases in a regular monotonic fashion as more ethyl acetate vapour desorbs. The other vapours show a similar change in activation energy value with the amount of vapour adsorbed. The dependence of the

FIG. 4.6 : Semiconductivity in a vitamin A alcohol powder cell (steady state condition) with the adsorption of different vapours at the same pressure (40 mm) and at a sample cell temperature of 18.5°C. Solid lines represent the temperature region of measurements, broken lines are extrapolations. Each line refers to a specific vapour adsorbed state : (1), toluene (E = 0.80 eV); (2), ethyl acetate (E = 1.06 eV); (3), n-heptane (E = 1.10 eV); (4), ethanol (E = 1.55 eV); (5), methanol (E = 1.82 eV). (To avoid overlapping with (2) the line corresponding to benzene vapour (E = 1.04 eV) is not shown). The value of $T_0 \approx 408°K$; $\sigma_0' = 2.65 \times 10^{-9} (\Omega \cdot cm)^{-1}$

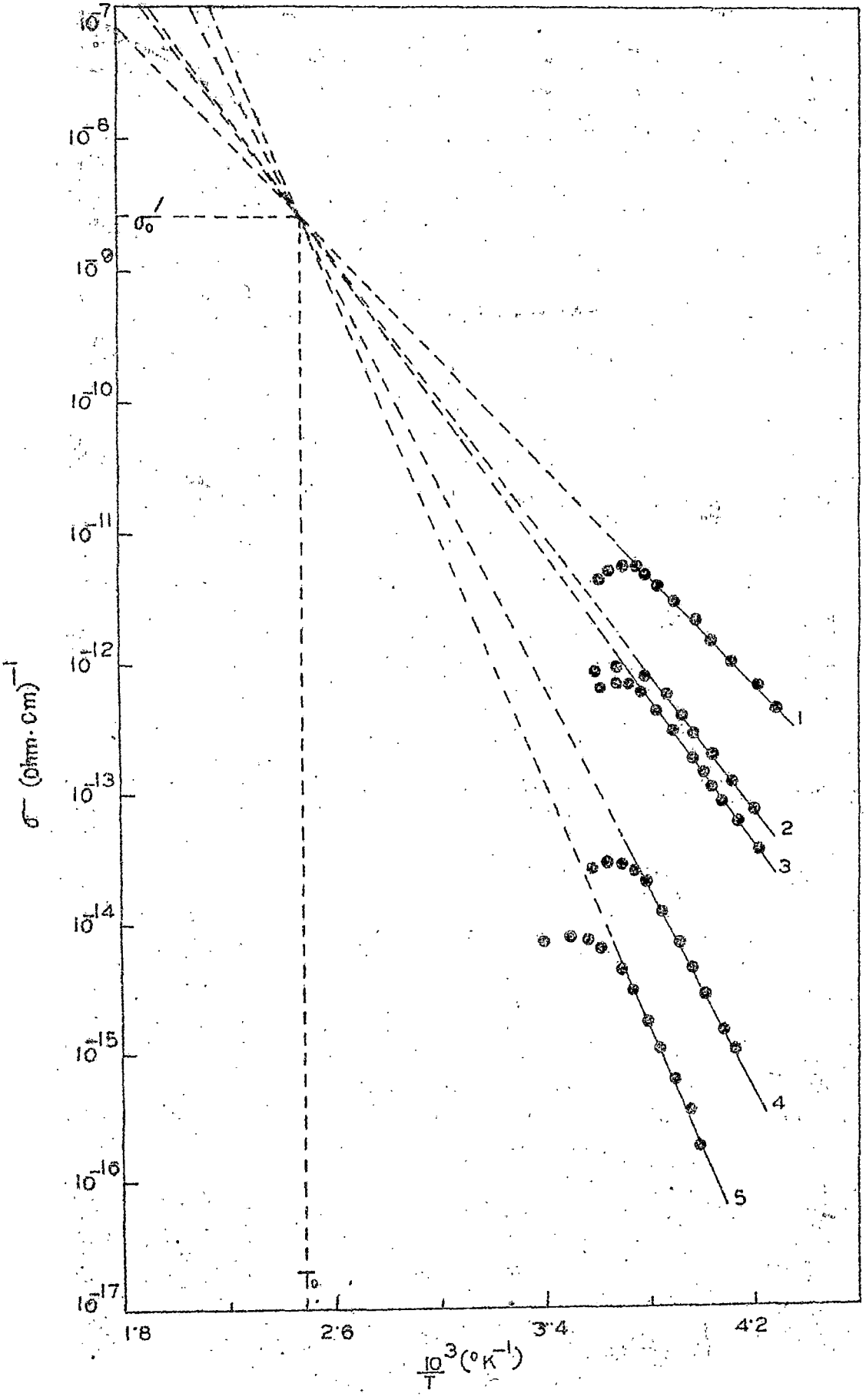
10^{-7}
10^{-8}
σ_0'
10^{-9}
10^{-10}
10^{-11}
10^{-12}
10^{-13}
10^{-14}
10^{-15}
10^{-16}
10^{-17}
σ (ohm·cm)$^{-1}$
T_0
1·8
2·6
3·4
4·2
$\frac{10^3}{T}$ (°K^{-1})
1
2
3
4
5

FIG. 4·6

FIG. 4.7 : Semiconductivity in a vitamin A acetate powder cell (steady state condition) with the adsorption of different vapours at the same pressure (40 mm) and at a sample cell temperature of 12.6°C. Solid lines represent the temperature region of measurements, broken lines are extrapolations. Each line refers to a specific vapour adsorbed state : (1), toluene (E = 0.442 eV); (2), benzene (E = 0.821 eV); (3), ethyl acetate (E = 0.896 eV); (4), n-heptane (E = 1.310 eV); (5), ethanol (E = 1.570 eV); (6), methanol (E = 2.070 eV). The value of $T_0 \approx 335^0K$; $\sigma_0' = 1.80 \times 10^{-10}$ $(\Omega \cdot cm)^{-1}$.

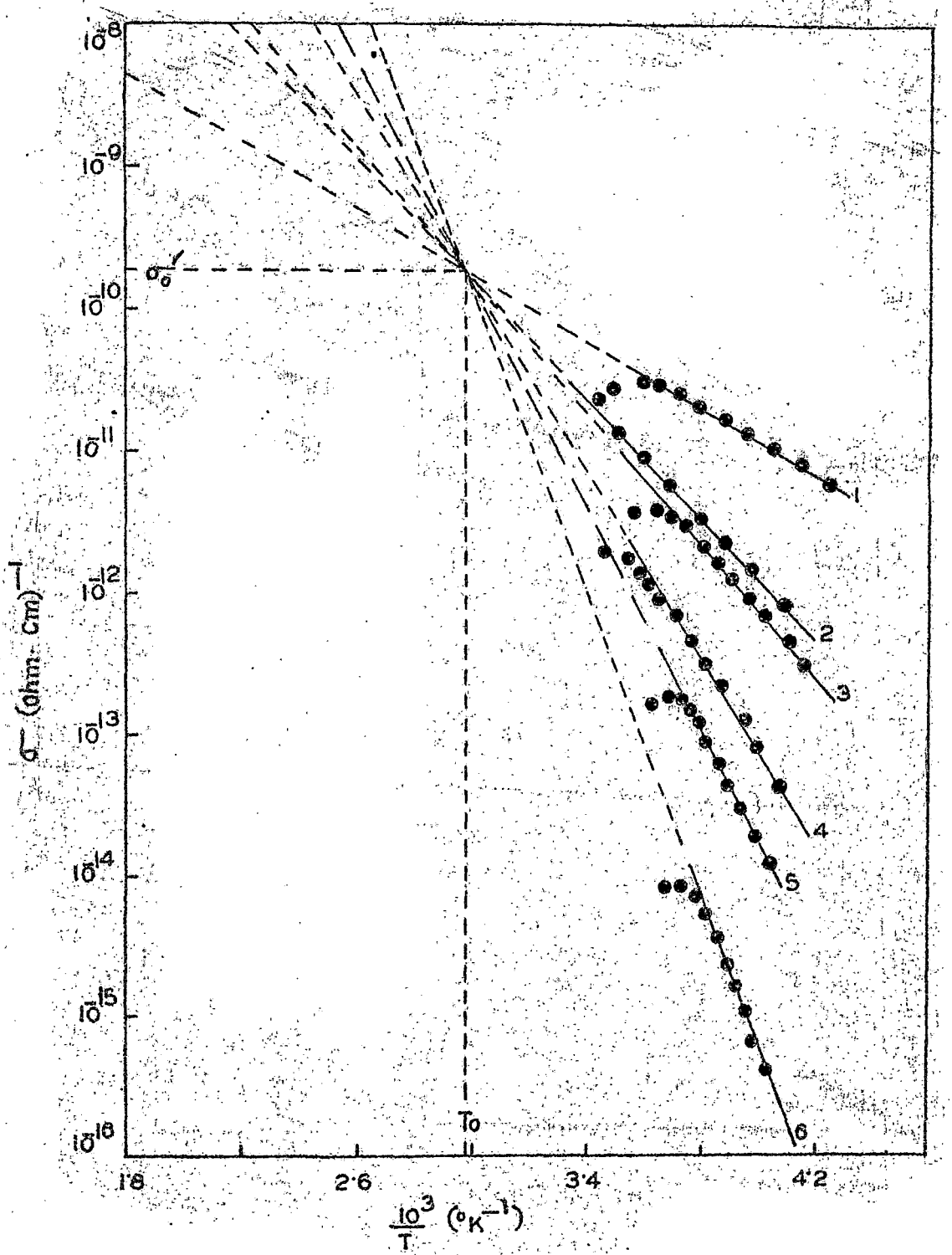
10^{-8}
10^{-9}
σ_0'
10^{-10}
10^{-11}
10^{-12}
10^{-13}
10^{-14}
10^{-15}
10^{-16}
σ (ohm-cm)$^{-1}$
1
2
3
4
5
6
T_0
1·8
2·6
3·4
4·2
$\frac{10^3}{T}$ (°K^{-1})

FIG. 4·7

FIG.4.8 : Semiconductivity in a β-apo-8'-carotenal powder cell (steady state condition) with the adsorption of different vapours at the same pressure (42 mm) and at a sample cell temperature of 18.5°C). Solid lines represent the temperature region of measurements, broken lines are extrapolations. Each line refers to a specific vapour adsorbed state : (1), ethanol (E= 4.80eV); (2), methanol (E= 5.04 eV); (3), ethyl acetate (E=5.58 eV); (4), toluene (E = 1.57 eV); (5), n-heptane (E= 1.40 eV). The value of $T_0 \approx 258^0K$; $\sigma_0' = 0.90 \times 10^{-16}$ $(\Omega \cdot cm)^{-1}$.

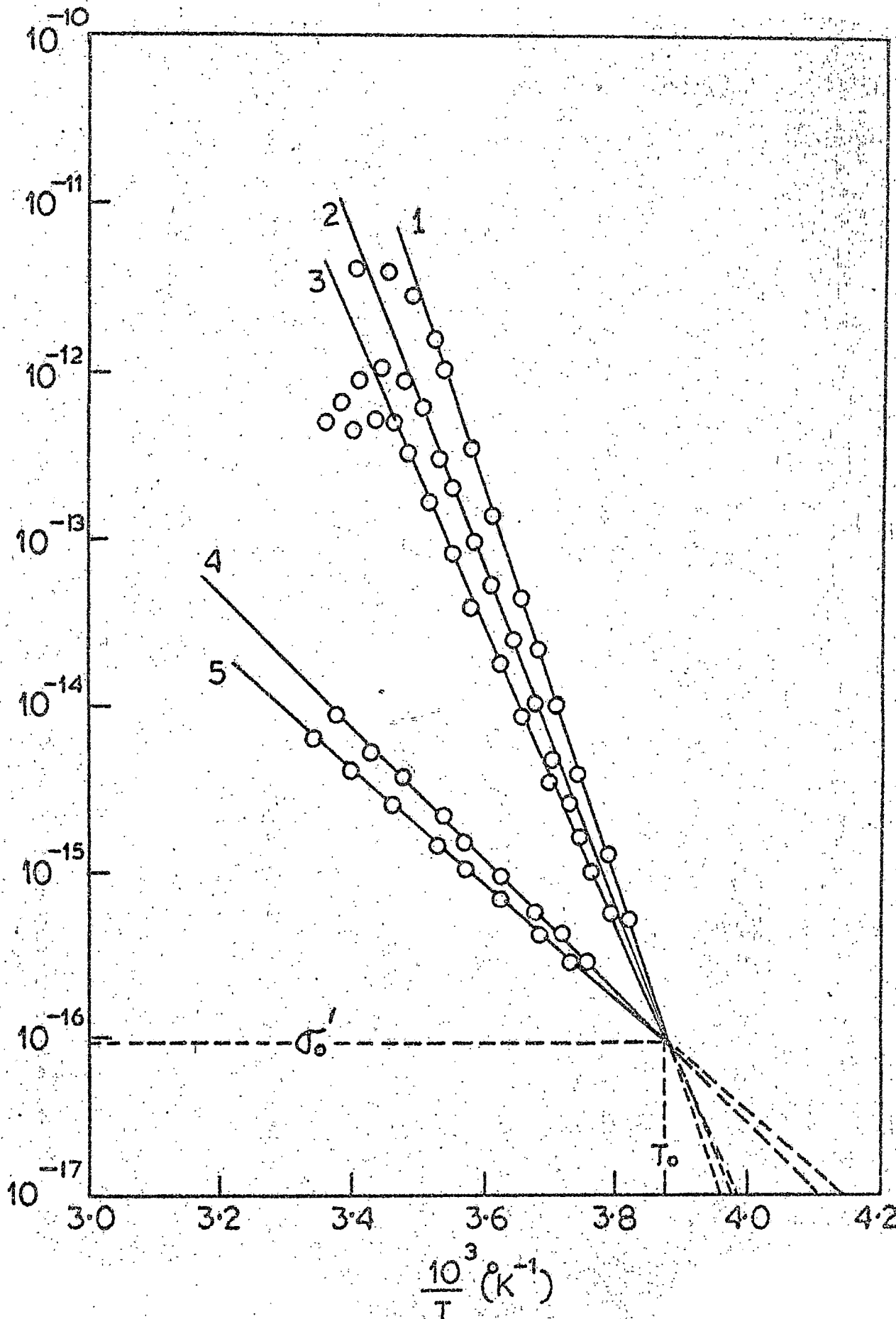
10^{-10}
10^{-11}
10^{-12}
10^{-13}
10^{-14}
10^{-15}
10^{-16}
10^{-17}
σ^{-1} (ohm.cm)
1
2
3
4
5
σ_o'
T_o
3·0
3·2
3·4
3·6
3·8
4·0
4·2
$\frac{10^3}{T}$ (°K^{-1})

FIG. 4·8

FIG. 4.9 : Semiconductivity in an octacene powder cell (steady state condition) with the adsorption of different vapours at the same pressure (50 mm) and at a sample cell temperature of 18.5°C. Solid lines represent the temperature region of measurements, broken lines are extrapolations. Each line refers to a specific vapour adsorbed state : (1), ethanol (E = 7.14 eV); (2), methanol (E = 6.63 eV); (3), ethyl acetate (E = 6.26 eV); (4), benzene (E = 1.71 eV); (5), toluene (E = 1.67 eV). The value of $T_0 \approx 272°K$; $\sigma_0' = 2.15 \times 10^{-16}$ $(\Omega \cdot cm)^{-1}$.

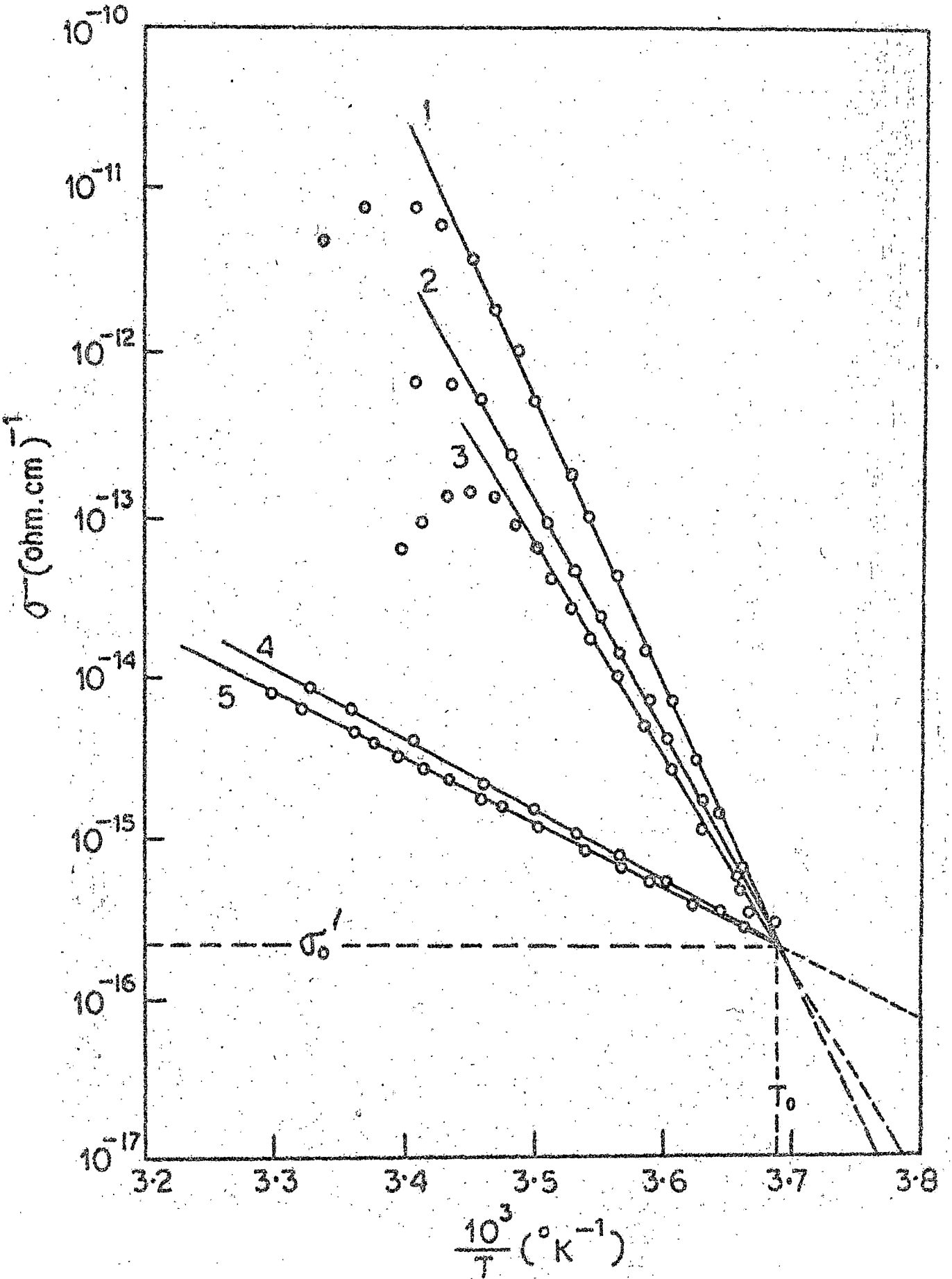
10^{-10}
10^{-11}
10^{-12}
10^{-13}
10^{-14}
10^{-15}
10^{-16}
10^{-17}
σ^{-1} (ohm.cm)$^{-1}$
1
2
3
4
5
σ_0'
T_0
3·2
3·3
3·4
3·5
3·6
3·7
3·8
$\frac{10^3}{T}$ ($^\circ K^{-1}$)

FIG. 4·9

FIG. 4.10 : Semiconductivity in a methyl bixin powder cell (steady state condition) with the adsorption of different vapours at the same pressure (60 mm) and at sample cell-temperature of 18.5°C. Solid lines represent temperature region of measurements, broken lines are extrapolations. Each line refers to a specific vapour adsorbed state : (1), ethanol (E = 4.43 eV); (2), methanol (E = 2.80 eV); (3), ethyl acetate (E = 2.26 eV); (4), benzene (E = 1.68 eV); (5), toluene (E = 1.44 eV). The value of $T_0 \approx 251^{\circ}K$; $\sigma_o' = 0.25 \times 10^{-16}$ $(\Omega . cm)^{-1}$.

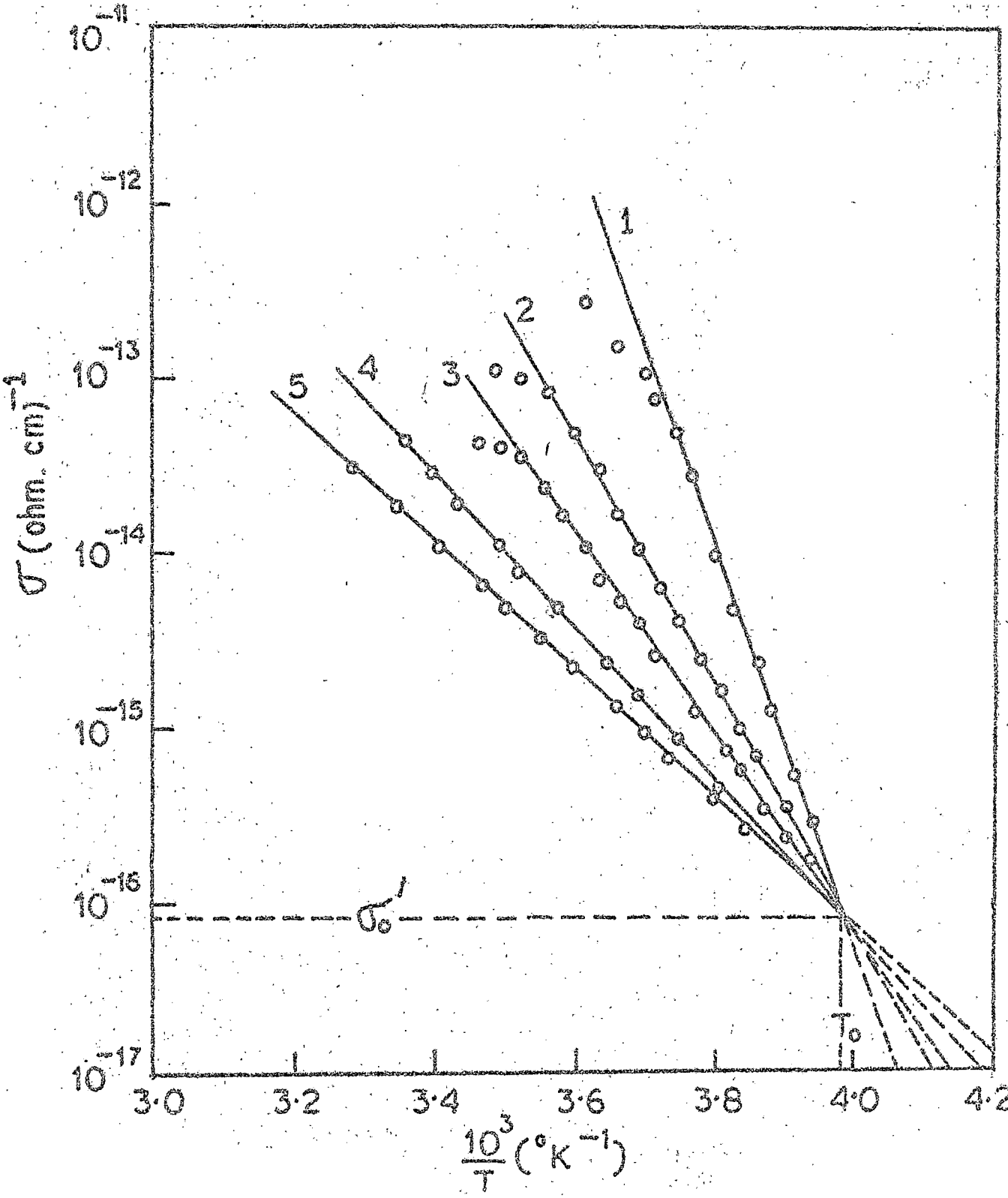
10^{-11}
10^{-12}
10^{-13}
10^{-14}
10^{-15}
10^{-16}
10^{-17}
σ (ohm. cm)$^{-1}$
1
2
3
4
5
σ_0'
T_0
3·0
3·2
3·4
3·6
3·8
4·0
4·2
$\frac{10^3}{T}$ (°K^{-1})

FIG. 4·10

FIG. 4.11 : Semiconductivity data for vitamin A alcohol powder cell (steady state condition) with the adsorption of different amounts of ethyl acetate vapour. Solid lines represent the temperature region of measurements, broken lines are extrapolations. The lines (1) $\longrightarrow$ (6) refer to the states with the decreasing amount of adsorbed vapour. The E values are (1) 0.94 eV; (2) 1.08 eV; (3) 1.19 eV; (4) 1.43 eV; (5) 1.62 eV. The value of $T_0 \approx 403^0K$; $\sigma_0' = 3.10 \times 10^{-9}$ $(\Omega . cm)^{-1}$.

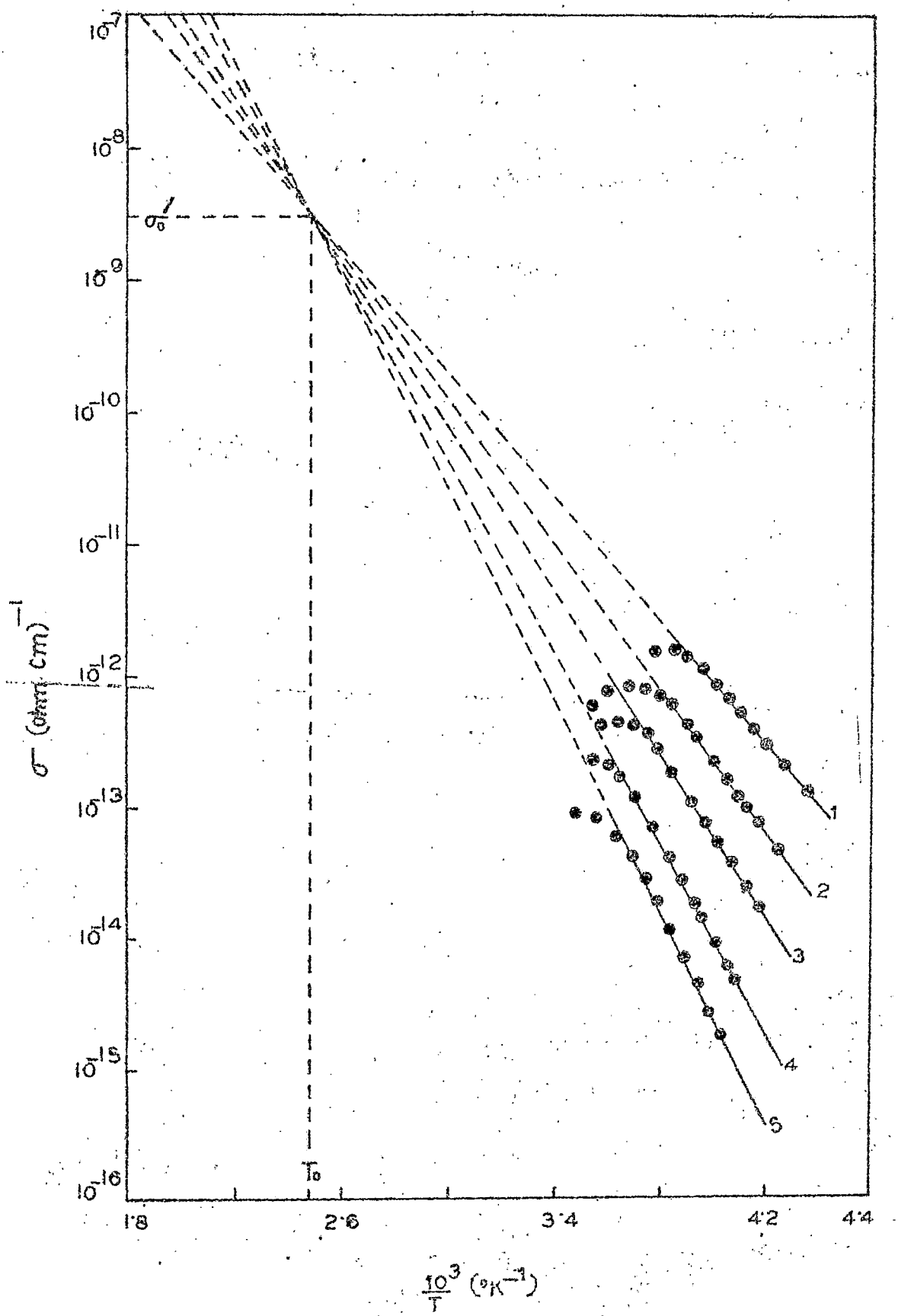
10^{-7}
10^{-8}
σ_0'
10^{-9}
10^{-10}
10^{-11}
10^{-12}
10^{-13}
10^{-14}
10^{-15}
10^{-16}
σ (ohm cm)$^{-1}$
T_0
1·8
2·6
3·4
4·2
4·4
$\frac{10^3}{T}$ ($^\circ K^{-1}$)
1
2
3
4
5

FIG. 4·11

FIG. 4.12 : Semiconductivity data for vitamin A acetate powder cell (steady state condition) with the adsorption of different amounts of ethyl acetate vapour. Solid lines represent the temperature region of measurements, broken lines are extrapolations. The lines (1) $\longrightarrow$ (5) refer to the states with the decreasing amount of adsorbed vapour. The E values are (1) 0.63 eV; (2) 0.89 eV; (3) 1.16 eV; (4) 1.52 eV; (5) 1.80 eV. The value of $T_0 \approx 334^0K$; $\sigma_0' = 1.65 \times 10^{-10}$ $(\Omega . cm)^{-1}$.

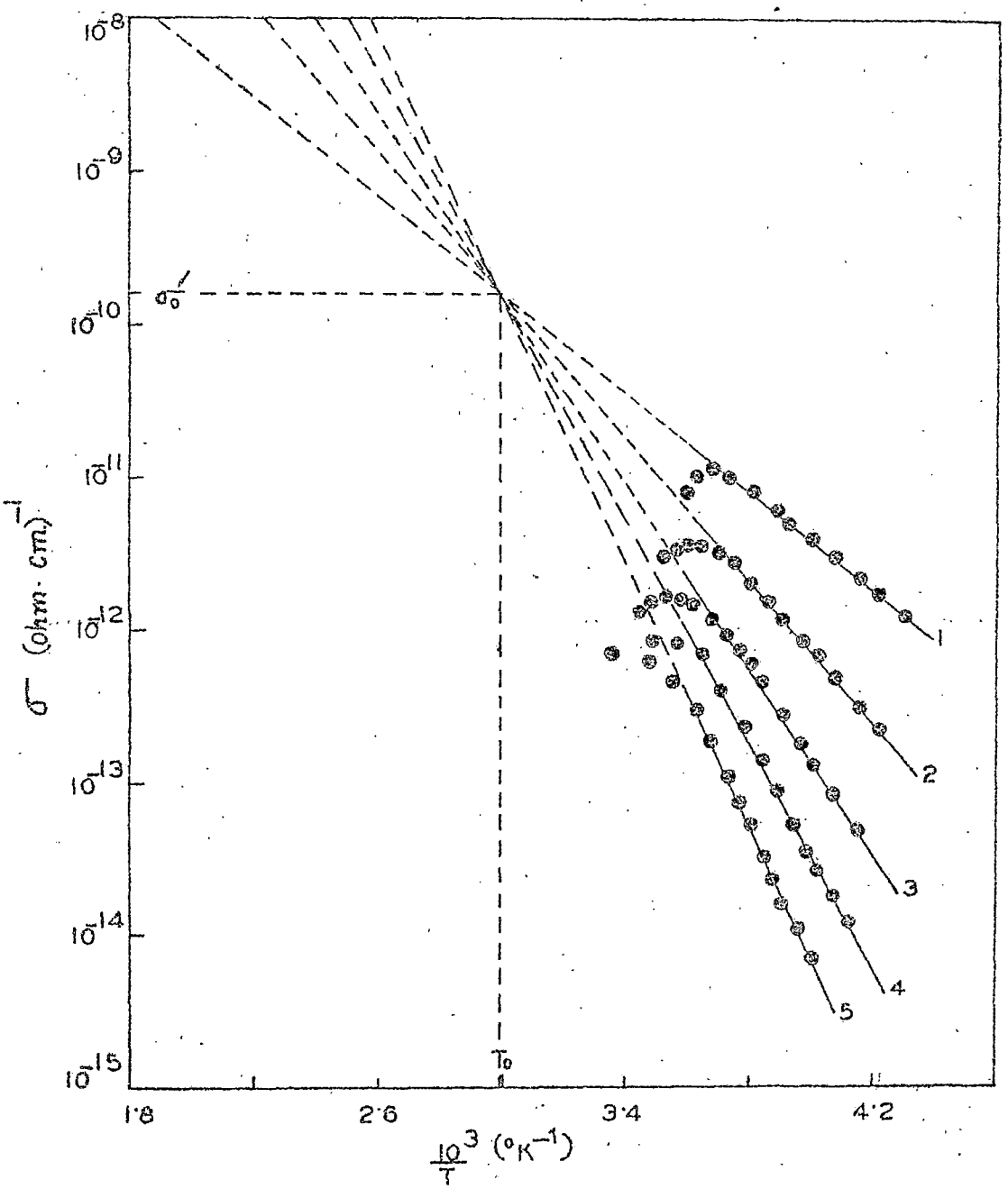
10^{-8}
10^{-9}
10^{-10}
10^{-11}
10^{-12}
10^{-13}
10^{-14}
10^{-15}
σ_0'
T_0
1
2
3
4
5
1·8
2·6
3·4
4·2
σ (ohm·cm)$^{-1}$
$\frac{10^3}{T}$ (°K^{-1})

FIG. 4·12

change in activation energy on the amount of vapour adsorbed in powder cells of β -apo-8'-carotenal, astacene and methyl bixin can be understood from the $\log \sigma$ vs. $\frac{1}{T}$ plots in Figs. 4.13 - 4.15 respectively. In case of methyl bixin the adsorbed vapour is ethanol and in the other two semiconductors ethyl acetate vapour has been used. However, in all these cases it has been observed that the slope of the straight lines in the low temperature region decreases with the decreasing amount of the adsorbed vapour. Thus, theseresults indicate that the value of the activation energy of these three semiconductors decreases in a regular monotonic fashion as more vapours desorbs from the sample. Similar change in activation energy with the amount of vapour adsorbed was also observed with other vapours.

4.2.3 The characteristic temperature for the polyene semiconductors

According to equation (4.1), the extrapolated intercept of the $\log \sigma$ vs. $\frac{1}{T}$ plot on the ordinate at $1/T = 0$ yields the value of σ_0. So from this equation (4.1), it is expected that the straight lines in the low temperature region in each of the $\log \sigma$ vs. $\frac{1}{T}$ plots should meet at a single point on the ordinate at $\frac{1}{T} = 0$ yielding a single value of σ_0 if the conductivity change is solely due to the change in activation energy E as in case of β -carotene[14]. But from the $\log \sigma$ vs. $\frac{1}{T}$ plots (Figs. 4.6 - 4.15) it is observed that no single value of σ_0 is obtained if either $T \to \infty$ or $E \to 0$. The extrapolated lines intercept the ordinate at a wide varieties of positions, but they all pass approximately through a single point at a temperature T_0, Characteristics of the semiconductor. This is exactly what is expected

FIG. 4.13 : Semiconductivity data for β -apo-8'-carotenal powder cell (steady state condition) with the adsorption of different amounts of ethyl acetate vapour. Solid lines represent the temperature region of measurements, broken lines are extrapolations. The lines (1) $\longrightarrow$ (5) refer to the states with the decreasing amount of adsorbed vapour. The E values are (1) 5.26 eV; (2) 3.90 eV; (3) 3.28 eV; (4) 2.19 eV; (5) 1.58 eV. The value of $T_o \approx 261\ ^oK$; $\sigma_o' = 170 \times 10^{-16}\ (\Omega \cdot cm)^{-1}$.

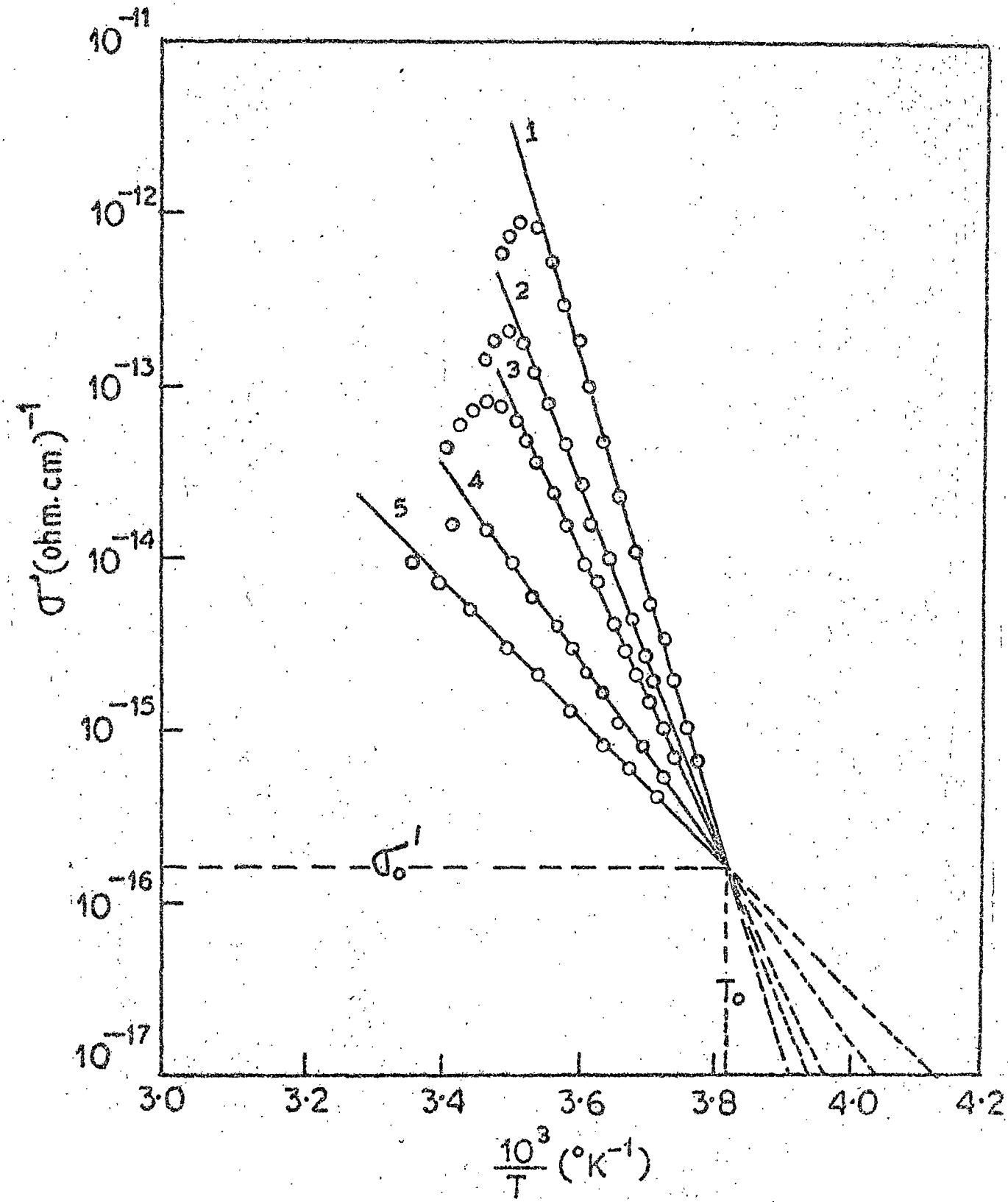
10^{-11}
10^{-12}
10^{-13}
10^{-14}
10^{-15}
10^{-16}
10^{-17}
σ^{-1} (ohm.cm)$^{-1}$
1
2
3
4
5
σ_0^{-1}
T_0
3·0
3·2
3·4
3·6
3·8
4·0
4·2
$\frac{10^3}{T}$ (°K^{-1})

FIG. 4·13

FIG. 4.14 : Semiconductivity data for azocene powder cell (steady state condition) with the adsorption of different amounts of ethyl acetate vapour. Solid lines represent the temperature region of measurements, broken lines are extrapolations. The lines (1) $\rightarrow$ (5) refer to the states with the decreasing amount of adsorbed vapour. The E values are (1) 4.93 eV; (2) 4.38 eV; (3) 3.13 eV; (4) 1.86 eV; (5) 1.31 eV. The value of $T_0 \approx 270^0$K; $\sigma_0' = 1.80 \times 10^{-16}$ $(\Omega . cm)^{-1}$.

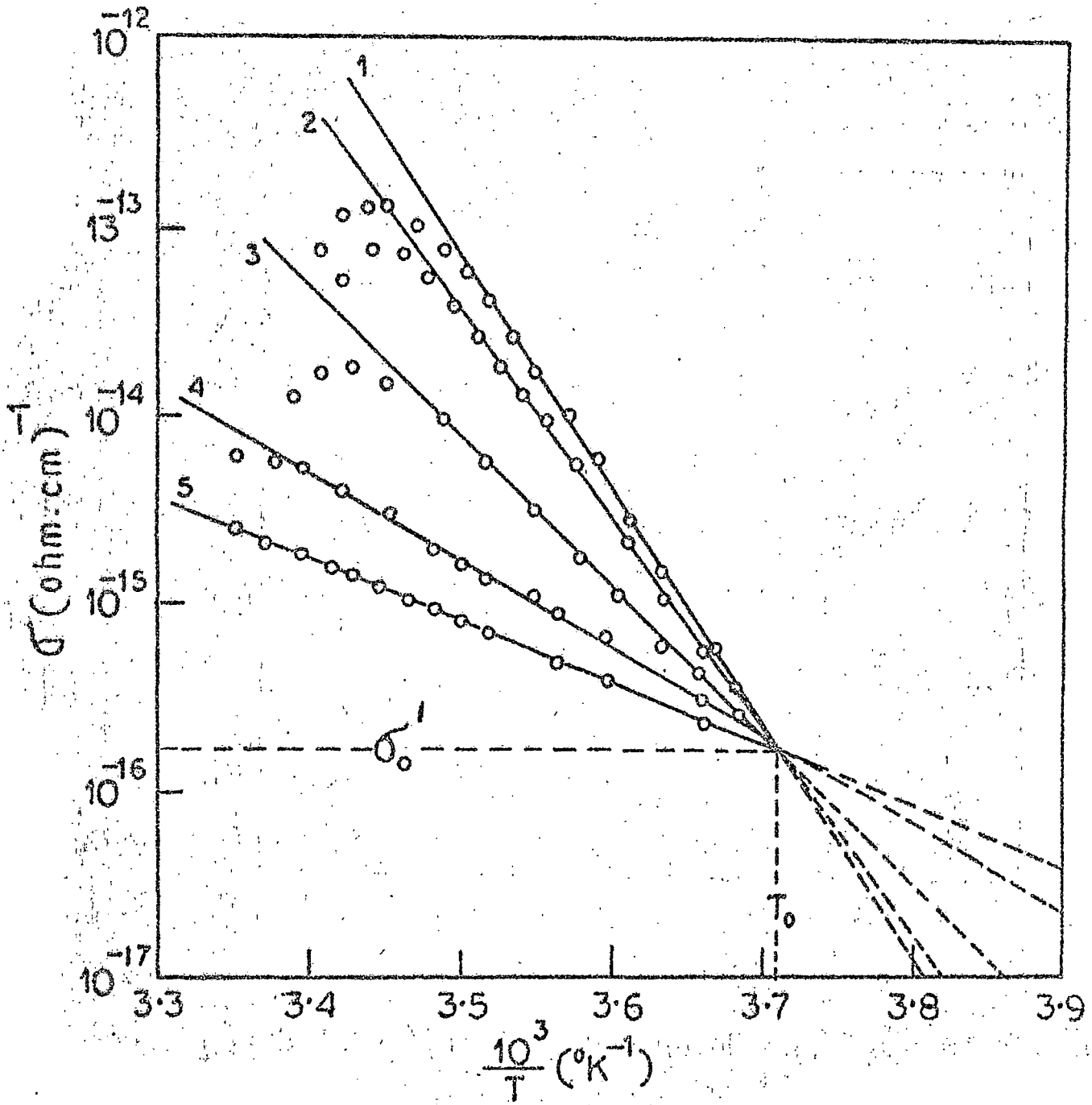
10^{-12}
10^{-13}
10^{-14}
10^{-15}
10^{-16}
10^{-17}
σ (ohm^{-1}cm^{-1})
1
2
3
4
5
σ_0'
T_0
3·3
3·4
3·5
3·6
3·7
3·8
3·9
$\frac{10^3}{T}$ (°K^{-1})

FIG. 4·14

FIG. 4.15 : Semiconductivity data for methyl bixin powder cell (steady state condition) with the adsorption of different amounts of ethanol vapour. Solid lines represent the temperature region of measurements, broken lines are extrapolations. The lines (1) → (6) refer to the states with the decreasing amount of adsorbed vapour. The E values are (1) 4.98 eV; (2) 3.94 eV; (3) 2.92 eV; (4) 1.93 eV; (5) 1.61 eV. The value of $T_0 \approx 253^0K$; $\sigma_0' = 1.95 \times 10^{-16}$ $(\Omega \cdot cm)^{-1}$.

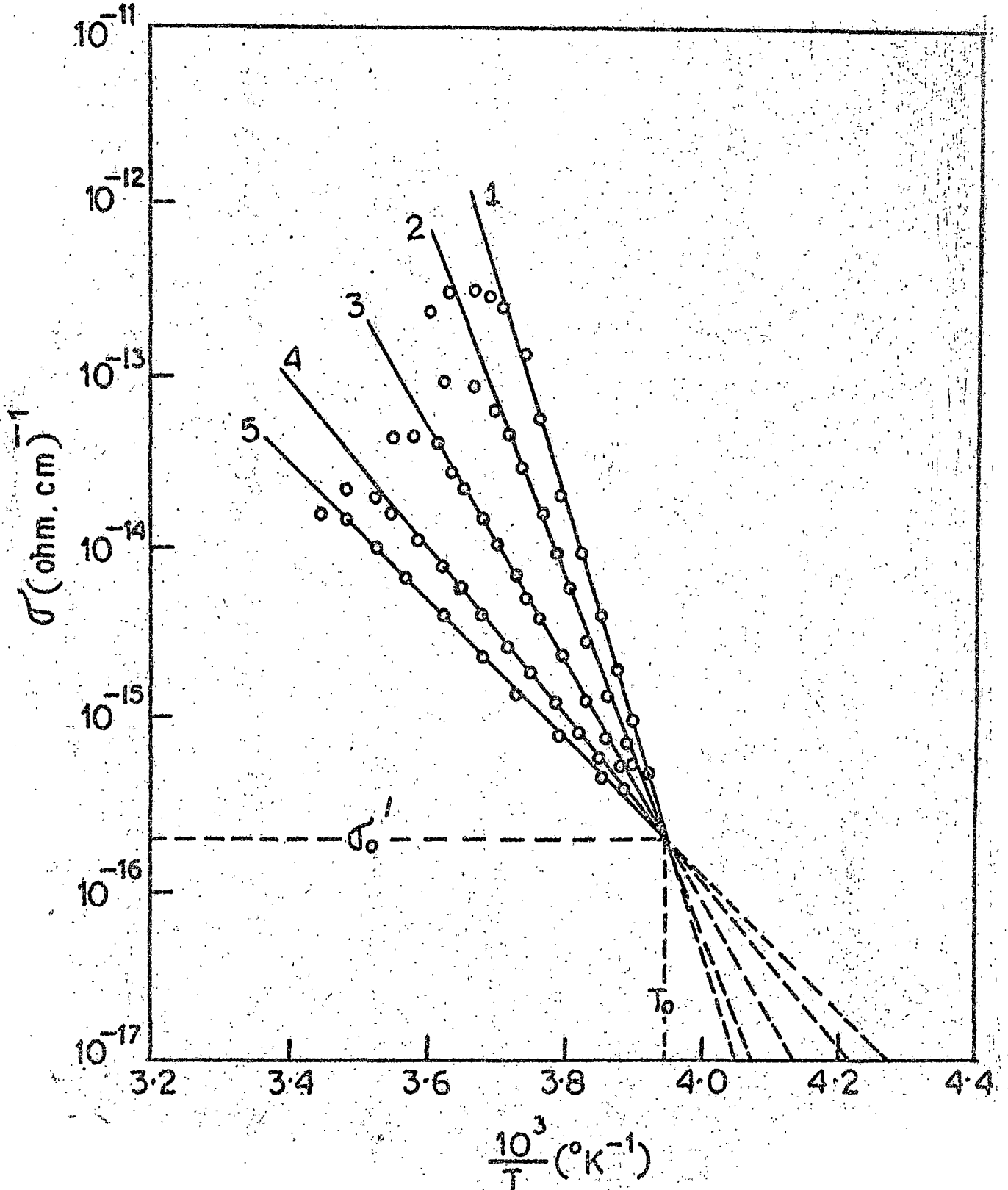
10^{-11}
10^{-12}
10^{-13}
10^{-14}
10^{-15}
10^{-16}
10^{-17}
σ (ohm. cm)$^{-1}$
1
2
3
4
5
σ_0'
T_0
3·2
3·4
3·6
3·8
4·0
4·2
4·4
$\frac{10^3}{T}$ ($^\circ K^{-1}$)

FIG. 4·15

from equation (4.3). At these characteristic temperatures (T_0), the value of $\sigma(T_0)$ gives the σ_0' values. The values of T_0's and σ_0''s obtained from different log σ vs. $\frac{1}{T}$ plots for the semiconductors studied are shown in table 4.1. From table 4.1 it is observed that the two sets of values of T_0's and σ_0''s are in good agreement.

The plots of log σ_0 vs. E are linear as expected from equation (4.4) [since $\log \sigma_0 = E/2kT_0 + \log \sigma_0'$] and are shown in Figs. 4.16 - 4.19 for vitamin A (alcohol and acetate), β-apo-8'-carotenal, astacene and methyl bixin respectively. The values of T_0 and σ_0' can be obtained from the slopes and intercepts respectively of the log σ_0 vs. E plots. The values of T_0 and σ_0' obtained from the log σ_0 vs. E plots for different polyenes are shown in table 4.2. Thus the values of T_0 and σ_0' (tables 4.1 and 4.2) obtained from various log σ vs. $\frac{1}{T}$ and log σ_0 vs. E plots are consistent and show excellent agreement[18]. Using the values of T_0's and σ_0''s obtained from the log σ_0 vs. E plots we have calculated the expected σ values and compare these with experimentally measured values. These are shown in the tables 4.3 - 4.12 for the various polyene semiconductors. The data presented in the tables 4.3 - 4.12 confirm the validity of equation (4.3) for the polyenes studied.

The plots of log $\sigma(\tau_1)$ against E are shown in Figs. 4.20-4.23 for vitamin A (alcohol and acetate), β-apo-8'-carotenal, astacene and methyl bixin respectively. In each case a good straight line is obtained as expected from equation (4.5). The value of the observed

Table - 4.1

The values of T_0's and σ_0''s obtained from different $\log \sigma$ vs. $\frac{1}{T}$ plots of some polyene semiconductors

Semiconductor	Value of T_0 (°K) obtained from the $\log\sigma$ vs. $\frac{1}{T}$ plots for		Value of σ_0' in $(\Omega \cdot cm)^{-1}$ obtained from the $\log\sigma$ vs. $\frac{1}{T}$ plots for	
	adsorption of different vapours	adsorption of different amounts of a particular vapour	adsorption of different vapours	adsorption of different amounts of a particular vapour
Vitamin A alcohol[1]	402	403	2.65×10^{-9}	3.10×10^{-9}
Vitamin A acetate[2]	335	334	1.80×10^{-10}	1.65×10^{-10}
β -apo-8'-carotenal[3]	268	261	0.90×10^{-16}	1.70×10^{-16}
Astacene[4]	272	270	2.15×10^{-16}	1.80×10^{-16}
Methyl bixin[5]	251	253	0.85×10^{-16}	1.95×10^{-16}

1. From Figs. 4.6 and 4.11;
2. From Figs. 4.7 and 4.12;
3. From Figs. 4.8 and 4.13;
4. From Figs. 4.9 and 4.14;
5. From Figs. 4.10 and 4.15.

FIG. 4.16 : Plots of the log σ_o values against the activation energies (E) for vitamin A (alcohol and acetate). The dark circles refer to different vapours and the open circles to different amounts of ethyl acetate vapour. Slopes and σ_o' values are 14.48 eV^{-1} and 2.80 x 10^{-9} $(\Omega \cdot cm)^{-1}$ for vitamin A alcohol and 17.52 eV^{-1} and 1.50 x 10^{-10} $(\Omega \cdot cm)^{-1}$ for vitamin A acetate respectively. The right and left scales refer to vitamin A alcohol and vitamin A acetate respectively.

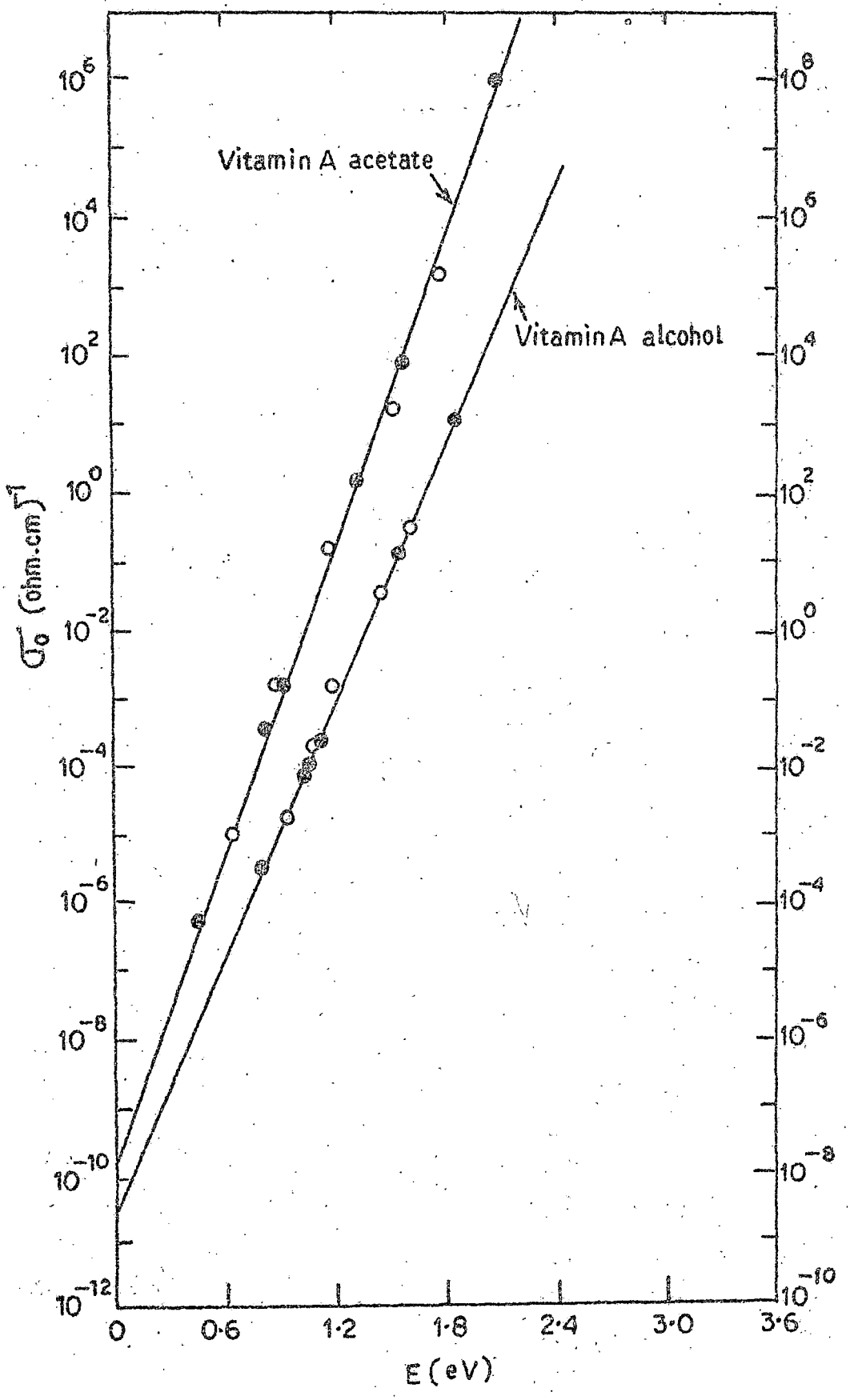
Vitamin A acetate
Vitamin A alcohol
σ_o (ohm.cm)$^{-1}$
10^{6}
10^{4}
10^{2}
10^{0}
10^{-2}
10^{-4}
10^{-6}
10^{-8}
10^{-10}
10^{-12}
10^{8}
10^{6}
10^{4}
10^{2}
10^{0}
10^{-2}
10^{-4}
10^{-6}
10^{-8}
10^{-10}
0
0·6
1·2
1·8
2·4
3·0
3·6
E (eV)

FIG. 4·16

FIG. 4.17 : Plot of the log σ_o values against the activation energies (E) for β -apo-8'-carotenal. The dark circles refer to different vapours and the open circles to different amounts of ethyl acetate vapour. The value of slope = 22.44 eV^{-1}; $\sigma_o' = 1.47 \times 10^{-16}$ $(\Omega \cdot cm)^{-1}$.

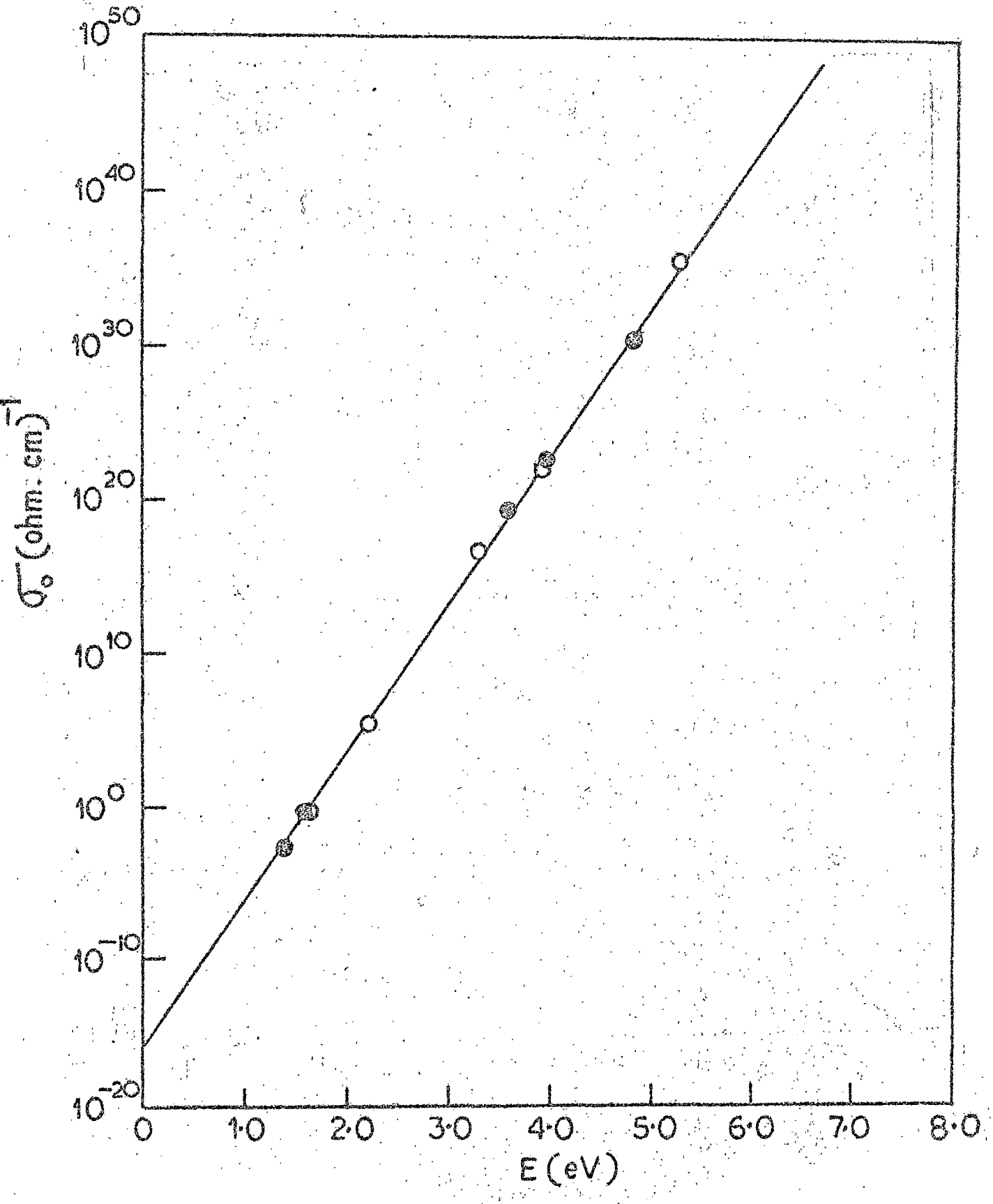
10^{50}
10^{40}
10^{30}
10^{20}
10^{10}
10^{0}
10^{-10}
10^{-20}
σ_o (ohm. cm)$^{-1}$
0
1·0
2·0
3·0
4·0
5·0
6·0
7·0
8·0
E (eV)

FIG. 4·17

FIG. 4.18 : Plot of log σ_o values against the activation energies (E) for acetacene. The dark circles refer to different vapours and the open circles to different amounts of ethyl acetate vapour. The value of slope = 21.64 eV^{-1}; $\sigma_o' = 2.00 \times 10^{-16}$ $(\Omega \cdot cm)^{-1}$.

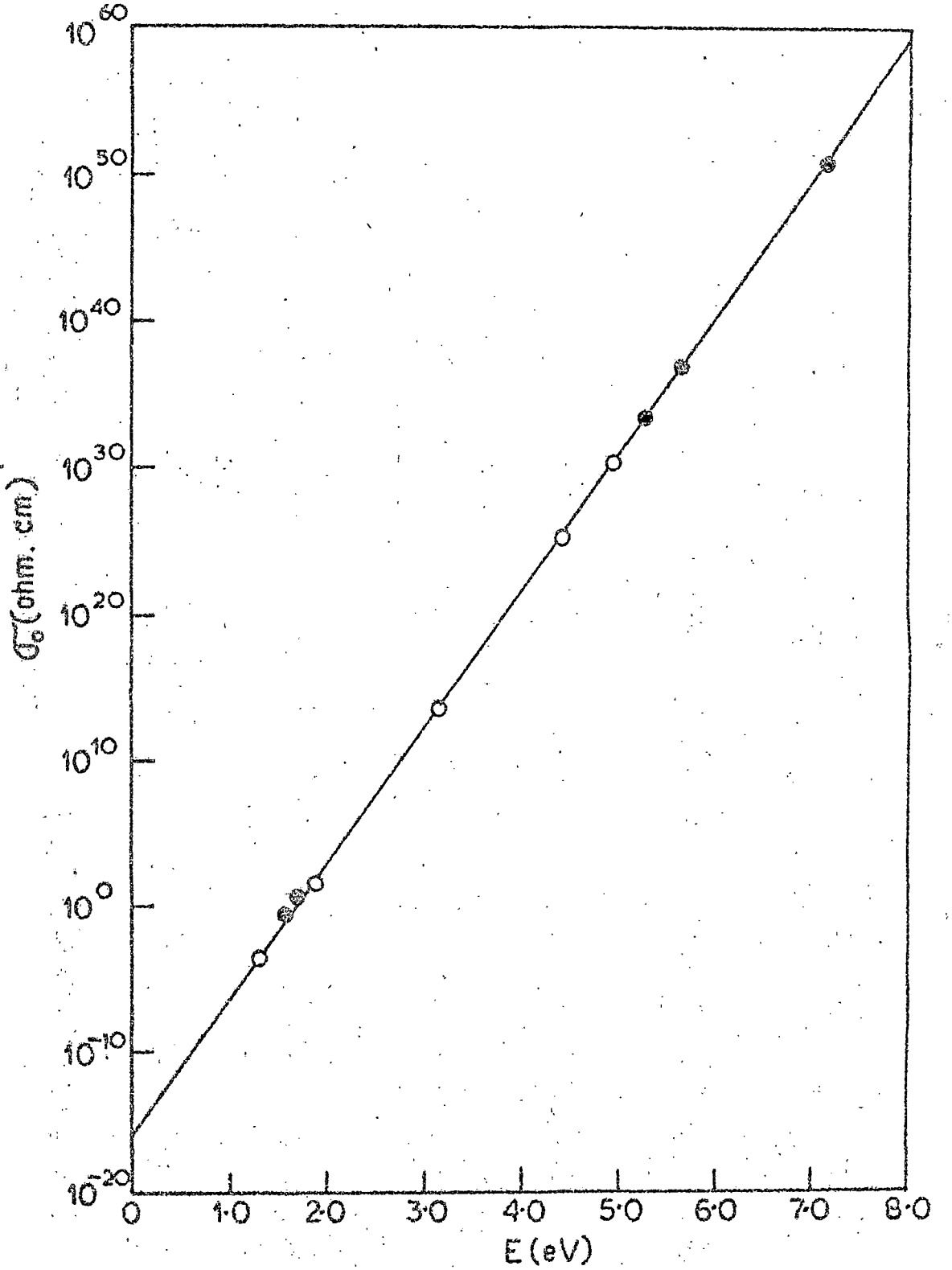
10^{60}
10^{50}
10^{40}
10^{30}
10^{20}
10^{10}
10^{0}
10^{-10}
10^{-20}
$\sigma_0 T$ (ohm. cm)$^{-1}$
0
1·0
2·0
3·0
4·0
5·0
6·0
7·0
8·0
E (eV)

FIG. 4·18

FIG. 4.19 : Plot of $\log \sigma_o$ values against the activation energies (E) for methyl bixin. The dark circles refer to different vapours and the open circles to different amounts of ethanol vapour. The value of slope = 23.31 eV^{-1}; $\sigma_o' = 1.68 \times 10^{-16} (\Omega \cdot cm)^{-1}$.

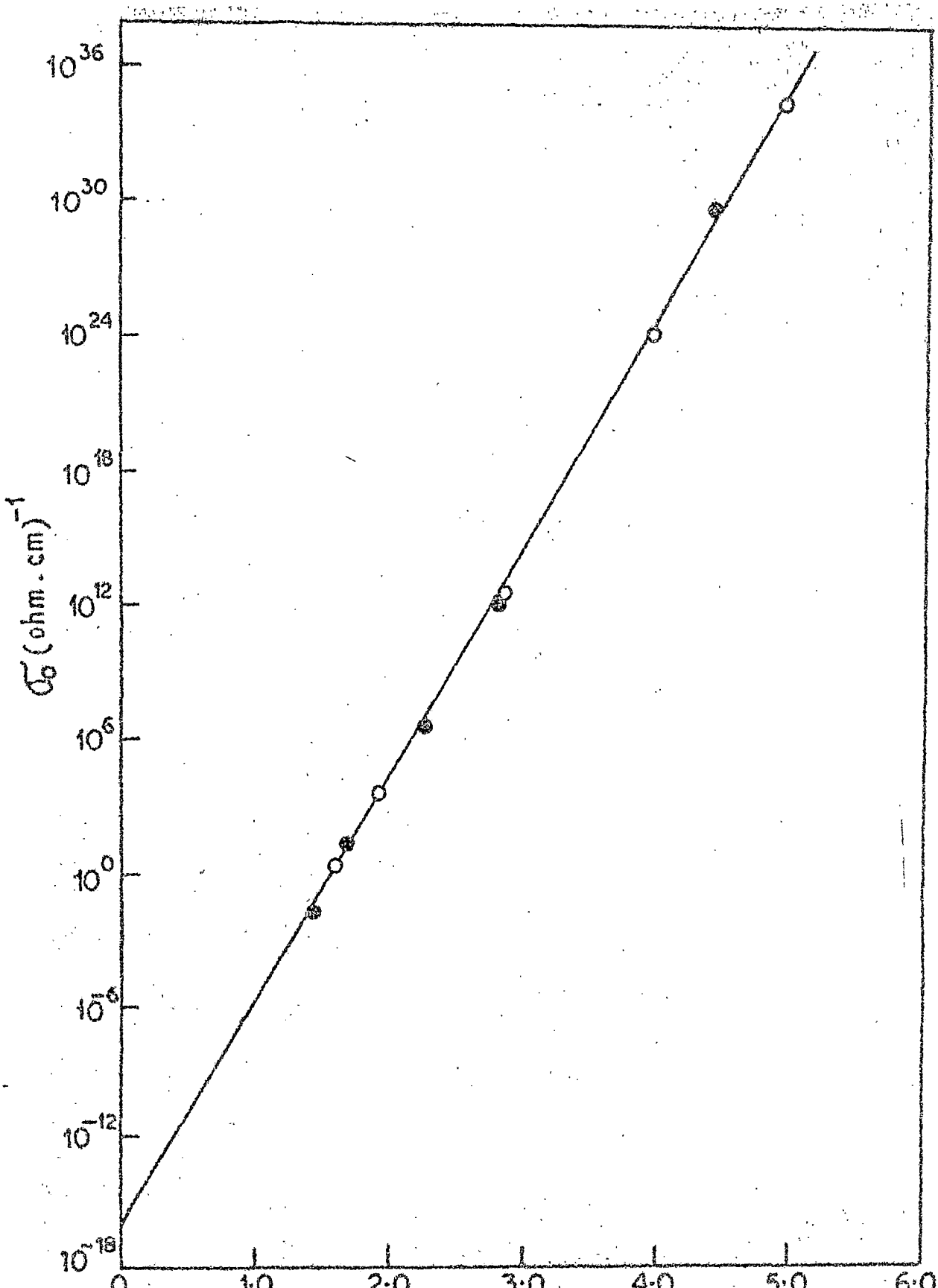
10^{36}
10^{30}
10^{24}
10^{18}
10^{12}
10^{6}
10^{0}
10^{-6}
10^{-12}
10^{-18}
σ_0 (ohm.cm)$^{-1}$
0
1·0
2·0
3·0
4·0
5·0
6·0
E (eV)

FIG. 4.19

Table - 4.2

Values of T_0 and σ_0' obtained from various log σ_0 vs. $\frac{1}{T}$ plots

Semiconductor	Value of T_0 (^{0}K)	Value of σ_0' in $(\Omega . cm)^{-1}$
Vitamin A alcohol[1]	404	2.60×10^{-9}
Vitamin A acetate[1]	333	1.50×10^{-10}
β -apo-8'-carotenal[2]	261	1.47×10^{-16}
Astacene[3]	270	2.00×10^{-16}
Methyl bixin[4]	251	1.68×10^{-16}

1. From Fig. 4.16;
2. From Fig. 4.17;
3. From Fig. 4.18;
4. From Fig. 4.19.

Table - 4.3

Semiconduction parameters for vitamin A alcohol on adsorption of various vapours according to equation (4.3)

Vapours adsorbed	Vitamin A alcohol $(2kT_0)^{-1} = 14.45\ eV^{-1}$ $\sigma_0' = 2.80 \times 10^{-9}\ (\Omega \cdot cm)^{-1}$		
	E(eV)	Calculated $\sigma_0 = \sigma_0' \exp(E/2kT_0)$ $(\Omega \cdot cm)^{-1}$	Measured* σ_0 $(\Omega \cdot cm)^{-1}$
Toluene	0.80	2.93×10^{-4}	4.10×10^{-4}
Benzene	1.04	9.41×10^{-3}	7.98×10^{-3}
Ethyl acetate	1.06	1.26×10^{-2}	1.15×10^{-2}
n-Heptane	1.10	2.24×10^{-2}	2.60×10^{-2}
Ethanol	1.56	1.49×10^{1}	1.30×10^{1}
Methanol	1.82	7.39×10^{2}	1.25×10^{3}

* From Fig. 4.6

Table - 4.4

Semiconduction parameters for vitamin A acetate on adsorption of various vapours according to equation (4.3)

Vapours adsorbed	Vitamin A acetate $(2kT_0)^{-1} = 17.52\ eV^{-1}$ $\sigma_0' = 1.50 \times 10^{-10}\ (\Omega.cm)^{-1}$		
	E(eV)	Calculated $\sigma_0 = \sigma_0' \exp(E/2kT_0)$ $(\Omega.cm)^{-1}$	Measured* σ_0 $(\Omega.cm)^{-1}$
Toluene	0.448	3.84×10^{-7}	6.1×10^{-7}
Benzene	0.821	2.65×10^{-4}	3.8×10^{-4}
Ethyl acetate	0.896	9.85×10^{-4}	1.7×10^{-3}
n-Heptane	1.310	1.39×10^{0}	1.2×10^{0}
Ethanol	1.570	1.32×10^{2}	7.0×10^{1}
Methanol	2.070	8.44×10^{5}	8.0×10^{5}

* From Fig. 4.7

Table - 4.5

Semiconduction parameters for β -apo-8'-carotenal on adsorption of various vapours according to equation (4.3)

Vapours adsorbed	β -apo-8'-carotenal $(2kT_0)^{-1} = 22.44\ eV^{-1}$ $\sigma_0' = 1.47 \times 10^{-16}\ (\Omega \cdot cm)^{-1}$		
	E(eV)	Calculated $\sigma_0 = \sigma_0' \exp(E/2kT_0)$ $(\Omega \cdot cm)^{-1}$	Measured* σ_0 $(\Omega \cdot cm)^{-1}$
Ethanol	4.80	8.83×10^{30}	2.6×10^{30}
Methanol	3.94	3.67×10^{22}	7.0×10^{22}
Ethyl acetate	3.58	1.13×10^{19}	2.8×10^{19}
Toluene	1.57	2.93×10^{-1}	2.9×10^{-1}
n-Heptane	1.40	6.47×10^{-3}	2.4×10^{-3}

* From Fig. 4.8

Table - 4.6

Semiconduction parameters for antacene on adsorption of various vapours according to equation (4.3)

Vapours adsorbed	Antacene $(2kT_0)^{-1} = 21.64\ eV^{-1}$ $\sigma_0' = 2.00 \times 10^{-16}\ (\Omega.cm)^{-1}$		
	E(eV)	Calculated $\sigma = \sigma_0' \exp(E/2kT_0)$ $(\Omega.cm)^{-1}$	Measured* σ_0 $(\Omega.cm)^{-1}$
Ethanol	7.14	8.53×10^{51}	0.7×10^{51}
Methanol	6.63	1.63×10^{37}	1.4×10^{37}
Ethyl acetate	5.36	5.43×10^{33}	3.9×10^{33}
Benzene	1.71	2.35×10^{0}	4.6×10^{0}
Toluene	1.57	1.14×10^{-1}	3.2×10^{-1}

* From Fig. 4.9

Table - 4.7

Semiconduction parameters for methyl bixin on adsorption of various vapours according to equation (4.3)

Vapours adsorbed	Methyl bixin $(2kT_0)^{-1} = 23.31\ eV^{-1}$ $\sigma_0' = 1.68 \times 10^{-16}\ (\Omega.cm)^{-1}$		
	E(eV)	Calculated $\sigma_0 = \sigma_0' \exp(E/2kT_0)$ $(\Omega.cm)^{-1}$	Measured* σ_0 $(\Omega.cm)^{-1}$
Ethanol	4.43	1.11×10^{20}	4.6×10^{20}
Methanol	2.80	3.60×10^{12}	1.2×10^{12}
Ethyl acetate	2.25	9.47×10^{6}	4.6×10^{6}
Benzene	1.68	1.60×10^{1}	2.8×10^{1}
Toluene	1.44	5.37×10^{-2}	4.0×10^{-2}

* From Fig. 4.10

Table - 4.8

Semiconduction parameters for vitamin A alcohol on adsorption of ethyl acetate vapour of different amounts according to equation (4.3)

Curve No. of Fig. 4.11	Vitamin A alcohol $(2k\tau_0)^{-1} = 14.45\ eV^{-1}$ $\sigma_0' = 2.80 \times 10^{-9}\ (\Omega \cdot cm)^{-1}$		
	E(eV)	Calculated $\sigma_0 = \sigma_0' \exp(E/2k\tau_0)$ $(\Omega \cdot cm)^{-1}$	Measured* σ_d $(\Omega \cdot cm)^{-1}$
1	0.94	2.22×10^{-3}	2.0×10^{-3}
2	1.08	1.68×10^{-2}	2.3×10^{-2}
3	1.19	8.22×10^{-2}	1.8×10^{-1}
4	1.43	2.64×10^{0}	3.5×10^{0}
5	1.62	4.11×10^{1}	3.0×10^{1}

Curve No. 1→5 corresponds to the decreasing amount of adsorbed ethyl acetate vapour.

* From Fig. 4.11

Table - 4.9

Semiconduction parameters for vitamin A acetate on adsorption of ethyl acetate vapour of different amounts according to equation (4.3)

Curve No. of Fig. 4.12	Vitamin A acetate $(2kT_0)^{-1} = 17.52\ eV^{-1}$, $\sigma_0' = 1.60 \times 10^{-10}\ (\Omega \cdot cm)^{-1}$		
	E(eV)	Calculated $\sigma_0 = \sigma_0' \exp(E/2kT_0)$ $(\Omega \cdot cm)^{-1}$	Measured* σ_0 $(\Omega \cdot cm)^{-1}$
1	0.63	9.32×10^{-6}	1.0×10^{-5}
2	0.89	8.87×10^{-4}	1.7×10^{-3}
3	1.16	1.00×10^{-1}	1.6×10^{-1}
4	1.62	5.51×10^{1}	1.5×10^{1}
5	1.80	7.43×10^{3}	1.2×10^{3}

Curve No. $1 \rightarrow 5$ corresponds to the decreasing amount of adsorbed ethyl acetate vapour.

* From Fig. 4.12

Table - 4.10

Semiconduction parameters for β -apo-8'-carotenal on adsorption of ethyl acetate vapour of different amounts according to equation (4.3)

Curve No. of Fig. 4.13	β -apo-8'-carotenal $(2kT_0)^{-1}$ = 22.44 eV^{-1} σ_0' = 1.47 x 10^{-16} $(\Omega \cdot cm)^{-1}$		
	E(eV)	Calculated $\sigma_0 = \sigma_0' \exp(E/2kT_0)$ $(\Omega \cdot cm)^{-1}$	Measured* σ_0 $(\Omega \cdot cm)^{-1}$
1	6.26	2.68 x 10^{35}	3.4 x 10^{35}
2	3.90	1.40 x 10^{22}	2.5 x 10^{22}
3	3.28	1.35 x 10^{16}	4.1 x 10^{16}
4	2.10	3.23 x 10^{5}	2.8 x 10^{5}
5	1.58	3.68 x 10^{-1}	5.1 x 10^{-1}

Curve No. 1 → 5 corresponds to the decreasing amount of adsorbed ethyl acetate vapour.

* From Fig. 4.13

Table - 4.11

Semiconduction parameters for antacene on adsorption of ethyl acetate vapour of different amounts according to equation (4.3)

Curve No. of Fig. 4.14	Antacene $(2kT_0)^{-1} = 21.64\ eV^{-1}$, $\sigma_0' = 2.00 \times 10^{-16}\ (\Omega \cdot cm)^{-1}$		
	E(eV)	Calculated $\sigma = \sigma_0' \exp(E/2kT_0)$ $(\Omega \cdot cm)^{-1}$	Measured* σ_0 $(\Omega \cdot cm)^{-1}$
1	4.93	4.30×10^{30}	2.1×10^{30}
2	4.38	2.91×10^{25}	2.7×10^{25}
3	3.13	5.21×10^{13}	3.4×10^{13}
4	1.86	6.04×10^{1}	2.7×10^{1}
5	1.31	4.10×10^{-4}	2.1×10^{-4}

Curve No. 1→ 5 corresponds to the decreasing amount of adsorbed ethyl acetate vapour.

* From Fig. 4.14

Table - 4.12

Semiconduction parameters for methyl bixin on adsorption of ethanol vapour of different amounts according to equation (4.3)

Curve No. of Fig. 4.15	Methyl bixin $(2kT_0)^{-1} = 23.31\ eV^{-1}$ $\sigma_0' = 1.58 \times 10^{-16}\ (\Omega \cdot cm)^{-1}$		
	E(eV)	Calculated $\sigma_0 = \sigma_0' exp(E/2kT_0)$ $(\Omega \cdot cm)^{-1}$	Measured* σ_0 $(\Omega \cdot cm)^{-1}$
1	4.98	4.10×10^{24}	2.1×10^{24}
2	3.94	1.22×10^{24}	1.5×10^{24}
3	2.82	5.68×10^{12}	3.0×10^{12}
4	1.92	4.32×10^{3}	4.6×10^{3}
5	1.61	3.14×10^{0}	2.3×10^{0}

Curve No. 1 → 5 corresponds to the decreasing amount of adsorbed ethanol vapour.

* From Fig. 4.16

FIG. 4.20 : Plots of log σ at a constant temperature ($1/T_1 = 3.30 \times 10^{-3}\ ^{\circ}K^{-1}$) vs. E for vitamin A (alcohol and acetate). The left and right scales correspond to vitamin A alcohol and vitamin A acetate respectively. The dark circles refer to different vapours and the open circles to different amounts of ethyl acetate vapour. Slopes and σ_o' values are $7.70\ eV^{-1}$ and $2.85 \times 10^{-9}\ (\Omega\ cm)^{-1}$ for vitamin A alcohol; $4.55\ eV^{-1}$ and $1.60 \times 10^{-10}\ (\Omega\ cm)^{-1}$ for vitamin A acetate respectively.

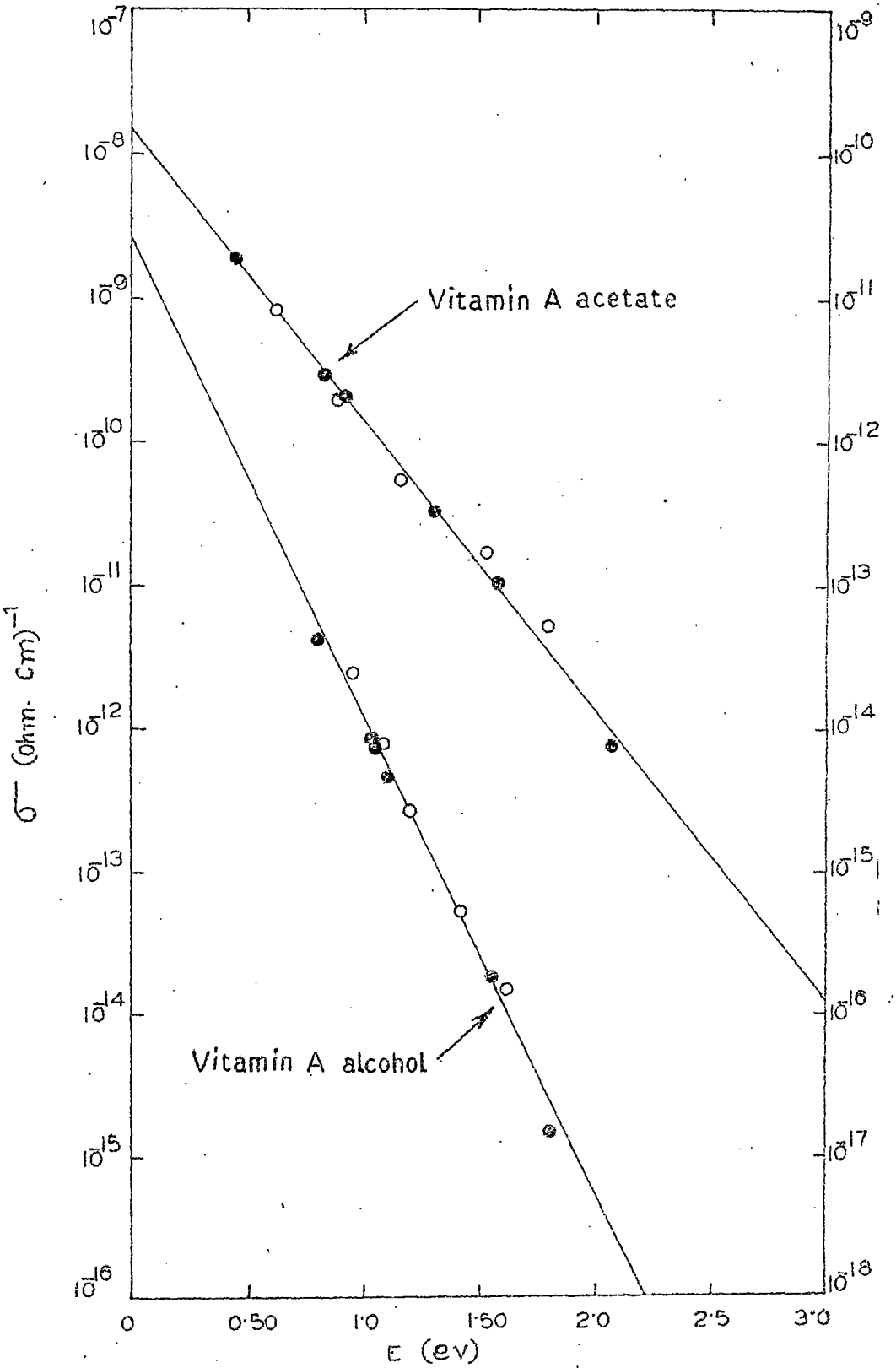
Vitamin A acetate
Vitamin A alcohol
σ (ohm. cm)⁻¹
E (eV)
0
0·50
1·0
1·50
2·0
2·5
3·0

FIG. 4·20

FIG. 4.21 : Plot of log σ at a constant temperature ($1/T = 3.60 \times 10^{-3} K^{-1}$) vs. E for β-apo-8'-carotenal. The dark circles refer to different vapours and the open circles to different amounts of ethyl acetate vapour.
The value of slope = 1.39 eV^{-1} ; $\sigma_o' = 1.25 \times 10^{-16} (\Omega \cdot cm)^{-1}$.

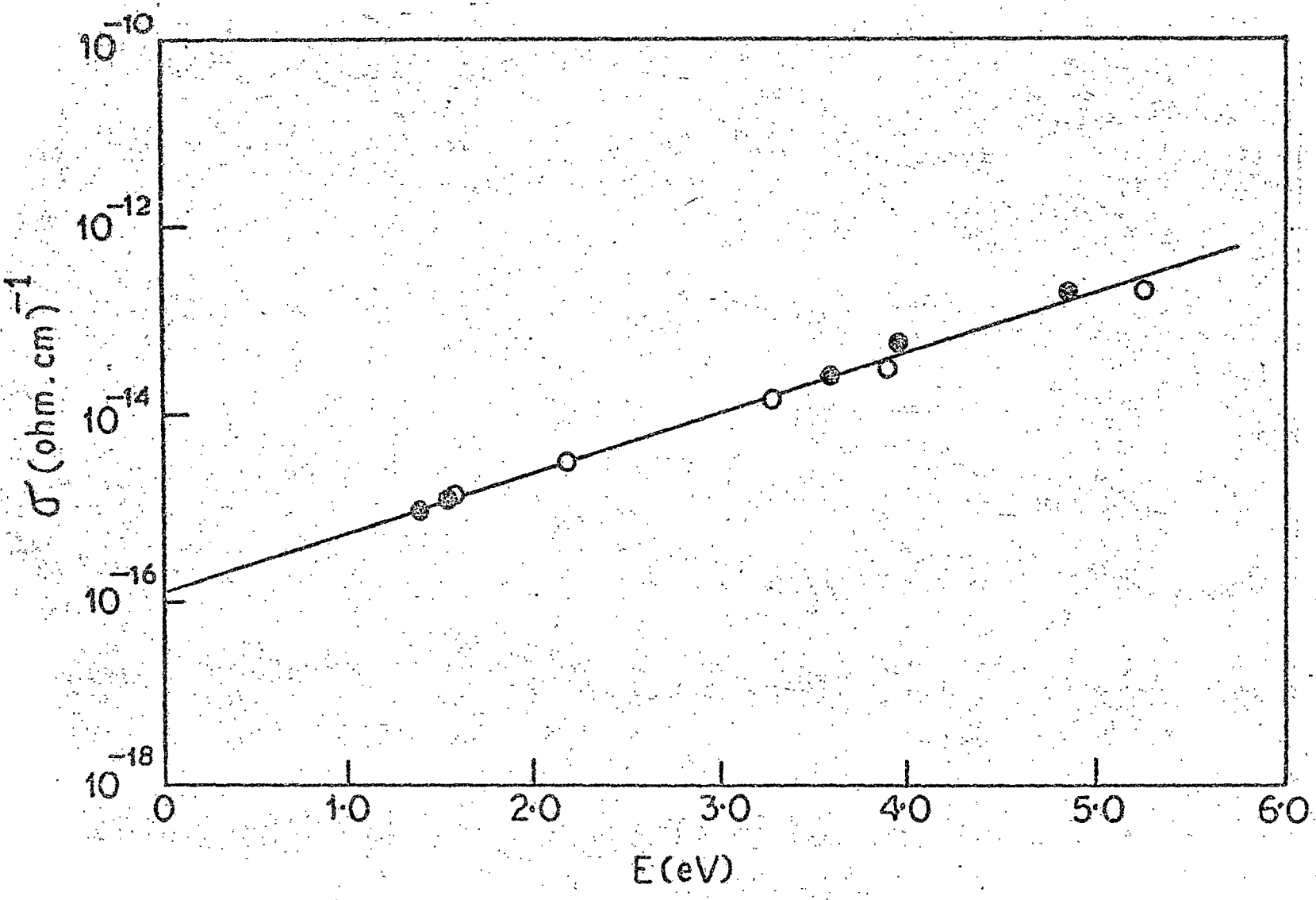

FIG. 4·21

FIG. 4.22 : Plot of log σ at a constant temperature ($\frac{1}{T}$ = 3.65 x 10^{-3} $^{o}K^{-1}$) vs. E for estacene. The dark circles refer to different vapours and the open circles to different amounts of ethyl acetate vapour. The value of slope = 0.86 eV^{-1}; σ_o' = 1.80 x 10^{-10} $(\Omega \cdot cm)^{-1}$.

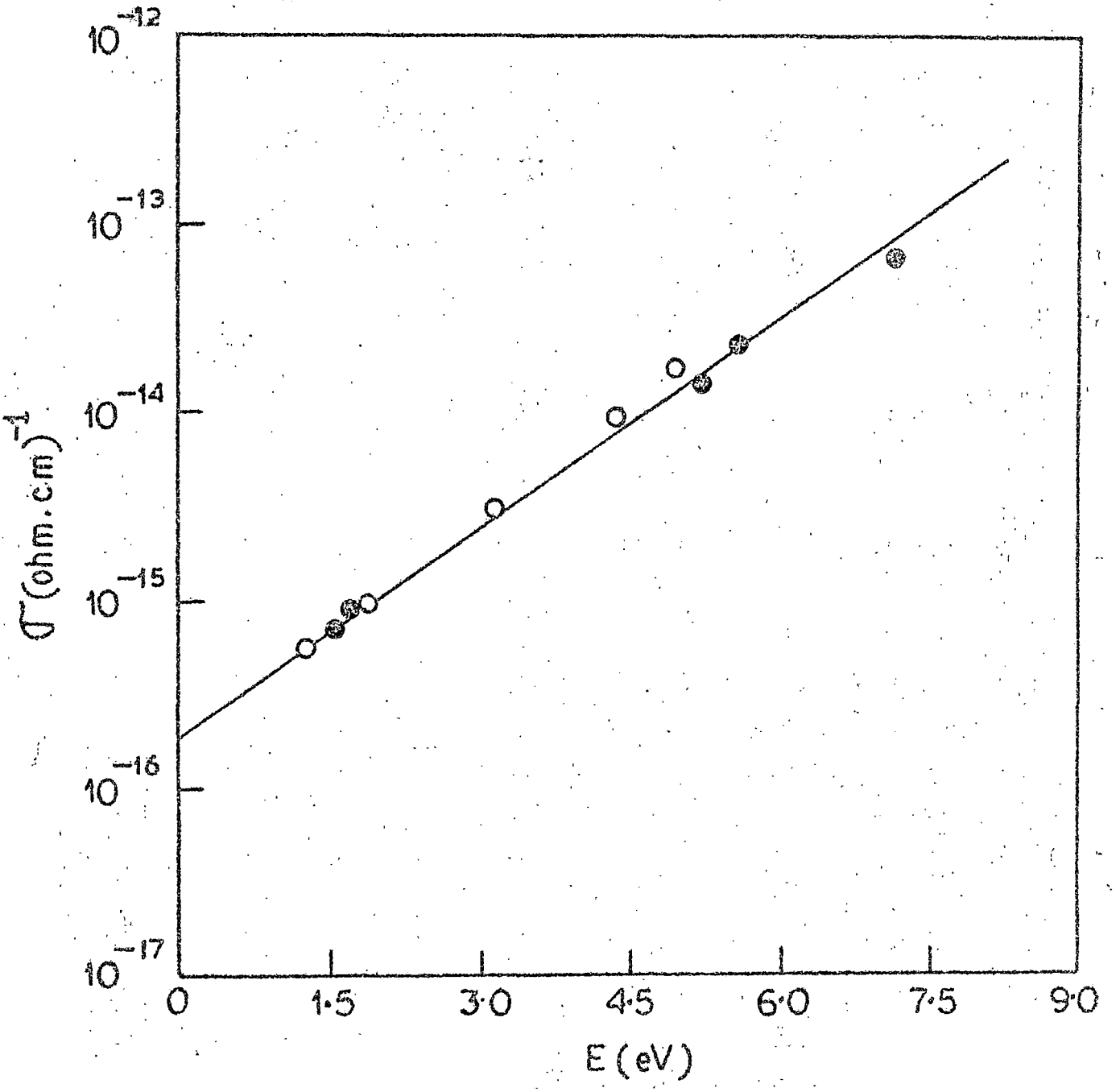
10^{-12}
10^{-13}
10^{-14}
10^{-15}
10^{-16}
10^{-17}
σ (ohm.cm)$^{-1}$
0
1·5
3·0
4·5
6·0
7·5
9·0
E (eV)

FIG. 4·22

FIG. 4.23 : Plot of $\log \sigma$ at a constant temperature ($\frac{1}{T_1} = 3.70 \times 10^{-3}\ ^{\circ}K^{-1}$) vs. E for methyl bixin. The dark circles refer to different vapours and open circles to different amounts of ethanol vapour. The value of slope = $1.60\ eV^{-1}$; $\sigma_o' = 1.00 \times 10^{-16}\ (\Omega \cdot cm)^{-1}$.

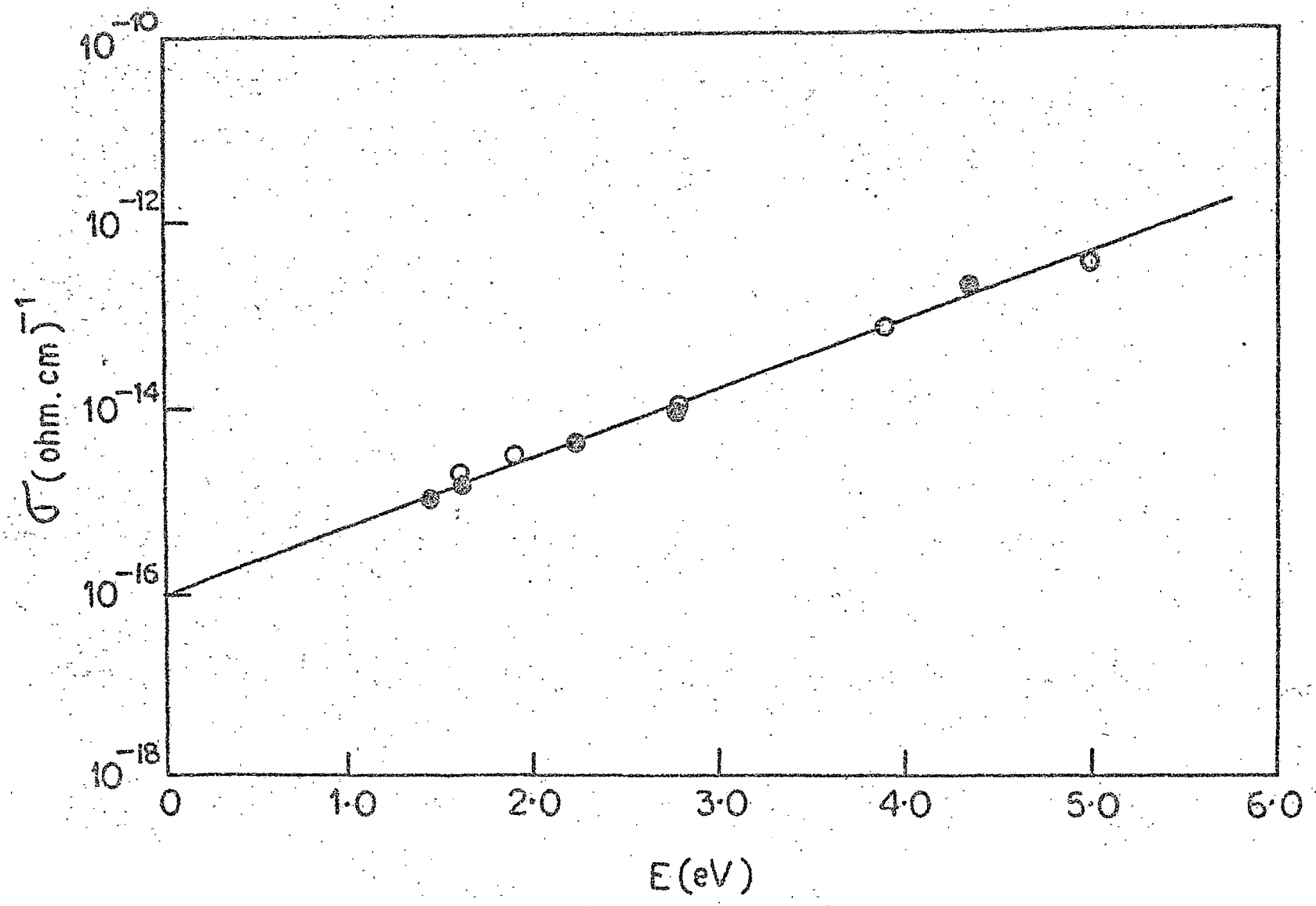

FIG. 4·23

slope of the line for each polyene is shown in table 4.13 for comparison with the value of the slope expected from the equation (4.5). The value of σ_o' obtained from each log σ vs. E plot is also shown in this table to compare this value with the values obtained from the log σ vs. $\frac{1}{T}$ and log σ_o vs. E plots. From the table 4.13 it is seen that the observed slopes from log σ vs. E plots are in excellent agreement with the slopes expected from equation (4.5). Also the σ_o' values obtained from log σ vs. E plots agree satisfactorily with the values obtained from the log σ_o vs. E and log σ vs. $\frac{1}{T}$ plots. Thus the high correlation between the relevant parameters in the semiconductors under study on adsorption of various vapours indicates that compensation rule is valid in these semiconductors and that σ_o and E are indeed physically related.[18,19]

4.3 Discussion

There are number of theses about the mechanism of conduction in organic semiconductors leading to compensation effect. The carrier injection model of Green[20] produces the type of activation energy dependence of the pre-exponential factor as observed experimentally but it does not provide any physical basis for the interpretation of T_o.

Kemeny and Rosenberg[21] observed compensation law in tunneling of small polaron through molecular barrier from thermally activated energy levels of molecules. Their model predicts that $T_o = \frac{\theta}{2}$ (where θ is the Debye-Temperature) and that at $T > T_o$, small polaron tunneling is not possible and compensation effect is not expected to be observed. Out of the five semiconductors studied, in case of three (β-apo-8'-

Table - 4.13

Expected (Eqn. 4.6) and observed slopes and observed σ_0' from the log σ vs. E plots for the polyene semiconductors

Semiconductor	Expected slope (eV^{-1})	Observed slope (eV^{-1})	Observed σ_0' $(\Omega \cdot cm)^{-1}$
Vitamin A alcohol[1]	7.73	7.70	2.85×10^{-9}
Vitamin A acetate[1]	4.66	4.56	1.60×10^{-10}
β -apo-8'-carotenal[2]	1.41	1.39	1.25×10^{-16}
Astacene[3]	0.91	0.86	1.80×10^{-16}
Methyl bixin[4]	1.70	1.69	1.00×10^{-16}

1. From Fig. 4.20 ;
2. From Fig. 4.21 ;
3. From Fig. 4.22 ;
4. From Fig. 4.23 .

carotenal, astacene and methyl bixin) the semiconductive behaviour of the compounds has been studied at $T > T_0$. The experimental results show that the compensation rule is also valid in these cases. Further, Debye- temperature for these semiconductors are not known. It has been reported[22] that the Debye-temperature for a series of crystals of large aromatic molecules lies in the range 100-130°K. It seems that the T_0 values measured are far too high to justify the polaron tunneling model.

Because of widespread occurrence[23] of the compensation effect (besides semiconduction process, it is observed in chemical reactions, catalytic process, thermal denaturation of macromolecules, thermal killing of unicellular organisms etc), Kemeny and Mahanti[11] have proposed a theory of electronic charge transport as involved in kinetic processes (also applicable to equilibrium processes) from the absolute rate theory equation[24,25] within two special models. The first one (quadratic polarons) involves the coupling of electrons with a set of oscillators, whereas the second one (magnetic polarons) involves the coupling of electrons with a set of spins. Both the models show that the activation entropy is proportional to the activation energy thus providing a compensation effect. The use of N number of oscillators or of spins to bring about the compensation effect seems to appear reasonable in view of the fact that the variable amount of adsorbed dielectric (vapour) screen off the interaction of a charge with a more distant parent molecules; N depending on the number of such molecules with which the charge effectively interacts. But in quadratic polaron model, the characteristic temperature T_0 is always

negative in contradiction to our observation. The spin polaron model gives a positive T_o but predicts no activation energy at very high temperatures. At a temperature around T_o, the process is activated and the activation energy becomes function of temperature i.e.

$$E(T) = E(0)\left[1 + \alpha \frac{T}{T_o}\right] \tag{4.6}$$

Here E(0) is the activation energy at low temperature and α is a function of temperature;

$$\alpha = \frac{1}{\log 2} \cdot \log\left[1 + \exp\left\{(-2\log 2)\frac{T_o}{T}\right\}\right] \tag{4.7}$$

Though our experiments were done in a limited range of temperature, the excellent linear plots in Figs. 4.6 - 4.15 do not suggest such temperature dependence.

Other theoretical attempts[3,10] to derive the compensation rule were restricted to the temperature dependence of the number of activated carriers in a model consisting of two electronic levels associated with each molecular site, the electronic states being coupled to a set of N oscillators associated with each molecular site. A change in the electronic state (due to vapour adsorption) gives rise to an activation entropy because of a change in vibrational frequencies. If one assumes the semiconduction equation as

$$\sigma(T) = \sigma_o' \exp\left(\frac{S}{k}\right) \exp\left(-\frac{E}{2kT}\right) \tag{4.8}$$

then the variation in both the electronic energy gap (E) and the

activation entropy (S) can account for compensation effect if the changes in these parameters are given by

$$E = E_0 + n E_1$$
$$S = S_0 + n S_1 \qquad \text{(4.9)}$$

where n is a definite number for each system and E_0, E_1, S_0 and S_1 are same for all the systems. In this case the characteristic temperature is given by $T_0 = E_1 / 2S_1$

Unfortunately due to the fact that the nature of the activated complex (due to vapour adsorption) is not precisely known, the activation entropy S (hence S_1) is a relatively obscure quantity and any quantitative estimate of T_0 is not possible.

The experimental results presented in this chapter show that the enhancement of conductivity is associated with a change in activation energy of the semiconductors on vapour adsorption. This change in activation energy depends on the chemical nature and also on the amounts of vapours adsorbed. In case of vitamin A alcohol and acetate the conductivity increases with the decrease of activation energy whereas in β-apo-8'-carotenal, astacene and methyl bixin the activation energy increases with the increase of conductivity. This behaviour, however, is quite understandable from the conductivity expression (4.3). If $T_0 > T$; where T is any temperature in the working temperature range, then $\left(\frac{1}{T_0} - \frac{1}{T}\right)$ becomes negative and the increase in σ at a particular temperature T is suggested with the decrease in the value of E. Thus for a semiconductor having the characteristic temperature (T_0) at a higher value than the working

temperatures, enhancement of its conductivity is expected with the decrease of its activation energy. This is what we have observed in case of vitamin A alcohol and acetate. Again, if $T_0 < T$, then $\left(\frac{1}{T_0} - \frac{1}{T}\right)$ becomes a positive quantity and so increase in σ at a temperature T is associated with an increase in activation energy. Thus a semiconductor having the characteristic temperature (T_0) at a lower value than the working temperatures should show an enhancement of its conductivity with the increase of its activation energy. We have observed such behaviour in case of β -apo-8'-carotenal, astacene and methyl bixin. Now it is clear from our experiment that the characteristic temperature (T_0) of a semiconductor plays an important role in the dark conduction process.

The characteristic temperature (T_0), however, has been thought to be a molecular property[2]. Our results also show distinct T_0 values (tables 4.1 and 4.2) for each of the polyenes. It is, however, not understood why T_0 has a high value for vitamin A and also for β - carotene[2] whereas for β -apo-8'-carotenal, astacene and methyl bixin T_0 is small though all these molecules belong to the long chain conjugated polyene group with alternating single and double bonds. Also the number of double bonds of the second group of polyenes lie in between vitamin A and β -carotene suggesting that this parameter is not related to T_0. Possibly it is the end group of the polyenes with which T_0 is somehow related. It is to be of interest to note that the two groups of the polyenes investigated are distinct in that the molecules of the second group, β -apo-8'-carotenal, astacene and methyl bixin, have a $>C=O$ group which is conjugated

with the polyene chain whereas the $>C=O$ group in vitamin A acetate is not conjugated with the main carbon chain and vitamin A alcohol has no carbonyl end group (shown in Part - I, Chapter 2, page - 33). Thus it seems that the presence of the conjugated carbonyl end group, in the second group of the polyenes studied is somehow related to the low value of T_o.

4.4 Conclusion

Our experimental results indicate that the compensation rule is valid for the polyene semiconductors studied and the activation energy (E) is physically related with σ_o . The distinct variation in the observed values of T_o of these semiconductors suggests the possibility of dependence of T_o on the molecular property of the semiconducting material. The characteristic temperature (T_o) of an organic semiconductor plays an important role in the dark conduction process.

References.

1. D.D. Eley, J. Polymer Sci., Pt. C., 17, 73 (1967).
2. B. Rosenberg, B. Bhowmik, H.C. Harder and E. Postow, J. Chem. Phys., 48, 4108 (1968).
3. D.D. Eley, A.S. Fawcett and M.R. Wills, Trans. Faraday. Soc., 64, 1513 (1968).
4. G.R. Johnston and L.E. Lyons, Aust. J. Chem., 23, 2137 (1970).
5. K. Ulbert, Aust. J. Chem., 23, 1247 (1970).
6. M. Masui, H. Nagasaka and K. Yahagi, Jpn. J. Appl. Phys., 16, 177 (1977).
7. F. Gutmann and L.E. Lyons, Organic Semiconductors (John-Wiley and Sons, Inc., New York, London and Sydney, 1967) p 428-435.
8. O. Exner, Nature, 201, 488, 1964.
9. G. Kemeny and I.M. Goklany, J. Theor. Biol., 40, 107 (1973).
10. T.A. Kaplan and S.D. Mahanti, J. Chem. Phys., 62, 100 (1975).
11. G. Kemeny and S.D. Mahanti, Proc. Nat. Acad. Sci., USA, 72, 999(1975).
12. G. Sawa, K. Kitagawa and M. Ieda, Jpn. J. Appl. Phys., 11, 416(1972).
13. B. Rosenberg, J. Chem. Phys., 36, 816 (1962).
14. T.N. Misra, B. Rosenberg and R. Switzer, J. Chem. Phys., 48, 2096 (1968).
15. A. Epstein and B.S. Wildi, J. Chem. Phys., 32, 324 (1960).
16. B. Rosenberg, Nature, 193, 364 (1962).
17. B. Rosenberg, Physical Processes in Radiation Biology edited by L. Augenstein, R. Mason and B. Rosenberg (Academic Press, New York and London, 1964) p 120.
18. B. Mallik, A. Ghosh and T.N. Misra, Bull.Chem.Soc. Jap., in press (1979).

19. B. Mallik, A. Ghosh and T.N. Misra, Jpn. J. Appl. Phys., 18, 331 (1979).

20. M.E. Green, J. Chem. Phys., 51, 3279 (1969).

21. G. Kemeny and B. Rosenberg, J. Chem. Phys., 53, 3549 (1970).

22. E.I. Mukhterov, A.A. Pichurin, A.I. Kitaigorodskii, Sov. Phys. Solid State (U.S.A.), 17, 1871 (1976).

23. G. Kemeny and B. Rosenberg, Nature, 243, 400 (1973).

24. S. Glasstone, K.J. Laidler and H. Eyring, The Theory of Rate Processes (McGraw-Hill, New York, 1941).

25. R.E. Weston, Jr. and H.A. Schwartz, Chemical Kinetics (Prentice-Hall, Englewood Cliffs, N.J., 1972).

APPENDIX

LIST OF PUBLICATIONS AND REPRINTS

LIST OF PUBLICATIONS

1. B. Mallik, K.M. Jain, K.G. Mandal and T.N. Misra, "Electronic Spectra of Polyenes : Evidence of a low-lying forbidden transition in some linear conjugated polyenes",
   Ind. J. Pure Appl. Phys., 13, 699 (1975).

2. B. Mallik, K.M. Jain, K.G. Mandal and T.N. Misra, " On the evidence of a low-lying forbidden π -electronic state in Methyl Biolin "
   Ind. J. Pure Appl. Phys., 15, 229 (1977).

3. B. Mallik, K.M. Jain and T.N. Misra, " Charge-transfer complexes of all-trans- β -carotene".
   Ind. J. Biochem. Biophys., 15, 233 (1978).

4. B. Mallik and T.N. Misra, " Charge-transfer complexes of some polyenes".
   Ind. J. Biochem. Biophys., (communicated)

5. B. Mallik, A. Ghosh and T.N. Misra, "Semiconductive properties of biologically important compounds : Gas adsorption effect on vitamin A (alcohol and acetate).
   Proc. Indian Acad. Sci. A, 88A, 25 (1979).

6. B. Mallik, A. Ghosh and T.N. Misra, " Compensation effect in semiconducting vitamin A (alcohol and acetate) "
   Jpn. J. Appl. Phys., 18, 331 (1979).

7. B. Mallik, A. Ghosh and T.N. Misra, " Pre-exponential factor in semiconducting vitamin A (alcohol and acetate)"

Bull. Chem. Soc. Jap., 52, 0000 (1979).

8. B. Mallik, A. Ghosh and T.N. Misra, " Compensation effect in some polyene semiconductors "

Bull. Chem. Soc. Jap., (communicated).

9* B. Mallik, K.M. Jain and T.N. Misra, "Electronic spectra of 9 -Nitro anthracene : Solvent effect on $^1A \longrightarrow {}^1L_a$ and $^1A \longrightarrow {}^1L_b$ transitions "

Ind. J. Pure Appl. Phys., 14, 53 (1976).

10* B. Mallik, K.M. Jain and T.N. Misra, " Electronic absorption spectra of 2-Nitrofluorene : Solvent effect on $^1A \longrightarrow {}^1L_a$ transition ",

Ind. J. Pure Appl. Phys., 15, 267 (1977).

11* B. Mallik, G.B. Talapatra and T.N. Misra, " Host crystal field effect on the electronic absorption spectra of tetracene guest in mixed crystals.

Ind. J. Phys., 53B, 00 (1979).

12* B. Mallik, K.M. Jain, Alpana Ghosh and T.N. Misra, "Semiconductive properties of organic compounds : Gas adsorption effect on 9-nitroanthracene ".

Ind. J. Phys., 52A, 543 (1978).

---

* Not included in this thesis.

Proc. Indian Acad. Sci., Vol. 88 A, Part 1, Number 1, February 1979, pp. 25–32.

Semiconductive properties of biologically important compounds: Gas adsorption effect on vitamin A (alcohol and acetate)

BISWANATH MALLIK, ALPANA GHOSH and T N MISRA
Optics Department, Indian Association for the Cultivation of Science, Jadavpur, Calcutta 700 032

MS received 1 September 1978; revised 27 November 1978

Abstract. The change in semiconductive properties of vitamin A (alcohol and acetate) after adsorption of various vapours on its crystallite surface has been studied at a constant sample temperature. A rapid enhancement in the semiconductivity has been observed. The rise in conductivity has been found to be exponential with increasing vapour pressure of the adsorbed gas. It has been suggested that charge transfer (CT) interaction may be responsible for such conductivity change. The adsorption process being efficiently reversible this CT complex is weakly bound.

The biological implication of these observations is discussed.

Keywords. Organic semiconductors; gas adsorption effect; gas adsorption kinetics; semiconductive study.

1. Introduction

The biological importance of vitamin A and other conjugated long chain polyenes is well known. These are known to have an important role in the primary mechanism of olfactory transduction (Misra *et al* 1968; Rosenberg *et al* 1968). The carotenoids present in the olfactory organ can form weakly-bound reversible complexes with adsorbed odourous gas molecules which increase the conductivity of the olfactory membrane leading to the electrical event of olfaction. Selectivity of smell comes from the interaction of the odourous molecules with one or the other carotenoid present in the olfactory epithelium. It has been shown that all-trans β-carotene is a poor receptor for the methyl acetate molecules but vitamin A alcohol responds very well with these molecules and the conduction properties of vitamin A change significantly on adsorption of the acetate molecules. The limited experiment done earlier with vitamin A alcohol showed the effect of adsorption of methyl acetate molecules only. We have now systematically studied the effect of adsorption of various gases on the semiconductive properties of vitamin A (alcohol and acetate) and have examined the kinetics of such adsorption. In this paper we present our results.

2. Experimental

The sample of vitamin A (alcohol and acetate) was obtained from Hoffman La-Roche, Bombay. We have used these compounds without further purification. Organic solvents used in this investigation were of high purity. The experimental set-up is shown in figure 1. The fine powder of the compounds was pressed in a sandwich cell between a conducting glass and a stainless steel electrode. The separation between the electrodes was maintained by a 2 mil. thick teflon spacer. A d.c. voltage of 22·5 V was applied across the cell which was placed on a thermal bar platform in a suitably designed conductivity chamber made of brass and fashioned with teflon. The temperature of the sandwich cell could be controlled from outside. There was a gas inlet and an outlet in the chamber for gas adsorption study. Temperature measurements were made by using a copper-constantan thermocouple attached at the top of the metal electrode and a millivolt potentiometer. All the conductivity measurements were made in dry nitrogen/vacuum atmosphere with an electrometer amplifier EA 815 of the Electronic Corporation of India Limited. To pass various vapours inside the chamber, dry nitrogen was used as a carrier which was passed through the bubbler containing the solvent kept at a required temperature to maintain a fixed partial vapour pressure less than the saturation vapour pressure at sample cell temperature. The pressure inside the conductivity chamber was kept constant by carefully controlling the inlet and the outlet flow. The sample cell was maintained at a constant temperature throughout each set of experiment.

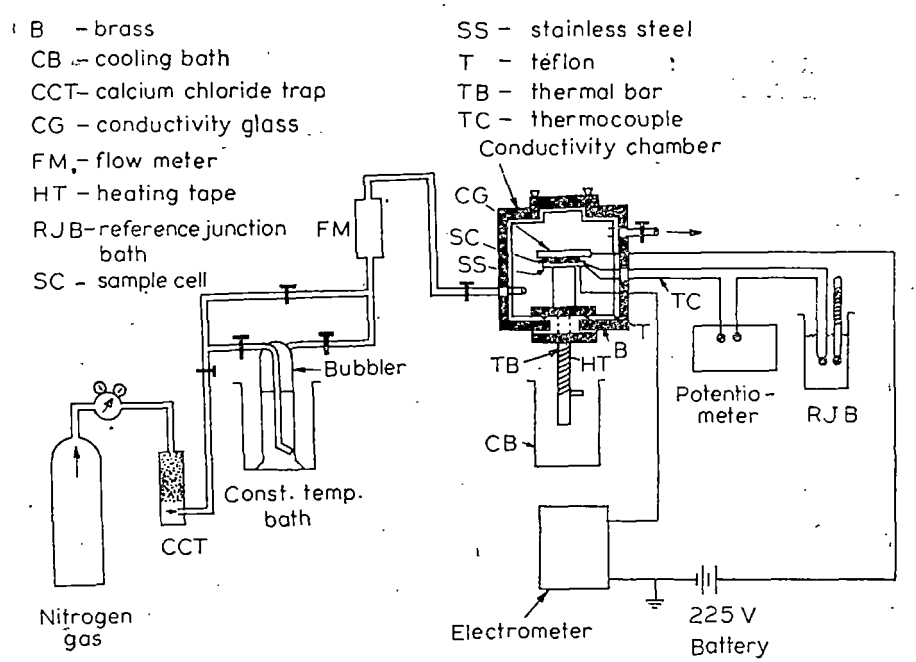

Figure 1. A schematic diagram of the apparatus used to test the effects of the adsorbed gases on the conductivity of vitamin A (alcohol and acetate).

3. Results

On adsorption of vapours on the crystallite surface of the compounds studied a rapid enhancement in the conductivity is observed. The adsorption process is fast and almost completely reversible. The initial value of the dark current is reached quickly simply by flushing the chamber with dry nitrogen (figure 2). Adsorption and desorption behaviour with vitamin A acetate is similar. The rise in the conductivity depends on the vapour pressure (figure 3). Different vapours at the same vapour pressure show different extents of enhancement of conductivity. The results are presented in table 1.

4. Discussion and conclusions

4.1. *Dependence of the conductivity on vapour pressure*

The rise in conductivity was studied at a constant temperature (25° C) as a function of partial pressure of ethyl acetate. The total gas mixture inside the chamber was at atmospheric pressure and the partial pressure of the vapour was the vapour pressure of the solvent used at the temperature of the experiment. For low amount

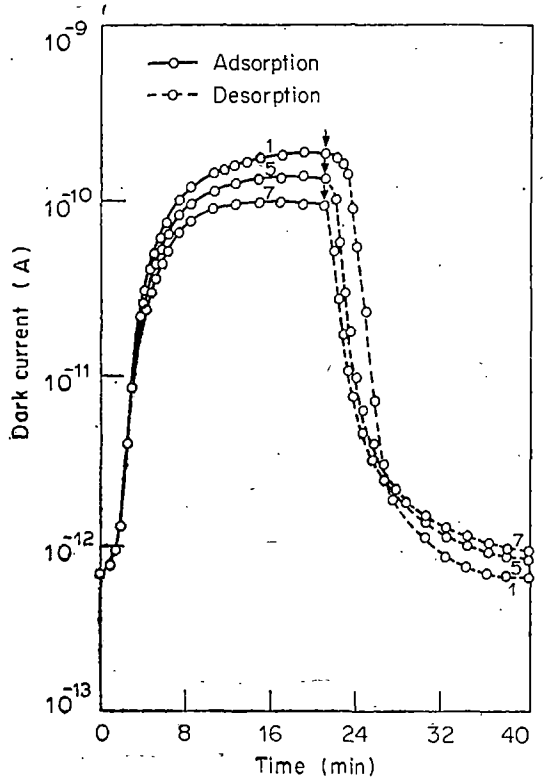

Figure 2. The change in dark current in a vitamin A alcohol powder cell kept at 25° C with repeated injection of ethyl acetate vapour (40·0 mm).

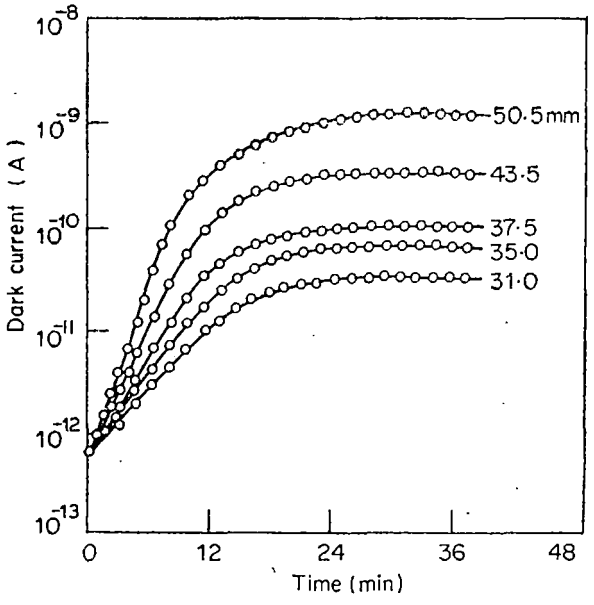

Figure 3. The change in dark current after adsorption of ethyl acetate vapour at different vapour pressure on vitamin A alcohol.

of vapour adsorption the conductivity after adsorption $\sigma_A(m)$ follows the relation (Misra *et al* 1968)

$$\sigma_A(m) = \sigma_V \exp(am) \tag{1}$$

where σ_V is the conductivity before adsorption of any vapour.

a is a constant and m is the amount of the vapour adsorbed. m depends on the partial pressure (p) of the reagent chemical. In the initial period, m depends also on the time of exposure. After some time, however, an equilibrium is established. Thus we assume that in the initial region

$$m(t) = Q(t) \cdot p \tag{2a}$$

Table 1. Rise in the dark current in vitamin A (alcohol and acetate) powder cells at 12·5° C due to adsorption of various vapours at the same pressure of 40 mm

Vapour	Dielectric constant at 25° C	Ionisation potential (eV)	σ_A/σ_V	
			Vitamin A (alcohol)	Vitamin A (acetate)
Toluene	2·38	8·81	$2·3 \times 10^4$	$5·0 \times 10^4$
Benzene	2·28 (20° C)	9·24	$6·7 \times 10^3$	$1·7 \times 10^4$
Ethylacetate	6·00	10·11	$6·5 \times 10^3$	$1·3 \times 10^4$
n-heptane	1·93 (20° C)	10·35	$4·0 \times 10^3$	$3·8 \times 10^3$
Ethanol	24·30	10·50	$3·0 \times 10^2$	$2·0 \times 10^3$
Methanol	32·60	10·85	$4·5 \times 10$	$3·2 \times 10^2$

where $Q(t)$ is a function of time. At equilibrium,

$$m_0 = Q_0 \cdot p \tag{2b}$$

where Q_0 now becomes independent of time. This is expected from Langmuir's adsorption isotherm, when a small fraction of the surface is covered by gas molecules. Hence,

$$\sigma_A \{m(t)\} = \sigma_V \exp\{a \cdot Q(t) \cdot p\} \tag{3a}$$

and at equilibrium

$$\sigma_A (m_0) = \sigma_V \exp(a \cdot Q_0 \cdot p). \tag{3b}$$

A plot of $\log \sigma_A(m_0)$ *versus* vapour pressure (p) at equilibrium is expected to be linear. Our experimental result in figure 4 shows a good agreement with this.

4.2. *Change in conductivity in different vapours*

When the powdered semiconductor is exposed to some vapour, the vapour molecules may enter the inter-space between the crystallites and form a dielectric medium different from the original one. If the conductivity change on adsorption of vapours is due to such physical mixing, a relationship between the conductivity enhancement and the dielectric constant of the vapours used is expected. But our experimental results for the conductivity rise at the same vapour pressure for different vapours (table 1) do not suggest this. The static dielectric constant (Treiber and Koren 1951) of the vapours used are in the order *n*-heptane < benzene < toluene < ethyl-acetate < ethanol < methanol which is not in agreement with the semiconduction current enhancemment (table 1). It has been reported (Pullman and Pullman 1963; Platt 1959; Mairanovsky *et al* 1975) that polyenes can act both as electron acceptors and electron donors. The adsorbed molecules may form a weak (D^+A^-) charge transfer complex with vitamin A

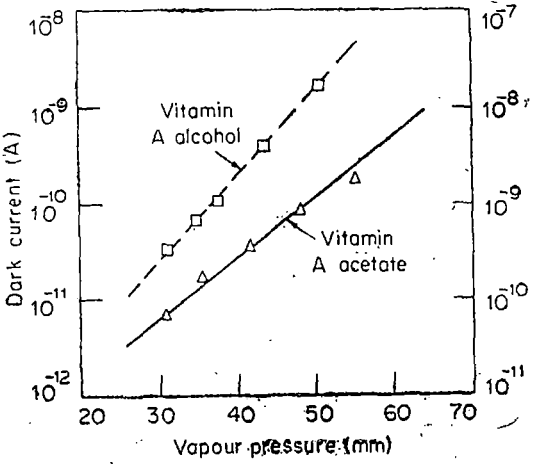

Figure 4. Change in the dark current of vitamin A (alcohol and acetate) powder cell as a function of the vapour pressure of ethyl acetate.

resulting in a change in the conductivity. In such a case, the current enhancement should show a relationship with the ionisation potential or the electron affinity of the reagent molecules. The reagent molecules used are generally electron donors (Foster 1969). Table 1 shows that in general as the ionisation potential (Gutmann and Lyons 1967; Lorquet 1965) of the vapour molecules decreases, semiconduction current enhances. These results show that the enhancement of conductivity is possibly due to the formation of donor-acceptor ($D^+ A^-$) complexes of these compounds with the vapour molecules adsorbed. The fact that the conductivity change is efficiently reversible shows that any C-T complexes formed are weakly bound.

4.3. *Kinetics*

The adsorption kinetics follows Roginsky-Zeldovich equation in a modified form (Rosenberg *et al* 1968; Eley and Leslie 1964). It was assumed that there is an activation energy associated with the adsorption rate, which increases linearly with the amount of adsorbed gas. Thus, the rate of adsorption (dm/dt) will be

$$dm/dt = A \exp(-\beta m/kT), \tag{4}$$

where β is a constant. Integrating (4), we get

$$m(t) = \frac{kT}{\beta} \log(t + t_0) + \text{constant} \tag{5}$$

From (1) and (5) we get,

$$\log \sigma_A = \frac{akT}{\beta} \log(t + t_0) + \text{constant}. \tag{6}$$

Thus, a linear plot of $\log \sigma_A$ *versus* $\log(t + t_0)$ is suggested from (6) and our experimental results in figure 5 are in good agreement with this. In the initial region, different slopes observed at different vapour pressures show the vapour pressure-dependence of β (since α is pressure-independent). The higher the partial vapour pressure, the larger is the slope. This justifies the assumption made in expression (2) and shows an inverse relationship between p and β (table 2).

Table 2. Vapour pressure dependence of the factor $\beta' = (\beta/\alpha)$ for ethyl acetate vapour adsorption kinetics.

Vitamin A (alcohol)		Vitamin A (acetate)	
Vapour pressure (mm)	β' (eV)	Vapour pressure (mm)	β' (eV)
31·0	$1{\cdot}202 \times 10^{-2}$	31·0	$0{\cdot}819 \times 10^{-2}$
35·0	$1{\cdot}005 \times 10^{-2}$	35·7	$0{\cdot}753 \times 10^{-2}$
37·5	$0{\cdot}930 \times 10^{-2}$	41·7	$0{\cdot}660 \times 10^{-2}$
43·5	$0{\cdot}759 \times 10^{-2}$	48·2	$0{\cdot}601 \times 10^{-2}$
50·5	$0{\cdot}643 \times 10^{-2}$	55·2	$0{\cdot}518 \times 10^{-2}$

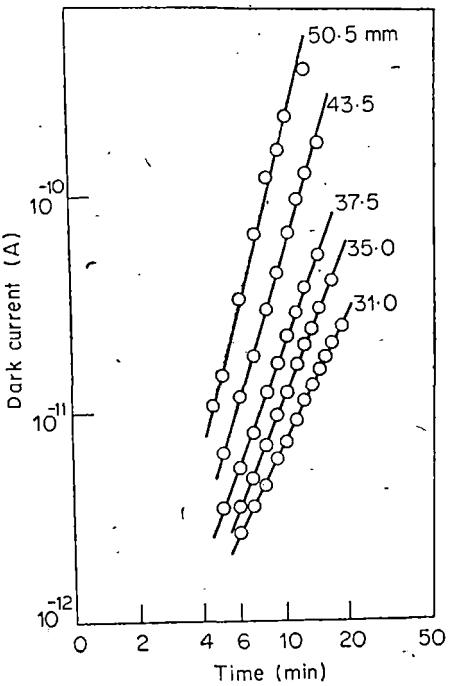

Figure 5. Adsorption kinetics data plotted according to Roginsky-Zeldovich equation for vitamin A alcohol.

The change in conductivity of β-carotene with repeated injection of odourous gas molecules in the chamber was found to decrease with the number of repetition of the exposure. This was related to fatigue effect in olfaction (Rosenberg *et al* 1968). In the present investigation, we have studied the change in conductivity of vitamin A with injection of ethyl acetate vapour in the chamber and have observed similar effect. This is shown in figure 2. However, our observed change is not large enough in comparison with that of β-carotene (Rosenberg *et al* 1968). This is possibly due to the fact that the present experiment was performed at a low vapour pressure and also at higher temperature of the sample. From the desorption curves in figure 2 it is observed that after a number of exposures to ethyl acetate vapour, a longer time is required to bring the current back to the original value on nitrogen flushing. This may be due to the fact that for long and repeated exposures strongly bound complexes are formed and such complexes unlike the weakly-bound CT type complexes, do not affect the conductivity change significantly.

Acknowledgements

Thanks are due to CSIR, New Delhi, for financial support to BM and to the Hoffman and La-Roche Co., Bombay, for a generous gift of the sample. Thanks are also due to Prof. G S Kastha for helpful discussion.

References

Eley D D and Leslie R B 1964 *Advances in Chemical Physics* (New York: Interscience Publishers) **7** 238

Foster R 1969 *Organic Charge-Transfer Complexes* (London and New York: Academic Press) p 396

Gutmann F and Lyons L E 1967 *Organic Semiconductors* (New York : John Wiley) p 669

Lorquet J C 1965 *Mol. Phys.* **9** 101

Misra T N, Rosenberg B and Switzer R 1968 *J. Chem. Phys.* **48** 2096

Mairanovsky V G, Engovatov A A, Ioffe N T and Samokhvalov G I J 1975 *Electroanal. Chem.* **66** 123

Pullman B and Pullman A 1963 *Quantum Biochemistry* (New York : Interscience Publishers) p 440

Platt J R 1959 *Science* **129** 372

Rosenberg B, Misra T N and Switzer R 1968 *Nature London* **217** 423

Treiber S and Koren M 1951 *Nat. Bur. Stand. Circ.* p 514

Indian Journal of Pure & Applied Physics
Vol. 13, October, 1975, pp. 699-702

Electronic Spectra of Polyenes : Evidence of a Low-lying Forbidden Transition in some Linear Conjugated Polyenes

BISWANATH MALLIK, KAPUR MAL JAIN, KRISHNAGOPAL MANDAL & T. N. MISRA

Department of Physics, North Bengal University, Darjeeling

Received 18 *April* 1975

Electronic absorption and emission spectra of *all-trans* vitamin A alcohol, *all-trans* vitamin A acetate, β-apo-8′-carotenal and astacene have been investigated. The effects of different solvents on the absorption and emission bands of these polyenes are appreciably different. This indicates that different excited states are involved in absorption and emission. Effect of adsorption of certain gases on the crystallite surface of β-apo-8′ carotenal and astacene has been discussed. On adsorption of certain gases, a new band appears on the low-energy side of the strongly allowed ^1B_u state. It has been concluded that in these long-chain polyenes there exists a low-lying-forbidden ^1A_g state below the strongly allowed ^1B_u state.

1. Introduction

IN RECENT YEARS, interest in the electronic spectra of linear conjugated polyenes[1-5] has been revived. Little experimental work has been done in this class of molecules in comparison to the effort expended in aromatic molecules. The strongly allowed transition in the visible and near UV region of the spectrum in the linear polyenes has been known so far to be the lowest excited singlet state, ^1B_u. The absorption and emission spectra of these molecules show very little or no overlap[3,6]. Some workers have tried to explain it on the basis of "Franck-Condon forbiddenness".

It has been shown by Schulten and Karplus[4] that when double excited configurational interaction is taken into account, a singlet (^1A_g) state appears below the strongly allowed ^1B_u state in some polyenes like butadiene, hexatriene and octatetraene. Hudson and Kohler[5] have presented some experimental evidence that there exists a low-lying forbidden state below the well-defined lowest π-electron state in α, ω-diphenyl octatetraene. Recently, Mandal and Misra[7] have shown that adsorption of certain gas molecules on the solid film makes this transition allowed. We have extended such investigations to some more polyenes. In addition, the effect of different solvents on absorption and emission spectra of these polyenes has been studied, and the results are presented in this paper.

2. Experimental Procedure

The polyenes employed in the present study are *all-trans* vitamin A alcohol, *all-trans* vitamin A acetate, β-apo-8′-carotenal and astacene. Compounds of high quality obtained from Hoffman-La Roche Co., Switzerland were used without further purification. Solvents used in this investigation were of the spectro-grade quality. The absorption spectra were recorded by a Perkin-Elmer recording Spectrophotometer-202 and Spectromom-202. The emission spectra were recorded by Aminoco Bowman spectrophoto fluorometer.

Thin films of polycrystals of the polyenes were made on the quartz surface by gently rubbing the material. Solid films thus made were exposed to vapours of various solvents. The exposure was made by holding the films for about 5 min over a beaker containing the chemicals. The films were thus exposed at the saturated vapour pressure of various chemicals at room temperature (25°C).

3. Results

In the polyenes studied, a very broad absorption band is generally observed. The absorption spectrum of β-apo-8′-carotenal in non-polar solvents, however, consists of three vibronic bands with the central one most intense. This structure represents an upper state fundamental of about 1000 cm^{-1}. In common polar solvents, this vibrational structure is completely lost and only a very broad absorption band is observed. It has been observed that the absorption bands are strongly solvent-dependent. In all the polyenes studied, the emission spectra do not show any vibrational structure and no mirror image relationship is observed with the intense absorption band. The room temperature absorption and emission spectra of different polyenes in ethyl acetate are shown in Fig. 1. Though the absorption and emission spectra of β-apo-8′-carotenal show some overlap, such overlaps very small for astacene and in case of *all-trans* Vitamin A (alcohol and acetate) practically no overlap is observed.

The effect of different solvents on the absorption and emission spectra of *all-trans* vitamin A alcohol is

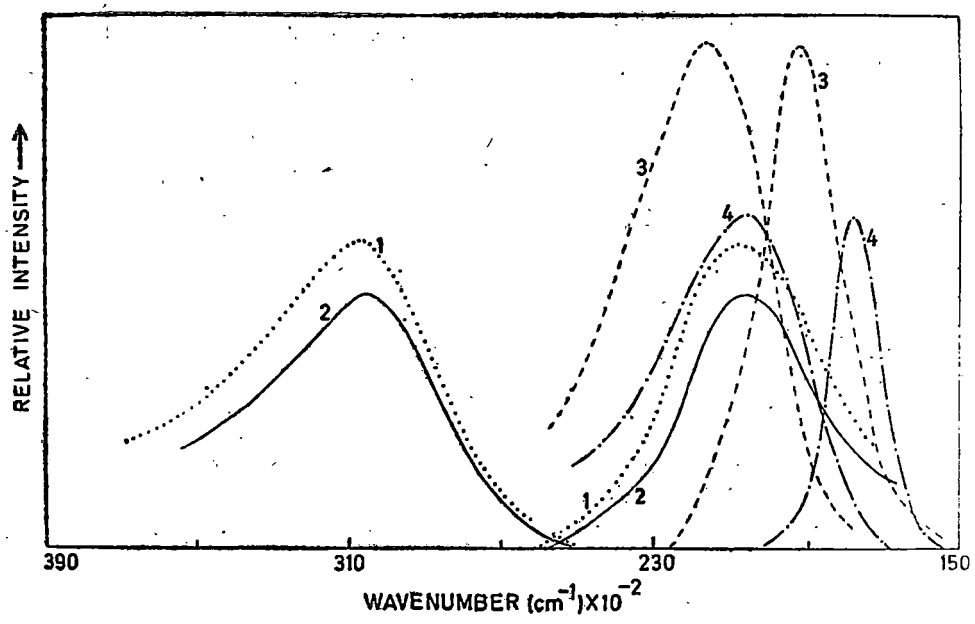

Fig. 1—Absorption and emission spectra of different polyenes in ethyl acetate at room temperature, [1, All-*trans* vitamin A alcohol; 2, all-*trans* vitamin A acetate; 3, β-apo-8′-carotenal; and 4, astacene]

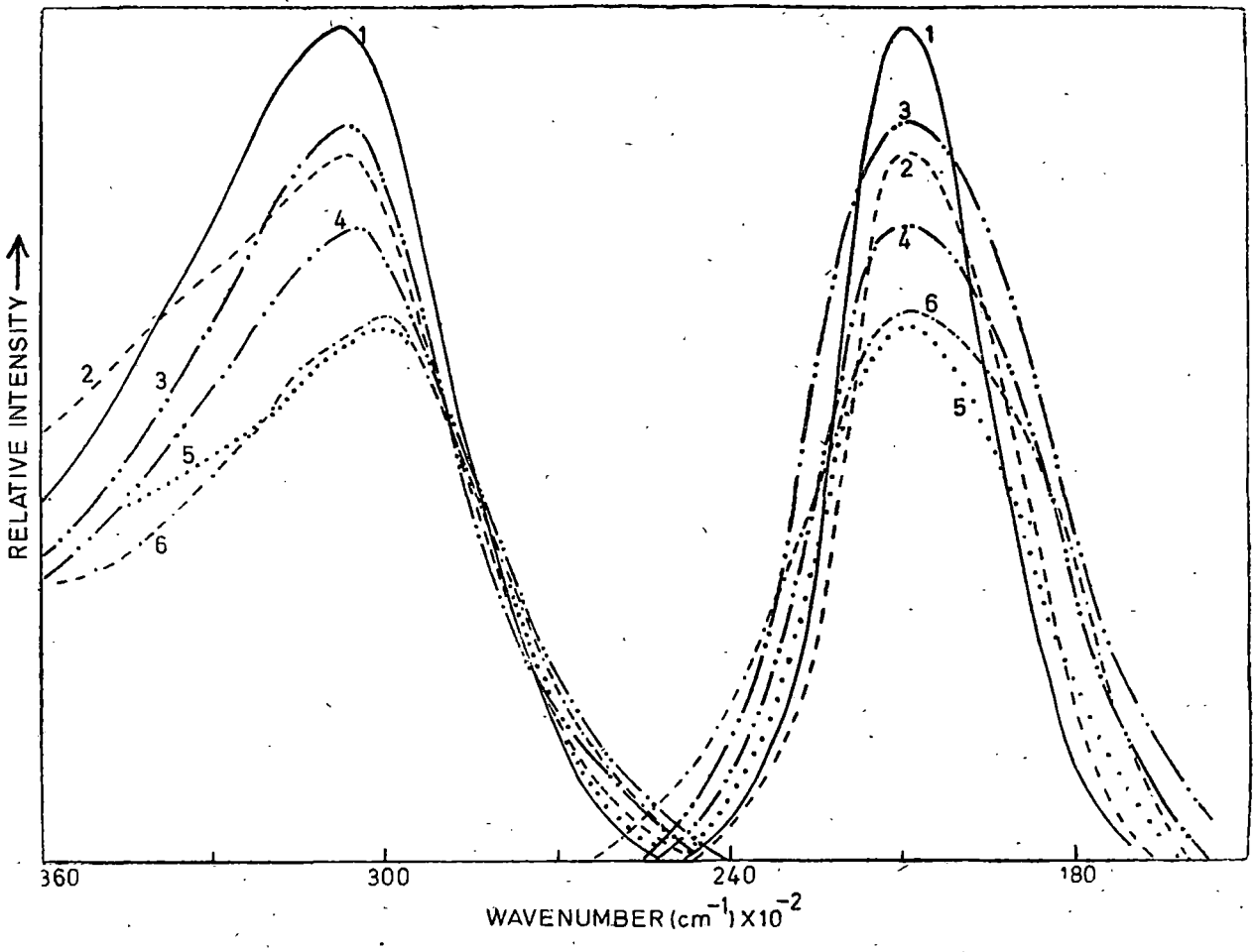

Fig. 2—Absorption and emission spectra of all-*trans* vitamin A alcohol in different solvents at room temperature [1, Methanol; 2, ethanol; 3, ethyl acetate; 4, 1, 4-dioxane; 5, carbon tetrachloride; and 6, benzene]

shown in Fig. 2. The absorption spectra show large solvent shift, but for emission spectra such shift is small.

The room temperature absorption spectra of β-apo-8′-carotenal and astacene in the solid state and after vapour adsorption are shown in Figs. 3 (a) and (b) respectively. To see the effect of the adsorption of gases on the solid film, various vapours were used.

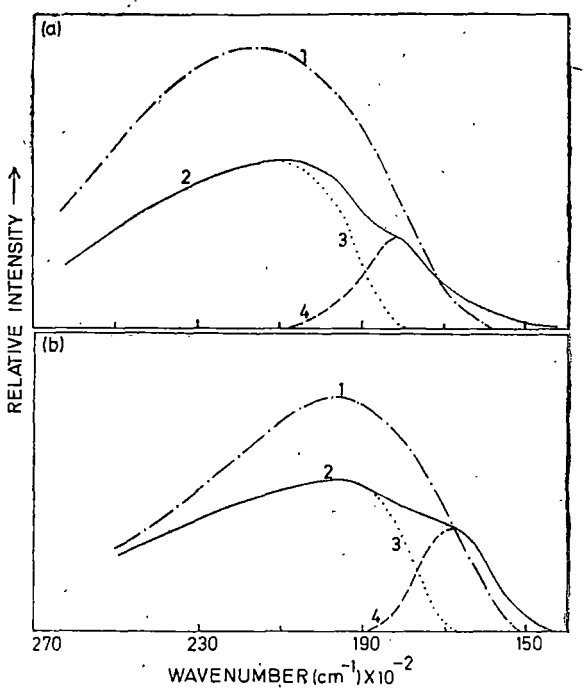

Fig. 3—(a): Absorption spectra of β-apo-8′-carotenal [1, Absorption spectrum for the solid film; and 2, absorption spectrum for the solid film after pyridine vapour adsorption. Resolution of the total adsorption; spectrum for the solid film after pyridine vapour adsorption ; 3, band of the solid film; and 4, new band]

(b) : Absorption spectra of astacene [1, Absorption spectrum for the solid film; and 2, absorption spectrum for the solid film after aniline vapour adsorption. Resolution of the total absorption spectrum for the solid film after aniline vapour adsorption: 3, band of the solid film; and 4, new band]

With all the vapours studied, the effect is similar except, that with certain of these the effect is more pronounced than with others. Pyridine vapour adsorption on β-apo-8′-carotenal affects the absorption spectra intensely whereas aniline vapour shows a strong effect on astacene spectrum.

The absorption spectrum of β-apo-8′-carotenal in the solid state, as shown in Fig. 3 (a), is a broad band. After exposure to various vapours, the solid state spectrum shows a marked change in which a new band appears at about ~~16660~~ 18200 cm^{-1}. The other band remains unchanged.

The absorption spectrum of astacene in the solid state is also a broad band. When solid film of this polyene is exposed to different vapours, a new band appears at about ~~18200~~ 16660 cm^{-1} along with the band observed before vapour adsorption.

4. Discussion

For strong absorption band of linear polyenes, the solvent shift[8] can be expressed in the form

$$\Delta\bar{\nu} = k.f.\ \frac{n^2-1}{n^2+2}$$

where k is a parameter which is constant for a given molecule, f is the oscillator strength for a particular transition and n is the refractive index of the solvent. The absorption band of the polyenes under investigation shows a large red shift with the increase of the refractive index of the solvents. But in case of emission, this shift is very small compared to that for absorption. In Table 1, values of $\bar{\nu}_{max}$ for the absorption and emission of some polyenes in various solvents are given. Our experimental results show that in all the polyenes studied, the plot of $\bar{\nu}_{max}$ for both absorption and emission against $(n^2-1)/(n^2+2)$ is a straight line. In Fig. 4, such plots are shown. The slope of the plot for absorption (which is a measure of the oscillator strength involved) is about seven times larger than that for emission. This difference in

Table 1—Solvent Effect on the Absorption and Emission Bands of Some Polyenes
($\bar{\nu}_{max}$ in cm^{-1})

		Vit. A alcohol		Vit. A acetate		β-apo-8′-carotenal		Astacene	
Solvent	$(n^2-1)/(n^2+2)$	$(\bar{\nu}max)_E$	$(\bar{\nu}max)_A$	$(\bar{\nu}max)_E$	$(\bar{\nu}max)_A$	$(\bar{\nu}max)_E$	$(\bar{\nu}max)_A$	$(\bar{\nu}max)_E$	$(\bar{\nu}max)_A$
Methanol	0·203	21008	30864	20833	30614	—	—	—	—
Acetone	0·219	—	—	—	—	19157	21880	18018	20746
Ethanol	0·221	20964	30769	20833	30581	—	—	—	—
Ethyl acetate	0·227	20942	30722	20730	30534	19157	21739	17857	20661
n-Hexane	0·228	—	—	—	—	19011	21790	—	—
1, 4-Dioxane	0·254	20942	30534	20790	30487	19083	21459	17921	20408
Cyclohexane	0·257	—	—	—	—	19120	21500	—	—
Carbon tetrachloride	0·275	20964	30303	20876	30030	19047	21270	17889	20242
Benzene	0·294	20920	30303	20790	30030	19083	21220	17889	20202

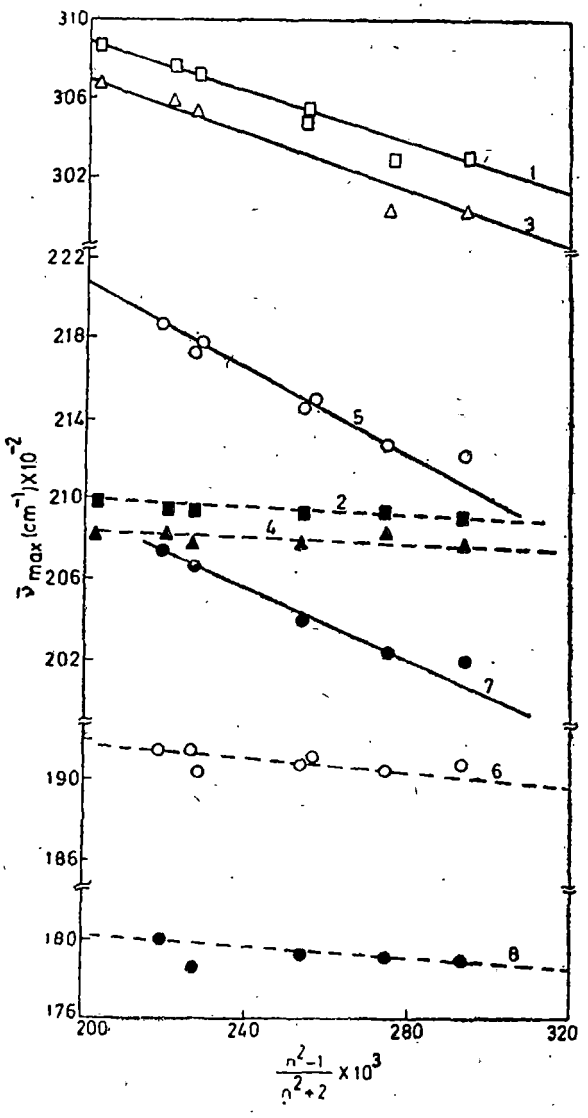

Fig. 4—Plots of $\bar{\nu}_{max}$ against $(n^2-1)/(n^2+2)$ for the lowest energy absorption band and the highest energy emission band of the polyenes studied

Polyene	Curve	
	Absorption	Emission
All-*trans* vitamin alcohol	1	2
All-*trans* vitamin acetate	3	4
Apo-8′-carotenal	5	6
Astacene	7	8

solvent behaviour and the small overlap of the absorption and emission bands indicate that the absorbing and emitting states of these polyenes are different. The existence of a low-lying π-electronic state below the strongly allowed ^1B_u state in these polyenes is thus indicated by such solvent behaviour.

We have observed that when certain vapours are absorbed on the surface of crystals, a new band appears in β-apo-8′-carotenal and astacene. There is a large overlap between the new band and the usually observed intense band. In order to get the longest wavelength band contour out of the total spectrum we have resolved qualitatively the whole spectrum into two parts—one corresponding to the new band and the other to the solid film spectrum before vapour adsorption. The resolved spectra are shown in Figs. 3 (a) and 3 (b).

We have studied the emission spectra of the polyenes in solution only. These emission bands in case of Vitamin A (alcohol and acetate) show good overlap and mirror image relationship with the new band[7]. In β-apo-8′-carotenal and astacene, the emission bands are slightly on the high energy side of the new band in the crystal film. In view of the fact that free molecular electronic energy states are generally lowered in the state of aggregation, the emission of these crystal film polyenes is expected to be on the lower energy side of that in solution, and one can then reasonably expect to get good overlap between the new absorption bands and the emission bands of these polyenes in the crystalline state. Unfortunately, the emission from the crystalline film of these polyenes could not be recorded. We conclude that the new absorption band which appears as a result of adsorption of gas molecules on the solid film of polyenes, corresponds to transition to the lowest excited state which is possibly a ^1A_g state. The adsorbed gas molecules introduce the perturbation required for the enhancement of the low-lying forbidden transition.

Acknowledgement

The authors express their thanks to Prof. R. K. Mishra, All India Institute of Medical Sciences, New Delhi, for providing with the laboratory facilities for the studies on emission spectra. The authors (B. M., K. M. J. and K. G. M.) express their thanks to the North Bengal University, CSIR, and the University Grants Commission respectively for the award of research fellowships.

References

1. Misra, T. N. & Rosenberg, B., *J. chem. Phys.*, **48** (1968), 5734.
2. Mandal, Krishnagopal & Misra, T. N., *Indian J. pure. appl. Phys.*, **10** (1972), 86.
3. Thomson, A. J., *J. chem. Phys.*, **51** (1969), 4106.
4. Schulten, K. & Karplus, M., *Chem. Phys. Lett.*, **14** (1972), 305.
5. Hudson, B. S. & Kohler, B. E., *Chem. Phys. Lett.*, **14** (1972), 299.
6. Cherry, R. J. & Chapman, D., *Trans. Faraday Soc.*, **64** (1968), 2304.
7. Mandal, Krishnagopal & Misra, T. N., *Chem. Phys. Lett.*, **27** (1974), 57.
8. Basu, S., *Advances in quantum chemistry*, Vol. 1, edited by P. O. Lowdin (Academic Press, Inc. New York), 1964, 145.

On the Evidence of a Low-lying Forbidden Π-Electronic State in Methylbixin

Electronic absorption and emission spectra of methylbixin have been studied. The solvent behaviour of absorption and emission bands is different. A large solvent shift appears in absorption whereas in emission such shift is very small. No mirror image relation between absorption and emission spectra exists. It has been suggested that in this polyene there exists a low-lying forbidden Π-electronic state (^1A_g) below the strongly allowed ^1B_u state.

According to semi-empirical and *a priori* calculations[1] the excited electronic states of linear polyenes are ^1B_u, ^1A_g, ^1A_g, and ^1B_u in order of increasing energy. The lowest singlet-singlet transition of polyenes is $^1A_g \rightarrow {}^1B_u$ and is strongly allowed. There is experimental evidence that there is no or little overlap between the origins of absorption and emission.[2,3] Attempts have been made[3] to explain it in terms of Franck-Condon forbiddenness. A recent theoretical work[4] has shown that inclusion of double-excitation configuration interaction for the excited states in addition to single-excitation configuration in semi-empirical and *a priori* calculations lowers significantly the lower ^1A_g state in the energy so that a forbidden ^1A_g state appears below the strongly allowed ^1B_u state. Recent experimental investigations[5-7] of polyenes have shown that there exists a low-lying forbidden Π-electronic state (^1A_g) below the well-studied lowest Π-electronic state ^1B_u. It is, therefore, expected that in polyenes the energy of absorption to ^1B_u state and of emission from ^1A_g state will show different solvent effects. In this note, we present our results on the effect of different solvents on the absorption and emission spectra of methylbixin.

The compound under investigation is obtained from Hoffman-La Roche Co., Switzerland and used without further purification. Solvents used are of spectrograde quality. The absorption and emission spectra are recorded at room temperature by Spectromom-202 spectrophotometer and Aminco Bowman spectrofluorometer, respectively.

The absorption and emission spectra of this polyene in benzene are shown in Fig. 1. It is observed that the absorption spectrum consists of three vibronic bands with the central one most intense. This structure is the upper state fundamental of about 1000 cm^{-1}. Due to the solvent-solute interaction this structure becomes blurred in some solvents. The effect of different solvents on the spectra results in a shift of the position of the band. It is found that the absorption and emission spectra shift differently when the solvent is changed. Also the absorption spectrum is much more solvent-dependent than the emission spectrum, the latter does not resemble the former and no mirror image relation between absorption and emission exists.

The absorption band of the polyene shifts more towards red with the increase of the refractive index of the solvents whereas this shift is comparatively very small in emission. This solvent shift is expressed in the form[8,9]

$$\Delta\bar{\nu} = k\,f(n^2-1)/(n^2+2)$$

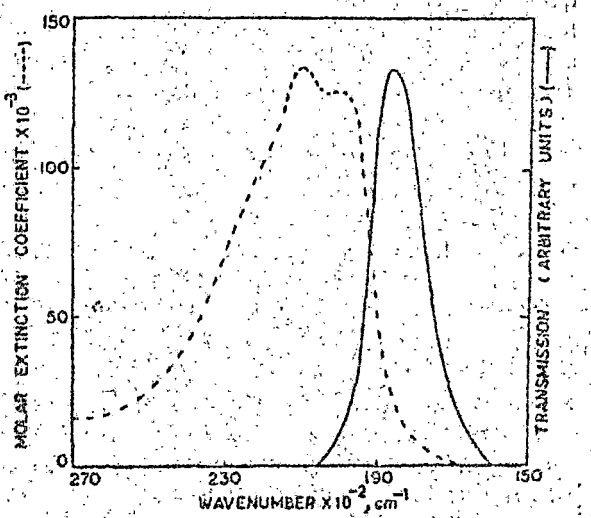

Fig. 1—Absorption (— — —) and emission (——) spectra of methylbixin in benzene

Table 1—Solvent Effect on the Absorption and Emission Bands of Methylbixin

Solvent	$\frac{n^2-1}{n^2+2}$	Transition Energy	
		Emission (in cm^{-1})	Absorption (in cm^{-1})
Acetone	0·2195	18796	21645
Ethanol	0·2217	18761	21598
Ethyl acetate	0·2272	18726	21505
1, 4-Dioxane	0·2546	18691	21220
Cyclohexane	0.2578	18796	21186
Carbon tetrachloride	0·2754	18726	20920
Benzene	0·2946	18691	20920

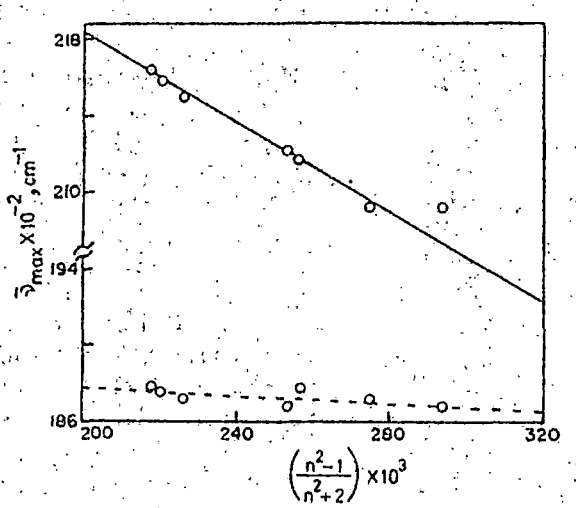

Fig. 2—Plot of $\bar{\nu}_{max}$ versus $(n^2-1)/(n^2+2)$ for absorption (———) and emission (– – –)

Here k is a parameter constant for a given molecule, f the oscillator strength for a particular transition and n the refractive index of the solvent. The positions ($\bar{\nu}_{max}$) of the lowest energy absorption and the highest energy emission bands in different solvents are shown in Table 1. Our experimental results show that the plot of $\bar{\nu}_{max}$ versus the solvent polarizability $(n^2-1)/(n^2+2)$ for both absorption and emission is a straight line as shown in Fig. 2. The slope of this plot gives a measure of the oscillator strength of the electronic transition and it is found that the oscillator strength for the transition involved in absorption is much greater than that for emission. This difference in solvent behaviour and the absence of mirror image relationship between absorption and emission lead to the suggestion that the electronic states involved in absorption and emission are different. Thus the solvent behaviour of absorption and emission indicates the presence of a low-lying forbidden Π-electronic state below the strongly allowed ^1B_u state in this polyene.

The authors are thankful to the University Grants Commission, New Delhi, for financial assistance.

References

1. Suzuki H, *Electronic absorption spectra and geometry of organic molecules* (Academic Press, New York), 1967.
2. Cherry R J & Chapman D, *Trans. Faraday Soc.*, 64 (1968), 2304.
3. Thomson A J, *J. chem. Phys.*, 51 (1969), 4106.
4. Schulten K & Karplus M, *Chem. Phys. Lett.*, 14 (1972), 305.
5. Hudson B S & Kohler B E, *Chem. Phys. Lett.*, 14 (1972), 299.
6. Mandal Krishnagopal & Misra T N, *Chem. Phys. Lett.*, 27 (1974), 57.
7. Mallik B, Jain K M, Mandal K G & Mishra T N, *Indian J. pure appl. Phys.*, 13 (1975), 699.
8. Basu S, *Advances in quantum chemistry*, Vol. 1, edited by P O Lowdin (Academic Press, New York), 1964, 145.
9. Hudson B S & Kohler B E, *J. chem. Phys.*, 59 (1973), 4984.

B Mallik, K M Jain, K G Mandal & T N Misra

Department of Physics, North Bengal University, Raja-Rammohunpur 734 430

Received 5 *January* 1976; *accepted* 19 *February* 1977

Reprinted from the *Indian Journal of Biochemistry & Biophysics* Vol. 15. No. 3 June 1978, pp. 233-235

Charge-transfer Complexes of *all-trans*-β-Carotene

BISWANATH MALLIK, K. M. JAIN* & T. N. MISRA
Indian Association for the Cultivation of Science, Jadavpur, Calcutta 700 032

Manuscript received 12 *December* 1977

On adsorption of some electron acceptor molecules on the solid films of *all-trans*-β-carotene, a new absorption band appears on the longer wavelength side of the spectrum in addition the original bands of *all-trans*-β-carotene. The position of this new band is dependent on the electron effinity (E_A) of the acceptor molecules. A linear relationship between the of ν_{max} the new band and E_A has abee observed. The ionization potential of *all-trans*-β-carotene has been estimated from the intercept of this plot. The value 5.44 ev obtained agrees satisfactorily with the experimental value. It has been concluded that *all-trans*-β-carotene behaves as an electron donor and forms charge-transfer complexes with suitable electron acceptors.

THE observation that β-carotene may form charge-transfer (CT) complexes was made by Platt[1] who suggested that donor-carotene-acceptor trimolecular complex could be involved in the primary photosynthesis process. In a mixture of β-carotene and iodine in $ClCH_2Cl$ solution Lupinski[2] observed a new absorption band at 10000 Å proposed as charge-transfer band of β-carotene....I^+ complex.

Ebrey[3], on the other hand, believed that the band observed by Lupinski, instead of being a charge-transfer band of donor-acceptor type, was a band of β-carotene shifted to longer wavelength due to charge-transfer effect, thus suggesting that β-carotene-1^+. complex has several resonance structures for the β-carotene ground state that would equalise bond length and cause its shifting to longer wavelength.

Significant change in semiconduction current and activation energy of β-carotene powder cell on adsorption of certain gases and vapours on the crystalline surface has been attributed to possible CT complex formation between β-carotene and the adsorbed vapour molecules[4]. We have studied spectroscopically the effect of adsorption of acceptor vapours on the solid film of β-carotene to see if CT complexes are really formed in the solid state. The results of such studies are presented in this paper.

The sample of *all-trans*-β-carotene of high quality has been obtained from Hoffman-La-Roche Co, Switzerland. We have used this compound without further purification. Thin films of polycrystals of this polyene have been made on the quartz surface by gently rubbing the material on it. The solid films thus made have been exposed to nitric acid, iodine, bromine and iodine monochloride vapours. These chemicals are of high quality. The absorption spectra at room temperature (28°C) were recorded immediately after exposing the solid films to vapours. Spectromom-202 spectrophotometer of Hungarian Optical Works was used.

*Present Address: : Physics Department, Govt. P. G. College Durg (M.P.)

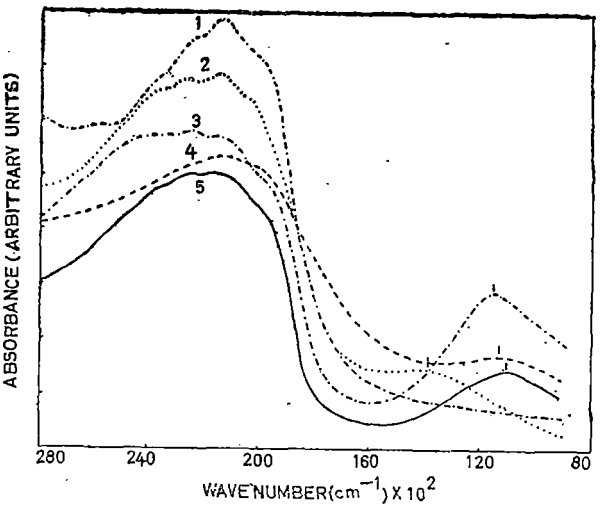

Fig. 1—Electronic absorption spectra of *all-trans*-β-carotene solid film after adsorption of different electron acceptor vapours. [(1), all-trans-β-carotene solid film; (2), nitric acid vapour adsorption; (3), iodine vapour adsorption; (4), bromine vapour adsorption; (5), iodine monochloride vapour adsorption]. (The position ν_{max} of the new bands is indicated by a vertical mark)]

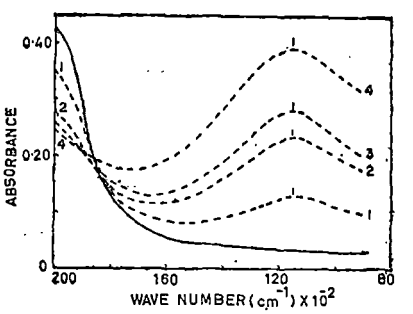

Fig. 2—Enhancement of the intensity of the new band with the amount of adsorbed acceptor molecules. [(—), no adsorption; (....), on adsorption of I_2 vapour; (1-4), in order of increasing amount of acceptor molecules)]

The room temperature absorption spectrum of all-trans-β-carotene in the solid state and the spectra after adsorption of different acceptor vapours are shown in Fig. 1. In the latter case, a new band appeas on the longer wavelength side of the spectra in addition to the original bands of β-carotene solid film. With the increasing amount of acceptor molecules adsorbed on the film surface, the intensity of this new band increases as is usually observed in the case of a charge-transfer band (Fig. 2). The position of this new band is found to be dependent on the acceptor vapours used and shows large red shift with increasing electron affinity of the acceptor molecules. Only acceptors fairly volatile at ordinary temperature are suitable for such experiment. As number of such acceptors are very limited, only a few acceptors could be used. The position of the new band appearing due to the adsorption of different acceptor vapours on the solid film of all-trans-β-carotene are summarized in Table 1.

TABLE 1—POSITION (ν_{max}) OF THE NEW BAND APPEARING ON ADSORPTION OF DIFFERENT ACCEPTOR VAPOURS ON THE SOLID FILM OF *all-trans*-β-CAROTENE

Acceptor used	E_A (ev)	Ref.	ν_{max} (cm^{-1})
Nitric acid	1.83	5	13900
Iodine	2.4	6	11550
Bromine	2.6	6	11300
ICl	2.7	6	11100

The Mulliken theory for charge-transfer complex formation leads to the equation[5].

$$h\nu_{CT} = I_D^V - E_A^V + C_1 + \frac{C_2}{I_D^V - E_A^V + C_1} \quad (1)$$

where $h\nu_{CT}$ is the energy of the lowest energy intermolecular CT band, I_D^V is the vertical ionization potential of the donor, E_A^V is the vertical electron affinity of the acceptor and C_1 and C_2 are constants. The last term is often small, so that its variation can be neglected, giving the equation

$$h\nu_{CT} = I_D^V - E_A^V + C_1 \quad ..(2)$$

Thus for a particular donor, a plot of $h\nu_{CT}$ against E_A^V should be linear. Unfortunately, reliable values of vertical electron affinities are very scare. The vertical electron affinity of nitric acid is not avaiable in the literature. Recently, Chen and Wentworth have emphasised that the correlation of $h\nu_{CT}$ with the absolute electron affinities (E_A) of acceptors is consistent with the usual linear equations and their associated assumptions. The adiabatic electron affinities of I_2, Br_2 and ICl, estimated theoretically by Person[6], were 2.4 ± 0.3, 2.6 ± 0.3 and 2.7 ± 0.3 ev respectively, agreeing satisfactorily with the experimental absolute values measured by Hughes *et al.*[7] We have, therefore, used these adiabatic electron affinity values as the absolute values. The value of E_A for nitric acid has been taken from Chen and Wentworth's table[5].

A plot of ν_{max} (cm^{-1}) of the new band against E_A gives a linear curve (Figs. 3). The ionization potenial of β-carotene can be estimated from this ν_{max} versus E_A plot. The intercept of this curve gives $I_D + C_1 = 2.44$ ev. In typical donor-acceptor CT complexes, $-C_1$ is usually around 3 ev[5,8]. This gives a value of the ionization potential of β-carotene as 5.44 ev. The experimental[9,10] value of the ionization potential of β-carotene is 5.5 ev. This agreement leads credence to the above linear plot and also to the CT concept for this complex. From Eq. 2, one expects a slope of unity for ν_{CT} *versus* E_A^V plot. Fig. 3 gives a slope of 0.44. This low value of slope could be due to that the electron affinity values used for the plot being absolute rather than vertical.

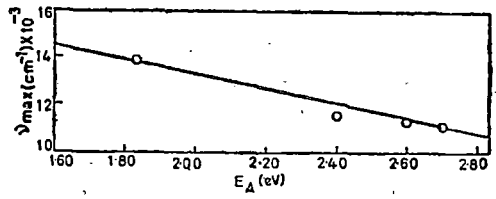

Fig. 3— Plot of ν_{max} (cm^{-1}) against E_A

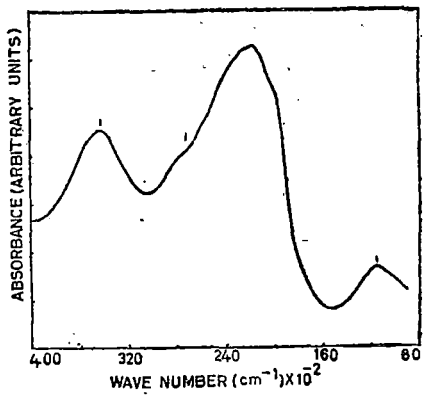

Fig. 4—Electronic absorption spectrum of *all-trans*-β-carotene solid film after adsorption of I_2 vapour. [The position of the new bands is indicated by a vertical mark]

Further, Eq. 2 is only approximate and there is no reason to expect that the last term in Eq. 1 is negligible for all the pairs of donors and acceptors. Indeed, such deviation of slope from unity is a general observation in these types of experiments[11,12].

The room-temperature absorption spectrum of *all-trans*-β-carotene in the region 40000—9000 cm^{-1} after adsorption of I_2 vapour is shown in Fig. 4. From the spectrum, it is observed that in addition to the new band in the longer wavelength side another weak new band is also observed at about 27200 cm^{-1}. This band is possibly the absorption band of I_3^- ion. The other absorption band of this molecular ion expected at about 33900 cm^{-1} has possibly been merged with the original band of *all-trans*-β-carotene at 35400 cm^{-1}. In the case of I_2, possibly through the reaction

$$\beta\text{-carotene} + 2I_2 \rightleftharpoons (\beta\text{-carotene I})^+ + I_3^-$$

β-carotene forms CT complex with iodine. The observed new band on the longer wavelength side arises from the transition between the complex in its ground state (β-carotene.... I^+) and the excited state of the complex (β-carotene$^+$....I)

Contrary to that suggested by Ebrey, our results indicate that at least in the solid state single resonance structure

$$C=C-(C=C)_n-C=C.....I^+$$

is quite stable and usual donor-acceptor complexes are formed.

Thanks are due to the Council of Scientific & Industrial Research, New Delhi for financial support

and to the Hoffman & La-Roche Co., Switzerland for a generous gift of the sample. Thanks are also due to Prof. G. S. Kastha for his kind interest.

References

1. PLATT J. R. (1959) *Science* **129**, 372.
2. LUPINSKI J. H. (1963) *J. phys. Chem.* **67**, 2725.
3. EBREY, T. G. (1967) *J. phys. Chem.* **71**, 1963.
4. ROSENBERG, B., MISRA, T. N. & SWITZER, R. (1968) *Nature* **217** 423.
5. CHEN, E. C. M. & WENTWORTH, W. E. (1975) *J. chem. Phys.* **63**, 3183.
6. PERION, W. B. (1963) *J. chem. Phys.* **38**, 109.
7. HUGHES, B. M., LIFSHITZ, C. & TIERNAN, T. O. (1973) *J. chem. Phys.* **59** (6), 3162.
8. FARRAGHER, A. L. & PAGE, F. M. (1967) *Trans. Faraday. Soc.* **63**, 2369.
9. VILESOV, F. I. (1960) *Dokl. Akad. Nauk. SSSR. Sèr. Fiz.* **132**, 632.
10. VILESOV, F. I. & TERENIN, A. N. (1960) *Dokl. Akad. Nauk. SSSR, Ser. Fiz.* **133**, 1059.
11. MCCONNEL, H., HAM, J. S. & PLATT, J. R. (1953) *J. chem. Phys.* **21**, 66.
12. FOSTER, R. (1960) *Tetrahedron* **10**, 96.

Jpn. J. Appl. Phys. Vol. 18 (1979), No. 3

Compensation Effect in Semiconducting Vitamin A (alcohol and acetate)

Biswanath Mallik, Alpana Ghosh and T. N. Misra

Optics Department, Indian Association for the Cultivation of Science, Jadavpur, Calcutta-700 032 India

(Received September 12, 1978)

Inorganic semiconductor the compensation rule, a linear relationship between the logarithm of the pre-exponential factor in the expression for specific conductivity and the semiconduction activation energy, has been a subject of great interest in the recent years.[1-4] The pre-exponential factor σ_0 is generally assumed to be a constant in the equation

$$\sigma(T) = \sigma_0 \exp(-E/2kT), \qquad (1)$$

where, $\sigma(T)$ is the specific conductivity at any absolute temperature T, E is the semiconduction activation energy and k is the Boltzmann constant. But experimental evidence shows that σ_0 contains exponential functions.[5] To study the compensation rule in a semiconductor E is generally varied by different ways and $\log \sigma_0$ is plotted against E. Recently, Masui *et al.*[1] have reported that this compensation rule is valid for uniaxially drawn low density polyethylene. Experimental results of Sawa *et al.*[2] show that in case of high energy irradiated polyethylene with different radiation doses also this rule is valid. However, adsorption of gases is known to change the semiconduction activation energies of many organic semiconductors.[6,7] Such change depends on the chemical nature and also on the amount of vapour adsorbed. We have used this method of varying the activation energy of semiconducting Vitamin A by adsorbing various vapours and different amounts of the same vapour on the crystallite surface. In this note we present our experimental results and show that the compensation rule is valid for semiconduction in solid Vitamin A (alcohol and acetate).

The samples of Vitamin A alcohol and acetate powder were obtained from Hoffmann-La Roche & Co. Ltd., Switzerland. The experimental procedure for the measurement of semiconduction activation energy of these compounds on vapour adsorption is similar to that of Misra *et al.*[7] The finely powdered compounds pressed in a sandwich cell between a conducting glass and a stainless steel electrode was maintained at a moderate pressure by spring clips. The separation between the electrodes was maintained by a 2 mil thick teflon spacer. A d.c. voltage of 22.5 volts from a dry battery pack was applied across the cell which was placed on a thermal bar platform in a suitably designed conductivity chamber made of brass and fashioned with teflon. There was an inlet and a outlet for gas in the chamber. The temperature of the cell which could be controlled from outside was measured by a copper constantan thermocouple attached to the metal electrode. The dark current was measured with Electrometer Amplifier EA815 of Electronic Corporation of India Limited. Chemicals used in this experiment were of spectrograde (E. Merck, B.D.H.) or equivalent quality. The semiconduction activation energy of Vitamin A (alcohol and acetate) with toluene (1), benzene (2), ethyl acetate (3), n-heptane (4), ethanol (5) and methanol (6) vapour and also with different amounts of ethyl acetate vapour adsorption have been determined from the Arrhenious plots of eq. (1).

At a constant temperature T_1, $\log \sigma$ [for $(1/T_1) = 3.80 \times 10^{-3}\ \mathrm{K}^{-1}$] is plotted against the measured values of activation energy (E). Linear plots as shown in Fig. 1 are obtained. The observed slopes in Fig. 1 are 7.70 and 4.55 eV^{-1} for Vitamin A alcohol and acetate respectively. The expected slope according to eq. (1) is 22.18 eV^{-1} for both the compounds. These low values of the observed slopes indicate that eq. (1) is not valid in these cases. To test the validity of the compensation rule $\log \sigma_0$ is plotted against E. The plots are linear (Fig. 2). Rosenberg *et al.*[4] have suggested the following equation for the specific conductivity which takes account of the compensation effect

$$\sigma = \sigma_0' \exp(E/2kT_0) \exp(-E/2kT) \qquad (2)$$

So that

$$\sigma_0 = \sigma_0' \exp(E/2kT_0), \qquad (3)$$

where T_0 is the characteristic temperature of the semiconducting material. σ_0' and T_0 for the same compound remain invariant. The

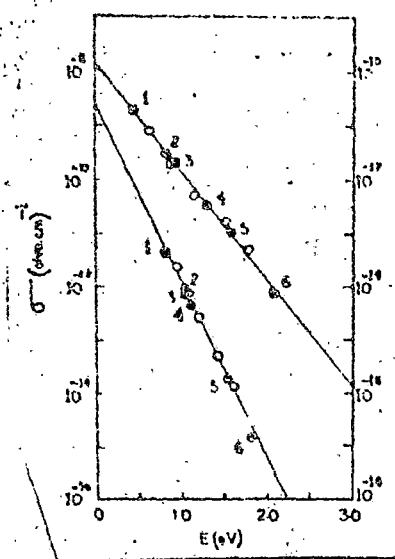

Fig. 1. Plot of $\log \sigma$ versus E at a constant temperature $[(1/T_1) = 3.80 \times 10^{-3}\ K^{-1}]$ for Vitamin A (alcohol and acetate).
Vitamin A alcohol: lower line (left scale);
Vitamin A acetate: top line (right scale).
—●— different vapours (the numbers indicate the specific vapour as stated in the text).
—○— different amounts of ethyl acetate vapour (activation energy decreases with the increasing amount of the vapour adsorbed).

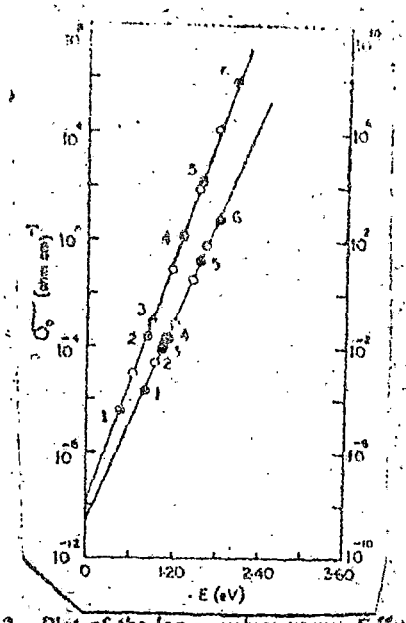

Fig. 2. Plot of the $\log \sigma_0$ values versus E [from eq. (1)] for Vitamin A (alcohol and acetate) at a constant temperature $[(1/T_1) = 3.80 \times 10^{-3}\ K^{-1}]$.
Vitamin A alcohol: lower line (right scale);
Vitamin A acetate: top line (left scale).
The closed and open circles indicate same as in Fig. 1.

value of the slope i.e. $(2kT_0)^{-1}$ obtained from Fig. 2 is 14.45 and 17.52 eV^{-1} for Vitamin A alcohol and acetate respectively.

From eq. (2) it is seen that for any particular temperature T_1 the specific conductivity is expressed by

$$\log \sigma(T_1) = \log \sigma_0' + \left[\frac{1}{T_0} - \frac{1}{T_1}\right]\frac{E}{2k} \qquad (4)$$

giving a slope equal to $[(1/T_0) - (1/T_1)](1/2k)$ and an intercept of $\log \sigma_0'$ for the linear plot $\log \sigma(T_1)$ vs E. The calculated slopes with $(2kT_0)^{-1}$ as obtained from Fig. 2 are 7.73 and 4.66 eV^{-1} for Vitamin A alcohol and acetate respectively. The experimentally observed slopes (Fig. 1) are in excellent agreement with this. The value of σ_0' obtained from Fig. 2 [2.80×10^{-9} and 1.50×10^{-10} $(\Omega \cdot cm)^{-1}$ for Vitamin A alcohol and acetate respectively] and Fig. 1 [2.85×10^{-9} and 1.60×10^{-10} $(\Omega \cdot cm)^{-1}$ for Vitamin A alcohol and acetate respectively] agree satisfactorily. Thus our results confirm the validity of the compensation rule in solid Vitamin A semiconductor.

We thank the Council of Scientific and Industrial Research, India for a Senior Research Fellowship (to B.M.) and Prof. G. S. Kastha for his kind interest in this problem. Thanks are also due to M/s. Hoffmann-La Roche & Co., Switzerland for a kind gift of the Vitamin A samples.

References

1) M. Masui, H. Nagasaka and K. Yahagi: *Jpn. J. Appl. Phys.* 16 (1977) 117.
2) G. Sawa, K. Kitagawa and M. Ieda: *Jpn. J. Appl. Phys.* 11 (1972) 416.
3) D. D. Eley, A. S. Fewcett and M. R. Willis: *Trans. Faraday Soc.* 64 (1968) 1513.
4) B. Rosenberg, B. Bhowmik, H. C. Harder and E. Postow: *J. Chem. Phys.* 49 (1968) 4108.
5) F. Gutmann and L. E. Lyons: *Organic Semiconductors* (Wiley, New York, 1967) p. 428.
6) B. Rosenberg: *J. Chem. Phys.* 36 (1962) 816.
7) T. N. Misra, B. Rosenberg and R. Switzer: *J. Chem. Phys.* 48 (1968) 2096.

BULLETIN OF THE CHEMICAL SOCIETY OF JAPAN, VOL. 52 (6), 0000—0000 (1979)

Pre-exponential Factor in Semiconducting Vitamin A (Alcohol and Acetate)

Biswanath Mallik, Alpana Ghosh, and T. N. Misra*

Optics Department, Indian Association for the Cultivation of Science, Jadavpur, Calcutta 700032, India

(Received August 30, 1978)

The semiconductive properties of vitamin A (alcohol and acetate) on adsorption of various vapors have been studied. The adsorbed vapors increase the semiconduction currents by several orders of magnitude and decrease the semiconduction activation energies. Such change depends on the chemical nature and also on the amount of vapor adsorbed. Semiconducting vitamin A follows the three-constant equation

$$\sigma(T) = \sigma_0' \exp(E/2kT_0) \exp(-E/2kT)$$

where the conventional pre-exponential factor σ_0 has been replaced by $\sigma_0' \exp(E/2kT_0)$ (the so called compensation effect). Here T_0 and σ_0' are constants for the substance and T_0 is called the characteristic temperature. Various methods used for evaluating these constants have yielded consistent results with $T_0 \approx 402$ K and $\sigma_0' \approx 2.8 \times 10^{-9}\ \Omega^{-1}\ \mathrm{cm}^{-1}$ for vitamin A alcohol and $T_0 \approx 335$ K and $\sigma_0' \approx 1.5 \times 10^{-10}\ \Omega^{-1}\ \mathrm{cm}^{-1}$ for vitamin A acetate. Excellent correlation obtained between the relevant parameters in semiconducting vitamin A indicates that σ_0 and E are physically related. Various models for conduction mechanism leading to compensation effect have been discussed. The measured activation energies on adsorption of same amount of various vapors show a linear relationship with the ionization potential of the adsorbed molecules suggesting that charge-transfer interaction is responsible for the semiconductivity enhancement.

The electrical conductivity of conjugated π-electronic organic compounds follows the operational definition of a semiconductor

$$\sigma(T) = \sigma_0 \exp(-E/2kT) \tag{1}$$

where $\sigma(T)$ is the specific conductivity at any absolute temperature T, σ_0 is a pre-exponential factor, E the semiconduction activation energy and k is Boltzmann constant ($E/2$ is often written as E', however, we shall use the former throughout this paper). Experimentally, E is obtained from the slope of the linear plot of $\log \sigma(T)$ *vs.* $1/T$. Recently, the so called pre-exponential factor σ_0 has been the subject of much discussion[1-6] as experimental evidence accumulated shows that σ_0 contain exponential functions. Gutmann and Lyons[7] showed a linear relationship of the form

$$\log \sigma_0 = \alpha E + \beta \tag{2}$$

holds good for one entire class of organic compounds, α and β being constants. Rosenberg[2,8] *et al.* showed evidence that if E is varied by hydration or complex formation relation (2) is valid for a single organic substance as well and they suggested an expression for the specific conductivity of the form

$$\sigma(T) = \sigma_0' \exp(E/2kT_0) \exp(-E/2kT) \tag{3}$$

thus introducing an additional constant T_0 called characteristic temperature. σ_0' and T_0 for the same compound remain invariant. The linear relationship between the logarithm of the pre-exponential factor and the activation energy is called the compensation effect. σ and E change in such a manner that their effect on σ_0 are mutually compensated. It has been pointed out by Johnston and Lyons[4] that the linear relationship between $\log \sigma_0$ and E may originate solely from the calculation of these parameters and the compensation effect requires no physical interpretation. However, they have suggested that if σ_0 and E are physically related, one should get a linear relationship between $\log \sigma$ and E yielding the semiconductive parameters in agreement with the values obtained from other sources. From Eq. 3, for any particular temperature T_1, the specific conductivity is given by

$$\log \sigma(T_1) = \log \sigma_0' + \left(\frac{1}{T_0} - \frac{1}{T_1}\right)\frac{E}{2k}.$$

Thus, the plot of $\log \sigma(T_1)$ *vs.* E is expected to be linear with a slope $(1/T_0 - 1/T_1)/2k$ and an intercept of $\log \sigma_0'$. The value of σ_0' obtained from this plot should also show a good agreement with the values obtained from the $\log \sigma_0$ *vs.* E and $\log \sigma$ *vs.* $1/T$ plots. In the experiment of Johnston and Lyons[4] the $\log \sigma_0$ *vs.* E plots were linear, but a very poor correlation between $\log \sigma$ and E was observed[9] in one component crystal of anthracene by changing its purity and doping with tetracene. Some recent theoretical works[9,10] suggest that in biological semiconductors the compensation effect arises due to the dark conduction process. In view of the scanty experimental works available on this effect, it was thought worthwhile to investigate the conduction process in more biological semiconductors. To test the validity of the compensation effect, E is generally varied by various ways and $\log \sigma_0$ is plotted against E. The adsorption of gases is known[8,11] to change the activation energies of organic semiconductors. Recently, being motivated to examine the hypothesis that vitamin A is involved in olfactory transduction mechanism,[12] we have studied the effect of adsorption of gases on solid vitamin A. Such adsorption changes the activation energy and enhances the conductivity. In this paper we present experimental evidence to indicate that the compensation rule is valid for solid vitamin A and that σ_0 and E are indeed physically related. Further, the formation of donor-acceptor complex between vitamin A and the adsorbed gas molecule is shown to be responsible for the observed activation energy change.

Experimental

High purity vitamin A alcohol and vitamin A acetate were obtained from Hoffmann-La Roche and Co. Ltd., Switzerland. These were used without any further purification. Sandwich cell technique with a conducting glass and a

stainless steel electrode was used. There was a gas inlet and an outlet in the conductivity chamber, made of brass and fashioned with Teflon, for gas adsorption study. The temperature of the sandwich cell could be controlled from outside. Temperature measurements were made using a copper-constantan thermocouple attached at the top of the metal electrode. The semiconduction currents were measured with an electrometer amplifier EA815 of the Electronic Corporation of India Ltd. Vapors of methanol, ethanol, heptane, ethyl acetate, benzene, and toluene were allowed to be adsorbed on the semiconductors. The reagent chemicals of spectrograde (E. Merck, B. D. H.) quality were used without further purification; otherwise repeated fractional distillation was done before use. To pass various vapors inside the chamber, dry nitrogen gas was used as carrier which was passed through a bubbler containing the reagent chemical. The partial pressure of the reagent vapor in the conductivity chamber was kept constant during adsorption at a pressure less than the saturation vapor pressure at the sample cell temperature by carefully adjusting the temperature of the bubbler. The partial pressure of the vapor was the saturation vapor pressure of the reagent chemical at the temperature of the bubbler. The same partial pressure (40 mm) was maintained inside the chamber for various vapors. Under this condition it is a valid assumption that the same amount of various vapors are adsorbed on the semiconductors. Repeated heating and cooling of the sample initially in vacuum and finally in dry nitrogen atmosphere ensured desorption of water vapor or any other adsorbed gases. Temperature (12.5 °C) of the sample cells and the inlet flow were kept constant during adsorption.

To determine the effect of adsorbed vapor on the semiconduction activation energy, the sample was allowed to come to a steady state in the chamber atmosphere containing the vapor with nitrogen. The pressure of the total gas mixture in the chamber was atmospheric pressure. The saturation current, after vapor adsorption was found to be almost constant even after four hours indicating that the conduction in the system is mainly electronic.[13,14] The sample cell was then rapidly cooled to about −40 °C and then the chamber was flushed gently with dry nitrogen gas. Semiconduction current was measured with increasing temperature of the sample cell. The outlet of the chamber was kept open to maintain atmospheric pressure inside the chamber.

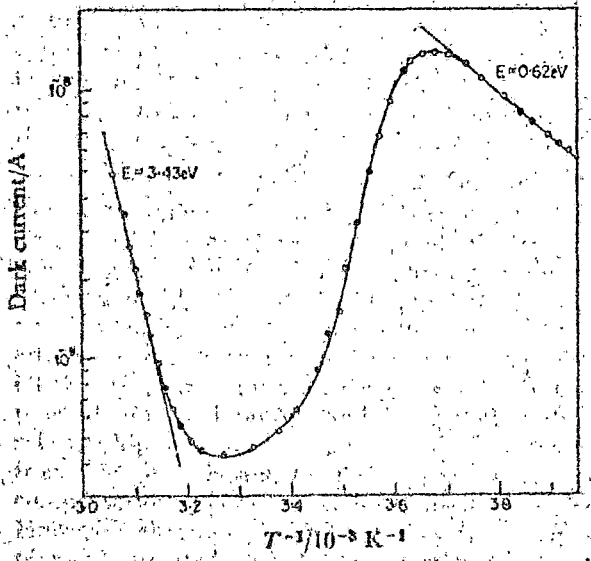

Fig. 1. Semiconductivity in a vitamin A acetate powder cell with desorption of ethyl acetate vapor as the temperature increases.

Results and Discussion

The semiconduction activation energy of crystalline powders of vitamin A (alcohol and acetate) has been measured several times in dry nitrogen atmosphere. The observed values are 2.06 and 3.50 eV (approx.) for the alcohol and acetate respectively. The adsorption of gases enhances the semiconduction current (by several orders of magnitude in some cases) and decreases the activation energy appreciably. The results of one such typical experiment is shown in Fig. 1. The straight line portion in the low temperature region shows the semiconducting properties of vitamin A acetate powder with adsorbed ethyl acetate vapor and the slope of this line gives the activation energy (0.62 eV) of this semiconducting system. The straight line portion in the high temperature region gives the activation energy of vitamin A acetate in nitrogen atmosphere. The observed value (3.43 eV) is slightly lower possibly due to incomplete desorption of adsorbed vapors. The intermediate portion shows the semiconduction behavior

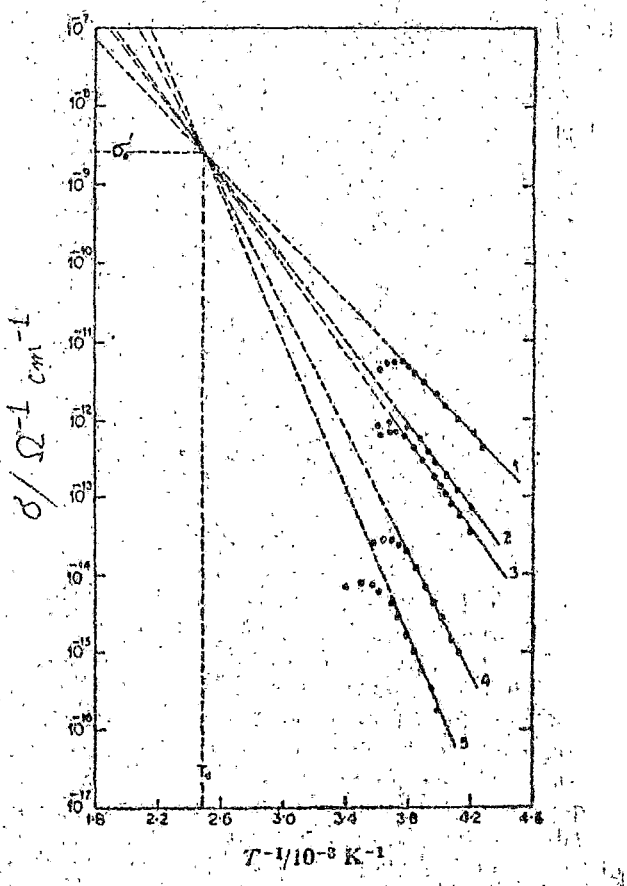

Fig. 2(a). Semiconductivity in vitamin A alcohol powder cell (steady state condition) with the adsorption of same amount of different vapors. Solid lines represent temperature region of measurements, dashed lines are extrapolations. Each line refers to a specific vapor adsorbed state. Vapors are (1) toluene; (2) ethyl acetate; (3) heptane; (4) ethanol; and (5) methanol. To avoid overlapping with (2) the line corresponding to benzene vapor is not shown. The value of T_0=402 K; $\sigma_0'=2.65\times10^{-8}\ \Omega^{-1}\ cm^{-1}$.

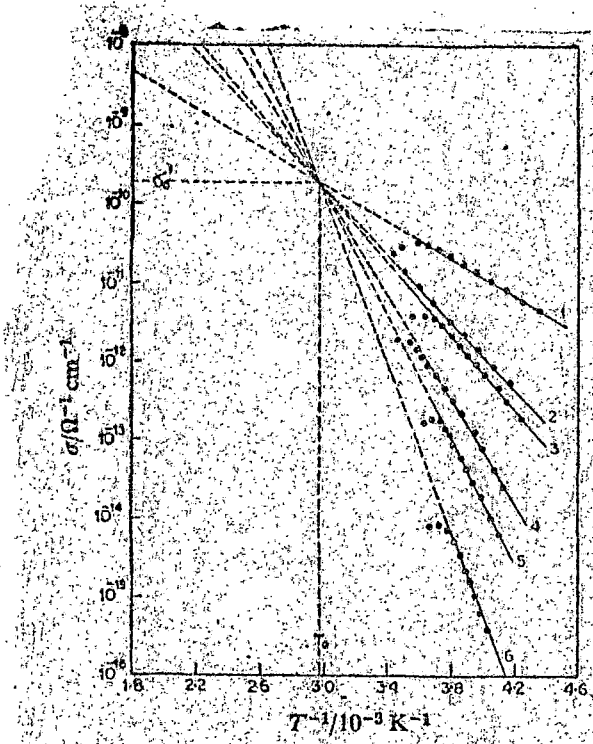

Fig. 2(b). Same as Fig. 2(a) for vitamin A acetate with adsorbed vapors (1) toluene; (2) benzene; (3) ethyl acetate; (4) heptane; (5) ethanol; and (6) methanol. $T_0 \simeq 335$ K; $\sigma_0' = 1.8 \times 10^{-10}\ \Omega^{-1}$ cm^{-1}.

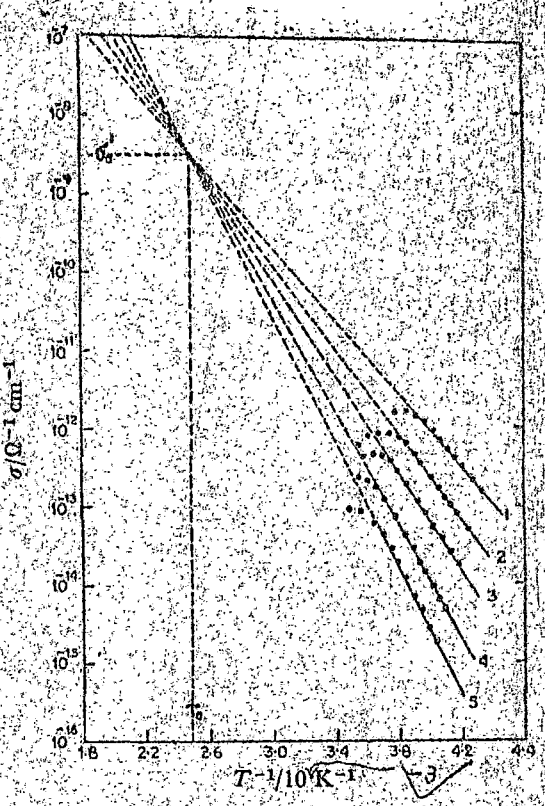

Fig. 3(a). Semiconductivity data for vitamin A alcohol powder cell (steady state condition) with adsorption of different amount of ethyl-acetate vapor. The lines (1) $\rightarrow$(5) refer to the states with the decreasing amount of adsorbed vapor. $T_0 \simeq 403$ K; $\sigma_0' = 3.1 \times 10^{-9}\ \Omega^{-1}$ cm^{-1}.

of the sandwich cell during desorption process. Similar curves were also obtained with other vapors.

The Characteristic Temperature for the Semiconducting Vitamin A. In Figs. 2(a) and 2(b) we show the straight portion in the low temperature region for a number of adsorbed vapors in vitamin A alcohol and acetate respectively. It is observed that with the same amount of vapor adsorbed, the activation energy values are different for different vapors. In this case no single value of σ_0 is found if either $T \rightarrow \infty$ or $E \rightarrow 0$ as is expected from Eq. 1. The extrapolated lines intercept the ordinate at a wide varieties of positions, but they all pass approximately through a single point at a temperature T_0, characteristic of the semiconductor. This is exactly what is expected from Eq. 3. Figs. 2(a) and 2(b) show $T_0 \simeq 402$ K for vitamin A alcohol and $T_0 \simeq 335$ K for vitamin A acetate. At these characteristic temperatures $\sigma(T_0) = \sigma_0'$ values of vitamin A alcohol and acetate are 2.65×10^{-9} and $1.8 \times 10^{-10}\ \Omega^{-1}$ cm^{-1} respectively. Adsorption of different amount of same vapor also changes the semiconduction activation energy to different extent. The plots of $\log \sigma(T)$ *vs.* $1/T$ for different amount of ethyl acetate vapor adsorbed on vitamin A alcohol and acetate semiconductors are shown in Figs. 3(a) and 3(b). These two sets also give values of T_0's and σ_0's [403 and 334 K and 3.1×10^{-9} and $1.65 \times 10^{-10}\ \Omega^{-1}$ cm^{-1} for vitamin A alcohol and acetate respectively] in good agreement with those obtained earlier.

If plotted in alternate fashion as $\log \sigma_0$ *vs.* E, the plots are linear as expected [since $\log \sigma_0 = E/(2kT_0) + \log \sigma_0'$] and are shown in Fig. 4. The value of T_0 obtained from the slopes are 404 and 333 K for vitamin A alcohol and

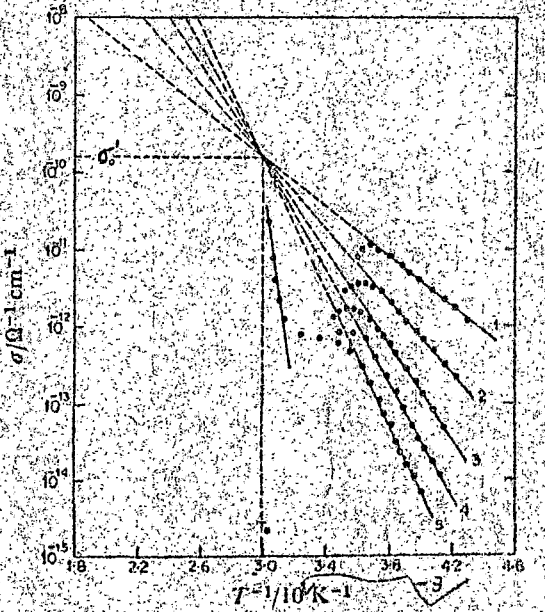

Fig. 3(b). Same as Fig. 3(a) for vitamin A acetate Here, $T_0 \simeq 334$ K; $\sigma_0' = 1.65 \times 10^{-10}\ \Omega^{-1}$ cm^{-1}.

acetate respectively. The σ_0' values obtained from the intercepts of these plots are 2.8×10^{-9} and 1.5×10^{-10} Ω^{-1} cm^{-1} for vitamin A alcohol and acetate respectively. Thus the values of T_0 and σ_0 obtained from various plots are consistent and show excellent agreement.

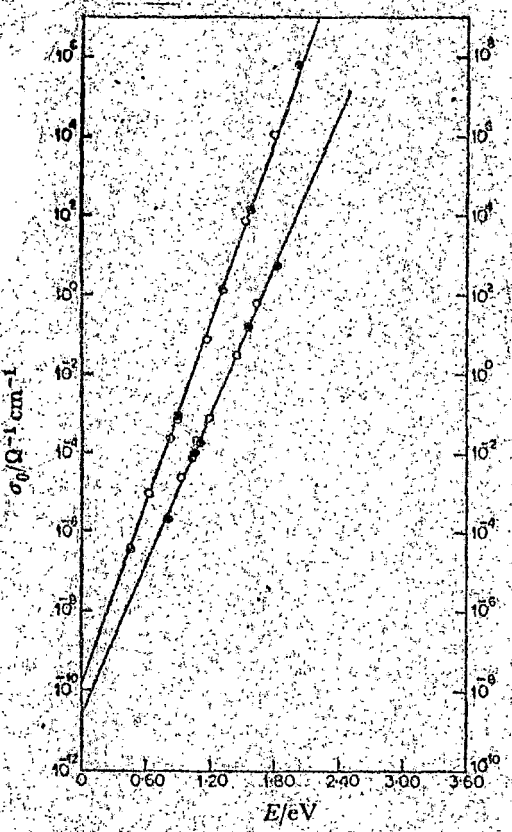

Fig. 4. Plot of the log σ_0 values [from Eq. 1] *vs.* the activation energies for vitamin A (alcohol and acetate) at a constant temperature [$1/T=3.8\times10^{-3}$ K^{-1}]. The lower line is for vitamin A alcohol (right scale) and the top line is for vitamin A acetate (left scale). The dark circles refer to different vapors and the open circles to different amounts of same vapor. Slopes and σ_0' values are 14.45 eV^{-1} and 2.8×10^{-9} Ω^{-1} cm^{-1} for vitamin A alcohol and 17.52 eV^{-1} and 1.5×10^{-10} Ω^{-1} cm^{-1} for vitamin A acetate respectively.

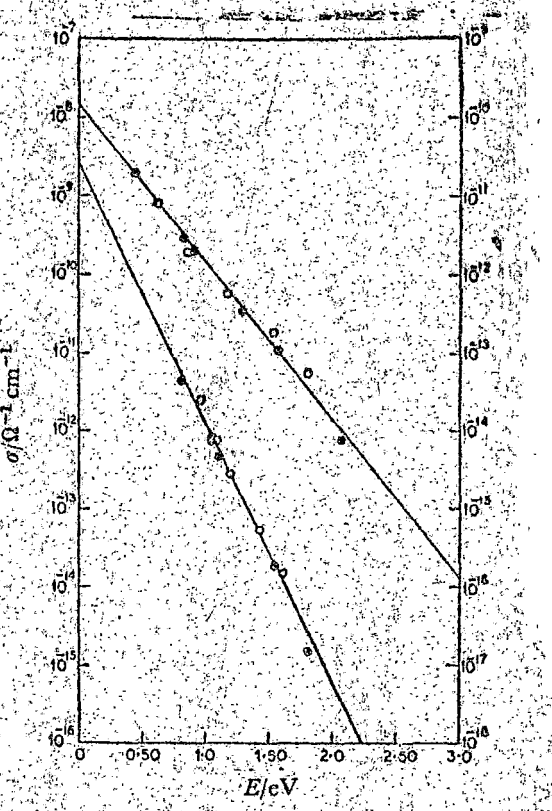

Fig. 5. Plot of the log σ values for vitamin A (alcohol and acetate) *vs.* E at a constant temperature ($1/T_1=3.8\times10^{-3}$ K^{-1}). The lower line refers to vitamin A alcohol (left scale) and the top line to vitamin A acetate (right scale). The dark circles refer to different vapors and the open circles to different amounts of same vapor. Slopes and σ_0' values are 7.70 eV^{-1} and 2.85×10^{-9} Ω^{-1} cm^{-1} for vitamin A alcohol; 4.55 eV^{-1} and 1.6×10^{-10} Ω^{-1} cm^{-1} for vitamin A acetate respectively.

Using the values of $1/2kT_0=14.45$ eV^{-1} and $\sigma_0'=2.8\times10^{-9}$ Ω^{-1} cm^{-1} for vitamin A alcohol, $1/2kT_0=17.52$ eV^{-1} and $\sigma_0'=1.5\times10^{-10}$ Ω^{-1} cm^{-1} for vitamin A acetate, we calculate the expected σ_0 values and compare these with experimentally measured values as obtained from the intercepts of the log σ *vs.* $1/T$ plots. These are shown in Tables 1 and 2. These data confirm the validity of Eq. 3 for vitamin A semiconductor.

The plots of log σ (T_1) *vs.* E are shown in Fig. 5 for $1/T_1=3.8\times10^{-3}$ K^{-1}. Taking $1/(2kT_0)=14.45$ and 17.52 eV^{-1} from Fig. 4, the expected slopes are 7.73 and 4.66 eV^{-1} for vitamin A alcohol and acetate respectively. The observed slopes in Fig. 5 are 7.70 and

Table 1. Semiconduction parameters for vitamin A (alcohol and acetate) on adsorption of various vapors according to Eq. 3

Vapors adsorbed	Ionization potential[a]	Vitamin A alcohol (solid state crystalline powder) $(2kT_0)^{-1}=14.45$ eV^{-1}, $\sigma_0'=2.8\times10^{-9}$ Ω^{-1} cm^{-1}			Vitamin A acetate (solid state crystalline powder) $(2kT_0)^{-1}=17.52$ eV^{-1}, $\sigma_0'=1.5\times10^{-10}$ Ω^{-1} cm^{-1}		
	eV	E eV	$\sigma_0'\exp[E/(2kT_0)]$ Ω^{-1} cm^{-1}	σ_0 Ω^{-1} cm^{-1}	E eV	$\sigma_0'\exp[E/(2kT_0)]$ Ω^{-1} cm^{-1}	σ_0 Ω^{-1} cm^{-1}
Toluene	8.81	0.80	2.93×10^{-4}	4.1×10^{-6}	0.448	3.84×10^{-7}	6.1×10^{-7}
Benzene	9.24	1.04	9.41×10^{-3}	7.98×10^{-3}	0.821	2.65×10^{-6}	3.8×10^{-6}
Ethyl acetate	10.11	1.05	1.26×10^{-2}	1.15×10^{-2}	0.896	9.85×10^{-6}	1.7×10^{-5}
Heptane	10.35	1.10	2.24×10^{-2}	2.6×10^{-2}	1.31	1.39×10^{0}	1.2×10^{0}
Ethanol	10.50	1.55	1.49×10^{1}	1.3×10^{1}	1.57	1.32×10^{0}	7.0×10^{1}
Methanol	10.85	1.82	7.39×10^{2}	1.25×10^{3}	2.07	8.44×10^{4}	8.0×10^{3}

a) Ref. 7, pp. 669—689.

Table 2. Semiconduction parameters for vitamin A (alcohol and acetate) on adsorption of ethyl-acetate vapor of different amounts

Vitamin A alcohol (Solid state crystalline powder) $(2kT_0)^{-1}=14.45\ eV^{-1}$; $\rho_0'=2.8\times10^{-9}\ \Omega^{-1}\ cm^{-1}$				Vitamin A acetate (Solid state crystalline powder) $(2kT_0)^{-1}=17.52\ eV^{-1}$; $\sigma_0'=1.5\times10^{-10}\ \Omega^{-1}\ cm^{-1}$			
Curve No. from Fig. 3(a)	E / eV	$\sigma_0' \exp[E/(2kT_0)]$ / $\Omega^{-1}\ cm^{-1}$	σ_0 / $\Omega^{-1}\ cm^{-1}$	Curve No. from Fig. 3(b)	E / eV	$\sigma_0' \exp[E/(2kT_0)]$ / $\Omega^{-1}\ cm^{-1}$	σ_0 / $\Omega^{-1}\ cm^{-1}$
1	0.94	2.22×10^{-3}	2.0×10^{-3}	1	0.63	9.32×10^{-6}	1.0×10^{-5}
2	1.08	1.68×10^{-2}	2.3×10^{-2}	2	0.89	8.87×10^{-4}	1.7×10^{-3}
3	1.19	8.22×10^{-2}	1.8×10^{-1}	3	1.16	1.00×10^{-1}	1.6×10^{-1}
4	1.43	2.64×10^{0}	3.5×10^{0}	4	1.52	5.51×10^{1}	1.5×10^{1}
5	1.62	4.11×10^{1}	3.0×10^{1}	5	1.80	7.43×10^{3}	1.2×10^{3}

Curve No. 1→5 corresponds to the decreasing amount of adsorbed ethyl acetate vapor.

4.55 eV^{-1} for these two compounds respectively. The agreement is excellent. Also the intercepts give $\sigma_0' \simeq 2.85\times10^{-9}\ \Omega^{-1}\ cm^{-1}$ for vitamin A alcohol and $\sigma_0' \simeq 1.6\times10^{-10}\ \Omega^{-1}\ cm^{-1}$ for vitamin A acetate. These values agree well with the values obtained from the log σ_0 *vs.* E and log σ *vs.* $1/T$ plots. Thus the high correlation between the relevant parameters in semiconducting vitamin A powder on adsorption of various vapors indicates that Compensation rule is valid in these biological semiconductors and that σ_0 and E are indeed physically related.

Type of Interaction between the Adsorbed Gas and the Semiconducting Material. It needs to be pointed out that the reason for the semiconduction activation energy change is not quite settled.[8,11] However, donor-acceptor complex formation has been widely held responsible for the increase of current in some semiconductors[15-17] due to gas adsorption. As the vapors used in this present investigation are good electron donors and polyenes are known to act both as electron donor and electron acceptor,[18,19] formation of charge-transfer complexes of vitamin A (alcohol and acetate) with the adsorbed vapors may be possible. It had generally been observed[20,21] that in solid charge-transfer complexes with a particular acceptor and a number of similar type of donors, the semiconduction activation energy as obtained from relation (1) and the energy ($h\nu_{CT}$) of the lowest charge-transfer band are linearly related by the expression

$$E = h\nu_{CT} - \delta = I_D - E_A + C_1 - \delta \qquad (4)$$

where, I_D is the vertical ionization potential of the donor, E_A is the vertical electron affinity of the acceptor, C_1 is a constant[22] and δ is also another constant of very low value.[20] In Fig. 6, we show a plot of E *vs.* I_D. A linear relationship is obtained as expected from Eq. 4. The slope of the line (0.6) however, is much less than unity. Such a value for the slope is a rather general observation[23,24] in $h\nu_{CT}$ *vs.* I_D plots. The intercept of this plot is −3.8 eV. The value of $-C_1$ is usually[22,25] around 3 eV. The electron affinity of anhydro vitamin A which is expected to be close to that of vitamin A (alcohol and acetate) has been reported to be[26] 0.7 eV. This gives a value of 0.1 eV for δ which is a very reasonable value.[21,22] This adds further credence to the proposed charge-transfer concept.

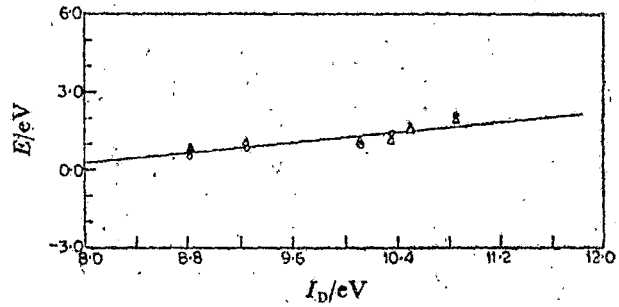

Fig. 6. Semiconductive activation energy (E) *vs.* ionization potential (I_D) of the adsorbed vapor molecules.
—○—: Vitamin A alcohol.
—△—: Vitamin A acetate.

There are number of theses about the mechanism of conduction in organic semiconductors leading to compensation effect. The carrier injection model of Green[27] produces the type of activation energy dependence of the pre-exponential factor as observed experimentally, but does not provide any physical basis for the interpretation of T_0. Significant difference in T_0 values for these two compounds suggests that T_0 is a molecular characteristic of these organic semiconductors. Kemeny and Rosenberg[28] observed compensation law in tunneling of small polaron through molecular barrier from thermally activated energy levels of molecules. Their model predicts that $T_0=\theta/2$ (where θ is the Debye temperature) and that at $T>T_0$, small polaron tunneling is not possible and compensation effect is not expected to be observed. No experimental study seems to have been reported on the semiconductive behavior of organic compounds at $T>T_0$. Debye temperature for vitamin A alcohol and acetate are not known. It has been reported[29] that the Debye temperature for a series of crystals of large aromatic molecules lies in the range 100—130 K. It seems that the T_0 values measured are far too high to justify the polaron tunneling model.

An interaction between the electrons and the vibrational motion has been thought[9,10] to be the mechanism behind compensation effect. A change in the electronic state (due to complex formation) gives rise to an activation entropy because of a change in vibrational frequencies. The variation in both the electronic energy gap

(E_g) and the activation entropy (S) can account for compensation effect if the changes in these parameters are given by

$$E_g = E_{g_0} + nE_{g_1} \text{ and } S = S_0 + nS_1$$

where n is a definite number for each system and E_{g_0}, E_{g_1}, S_0 and S_1 are same for all the systems. In this case the characteristic temperature is given by

$$T_0 = E_{g_1}/(2S_1) .$$

Unfortunately due to the fact that the nature of the activated complex is not precisely known, the activation entropy S (hence S_1) is a relatively obscure quantity and any quantitative estimate of T_0 is not possible.

We thank the Council of Scientific and Industrial Research, India for a Senior Research Fellowship (to B. M.) and Prof. G. S. Kastha for his kind interest in this problem. Thanks are also due to M/s Hoffmann-La Roche and Co., Switzerland for a kind gift of the polyenes.

References

1) D. D. Eley, *J. Polym. Sci., Part C*, **17**, 73 (1967).
2) B. Rosenberg, B. Bhowmik, H. C. Harder, and E. Postow, *J. Chem. Phys.*, **49**, 4108 (1968).
3) D. D. Eley, A. S. Fawcett, and M. R. Wills, *Trans. Faraday Soc.*, **64**, 1513 (1968).
4) G. R. Johnston and L. E. Lyons, *Aust. J. Chem.*, **23**, 2187 (1970).
5) Ulbert, *Aust. J. Chem.*, **23**, 1347 (1970).
6) M. Masui, H. Nagasaka, and K. Yahagi, *Jpn. J. Appl. Phys.*, **16**, 177 (1977).
7) F. Gutmann and L. E. Lyons, "Organic Semiconductors," John-Wiley, New York (1967), pp. 428—435.
8) B. Rosenberg, *J. Chem. Phys.*, **36**, 816 (1962).
9) G. Kemeny and I. M. Goklany, *J. Theor. Biol.*, **40**, 107 (1973).
10) T. A. Kaplan and S. D. Mahanti, *J. Chem. Phys.*, **62**, 100 (1975).
11) T. N. Misra, B. Rosenberg, and R. Switzer, *J. Chem. Phys.*, **48**, 2096 (1968).
12) B. Rosenberg, T. N. Misra, and R. Switzer, *Nature*, **217**, 423 (1968).
13) B. Rosenberg, *Nature*, **193**, 304 (1962).
14) B. Rosenberg, "Physical Processes in Radiation Biology," Academic Press (1969), p. 119.
15) M. M. Labes and O. N. Rudyj, *J. Am. Chem. Soc.*, **85**, 2055 (1963).
16) P. J. Reucroft, O. N. Rudyj, and M. M. Labes, *J. Am. Chem. Soc.*, **85**, 2059 (1963).
17) P. J. Reucroft, O. N. Rudyj, R. E. Salomon, and M. M. Labes, *J. Phys. Chem.*, **69**, 779 (1962).
18) B. Pullman A. Pullman, "Quantum Biochemistry," Interscience New York (1963), p. 440.
19) J. R. Platt, *Science*, **129**, 372 (1959).
20) H. Kuroda, K. Yoshihara, and M. Akamatu, *Bull. Chem. Soc. Jpn.* **35**, 1604 (1962).
21) H. Kuroda, M. Kobayashi, M. Kinoshita, and S. Takemoto, *J. Chem. Phys.*, **36**, 457 (1962).
22) E. C. M. Chen and W. E. Wentworth, *J. Chem. Phys.*, **63**, 3183 (1975).
23) H. McConnel, J. S. Ham, and J. R. Platt, *J. Chem. Phys.*, **21**, 66 (1953).
24) R. Foster, *Tetrahedron*, **10**, 96 (1960).
25) A. L. Farragher and F. M. Page, *Trans. Faraday Soc.*, **63**, 2369 (1967).
26) V. G. Mairanovaky, A. A. Engovatov, N. T. Ioffe, and G. I. Samokhvalov, *J. Electroanal. Chem.*, **66**, 123 (1975).
27) M. E. Green, *J. Chem. Phys.*, **51**, 3279 (1969).
28) G. Kemeny and B. Rosenberg, *J. Chem. Phys.*, **53**, 3549 (1970).
29) E. I. Mukhtarov, A. A. Pichurin, and A. I. Kitaigorodskii, *Sov. Phys. Solid State (U. S. A.)*, **17**, 1871 (1975).